PROGRESS SERIES

METAL PHYSICS

2

PROGRESS IN METAL PHYSICS

2

Editor
BRUCE CHALMERS, D.Sc., Ph.D.

LONDON
BUTTERWORTHS SCIENTIFIC PUBLICATIONS
1950

BUTTERWORTHS SCIENTIFIC PUBLICATIONS LTD
BELL YARD · TEMPLE BAR · LONDON, W.C.2

BUTTERWORTH & CO (AFRICA) LTD · DURBAN

BUTTERWORTH & CO (AUSTRALIA) LTD · SYDNEY
MELBOURNE · BRISBANE · WELLINGTON · AUCKLAND

BUTTERWORTH & CO (CANADA) LTD · TORONTO

U.S.A. edition published by

INTERSCIENCE PUBLISHERS INC
250 FIFTH AVENUE · NEW YORK, I, N.Y

December 1950

Set in Monotype Baskerville type
Printed in Great Britain by THE KYNOCH PRESS, Witton, Birmingham

CONTENTS

FOREWORD TO VOLUME 1

THE study of the physical properties of metals has developed through a number of stages. The first was that in which the mechanical properties were correlated empirically with the heat treatment to which the metal had been subjected and, sometimes, to the chemical composition. At this stage the successful treatment of metals was an art, in the sense that experience rather than understanding led to the most satisfactory results. The next stage, in which the internal structure of the metal was examined, was based originally on the use of the microscope and it was found that many experimental facts could be explained in terms of effects that were of the right size to be seen under magnifications of less than about two thousand. The development of the x-ray diffraction techniques allowed phenomena of a smaller order of magnitude to be examined, and much of the existing information was found to be comprehensible in terms of the geometry of the crystal structure of the various phases that were visible under the microscope.

More recent development can perhaps best be discussed by a division of the field into what may be termed 'statics' and 'dynamics'. Under the former heading is the study of the conditions which govern the structure of a metal or alloy when it is in thermodynamic and mechanical equilibrium. The theories of the phrases that are present in equilibrium and of the elastic constants have made remarkable progress in terms of rapidly developing theory of the part played by electrons in the metal.

Under the heading 'dynamic' effects we may include both the conditions governing the approach to equilibrium in respect of the phases that are present, in which diffusion plays an important part, and the response of a metal to forces which are sufficient to cause non-recoverable or plastic mechanical deformation.

These and associated subjects have advanced so rapidly that it has become difficult for research workers in one part of the field to remain up to date in other branches. It is the purpose of this volume, which is the first of an annual series, to present authoritative reviews of the present state of knowledge in specialized aspects of the field that includes both physical metallurgy and metal physics. It is not intended that any one volume should form a complete textbook on these subjects. It is hoped rather that a few subjects of current interest should be discussed rather fully so as to cover, in the course of several years, all the more important aspects in which progress is being made. In order to make the series reasonably self contained it is proposed that the necessary 'historical' background should be included the first time a particular subject is discussed. Subsequent articles on such subjects will generally only cover the more recent progress.

B. CHALMERS

FOREWORD TO VOLUME 2

PROGRESS in metal physics has been rapid and extensive since the preparation of the first volume of this series and much significant work has appeared even since the planning of the present volume. It is because of the rapid progress that is being made in the particular field of polygonization that it was thought desirable to include three papers on closely allied topics. It is hoped that this will give a more comprehensive and balanced account than would have been possible in a single paper so soon after the ideas had been formulated. In other respects this volume follows the policy set forth in the foreword to Volume 1. The subjects chosen are all new ones, as far as this series is concerned, although they have all been under investigation for a considerable time; in each of them there has been significant progress in the last few years.

B. CHALMERS

ACKNOWLEDGEMENTS

THE following illustrations appear by permission of the authors and the sources stated below·

American Institute of Mining and Metallurgical Engineers
FREDRICKSON, J. W. and EYRING, H. *Figures 12, 13, 14 pp 72, 77, 78*
KAUZMANN, W. *Figure 11 p 71*
RHINES, F N. and MEHL, R F. *Figure 4 p 61*

Cambridge University Press
BARRER, R M. (Diffusion in and through Solids) *Figure 2 p 58*

Edward Arnold & Co.
COTTRELL, A. H. (Theoretical Structural Metallurgy) *Figure 9 p 68*

Institute of Metals
BORELIUS, G *Figure 26 p 36*

Melbourne University Press
BOAS, W. *Table VIII p 116*

Metal Industry
WARRINGTON, H G. *Figures 3, 4, 5; art insert p 128*

Metaux et Corrosion
LACOMBE, P. and BERGHEZAN, A. *Figure 12 p 170*

Physical Review
QUIMBY, S. L. and SIEGEL, S. *Figure 3 p 108*
SIEGEL, S. *Figure 4 p 108*

Physical Society
CAHN, R. W *Figures 3, 14 p 155, art insert p 165*
GUINIER, A. *Figure 28 p 37*

Reviews of Modern Physics
NIX, F. C. and SHOCKLEY, W *Figures 32, 34, 36 pp 40, 41, 44*

Royal Society
BRADLEY, A. J. and ROGERS, J. W. *Figures 11, 23 pp 8, 32*
SYKES, C. and JONES, F. W. *Figures 29, 31, 33, 35; art insert p 38, pp 40, 41, 42*
WEBSTER, L. *Figure 8 p 111*

1

ORDER-DISORDER CHANGES IN ALLOYS

H. Lipson

THE SUBJECT of the order-disorder transformation in alloys has already been extensively covered; in addition to sections devoted to the subject in a number of books,[1-4] many reviews[5-10] exist, a particularly comprehensive one having been written by NIX and SHOCKLEY[7] in 1938. Each of these reviews, however, has stressed one particular aspect of the subject—Nix and Shockley, for example, were concerned mainly with theory—and none of them contains a reasonably full summary of the different types of superlattice that occur in practice. In addition, new methods of experimentation, particularly with x-rays, have been devised during the last few years for examining in greater detail the kinetics of the transformations.

An attempt is made here to describe superlattice structures as completely as possible, and to show how the x-ray diffraction effects arise. The theoretical side of the subject will be dismissed rather briefly, since it is covered so well by Nix and Shockley, and for similar reasons the section on experimental work is mainly concerned with the underlying principles rather than with practical details. Again, the results of experiment are chiefly concerned with introducing the ideas that have arisen since 1938, and these ideas provide a pointer to the way in which progress is likely to take place in the future. The article may thus, in a general way, be regarded as complementary to that of Nix and Shockley, in addition to providing a guide to work that has been published since their paper was written.

SUPERLATTICE STRUCTURES

Explanation of the Term Superlattice—A crystal is composed of atoms arranged in regular three dimensional array. Since the array is regular, in order to specify a structure it is not necessary to indicate the positions of all the atoms; we need to specify only that group of atoms which is repeated to form the whole crystal together with the three units of translation. If we apply these units of translation to a single point we produce what is known as the lattice of the crystal, the

framework without the atoms. The parallelepiped of which the three units of translation are the edges is called the unit cell, and a unit cell can be found by joining any one atom to the three nearest atoms that are similar and have similar environments, provided that the four atoms are not in the same plane.

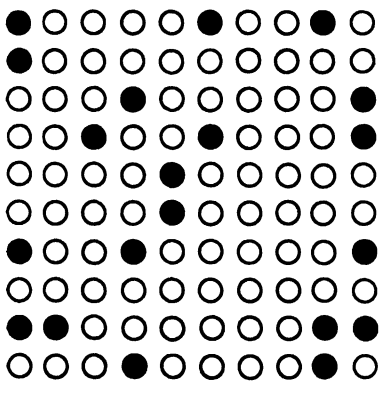

Figure 1. Random solid solution of 20% B atoms in A atoms

Metallurgists often use the term lattice to represent the complete structure, whereas, of course, it is an abstraction useful only in describing structures. The error has arisen because many metallic structures can be completely specified by placing a single atom at each point of a lattice; for example, copper has its atoms arranged on the points of a face-centred cubic lattice, and iron has its atoms arranged on the points of a body-centred cubic lattice. (These lattices are both formed by equal, mutually perpendicular, translations, but the former has extra lattice points at the centres of the faces of the unit cell, and the latter has an extra point at the centre of gravity of the unit cell. It is important to note that, although the cubic unit cell is the simplest to use, it is not the smallest in volume.)

This concept is satisfactory for pure metals, but requires modification for solid solutions. Suppose we have a solid solution of 20 per cent of element *B* in element *A*; if we place an atom *B* at a lattice point, the lattice translations may not lead to an atom *B*. For solid solutions, therefore, we regard the lattice as a collection of atomic sites; whether an *A* atom or a *B* atom occupies a particular site depends upon several factors, the chief of which may be pure chance. Thus, we assume that the atoms are arranged at random, as shown in two dimensions in *Figure 1*. This figure was produced by means of a well shuffled mixture of two types of card in the ratio of 4 to 1; when one type was turned up an open circle was drawn at a lattice point, and when the other type was turned up a black circle was drawn.

There is another point to be remembered: if the two atoms are of different sizes they will tend to displace each other from the lattice

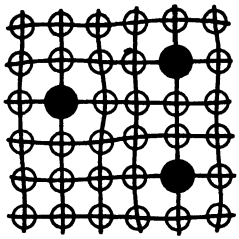

Figure 2. Distortion of lattice caused by solution of larger atoms

points, and the structure will not be quite regular, as is shown in *Figure 2*. This matter has been considered quantitatively by WASASTJERNA,[11] and is of importance in the theory of superlattice formation, to be considered later.

Although in many alloy systems chance appears to be the main factor in deciding the apportionment of the atoms, it is not always so; there may be particular reasons why dissimilar atoms tend to avoid or to attract each other. If, in a binary alloy, dissimilar atoms avoid each other, a two-phase system will be formed; whereas if they attract, a superlattice structure will be formed. If, in an alloy of equal atomic proportions, the presence of one type of atom on a lattice point demands that each neighbouring point shall be occupied by an atom of the other type, we arrive at the structure shown in *Figure 3*; a corresponding structure with random distribution of atoms is shown in *Figure 4*.

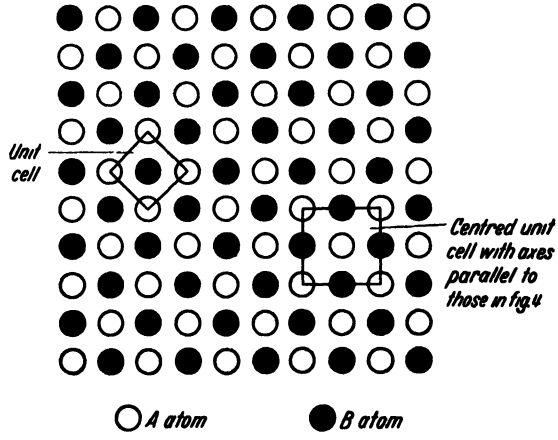

Figure 3. Superlattice structure of composition AB

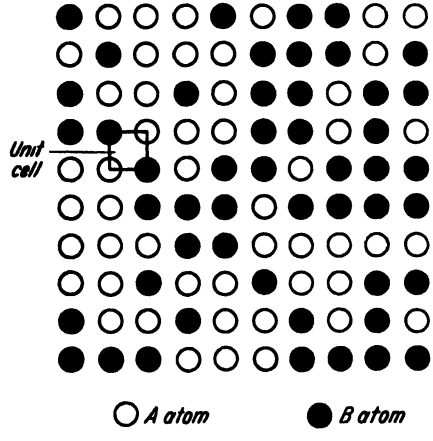

Figure 4. Disordered solid solution of composition AB

The structure shown in *Figure 3* is said to be ordered, and that shown in *Figure 4* is said to be disordered. The former may also be said to be a superlattice structure, the term originating in the following way. To find the unit cell of the disordered structure we join nearest atomic sites as shown in *Figure 4*; as we have already seen, we cannot join similar atoms, but with the ordered

structure we can join similar atoms, as shown in *Figure 3*. This leads to a larger unit cell with axes inclined at 45° to those of the disordered unit cell, or, if we wish to retain the directions of the axes of the disordered unit cell, we may choose a centred cell which is still larger. These larger unit cells, which are derived from a smaller one, lead to the name superlattice.

Types of Superlattices in Alloys

Ordered structures are found in many alloy systems, but there are only a few fundamentally important types. These are most easily

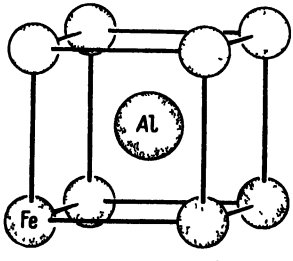

Figure 5. Structure of FeAl

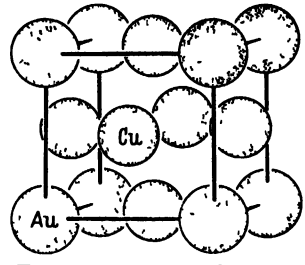

Figure 6. Structure of $AuCu_3$

described by giving the coordinates (x, y, z) of the atoms in the unit cell, each coordinate being a fraction of the corresponding cell edge. Thus an atom at the centre of gravity of a unit cell would have coordinates $(\frac{1}{2}, \frac{1}{2}, \frac{1}{2})$.

1 FeAl—The most common type of superlattice is that typified by the alloy FeAl. This is based upon the body-centred cubic structure of α-iron, but has iron atoms at (0, 0, 0) and aluminium atoms at $(\frac{1}{2}, \frac{1}{2}, \frac{1}{2})$, as shown in *Figure 5*. It should be noted that the complete structure can be specified equally well by interchanging the aluminium and iron atoms. Both atoms still have similar environments.

This superlattice has the same unit cell as the disordered structure, but the lattice now is not centred. The structure is often called body-centred cubic with a superlattice, but superlattice implies that the lattice is no longer body-centred.

2 $AuCu_3$—This ordered structure is based upon the face-centred lattice of copper or of gold. It is not as common as the FeAl type, but is much more interesting practically, as will be shown later. The structure can be described as having copper atoms at the centres of the faces of the unit cell $(0,\frac{1}{2},\frac{1}{2})$, $(\frac{1}{2},0,\frac{1}{2})$ and $(\frac{1}{2},\frac{1}{2},0)$ and gold atoms at the corners (0,0,0) (*Figure 6*). Three other descriptions, with the gold

atoms at one of the points $(0,\frac{1}{2},\frac{1}{2})$, $(\frac{1}{2},0,\frac{1}{2})$ or $(\frac{1}{2},\frac{1}{2},0)$, are also possible.

As for FeAl, this superlattice has the same unit cell as for the disordered structure, but the lattice is primitive, not centred.

3 Fe_3Al—Like FeAl, this type of superlattice is based upon the structure of α-iron. The unit cell, however, has to be doubled in each direction, being still cubic but containing sixteen atoms instead of two. Of these sixteen atoms, twelve are iron, at (0,0,0), $(\frac{1}{2},0,0)$, $(0,\frac{1}{2},0)$, $(0,0,\frac{1}{2})$, $(0,\frac{1}{2},\frac{1}{2})$, $(\frac{1}{2},0,\frac{1}{2})$, $(\frac{1}{2},\frac{1}{2},0)$, $(\frac{1}{2},\frac{1}{2},\frac{1}{2})$, $(\frac{1}{4},\frac{1}{4},\frac{1}{4})$, $(\frac{1}{4},\frac{3}{4},\frac{3}{4})$, $(\frac{3}{4},\frac{1}{4},\frac{3}{4})$, and $(\frac{3}{4},\frac{3}{4},\frac{1}{4})$, and four are aluminium, at $(\frac{3}{4},\frac{3}{4},\frac{3}{4})$, $(\frac{3}{4},\frac{1}{4},\frac{1}{4})$, $(\frac{1}{4},\frac{3}{4},\frac{1}{4})$ and $(\frac{1}{4},\frac{1}{4},\frac{3}{4})$. This structure is shown in *Figure 7*, from which it will be seen that the aluminium atoms are arranged tetrahedrally in the unit cell. It is interesting to note that, although the disordered structure is body-centred, the ordered structure is face-centred; if any atomic site is considered, those sites related to it by translations $(0,\frac{1}{2},\frac{1}{2})$, $(\frac{1}{2},0,\frac{1}{2})$ and $(\frac{1}{2},\frac{1}{2},0)$ are occupied by similar atoms. Other descriptions of the structure are again possible, but they all satisfy this condition.

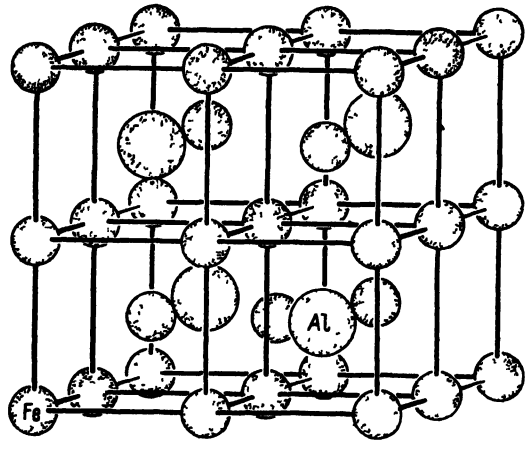

Figure 7 *Structure of* Fe_3Al

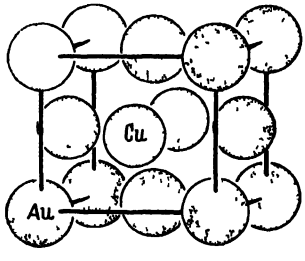

Figure 8 *Structure of* AuCu

4 AuCu—This structure is based upon the face-centred cubic structure, but there is an important modification. *Figure 8* shows gold atoms at (0,0,0) and $(\frac{1}{2},\frac{1}{2},0)$ and copper atoms at $(0,\frac{1}{2},\frac{1}{2})$ and $(\frac{1}{2},0,\frac{1}{2})$, like atoms filling alternate planes. Thus the distribution of atoms in a side face differs from that in the base. The crystal has lost the cubic symmetry which the disordered structure possesses; the structure is tetragonal and the unit cell edges are no longer equal, the base edge being slightly longer than vertical edge in *Figure 8*.

5 Mg_3Cd—So far we have dealt only with superlattices based upon cubic structures, but other types are also possible. The structure of Mg_3Cd is based upon the hexagonal close-packed structure. This has a hexagonal unit cell, for which two edges a are equal and inclined at 120°, the edge c being of unequal length and perpendicular to the other two. The positions of the atoms are (0,0,0) and $(\frac{1}{3},\frac{2}{3},\frac{1}{2})$. The ordered structure is represented by doubling the cell edges a and making one atom in four in each of the layers at $z = 0$ and $z = \frac{1}{2}$ different from the other three; the two layers are so disposed that each of the minority atoms is in contact with three majority atoms in all the layers adjacent to it (*Figure 9*).

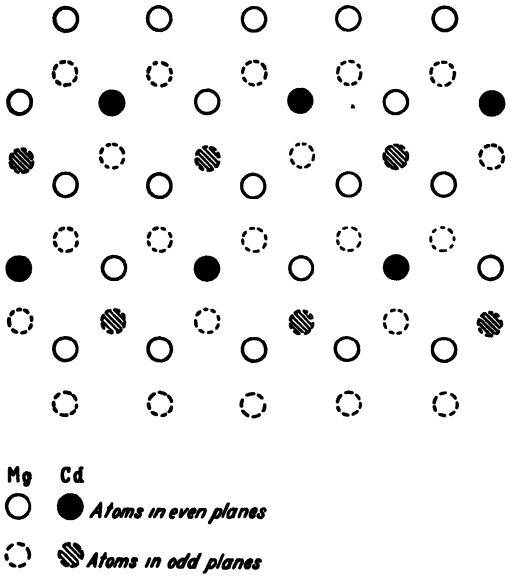

Figure 9. Relative dispositions of atoms in Mg_3Cd *structure*

6 Interstitial Superlattice Structures—In addition to substitutional solid solutions, in which one type of atom replaces another, it is possible to have interstitial solid solutions, in which the solute atoms are accommodated in the interstices between the solvent atoms. These structures are not very common because there are only a few atoms that are small enough to be so accommodated, and even when the atoms are small enough they seem to be accommodated only with some difficulty.

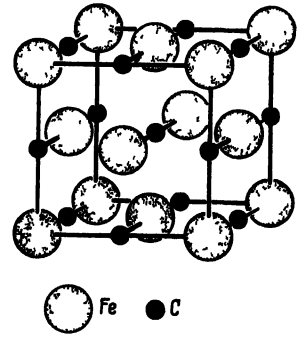

Figure 10. Structure of γ*-iron, showing possible positions of carbon atoms. Only a small proportion of these positions can be occupied*

The two atoms that form interstitial structures most readily are carbon and nitrogen. Of particular importance is the solution of carbon in iron, both in the face-centred γ-form (austenite), where the carbon atoms fit readily in the octahedral interstices (*Figure 10*), and in the body-centred form

(martensite), where the carbon atoms fit only with a great deal of strain. As will be shown later, it is probable that both these structures are ordered.

Nitrogen also forms ordered interstitial structures when dissolved in iron. The material Fe_4N, for example, has the same structure as the solution of carbon in γ-iron.[12] In addition, however, structures based on hexagonal close packing, but debased to orthorhombic symmetry, also exist.[13]

7 Other Possibilities—It is difficult to decide where to draw the line in enumerating superlattice structures. As we have seen, there are ordered structures formed with the same unit cell as the disordered, with only a change of lattice type (FeAl and $AuCu_3$), there are structures in which the unit cell of the ordered structure is a multiple of that of the disordered structure (Fe_3Al and Mg_3Cd), and there are structures in which the symmetry is reduced (AuCu). There are other examples[14] of this last type: Ni_2Al_3 is based upon the FeAl ordered structure, distorted in such a way that the symmetry is hexagonal. But here another effect arises: the addition of aluminium to NiAl is such as to introduce vacant sites into the structure. At first these are disposed at random, but with extra aluminium they arrange themselves with hexagonal symmetry. Thus the alloy Ni_2Al_3 may almost be considered as a ternary alloy of nickel, aluminium and holes.

These vacant sites do not always accommodate themselves so neatly, but often involve small displacements of neighbouring atoms. The most famous example[15] of this is provided by the alloy Cu_5Zn_8, the unit cell of which is produced by trebling each of the edges of the body-centred cubic cell. The two atoms at (0,0,0) and $(\frac{1}{2},\frac{1}{2},\frac{1}{2})$ in this large unit cell are then removed and the remaining fifty two atoms are redistributed to fill the gaps so created. This structure is essentially a superlattice structure, and a large number of such structures has been worked out on these principles, chiefly by BRADLEY. Nevertheless it is not usual to describe these structures as superlattices, the term being confined to those structures in which there are no displacements of the atoms from their relative positions in the disordered structures.

8 Ternary Alloys—When a third element is added to an ordered structure it may distribute itself in either an irregular or a regular way, no new superlattice being produced in the former instance, but a large number of new possibilities opening up with regular distribution. For

example, the alloy Cu_2MnAl[16] has a superlattice of the Fe_3Al type in which the manganese and aluminium atoms are regularly distributed, as shown in *Figure 11*. Nevertheless, such ternary structures do not introduce any new principles, and the evidence from binary alloys has been sufficient to establish, in great detail, the theory of the order-disorder change.

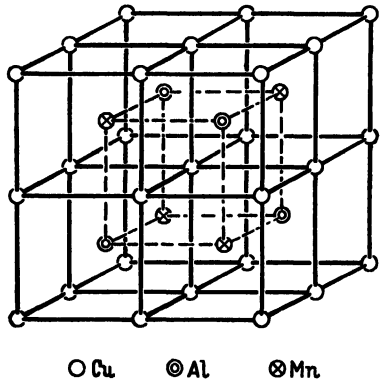

Figure 11. Distribution of copper, aluminium and manganese atoms in the quenched Heusler alloy

Short-range and Long-range Order—The ordered structures described so far have all been perfect, the probability that a site is occupied by a particular type of atom being either zero or unity. If the proportions of atoms are not correct for this condition to be fulfilled, for example if an alloy of iron and aluminium is not precisely equiatomic, then some disorder must be present. But the interesting points about many superlattice structures are that some disorder may be present even if the ratio of the numbers of atoms is correct, and that the amount of disorder can be caused to vary by heat treatment. A great deal of experimental work has been based upon this fact and this in its turn has provided the data for one of the most satisfactory theoretical treatments of reactions in the solid state.

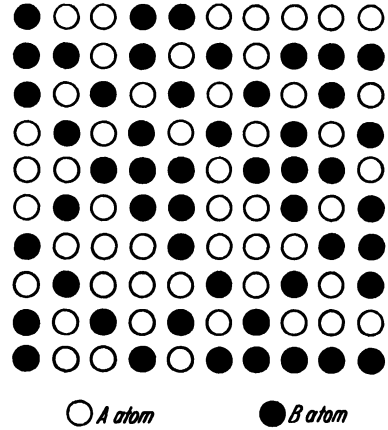

Figure 12 Solid solution of composition AB with $p = 0{\cdot}8$

Disorder may be of two types, which can best be explained with reference to a two dimensional structure containing equal numbers of atoms, A and B. Suppose that the structure has two different types of site, α at the corners of the unit cell and β at the centres of the faces. For perfect order, the probability that A atoms are on α-sites is unity, and thus the probability that B atoms are on β-sites is also unity. If the probability that A atoms are on α-sites is p, the probability that B

atoms are on α-sites is $1 - p$, the probability that A atoms are on β-sites is $1 - p$, and the probability the B atoms are on β-sites is p. Such a structure, in which the value of p is 0·8, is shown in *Figure 12*. This figure was constructed by interchanging one fifth of the atoms in *Figure 3* at random. The value of p is constant over the whole crystal, and the order is known as long-range order.

The random structure shown in *Figure 4* has a value of $p = \frac{1}{2}$, and it might be thought that this value of p is sufficient to indicate a completely disordered structure. This is not so, for this value of p can

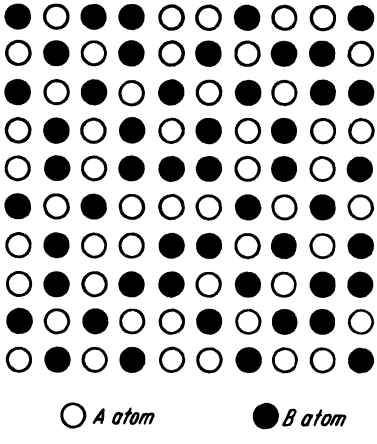

Figure 13a Solid solution of composition AB with short-range order

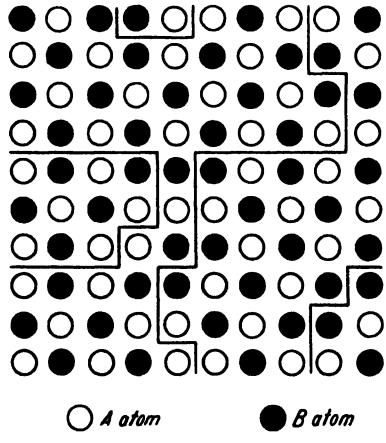

Figure 13b Structure shown in Figure 13a, with regions of perfect order (anti-phase domains) delineated

result even for practically complete order, as is shown in *Figure 13a*. In this figure the probability that A and B atoms are adjacent is quite large but is nevertheless not unity. Thus although there is no long-range order, since $p \simeq \frac{1}{2}$, there is another type of order, which is called local order or short-range order.

Anti-phase Domains—Examination of *Figure 13a* shows that local order can be regarded in another light, which is illustrated in *Figure 13b*. In this figure regions are marked out in which there is perfect order, and it can thus be seen that a crystal with local order can be regarded as a collection of small crystals with long-range order. These smaller crystals are not, of course, unrelated. As far as the atomic sites are concerned, they are part of the same regular formation. But as a boundary is crossed it will be noted that the sequence of atoms changes,

and for this reason the regions of perfect order are called anti-phase domains. This term arises by regarding the two different atoms respectively as the positive and negative parts of a wave: the change from one domain to another thus corresponds to a change of phase of π; that is, the two domains are exactly out of phase with each other.

THEORY OF THE ORDER-DISORDER TRANSFORMATION

The theory of the order-disorder phenomena is essentially simple since no changes in atomic sites are involved. (The problem may be contrasted with that of melting, where the regular arrangement of atoms gives place to an irregular packing. The theory of this process is far from being understood in as much detail as that of the order-disorder change.[17,18]) Nevertheless, although the general outline is satisfactory, the theory does not suffice to give quantitative agreement with experimental results, and in the attempts to remedy this defect many theoretical difficulties arise; to follow the subject completely, considerable mathematical equipment is necessary.

The main outlines have been treated in papers by BRAGG and WILLIAMS,[19-21] BETHE,[22] DEHLINGER,[23] BORELIUS,[24, 25] PEIERLS,[26] and FOWLER and GUGGENHEIMER.[27] EISENSCHITZ,[28, 29] KIRKWOOD,[30] CHANG[31] and others[32-41] have introduced modifications in attempts to bring these theories more into accord with what must actually take place in the atomic movement. The earlier findings have been admirably summarized in the paper by Nix and Shockley, on which the following account is based.

Definitions of Degree of Order—The adoption of some parameter to express degree of order constitutes the first necessity. The quantity p may be used, but it is unsatisfactory because it is not zero for a disordered alloy. For zero order in an alloy of composition AB, $p = \frac{1}{2}$. Bragg and Williams therefore adopt the quantity $s = 2p - 1$, which is zero for complete disorder ($p = \frac{1}{2}$) and unity for complete order ($p = 1$). (Bragg and Williams use the symbol S, but in view of the general acceptance of this symbol for entropy, which is important in the theory of these changes, the symbol s seems to be preferable.) A more general definition which is suitable for compositions other than AB is

$$(p - r)/(1 - r)$$

where r is the fraction of atoms of type A.

This definition of order does not, however, take short-range order into account. As we have seen, a structure (*Figure 13*a) may be highly ordered and yet have $s = 0$. Since, according to Peierls, the forces that dictate the structure to be adopted are short-range forces—a hypothesis that seems eminently reasonable since it is difficult to imagine these forces acting over many atomic diameters—a theory based on long-range order only is not likely to be completely satisfactory.[26] Bethe therefore suggests another parameter for specifying the degree of order.[22]

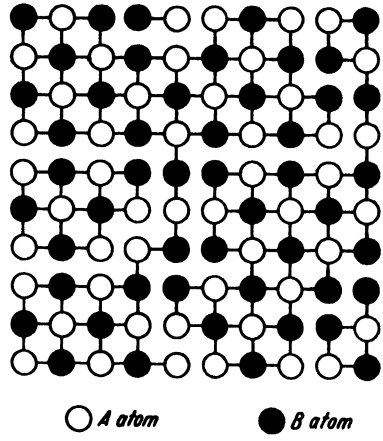

*Figure 13*c. *Structure shown in Figure 13*a, *with bonds between dissimilar atoms marked; the number of such bonds is* 142

This parameter is based upon the immediate environment of a particular atom, and not upon the whole crystal. In a crystal containing N atoms, each of which has z nearest neighbours, there are $Nz/2$ bonds. (The factor 2 enters because the pairing of two particular atoms is the same whichever is taken first.) A certain fraction of these bonds will be between unlike atoms; suppose this fraction be q. In a completely ordered structure q will be large, perhaps even unity, as it is for the two dimensional structure shown in *Figure 3*; let us call this value q_m. For a random structure such as that shown in *Figure 4*, q will have a smaller value dependent only on the ratio of the atoms present; let us call this value q_r.

Then the short-range order parameter σ is given by:

$$\sigma = \frac{q - q_r}{q_m - q_r}$$

This parameter can be illustrated by *Figure 13*a where there are 180 pairs of nearest neighbours. Because the perimeter atoms have only three nearest neighbours instead of four, this number is not 200, as we should expect from the expression $Nz/2$: in an actual structure, of course, we are justified in neglecting such surface effects since much larger numbers of atoms are involved. The number of unlike pairs, marked in *Figure 13*c by lines joining the circles, is 142, and thus the value of q is $142/180 = 0{\cdot}79$. The value of q_m is, of course, unity, and

the value of q_r is 0·5, as can be seen by counting the number of unlike pairs in *Figure 4*. Thus the value of σ is:

$$\frac{0{\cdot}79 - 0{\cdot}50}{1{\cdot}00 - 0{\cdot}50} = 0{\cdot}58$$

In the disordered structure of copper-zinc alloy each atom is on the average in contact with as many copper atoms as zinc atoms; q_r is therefore equal to $\frac{1}{2}$, as it is for the structure in *Figure 4*. Also q_m, in the ordered structure, is equal to unity, and therefore

$$\sigma = 2q - 1$$

Now for the completely long-range ordered structure $p = q$, and thus $\sigma = s$. Thus if one parameter is unity, the other is also, and only one is needed to specify a completely ordered structure. For a partly ordered structure, however, both parameters must be specified, the only relation between them being that $s \leqslant \sigma$.

In the disordered structure of $AuCu_3$, each copper atom is surrounded on the average by nine copper atoms and three gold atoms, and so contributes three unlike pairs. Similarly each gold atom contributes nine unlike pairs. Since there are three times as many copper as gold atoms, the fraction of unlike pairs is on the average $\frac{1}{4}$ for each lattice site. For the ordered structure each copper atom is in contact with eight copper atoms and four gold atoms, and each gold atom is in contact with twelve copper atoms and the fraction of unlike pairs is $(3 \times \frac{1}{3} + 1 \times 1)/4 = \frac{1}{2}$. Thus for this structure

$$\sigma = (q - \tfrac{1}{4})/(\tfrac{1}{2} - \tfrac{1}{4}) = 4q - 1$$

For this composition, therefore, the short-range parameter does not have the same form as the long-range parameter. This follows from the fact that for the composition AB_3 p approaches unity and q approaches $\frac{1}{2}$ as complete order is attained; for the composition AB both p and q approach unity.

Mechanism of Ordering—Any theory of the order-disorder change must first explain how order can arise in a disordered alloy. In a disordered structure there is no distinction between the sites, and thus it is difficult to see on what basis order can develop. The only rational explanation is that some ordered arrangement of a few atoms happens by chance, that this causes any similar arrangement of neighbouring atoms to have lower free energy, and that, because of this, neighbouring groups are similarly influenced, and so order spreads throughout the crystal.

Such phenomena are called cooperational. Attainment of further order depends upon the degree of order that already exists. It may be compared to the behaviour of a crowd of people: if one or two look up fixedly at the sky others may not be induced to do likewise, but if more people look upwards, the inducement to others to do so becomes greater, until when nearly everyone is looking upwards the instinct to look upwards also becomes almost irresistible even in the most obstinate individuals.

Bragg and Williams expressed this cooperational tendency by ascribing an energy V to the process of interchange of two atoms.[19] V must obviously depend upon s in such a way that it is zero when s is zero and increases as s increases. V may be regarded as the increase in energy of a crystal when two unlike atoms change to incorrect sites. The simplest assumption is that V is proportional to s, thus:

$$V = V_0 s$$

This means that, when there is no order, no energy change is involved in the interchange (or, more accurately, the energy change is as likely to be positive as negative), and that when there is complete order the interchange involves an energy of V_0. Thus as soon as a certain amount of order exists, the internal energy of the crystal is still further reduced by extension of the order.

Opposing this tendency is the action of temperature: the energy of the atoms manifests itself as kinetic energy, which, as it increases with temperature, may cause atoms to interchange places. Atoms are more likely to go on to right sites than on to wrong sites, but when there are only a few atoms on wrong sites the effect of temperature may be to send, on the balance, more atoms on to wrong sites than on to right sites, merely because there are so many more atoms which can be affected in this way. Thus the state of order must be regarded as one of dynamic equilibrium, and for any temperature there will be a degree of order which may be characteristic of that temperature.

Thus minimum internal energy is not the only consideration in deciding what structure will be adopted; if it were, then complete order would always exist. This fact can be expressed by making s dependent upon V; the easier it is for atoms to interchange, the less the degree of order, because there is little to hold the atoms in the right places if they should happen to go there. The equation relating s and V is not, however, the same as the previous equation: first, the parameter V_0

must be a function of temperature, whereas V as a function of order must be independent of temperature, and secondly s must approach unity asymptotically as V increases. Thus the two equations

$$V = V_0 s \qquad \text{and} \qquad s = \mathrm{s}(V)$$

represent simultaneous equations whose solution or solutions give equilibrium conditions for the alloy. The solution may be obtained graphically as shown in *Figure 14*, which represents the curve for $\mathrm{s}(V)$

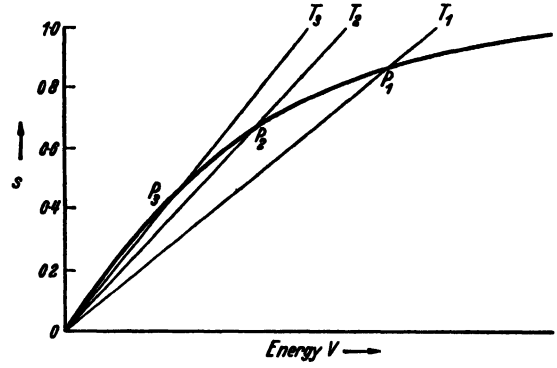

Figure 14 Curve of s as a function of V for an alloy of type AB, *the three straight lines representing equations* $V = V_0 s$ *for different temperatures*

obtained by Bragg and Williams for an alloy of the type AB, together with a number of straight lines $\mathrm{V}(s)$ representing the first equation for different values of temperature. The points P_1, P_2 and P_3 represent solutions to the equations for the corresponding temperatures.

Before enlarging upon this it is necessary to discuss the other solution, which is independent of temperature, namely $s = 0$. This solution is the one which expresses the fact that with zero order there is no tendency for order to begin. A slight variation of s will, however, lead to a finite value of V (this is represented by a small movement along the $\mathrm{V}(s)$ curve). The value of s corresponding to this value of V is greater than the value of s causing it: thus s will continue to increase until the point P_1 is reached and to attain stable equilibrium the curves must intersect at a point where the $\mathrm{s}(V)$ curve has a smaller slope than the $\mathrm{V}(s)$ curve.

As the temperature increases, the slope of the $\mathrm{V}(s)$ curve increases, and thus cuts the $\mathrm{s}(V)$ curve at lower values of s until finally the curves become tangential and the order decreases catastrophically to zero.

The temperature at which this happens is the critical temperature. Above this temperature, $s = 0$ represents the only solution to the two equations, and it is now a stable solution since the $s(V)$ curve has a smaller slope than the $V(s)$ curve.

For alloys of the type AB_3 still more interesting results are found. The $s(V)$ curve now has a point of inflection, and consequently three solutions are possible for certain temperatures. Below temperatures

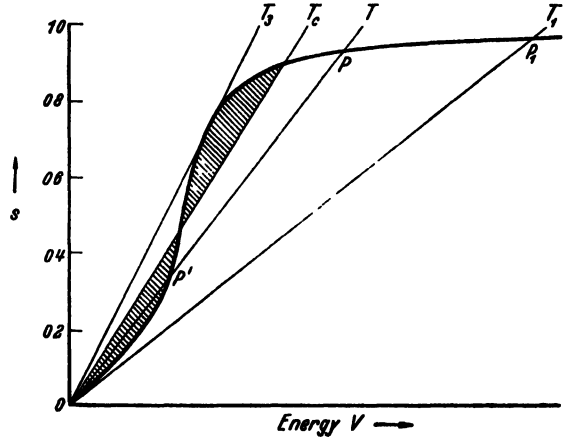

Figure 15. Curve of s as a function of V for an alloy of type AB_3, the four straight lines representing equations $V = V_0 s$ for different temperatures

corresponding to T_1 in *Figure 15* only one solution is possible and this is represented by the point P_1 as for the alloy AB. Above this temperature there are three solutions, corresponding to $s = 0$, the point P' and the point P.

It is obvious that the first and last solutions both represent stable states, but one is only metastable. The region of stability is determined by drawing a line, representing the temperature T_c, which makes the two shaded areas equal. For temperatures below T_c and above T_1 the disordered structure is metastable with respect to the ordered structure, for temperatures above T_c and below T_3 the ordered structure is metastable with respect to the disordered structure and above T_3 the disordered structure is the only stable one.

This theory leads to an essential difference between the two types of alloy, AB and AB_3. In the former the change of order should be continuous with temperature, although the change becomes more rapid

as temperature increases and finally becomes extremely fast. The change is known as a second-order change,[42] and is characterized by a variation in specific heat, but no latent heat. For the AB_3 alloy, however, there is a discontinuous change at the critical temperature in addition to the partial change of order that takes place below this temperature. Thus there is a change of specific heat culminating in a latent heat at the critical temperature which is characteristic of a first order change.

Although the theory is successful in explaining the more obvious features of the order-disorder change, the basis is not fundamentally satisfying. Bragg and Williams themselves point out that it is coarse-grained, as it makes the behaviour of a pair of atoms dependent upon knowledge of the state of affairs in the whole crystal. To overcome this defect Bethe has developed a theory[22] based on the short-range order parameter σ. This theory deals with a small group of atoms enclosed within a larger group with an ordered arrangement. The pattern of sites is then defined by the outer grouping and the interchanges of atoms on the inner sites can be treated mathematically. Since the results thus obtained are qualitatively similar to those of the Bragg-Williams theory, it is not proposed to discuss Bethe's work in detail here.

Thermodynamic Principles—The order-disorder change can also be treated by thermodynamic principles and provides a particularly satisfactory example of the application of these principles. This is again due to the fact that no changes in atomic sites are involved, only changes of atoms on the sites; the total entropy of the system need therefore not be considered but only the changes in entropy due to the changes in atomic configurations. This is known as the configurational entropy.

The entropy has to be examined because it enters into the expression for the free energy, which must be a minimum for the stability of a condensed (non-gaseous) system. Free energy is defined as $U - TS$, where U is the internal energy, T is the temperature and S the entropy of the system. In mechanical systems we regard the stability as dependent only upon minimum potential energy, which corresponds to the internal energy of a crystal.

This condition is approximately true at low temperatures. But for higher temperatures a closer analogy is given by a mechanical system to which a variable force is being applied and it is possible then that

the system will adopt configurations quite inconsistent with the principle of minimum potential energy.

This applies to crystals, where at low temperatures the atoms will tend to have minimum internal energy, implying that they will pack together as well as possible, forming either an ordered structure or two separate phases. Such tendencies to regular arrangement are well illustrated by the experiments of BRAGG and NYE[43, 44] with equally sized bubbles. It must be remembered that the tendency to order is due to the similarity of atoms and that in a system of unequal units regularity is extremely improbable. This improbability is merely an expression of the fact that there are more possibilities of making an irregular arrangement than of making a regular one.

By Boltzmann's principle, the entropy of a given system is related to the probability of that system—that is, to the number of different ways in which the system can exist. The general tendency of a system towards maximum entropy merely means that it tends to disorder because there are so many more ways of specifying a disordered system than of specifying an ordered one. Crystals disobey the principle because at ordinary temperatures the condition of minimum internal energy outweighs the condition of maximum entropy, but as the temperature increases the second condition becomes more important and finally the crystal melts.

The order-disorder change can be regarded as a similar effect on a different scale. Superimposed on the regular arrangement of the atoms there is a regular arrangement of the different atoms. Such a regular arrangement can be made in only a few ways; the structure in *Figure 3* can be drawn in only two ways, with a full circle or an open circle at the origin. But the disordered structure in *Figure 4* has a large number of alternatives and so is more probable; it has a greater entropy.

This theory can be applied quantitatively with fair success. An ordered crystal of CuZn containing N atoms can be arranged in 2 different ways and a disordered crystal in 2^N different ways (the fact that the last atom has Hobson's choice may be neglected if N is large). Thus the difference in entropy by Boltzmann's theorem is:

$$\Delta s = k \log_e 2^N - k \log_e 2$$

where k is Boltzmann's constant ($1{\cdot}38 \times 10^{-16}$ erg per degree). This difference is equal to $(N - 1)k \log_e 2$. If we consider one gram atom of the crystal (an average for copper and zinc may be taken),

the energy change $T\Delta S$, becomes equal to $R \log_e 2$, where R is the gas constant and has a numerical value of 1·38 cal/gm atom/°C in comparison with the observed value of 1·01 cal/gm atom/°C. Thus we see that this simple theory accounts very well for the magnitude of the energy change on ordering. For more precise agreement account has to be taken of the fact that order does not disappear completely at the critical temperature, some short-range order remaining.

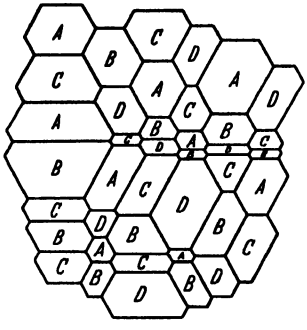

Figure 16. Two dimensional representation of four anti-phase domains, A, B, C, D

The thermodynamic approach to the problem has been developed by BORELIUS,[45] who has attempted to calculate the internal energy and entropy in terms of the degree of order. The expressions he formulates contain a number of arbitrary constants that he deduces from experimental results. This method of approach is fundamentally different from those already described and it is remarkable how closely the results of all the methods agree in general outline.

Stability of Short-range Order—The presence of short-range order both above and below the critical temperature can readily be explained on the thermodynamic basis. Above the critical temperature the entropy is not decreased greatly by the short-range order, but the internal energy is presumably decreased considerably; below the critical temperature short-range order causes the internal energy to be nearly a minimum, yet with considerably increased entropy. A compromise between the two opposing tendencies offers a suitable solution, both sides almost obtaining what they require but neither side being completely satisfied.

In view of these observations, it is surprising that short-range order below the critical temperature is so rarely observed. As far as the author is aware it has been reported only for the alloy $AuCu_3$,[46] although JONES and SYKES think that it may exist in Cu_3Pd.[47] The following considerations provide a possible explanation of this fact.

In *Figure 16* a (two dimensional) crystal is supposed to be divided into four types, A, B, C and D, of domains of similar order. It can be seen that it is readily possible to construct such a diagram without

contact between two similar domains; if two similar domains were in contact they would, of course, constitute only one domain.

Such a crystal would have extra internal energy at the lines of separation of the domains, and in order to reduce this energy the lines would contract until they were straight, and made equal angles with each other, in conformity with the principles of surface tension. This represents a stable structure. Suppose, however, that four types of domain are not possible, as with the FeAl type of superlattice which allows only two types of domain, one with iron atoms at the corners, the other with iron atoms at the centres of the unit cells. This may be taken into account by supposing that domains *A* and *C* are similar to each other and that *B* and *D* are also similar. Then effectively we have the arrangement shown in *Figure 17*, in which there are two types of domain with irregular boundaries. According to theory, therefore, the boundaries should contract until they are a minimum and it is not difficult to see that this can occur only if either there is a single domain, or the boundaries between the domains are straight lines.

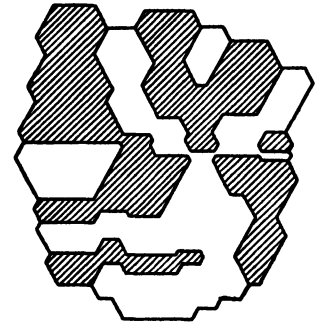

Figure 17. Modification of Figure 16, with A = B and C = D, showing irregular boundaries of anti-phase domains

It can be shown that it is possible for a three dimensional crystal to have stable short-range order below the critical temperature only if there are at least four different types of domain. Thus short-range order is possible with structures such as Fe_3Al or $AuCu_3$. Each crystal would then contain domains whose boundaries obey the same relations as a foam in which the pressure is constant at all points. BRAGG[48] has called such a structure a 'foam structure'. Although it is possible for the alloy Fe_3Al, it has not been reported for this alloy, and $AuCu_3$ remains the sole definite example.

EXPERIMENTAL INVESTIGATION

Detection of Long-range Order—Of the various methods of investigating order-disorder changes, x-ray diffraction is the most direct. The idea of ordering had been postulated by TAMMANN[49] in 1919 to account for the chemical behaviour of certain alloys of copper and gold, but x-ray

diffraction methods were not then sufficiently advanced to make direct verification possible. It was not until 1923 that BAIN[50] detected, on x-ray photographs of $AuCu_3$, lines that could only be attributed to a superlattice, and his conclusions were firmly established by JOHANNSON and LINDE[51] in 1925.

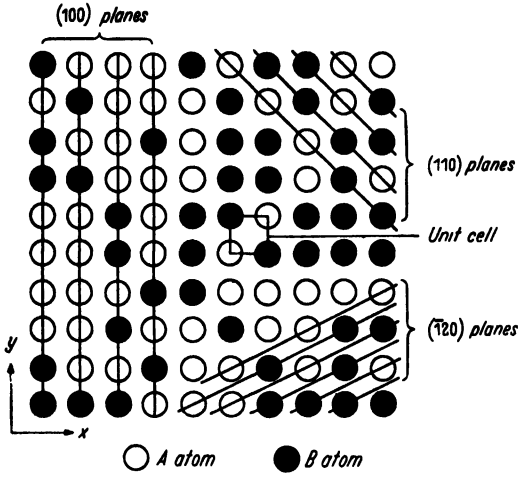

Figure 18. Traces of various lattice planes in a random solid solution

To explain the origin of these lines we have to consider the theory of x-ray diffraction. When x-rays fall upon matter, they cause each electron to vibrate and so to become a source of x-rays and this familiar effect is known as scattering. If the piece of matter has a periodic structure, as almost all solid matter has, the scattered rays interfere with each other in such a manner as not to disperse appreciable intensity in any direction unless the x-rays are incident in certain directions with respect to the crystal. The theory was treated rigidly by LAUE in 1912, but the rapid development of the subject had to await the more physical approach of Bragg in 1913.

Bragg regarded the crystal as composed of sets of planes that could 'reflect' the x-rays. Reflection in this sense is not specular; it can only take place if the rays are incident at particular angles, these angles θ being given by the relation

$$n\lambda = 2d \sin \theta$$

where n is an integer, λ is the wavelength and d is the distance apart of the planes.

This concept is illustrated in *Figure 18*, which is a reproduction of *Figure 4*, various sets of lattice lines having been drawn to represent the lattice planes that would exist in a three dimensional structure. It will be noted that all the lattice lines pass through atomic centres. This is true for a simple structure such as that of *Figure 4*, but not in general; the atoms may lie anywhere between the lines, but they must satisfy

the condition that the distribution of atoms between the lines is the same for any one set of lines.

From the few sets of lines drawn in *Figure 18* it is obvious that in any ordinary crystal a large number of sets of lattice planes is possible. These planes are specified by the three quantities representing the directions of their normals, these three quantities being proportional, in a cubic crystal, to the direction cosines of the normals. Because of the properties of the lattice the three quantities can be represented by integral numbers, $h\ k\ l$, the Miller indices, each index being inversely proportional to the intercept the plane makes on the three axes of the lattice. In *Figure 18* the planes drawn are (100) which make intercepts of 1 and ∞ on the x and y axes respectively, (110) which make intercepts of 1 and 1 on these axes and $(\bar{1}20)$ which make intercepts of -1 and $\frac{1}{2}$. We see that as the indices increase, the spacing $d(h,k,l)$ decreases and the density of atoms in the planes decreases.

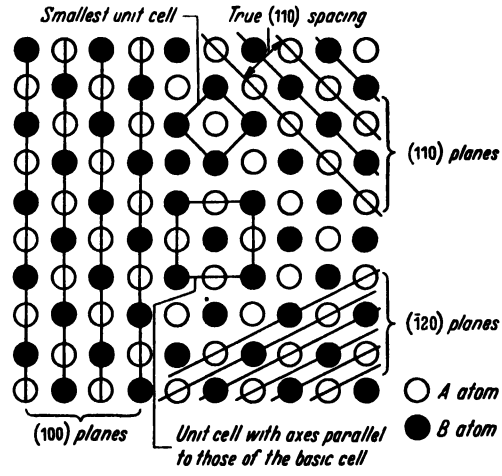

Figure 19 Traces of various lattice planes in an ordered structure, showing doubling of (110) *spacing The enlargement of the unit cell, compared with that of Figure 18, is also shown*

The various planes in *Figure 18* must, because of the randomness of the original arrangement, on the average contain equal numbers of the two types of atoms, and it can therefore be assumed that each of the sites contains an average atom; this concept works quite well for most x-ray investigations. But when the structure becomes ordered this rule breaks down, at least for certain sets of planes. For example, the (100) planes in *Figure 19*, which is a representation of an ordered structure, still contain equal numbers of the two types of atoms; so do the $(\bar{1}20)$ planes; but the (110) planes contain alternately atoms of one sort and atoms of the other sort. From this it may be deduced that the x-ray reflections from the planes (100) and $(\bar{1}20)$ and any planes of which the sum of the indices is odd will not be affected by the

ordering, but that the planes (110) and any planes of which the sum of the indices is even will be affected.

The nature of the change can be envisaged with reference to the lattice concept introduced in the first section of this article. It was seen that ordering is equivalent to the production of a lattice with a larger unit cell, and corresponding to this enlargement there is the possibility of larger interplanar spacings. Thus the spacing of (100) is now doubled, but since these planes are interleaved with exactly similar planes of atoms the effective spacing remains unchanged. The same is true of the planes ($\bar{1}20$) but not of the planes (110), which alternately contain different atoms, and since the spacing is the distance between one plane of atoms and the nearest plane of similar atoms, the spacing is effectively doubled. The importance of the statement that atoms do not necessarily lie on the lattice planes in a crystal can thus be seen.

Since the (110) spacing is doubled, twice as many values of n are possible in Bragg's equation, and hence twice as many values of θ. Thus extra x-ray reflections become possible when ordering takes place, and these provide the only direct evidence for ordering. These reflections are called superlattice reflections and are illustrated in *Figure 20*, which shows powder photographs of various types of ordered structures, together with those of the disordered structures from which they are derived.

For a general treatment of the subject it is obviously necessary to approach the problem analytically. This is provided by the general theory of x-ray diffraction,[52] which results in the following expression for the relative amplitudes of the rays 'reflected' from the various sets of planes $h\,k\,l$:

$$\mathrm{F}(h,k,l) = \Sigma f \cos 2\pi(hx + ky + lz)$$

where f is a quantity (the scattering factor) representing the scattering, at the same angle θ, of a single atom, and x, y and z are the coordinates of the atoms in the unit cell (the structural parameters) expressed as fractions of the cell edges. The summation is taken over all the atoms in the unit cell, and the quantity $\mathrm{F}(h,k,l)$ is known as the structure factor. (This expression is not perfectly general, but it applies to all the structures considered here if the quantities involved are appropriately specified.)

The significance of the expression for $\mathrm{F}(h,k,l)$ is demonstrated when

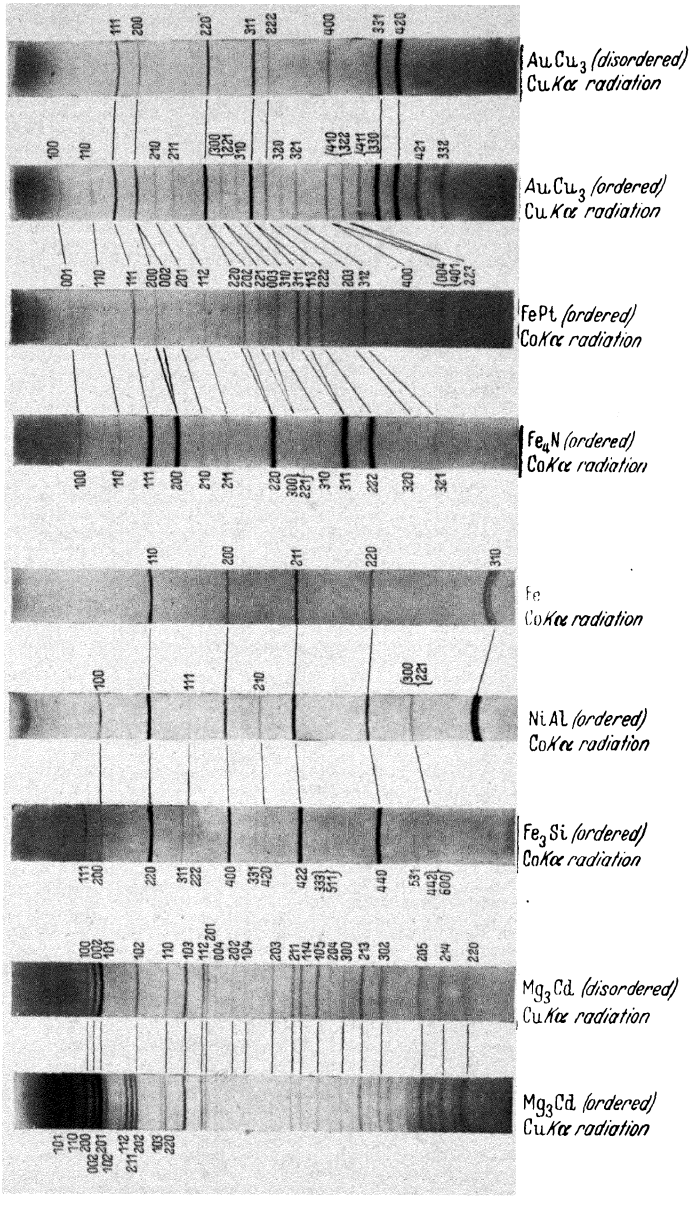

Figure 20. X-ray powder photographs of various disordered and ordered structures

applied to the structure of α-iron, which has atoms at (0,0,0) and $(\frac{1}{2},\frac{1}{2},\frac{1}{2})$. The value of F is then:

$$f\cos 0 + f\cos 2\pi(\tfrac{1}{2}h + \tfrac{1}{2}k + \tfrac{1}{2}l) = f\{1 + \cos\pi(h + k + l)\}$$

This value depends upon the indices h, k and l, but it can be seen that if $h + k + l$ is odd, $F(h,k,l)$ must be zero. That is, α-iron gives no reflections for which the sum of the indices is odd.

The ordered structure FeAl, however, has iron atoms at (0,0,0) and aluminium atoms at $(\frac{1}{2},\frac{1}{2},\frac{1}{2})$. Thus the expression for the structure factor is:

$$F(h,k,l) = f_{Fe}\cos 0 + f_{Al}\cos\pi(h + k + l)$$

This is not now zero when $h + k + l$ is odd, since the scattering factors of the two elements are not equal at any angle of diffraction. Thus the superlattice reflections are those with indices whose sum is odd. The reflections with indices whose sum is even are unaffected, since their structure factors are equal to $f_{Fe} + f_{Al}$.

Applying these methods to the other structures, we can derive similar relations. Such relations for the three cubic types of superlattice are shown in *Table I.*

Table I. Rules for Indices of Main Lines and Superlattice Lines in Cubic Structures

Structure Type	*Main Lattice Lines (Disordered Structure)*	*Superlattice Lines*
FeAl	*$h + k + l$ even*	*$h + k + l$ odd*
Fe_3Al	*h, k and l all even and $h + k + l$ a multiple of 4*	*h, k and l all even or all odd and $h + k + l$ not a multiple of 4*
$AuCu_3$	*h, k and l all even or all odd*	*h, k and l not all even or all odd*

These rules are illustrated by the indices accompanying the photographs in *Figure 20.*

The presence of superlattice lines on the x-ray photograph of an ordered alloy raises the interesting problem as to the origin of this extra scattered intensity. The total intensity of x-rays scattered by a given mass should be independent of the arrangement of atoms in that mass, yet it appears that in the process of ordering the scattering is increased,

since the main lattice lines remain constant and the superlattice lines are produced.

The solution of this problem is connected with the background of the x-ray photographs. Even if photographs are taken with purely monochromatic radiation (most x-ray photographs are taken with a great deal of white radiation as well), a certain amount of intensity is scattered at other than the Bragg angles, and this has been shown to be due to the displacements of the atoms from the lattice sites. Some of this displacement is a temperature effect,[53] since, to a pulse of x-rays, the atoms appear to be stationary, but some of it is also the actual physical displacement caused by the differences in sizes of the atoms.[11] When ordering takes place, this latter displacement tends to disappear, and thus the background scattering decreases. This decrease should account for the intensity scattered in the superlattice lines.

This appears to be supported in practice. As explained later, ordering in the alloy $AuCu_3$ is manifested by the appearance of superlattice lines that are broad at first and become sharper as the alloy is annealed.[54, 55] As far as can be ascertained, the intensities of the lines have a constant value; they are produced, as it were, by a gathering together of the background of the x-ray photographs until, with perfect order, the lines are quite sharp and the background is due solely to the temperature motion.

Measurement of Long-range Order—The rules outlined in *Table I* enable us to detect ordering in alloys and to decide what type of superlattice is present. As we have seen, the structure factor for the odd reflections from the FeAl type of structure changes from zero to $f_A - f_B$ as order increases. Thus it should be possible, by measuring the intensities of the superlattice lines, to deduce the degree of order present. If, for example, the probability that the A atoms are on α-sites is 80 per cent, the effective value of f_A is $\frac{4}{5}f_A + \frac{1}{5}f_B$ and the effective value of f_B is $\frac{4}{5}f_B + \frac{1}{5}f_A$. Thus the value of the structure factor for the superlattice reflections is:

$$(\tfrac{4}{5}f_A + \tfrac{1}{5}f_B) - (\tfrac{4}{5}f_B + \tfrac{1}{5}f_A) = \tfrac{3}{5}f_A - \tfrac{3}{5}f_B$$

This is only 3/5 of the value for complete order, and therefore the intensities, which are proportional to the square of the structure factor, are reduced to 9/25 of the value they would have for complete order. Thus we see that the intensities of the superlattice lines are very sensitive to changes in the degree of order.

There is, however, an experimental difficulty in this type of work that can lead to considerable errors. This difficulty is important in most kinds of x-ray investigation, and particularly for the simple structures that occur in metals and alloys. The effect is known as extinction, [56, 57] and is due to interference between the undiffracted rays and those reflected twice by the same sets of planes. From *Figure 21* it can be seen that any rays that are reflected from a set of lattice planes must be reflected from the other side of the planes into the direction of the undiffracted rays. It so happens that the twice reflected rays are 180° out of phase with the undiffracted rays, and so the undiffracted beam is weakened. This weakening takes place, however, only when the beam is being reflected, and is a function of the intensity of reflection. Thus arises the difficulty of measuring a quantity which can only be derived after the evaluation of a factor depending upon the quantity to be measured.

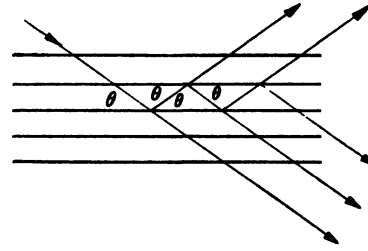

Figure 21 Diagram showing how X-rays are multiply reflected from a set of lattice planes

In general the effect is small, as most x-ray reflections are weak, and the twice reflected beams are of negligible intensity compared with the undiffracted beam. This is certainly true for superlattice reflections, which, as we have seen, have an amplitude that is dependent upon the difference between the scattering factors of two atoms. But it does not apply to the main lattice reflections, particularly those with low indices, for which the scattering factors of the atoms are large. In the cubic structures considered the atoms all lie in the lattice planes and so scatter exactly in phase. Thus considerable reduction of the intensities of the main lattice lines by extinction[58] might be expected. This effect militates against the accurate measurement of the degree of order in a crystal, and tends always to make the degree of order appear too high.

Another difficulty in measuring the degree of order in alloys occurs when the elements are nearly equal in atomic number so that the difference between their scattering factors is extremely small. For copper and zinc, for example, the atomic numbers are 29 and 30, so that the ratio of the difference of their scattering factors to their sum is approximately 1/60. Since the intensity of an x-ray reflection is proportional to the square of the structure factor, the intensities of the

superlattice lines are only about 1/3600 of the intensities of the main lattice lines and x-ray film cannot record such a range of intensities. The copper-zinc system is an extremely important one, and for a long time the existence of a superlattice at the composition CuZn was only inferred from thermal measurements. The method of observation of the superlattice lines will be described later.

The above reasoning would suggest that superlattice lines should be stronger when the two elements concerned differ greatly in atomic number. This is so only when we consider substitutional solid solutions. For interstitial solid solutions the opposite is true: the superlattice lines show more clearly the heavier the solute atom. As has already been pointed out, the only atoms that can form interstitial solid solutions are the small ones, and these are also the lightest. If the atom, for instance hydrogen, has negligible scattering power, then the x-ray diffraction pattern is not affected by its presence, and so the superlattice cannot be detected. If the atom is rather heavier, then superlattice lines may be detectable.

These facts can be illustrated by considering an example such as Fe_4N.[12] This has iron atoms in the face-centred cubic positions, (0,0,0), $(0,\frac{1}{2},\frac{1}{2})$, $(\frac{1}{2},0,\frac{1}{2})$ and $(\frac{1}{2},\frac{1}{2},0)$, and has the nitrogen atom at $(\frac{1}{2},\frac{1}{2},\frac{1}{2})$. The structure factor formula is thus:

$$f_{Fe}[1 + \cos \pi(k + l) + \cos \pi(k + h) + \cos \pi (h + k)] + f_N \cos \pi (h + k + l)$$

If h, k and l are all even this reduces to $4f_{Fe} + f_N$; thus these main lattice lines are slightly enhanced by the presence of the nitrogen atoms. If h, k and l are all odd, the expression reduces to $4f_{Fe} - f_N$. Thus these main lattice lines are slightly decreased in intensity. The superlattice lines, those with mixed indices, have structure factors of magnitude f_N and are thus very weak indeed. If the scattering factors are assumed to be proportional to the atomic numbers, then the intensities of the main even lines *e.g.* (200), of the main odd lines *e.g.* (111), and of the superlattice lines *e.g.* (100), are in the ratios:

$$(104 + 7)^2 : (104 - 7)^2 : 7^2$$

i.e. 1·23 : 0·94 : 0·005

Taking the range of visibility as 1 : 0·002, it will be seen that the superlattice lines should be only just detectable.

Nevertheless much more direct proof is possible. While the effect of the nitrogen on the superlattice lines is small, its effect on the intensities

of the main lattice lines is considerable. The ratio 1·23 : 0·94 can be quite satisfactorily established photometrically, although it is not obvious to the eye since several other factors have to be allowed for. Thus to establish the positions of the interstitial atoms the evidence from the main lattice lines is of considerable value and can be used, as will be described later, even when the superlattice lines cannot be seen at all.

Measurement of Short-range Order—Short-range order is a more difficult problem to deal with, and only recently has really effective work been done on its measurement, particularly in the alloy $AuCu_3$. The degree of long-range order may be zero in a crystal that contains a considerable degree of short-range order, but that does not mean that the superlattice reflections will be of zero intensity. This can be seen by imagining each perfectly ordered region to be a domain separated physically from the other regions, thus producing a set of small perfect crystals, each of which would give its own diffraction pattern of main lines and superlattice lines. The composite pattern may therefore be expected to have the same appearance as for a group of crystals with long-range order only.

Another effect obtrudes itself, however, if the domains become small: the x-ray reflections become broadened.[59–62] The word small is used in a relative sense, almost all crystals being small by ordinary standards. But x-ray wavelengths are very small indeed, and by x-ray standards almost all crystals are very large. Only when they come down to the dimensions of a few hundred x-ray wavelengths can they really be considered small.

The broadening is an optical effect that occurs when the number of scattering elements in a diffraction grating becomes small. A single element, if small enough, gives no variations in its diffraction pattern. Two neighbouring elements, however, give fringes in which the intensity alternates sinusoidally between maximum and zero. The addition of further elements produces sharper maxima and finally the ordinary sharp lines that are observed with good diffraction gratings and perfect crystals.

The sharpness, then, is a measure of the size of the crystals producing the reflections. If the reflections are as sharp as can be expected with the apparatus used, it may be deduced that the crystals are at least 10^{-5} cm in size. When appreciable broadening occurs, which may be

represented by β, then the crystal size t can be measured[62] by the relation $\beta = \lambda/t \cos \theta$. This effect, however, is not observed for all the reflections from a crystal with short-range order. The crystal is not separated physically into its separate domains, and, as far as the main lattice lines are concerned, the crystal is not separated into domains at all, since these reflections are unaffected by interchange of the two types of atom.

Thus we have the rather remarkable effect that some of the lines, the main lattice lines, remain sharp, while the other lines, the superlattice lines, vary in breadth. The variation can be extremely large, and when the domains are merely a few unit cells across only the reflections of lowest angle *i.e.* the strongest, can be observed at all. These may be so broad that they are detectable only with very careful work, and it is for this reason that short-range order has not been greatly studied in the past.

Effects of Change in Symmetry—When a cubic disordered structure changes into a cubic ordered structure no changes in the relative spacings of the various lines occur, because these spacings have fixed relationships to each other. There is a small overall change,[63, 64] representing the fact that the disordered collection of atoms is bound to occupy a larger volume than the ordered collection, but this can, to a first approximation, be neglected.

When the symmetry changes, however, a new variable is introduced, since the ratio of two axes (as in AuCu) may change with the degree of order, and this, as we have seen in *Figure 20*, may produce quite appreciable changes. For a cubic structure the spacings of planes such as (200), (020) and (002) are necessarily equal, but when the symmetry alters this is not so: we have seen that AuCu becomes tetragonal, and with the c axis smaller than a and b, which remain equal. Thus while the spacings (200) and (020) are equal and so produce a single line on an x-ray photograph, the spacing (002) is smaller and so produces a reflection at a slightly higher angle. Thus we find the original cubic line split into two components, the one at higher angle having half the intensity of the other. For other sets of indices different relations exist; for example the line (420) will have three components when the structure becomes tetragonal, 420 + 240, 402 + 042, and 204 + 024.

Since the axial ratio is presumably a function of the degree of order, the separation of the components with related indices can be taken as

a measure of the degree of order.[45] It provides a sensitive method of following order-disorder changes, since it depends upon the measurement of positions of lines, which can be done accurately, rather than on the measurement of the intensities of weak lines or on the measurement of small differences in the intensities of strong lines. If one accepts the theory of WILSON[65] it can also provide an absolute measure of the degree of order, but no practical use seems to have been made of this theory so far.

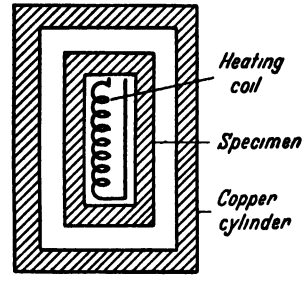

Figure 22 Diagrammatic representation of Sykes and Jones' specific heat apparatus

Thermal Measurements—Although x-ray measurements provide the only direct way of establishing the existence of an ordered structure, they are not particularly valuable in providing quantitative measurements against which the theory may be tested. When the existence of an ordered structure has been established, thermal methods can be brought into use, and these methods have been much more successful in providing the quantitative measurements required.

The quantity that is measured is essentially the change in internal energy which occurs when the atoms rearrange themselves, although it can be expressed in different ways. Suppose, for example, there is a sudden change in the degree of order at the critical temperature, such as theory (p 16) would demand for the alloy $AuCu_3$; this manifests itself as a latent heat. But if there is a change from complete order to zero order over a range in temperature, there is merely an anomalously large specific heat.

Ordinary methods for the measurement of specific heats are not satisfactory because the specific heat changes so rapidly that it has to be determined at fixed temperatures *i.e.* over ranges of temperature that are vanishingly small. The method that has been used for the investigation of CuZn and $AuCu_3$[66] is illustrated diagrammatically in *Figure 22*. A small cylinder of the alloy, closed at one end, contains a heating coil; its temperature can be measured by means of a thermocouple embedded in the metal and an external thermocouple measures the temperature of the surroundings. The whole is placed in a furnace the temperature of which can be gradually raised.

As the temperature of the furnace increases, the temperature of the

alloy cylinder will lag behind, and in order that the two thermocouples should indicate the same temperature heat must be supplied to the cylinder. The amount of electrical energy necessary to ensure this can be controlled manually, and the rate of provision of energy can thus be measured as the temperature of the furnace rises. Some degree of skill is needed to keep the two temperatures equal, or rather to correct the small differences of temperature that inevitably arise, but the method is particularly useful as no cooling or heating correction is required since the specimen and the furnace are always effectively at the same temperature.

For a material in which there is no change of order the specific heat will show no abnormal value. But if disorder starts some energy will be absorbed in the change and this has to be supplied by the heating coil. Thus the rate of supply of heat has to be increased and reaches a maximum at the critical temperature when it falls suddenly to more normal values. This stage of the proceedings requires a certain amount of skill. If calibrated instruments are used the apparatus is capable of considerable accuracy. Unfortunately it cannot be used with falling temperature, but in spite of this defect it has provided very valuable evidence.

The same apparatus can be used to determine the total energy change involved in taking the alloy from a certain state of order up to the disordered state, or, at least, up to the state of order that exists above the critical temperature. Of course, this information could be obtained by integration of the specific heat data, but the following experiment, described by SYKES and JONES,[66] provides a more direct approach. The alloy is initially at a temperature T_1 in the copper block, while the temperature of the furnace is raised to just above the critical temperature. The current through the inner coil is controlled (by hand) so that the temperature of the specimen is always within 0·1°C of that of the copper block. This current also passes through a copper voltameter, and the total energy is thus given directly by the amount of copper deposited.

Resistance Measurements—Electrical resistance is greatly dependent upon degree of order in an alloy, but nevertheless it is not a particularly useful property for testing theory in that the dependence of resistivity on degree of order has not yet been theoretically derived. Yet values of the resistivity of an alloy with various degrees of order can provide

important evidence on some details of the internal structure, as will be shown later.

The sensitivity of the dependence of resistance upon ordering is an expression of the effect of imperfections on this property. Pure metals are the best conductors and even slight impurity can produce a large change. The theoretical explanation of this is that conduction is due to the passage of the outer electrons of the constituent atoms from one atom to another. The electronic system is common to all the atoms,[67] and this may be expressed by stating that a crystal of a metal is a single molecule with a complicated electronic system. Most of the electrons are moving with high velocities, but on the whole there is no resultant motion in any one direction, as only when a potential difference is applied do more electrons move one way and so provide a current.

Theory also suggests that a perfect crystal should be a perfect conductor,[68] resistance being due to the lack of regularity of the paths available to the electrons. Such lack of regularity is produced by the random thermal vibrations of the atoms, and therefore the resistance of a metal increases with temperature. Lack of regularity is also provided in a much more marked degree by foreign atoms in solution, and this explains both the great increase of resistivity with impurity content and the lesser dependence of the resistivity of alloys upon temperature.

The effect which ordering should produce on resistivity can thus be seen. With a disordered alloy there are considerable irregularities as shown in *Figure 2*, and the resistance would be expected to be high. When ordering is complete the regularities disappear and low resistance would be expected. These results are found in practice, as will be seen later. The effect of short-range order is to produce a residual increase in resistance which may be expressed as reflection of the conduction electrons from the boundaries of the domains.[68]

RESULTS OF EXPERIMENT

X-ray Diffraction, Long-range Order—The most exhaustive work so far attempted is that of BRADLEY and JAY[69] on the alloys of iron and aluminium with aluminium contents ranging from 0 per cent to 50 per cent. This range of alloys contains two superlattice types, Fe_3Al and FeAl, and Bradley and Jay set themselves the problem of finding out how the atoms redistributed themselves as more aluminium was added.

They took x-ray powder photographs of alloys of various compositions and these photographs were then photometered in order to find the distribution of intensities between the superlattice lines and the main lattice lines (*Figure 20*). It will be appreciated that, since the presence of lines (111) and (200) indicates the existence of the Fe_3Al type of superlattice, and the absence of the former line indicates the FeAl type of superlattice, measurement of the relative intensities of these lines should indicate the proportions of atoms in the various positions.

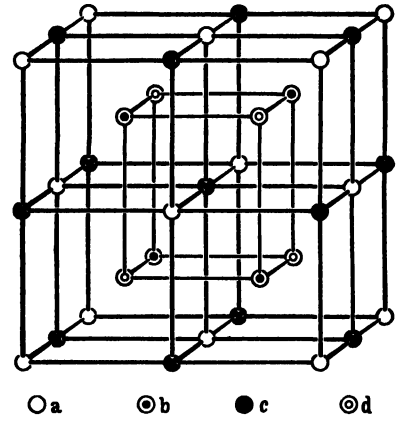

Figure 23 Four different positions in Fe_3Al

Bradley and Jay expressed their results with reference to four different types of positions, as shown in *Figure 23*. By comparison with *Figure 7* it will be seen the Fe_3Al structure can be represented by putting iron atoms at positions a, c and d, and aluminium atoms at b, while the FeAl structure can be represented by putting iron atoms at a and c, and aluminium atoms at b and d. For other structures only certain proportions of one sort of atom are at any given set of positions, and thus a structure at a given composition can be represented by plotting four points representing the percentage of aluminium atoms in a, b, c or d positions.

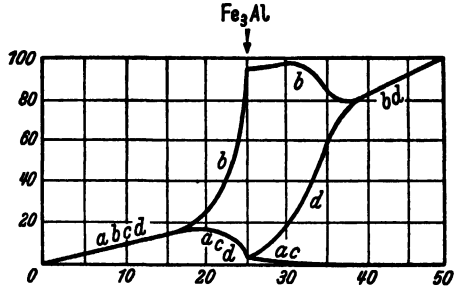

Figure 24a. Distribution of aluminium atoms on the four types of sites in annealed Fe–Al *alloys*

The results are represented in *Figures 24a* and b. *Figure 24a* refers to annealed alloys, and for small concentrations of aluminium the aluminium atoms

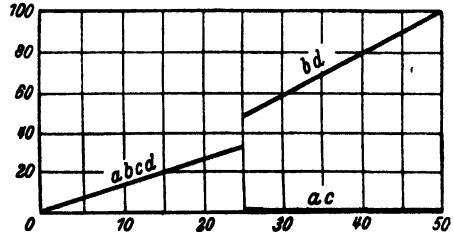

Figure 24b. Distribution of aluminium atoms on the four types of sites in quenched Fe–Al *alloys*

are distributed at random on the various sites. Thus the curves for the four sets of positions are all identical, consisting of a straight line of unit slope. Above about 18 per cent, however, ordering begins: the aluminium atoms cease to occupy the positions a, c and d and as far as possible occupy the positions b, until the perfect Fe_3Al structure is produced with 25 per cent of aluminium atoms. (It will be remembered that these results may not have absolute significance, since they depend greatly on extinction which was not allowed for.) Up to about 30 per cent, the b positions remain practically fully occupied, and the extra aluminium atoms all go into the d positions. Above 30 per cent the b and d positions tend to equalize their aluminium content, until finally they are both completely occupied by aluminium atoms.

The results for alloys quenched from about 600°C (*Figure 24*b) are completely different. The straight line up to 25 per cent aluminium indicates that no superlattice at all is formed in this range of composition. Ordering then takes place sharply; half of the b positions and half of the d positions, both at random, are occupied by aluminium atoms, and the other positions contain no aluminium atoms at all. As the concentration of aluminium becomes greater, the proportions of aluminium atoms in the b and d positions increase together until they are both completely occupied to give the FeAl structure.

These results, particularly those for the annealed alloys, are important because they give an indication of the principles upon which ordering takes place. BRAGG[70] has pointed out that the ordering so conducts itself that aluminium atoms tend to avoid each other. At small concentrations the aluminium atoms are so far apart that this effect is of no importance, but as the concentration increases the aluminium atoms tend to avoid being in neighbouring unit cells: they can do this with 25 per cent concentration only by adopting the Fe_3Al structure. Above this concentration the rule cannot be obeyed, since there are too many aluminium atoms, but the surplus atoms then tend to avoid being nearest neighbours. Above about 38 per cent this tendency is predominant until at 50 per cent even this condition is completely fulfilled and practically no more aluminium atoms can be tolerated. With higher concentrations much more complicated atomic arrangements result.

The superlattice lines of Fe_3Al are easily detectable because of the large difference between the scattering factors of iron and aluminium.

As was pointed out on p 25, however, the superlattice lines of copper-zinc alloy are extremely faint because of the similarity of the two atoms, and special methods had to be employed to detect them. These methods take into account the slight dependence of scattering factors on the wavelength of the radiation which is being diffracted;[71] if the wavelength is near to that which the element would itself emit as target of an x-ray tube, then the scattering factor is reduced. The curves connecting the depression of the scattering factors of zinc and copper with wavelength are shown in *Figure 25*, the curve for zinc being displaced upwards by one unit to represent its excess scattering factor with respect to that of copper. It will be seen that the scattering factors differ most when the wavelength is about 1·39 Å, and the nearest characteristic $K\alpha$ wavelength to this is that of zinc itself, 1·44 Å. JONES and SYKES[72] therefore took a powder photograph of copper-zinc powder with Zn$K\alpha$ radiation and the superlattice lines were quite definitely detectable.

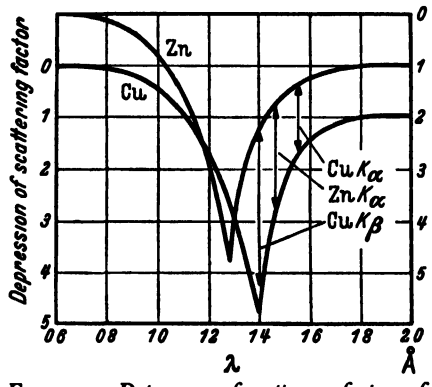

Figure 25. Depression of scattering factors of Cu(*left*) *and* Zn(*right*) *for wavelengths in the neighbourhood of the K absorption edges The diagram shows that* Zn$K\alpha$ *radiation is the best* α *radiation for emphasizing the difference between* Cu *and* Zn, *but that* Cu$K\beta$ *would be even better*

The method was first used by BRADLEY and RODGERS[16] to differentiate between the manganese and copper atoms in the Heusler alloy Cu_2MnAl. This alloy was known to have a superlattice of the Fe_3Al type, but it was not known whether the copper and manganese atoms ordered themselves as well. By the use of Fe$K\alpha$ radiation, which depresses the scattering factor of manganese more than that of copper, Bradley and Rodgers were able to show that these two atoms were also ordered upon the sites available when the aluminium atoms had been placed. The same methods have been used by HOWARTH[73] and LEECH and SYKES[74] in attempts to detect superlattices in the alloys Fe_3Ni and $FeNi_3$, and by ELLIS and GREINER[75] to detect a superlattice in the alloy FeCo.

As was explained on p 6, interstitial superlattices are nearly always difficult to detect because of the small scattering factors of the interstitial

atoms. An example of the use of accurate measurement of the intensities of the main lines is given by the work of JACK[12] on the alloy Fe_4N; an outline of this work was given on p 26.

In this alloy the superlattice lines were just detectable. A more extreme instance, for which the superlattice could be detected only by extremely accurate measurement of the intensities of the main lines, is that of austenite, face-centred cubic iron with carbon in solution. For many years there had been some controversy about the positions of the carbon atoms, there being several interstices into which it was possible for them to go, but PETCH[76] was able to show that the largest ones were chosen. These interstices are the same as those in which the nitrogen atoms are situated in Fe_4N, but the experimental difficulties were greater in the work on austenite because only a small proportion of the interstices are occupied at the saturation solubility of carbon in austenite.

The difficulty of having to observe weak diffracted beams can be avoided by means of the newly developed subject of neutron diffraction.[77, 78] The atomic neutron-scattering factors, or scattering cross sections as they are called, vary from atom to atom quite differently from x-ray scattering factors; they are not related to atomic number, heavy hydrogen, for example, being by far the best scatterer of neutrons. Thus it is extremely probable that neighbouring elements in the periodic table have quite different scattering factors, and so the superlattice reflections from alloys such as $FeNi_3$ should be easily detectable.[79–82] In a similar way it may be possible to establish the positions of the light atoms in interstitial structures by neutron diffraction.

Because of the difficulties, both theoretical and practical, in measuring long-range order accurately by means of x-ray intensities, no completely satisfactory work has yet been reported on the variation of order with temperature or with heat treatment for a particular alloy. WILCHINSKY[83] has attempted to measure the degree of order in $AuCu_3$ as a function of temperature, and reports very little change up to the critical temperature when the long-range order parameter dropped from 0·79 to zero. Because of the extinction difficulty, however, these results may be only qualitatively correct. When symmetry changes are also involved, as we have seen on p 28, the changes in position of a given line can be used to follow changes in order. In the AuCu alloy, for example, the line 311 from the disordered (cubic) structure should

split into lines 311 and 113 when the transformation to the ordered (tetragonal) structure takes place, and this change can be readily observed. Borelius reports[45] such an examination of the changes in the AuCu alloy heated for different lengths of time at 290°C and 395°C. He makes use of the changes of position of the line 311, but does not mention the effect of the splitting of this reflection.

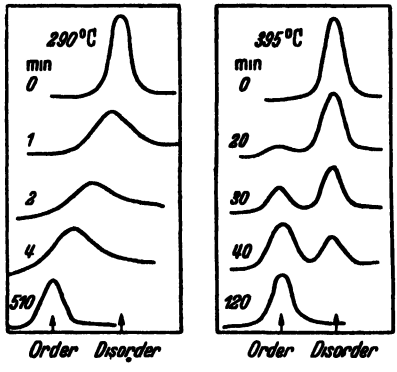

Figure 26. Microphotometer curves showing the changes in the powder photographs of AuCu *with various times of annealing at* 290°*C and* 395°*C*

There are two possible ways in which we can envisage the occurrence of the transformation: first, the disordered structure may gradually disappear, being replaced by the ordered structure; secondly, the axial ratio may change gradually from unity to the equilibrium value. The former effect would be evidenced by a gradual decrease of the intensities of the cubic lines, and a gradual increase of the intensities of the tetragonal lines, no changes in position being observed; the latter would be evidenced by a gradual shift of the cubic lines to their positions for the tetragonal structure.

Borelius has found that both effects occur: as shown in *Figure 26*, at the lower temperature the change is a gradual one through intermediate states from disorder to order; at the higher temperature the change is discontinuous. Borelius claims that this proves the existence at the higher temperature of a potential barrier between the ordered and disordered states, this barrier disappearing at the lower temperature.

The change in symmetry in the alloy AuCu requires that some consideration be given to the overall changes in the structure. Although the axial ratio changes by about one per cent, the bulk material itself should not show corresponding variations, and this can only happen if the changes balance over the whole of any one crystal. A more explicit statement is as follows: in a tetragonal crystal one of the axes is different from the other two, but this difference does not exist in the disordered cubic alloy; therefore, if order begins at different points in a crystal, it is to be expected that the particular axis that is to be the tetragonal

axis is chosen by chance, and that over the whole crystal they will be distributed at random over the three possible directions.

This is a matter of some importance. The transformation will presumably take place with as small atomic displacements as possible, and, as shown in two dimensions in *Figure 27*, if the domains of similar order are at all large the atomic displacements near the boundaries must also be large. A great deal of strain must occur at the boundaries,

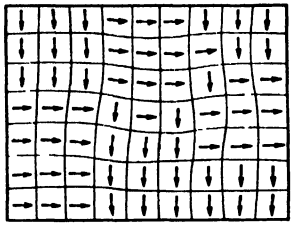

Figure 27. Distortion of lattice due to occurrence of tetragonal anti-phase domains. The arrows show the direction of the shorter axis, although some of these directions are rather doubtful

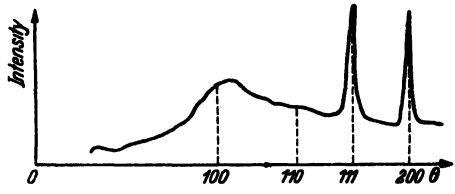

Figure 28. Photometer curves of powder photograph of quenched $AuCu_3$, *showing broad maxima indicative of short-range order*

and it is possible that this strain can account for some of the remarkable magnetic properties of alloys with this structure, to be reported in a later section (p 43).

X-ray Diffraction, Short-range Order—The measurement of short-range order, involving as it does the detection of diffuse lines which may also not be very strong, has not attracted as many investigators as the measurement of long-range order; fairly elaborate apparatus is required if these lines are not to be lost by submergence in the background that always exists on ordinary powder photographs.

BETTERIDGE[84] has described some experimental work on $AuCu_3$ in which the degree of short-range order, calculated theoretically by PEIERLS,[26] is related to changes in lattice parameter. A direct determination of the degree of short-range order would, however, be more desirable. GUINIER[85] has tackled the problem by using a specially designed camera with x-rays reflected from a crystal of quartz; the x-rays should then contain only a single wavelength (or, more precisely, a narrow band of wavelengths). With this apparatus ordinary materials give almost zero scattering in between the x-ray reflections, and so any extraordinary diffraction effects that may occur are more easily

detected. Guinier has in this way been able to demonstrate the existence of short-range order in the alloy AgAu, chosen because the almost exact equality of the atomic diameters should result in the absence of lattice distortion. Powder photographs show a well defined peak at the position where the 100 reflection would occur.

The alloy AgAu does not, however, form a superlattice. Much more interesting effects are shown by the alloy $AuCu_3$, in which the effects of both long-range and short-range order exist, and this alloy has been studied by Wilchinsky and also by Guinier. Both find, in an alloy quenched from above the critical temperature, maxima in the diffracted intensity at the positions of the reflections 100 and 110, as shown in *Figure 28*, which is a representation of Guinier's results.

Investigations such as these can be followed up by observing changes of the diffraction pattern when the specimen is annealed below the critical temperature. It was seen on p 27 how the existence of short-range order leads to broadening of the superlattice lines, and that this broadening can be related to the size of the domains over which the order is perfect. Thus, as the alloy is annealed, the lines gradually become sharper until they are as sharp as the main lattice lines. This effect is beautifully illustrated by the set of photographs,[55] due to Jones and Sykes, shown in *Figure 29*. These workers attempted to relate the breadths to the sizes of the domains by the use of the relation for small crystals, but different results were obtained from different reflections; in particular 100 gave almost twice the size that was given by 110. It appeared, then, that this simple theory was not adequate to account for the observed effects. WILSON,[86, 87] acting on certain suggestions of Jones and Sykes, tried to treat the problem on more general optical considerations, and showed that extremely good agreement (within 10 per cent, which is perhaps as much as can be expected for this type of work) can be obtained on the assumption that where one type of domain changes to another the change is favoured if it does not bring gold atoms into contact.

This result suggests another, and extremely powerful, method of tackling the problem experimentally. Wilson's theoretical treatment is based upon the single crystal, and has to be modified for adaptation to the interpretation of powder photographs. It would therefore seem more satisfactory to obtain the data from a single crystal and to test these data against theory. Part of the mathematical treatment is thus

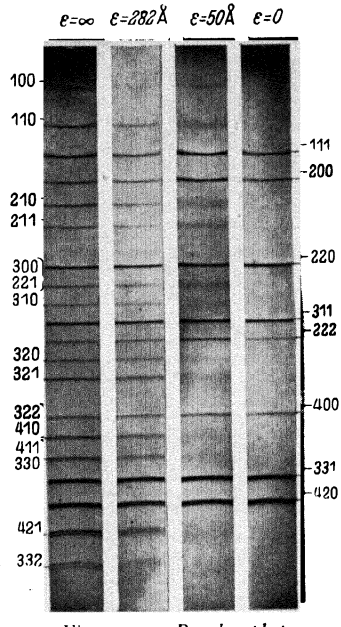

Figure 29. Powder photographs of $AuCu_3$ *alloy in different stages of transformation, showing increased broadening of the superlattice lines as the anti-phase domains decrease in size*

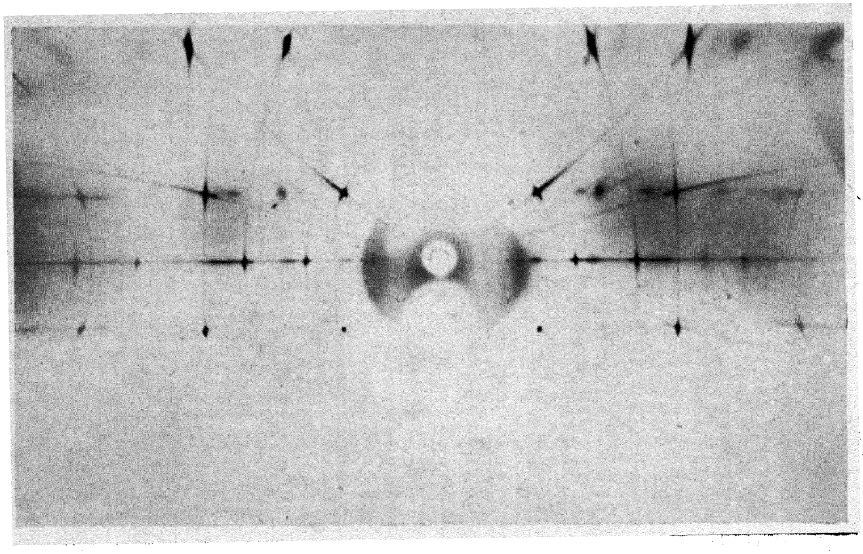

Figure 30. Rotation photograph of $AuCu_3$ *single crystal, showing broadened superlattice spots. (The main spots are very much overexposed and this has emphasized the streaks due to the white radiation and those due to the disoriented part of the alloy)*

dispensed with and, what is more important, much more detail should be given in that the diffraction pattern can be explored in three dimensions rather than the one dimension of a powder photograph.

Several investigators have taken up the problem. STRIJK and MACGILLAVRY[88] used a crystal that was elongated parallel to the (110) direction, and examined only the x-ray reflections in the plane perpendicular to this; consequently they did not gain the maximum information possible. GUINIER and GRIFFOUL[89-91] and EDMUNDS, HINDE and LIPSON[92] have used smaller crystals and have made the necessary three dimensional survey. Their results agree qualitatively well with WILSON's theory,[93] but no quantitative results have yet been reported. COWLEY[94] has used a crystal above the critical temperature and has examined the diffraction pattern due to short-range order and again the results of this investigation are awaited with interest.

Another advantage results from the use of single crystals: the superlattice reflections are much more clearly seen than when they are spread out into arcs on a powder photograph. Thus the order-disorder change can be followed down to quite small size of domains, probably as far as the powder method can cope with when crystal reflected radiation is used. The single-crystal rotation photograph shown in *Figure 30* gives an idea of the detail that can be seen.

By observing the changes in the shapes and sizes of the superlattice reflections as the alloy is subjected to different heat treatments it should be possible to gain information about the mechanism of ordering. Particularly interesting facts may emerge from the comparison of these results with those of Warren obtained from crystals above the critical temperature.

The single-crystal diffraction pattern contains all the evidence concerning the structural details and hence it should be possible to determine the degrees of long-range and short-range order. The difficulties in the former determination have already been stated (p 25), but for short-range order the difficulties are theoretical rather than practical. A treatment has been described by MACGILLAVRY and STRIJK;[95] it is based on the PATTERSON[96] treatment of the more usual x-ray diffraction patterns and is too complicated to describe here.

Thermal Measurements—Sykes and Jones have used thermal methods extensively in a study of the alloys $AuCu_3$ and CuZn. *Figure 31* shows the results of measurement of the specific heat of $AuCu_3$ by means of

the apparatus described on p 29, the alloy having been cooled from 450°C at 30°C per hour to put it into a state of maximum order. Up to 200°C the specific heat is equal to that calculated by means of the Dulong-Petit law, that is, the specific heat is equal to the weighted mean of the specific heats of the separate elements; for comparison, the curve for this normal specific heat is also shown in *Figure 31*. It may thus be presumed that below 200°C no transformation is taking place. Above this temperature, however, the specific heat shows an abnormal increase, reaching a maximum value of 2 cal/gm/°C, twice that of water. This value is so large that it may be assumed that, if the experiment had been conducted infinitely slowly, the specific heat would have been infinite—that is, that there would have been a latent heat, as required by theory (p 16). Above the critical temperature the specific heat drops abruptly, but not quite to the Dulong-Petit value, and this can be explained by the persistence of a certain degree of short-range order, which disappears only slowly as the temperature is increased. For the copper-zinc alloy (β-brass) a similar curve of specific heat was derived, except that the maximum value was only 0·25 cal/gm/°C, and this therefore does not indicate any latent heat, which again is in accordance with theory.

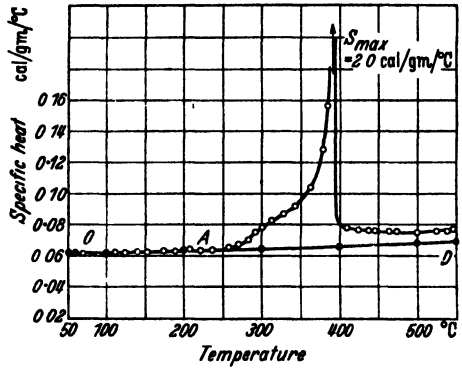

Figure 31. Specific heat of $AuCu_3$ *as a function of temperature, after the specimen had been cooled at 30°C per hour*

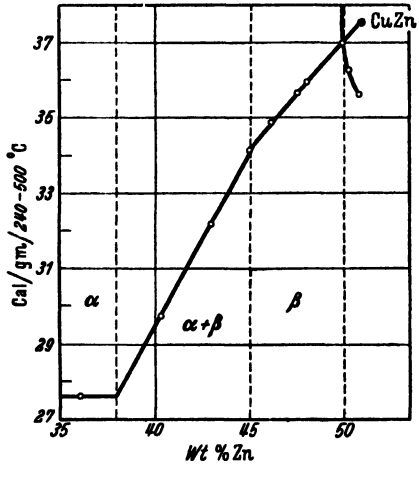

Figure 32 Energy consumed in transforming a series of Cu–Zn *alloys from 240°C to 500°C*

The work of SYKES and WILKINSON[97] on CuZn may be quoted as an

example of the derivation of total heats of transformation. The results of their investigation of the total heat of transformation as a function of composition are shown in *Figure 32*. It will be noted that the total heat of transformation, in this case between the temperatures of 240°C and 500°C, increases as the ideal composition is approached, as would be expected since at the ideal composition, CuZn, all the atoms must be exactly ordered, whereas at any other composition some of the atoms must be in the wrong places. As so often happens in alloy phase diagrams, the ideal composition is not included in the range of homogeneity of the phase,[98] and therefore the data for this composition have to be inferred by extrapolation, as shown in *Figure 32*. The observed range of variation between the extremes of the β-phase field is in good agreement with the calculations of EASTHOPE.[99]

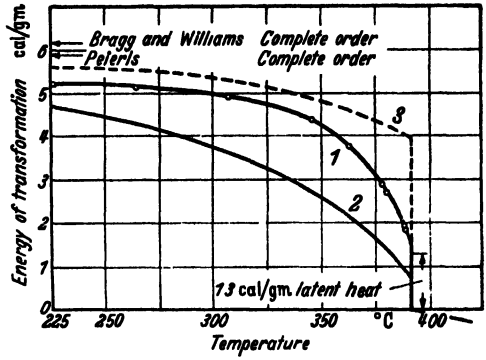

Figure 33. The energy of transformation of $AuCu_3$ *as a function of temperature: 1 experimental results 2 prediction of the Bragg-Williams theory 3 prediction of Peierl's theory*

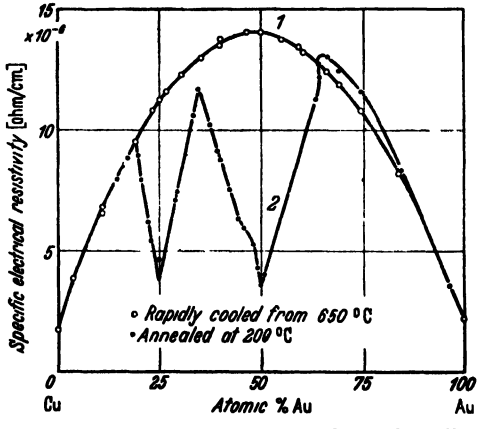

Figure 34. Electrical resistivity of Au–Cu *alloys 1 rapidly cooled 2 annealed at* 200°C

While these results show qualitative agreement with theory which is surprisingly good in view of the simple underlying assumptions, the agreement is by no means exact. This is shown in *Figure 33*, where the experimental results are compared with the predictions of the theories of BETHE[22] and of BRAGG and WILLIAMS.[19–21] By a slight modification of Bethe's theory Chang has deduced[31] a curve in rather better agreement with experiment than either of those shown in *Figure 33*.

Resistance Measurements—Since electrical resistivity depends greatly upon degree of order, measurements of this property are particularly suitable for showing the presence of order in alloy systems. This is shown very well by the work of JOHANNSON and LINDE[100] on copper-gold alloys: their measurements of the resistivity of annealed and quenched alloys are shown in *Figure 34* as functions of composition, and the curves show, as clearly as any physical measurements could be expected to show, that there are singularities at the compositions $AuCu_3$ and AuCu; they also indicate that there is no singularity at the composition Au_3Cu.

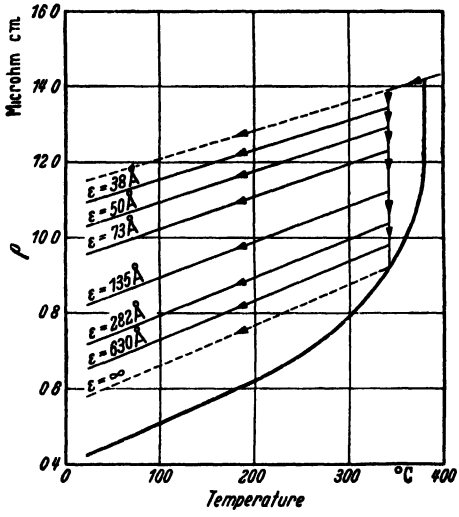

Figure 35. Electrical resistivity of $AuCu_3$ *as a function of temperature for different sizes of anti-phase domains*

A detailed examination[55] of the resistivity of the alloy $AuCu_3$ has been carried out by Jones and Sykes. By quenching the alloy in different states of order they were able to measure the resistivity as a function of temperature for different degrees of short-range order; their results, however, shown in *Figure 35*, are expressed in terms of domain size, ϵ, derived from the breadths of the corresponding x-ray diffraction lines.

Expressed in this form, the results show that the resistivity is linearly related to the inverse of ϵ; this can be interpreted by assuming that the resistance is proportional to the area of domain boundaries per unit volume, these boundaries acting as partial 'reflectors' of the conduction electrons. From the variation of lattice parameter with ϵ, Jones and Sykes also deduce that the boundaries are about one unit cell thick. Nevertheless it is possible, as will be shown later, that the idea of domains and boundaries is too precise to form an accurate picture of the structure, and they will have to be replaced ultimately by rather more vague conceptions of probability.

Magnetic Measurements—Magnetic measurements,[101–105] whether of diamagnetic or paramagnetic susceptibility, or of coercivity in

ferromagnetic alloys, fall into a different class from the phenomena so far described. The information they give does not clarify the ordering process itself, but tends rather to help in the elucidation of the nature of the magnetic properties themselves.

As an example, the study of the alloy FePt[105] may be quoted. This alloy is ferromagnetic, and with certain heat treatments can have a coercivity of about 1,500 oersted. This extremely high value suggested that a study of its structure, and its correlation with coercivity, would be worth while. The structure was found to be similar to that of AuCu, and no change was found with heat treatment; yet from this structure a reasonable explanation of the high coercivity could be adduced.

This explanation is as follows. It is presumed that at high temperatures the alloy is face-centred cubic, although this cannot be proved by quenching; the evidence lies in the fact that a coarse-grained specimen shows groupings of x-ray reflections such as 200 and 002 which can only be explained if the tetragonal crystals had developed from single cubic crystals. If this is so, there should be considerable strain at the junctions of these tetragonal crystals, as shown for two dimensions in *Figure 27*, and if the alloy is quenched rapidly from the cubic state it is possible that these strains do not have time to release themselves. Certain theories of ferromagnetism suggest that such strains are the principal requirement for high coercivity.

This theory agrees well with the experimental facts. Rapid cooling from high temperatures leads to the greatest values of the coercivity; annealing, which presumably would relieve the strains, leads to much lower values. The alloy[105] CoPt, which has the same structure, has been shown to be capable of still higher values of coercivity, and, moreover, its high-temperature cubic structure can be preserved by quenching. Unfortunately it has not been studied in anything like as much detail as the alloy FePt; the apparatus required for measuring such high coercivities has to be specially designed and requires supplies that are not generally available.

Mechanical Properties—The process of ordering does not, in itself, seem to affect the gross mechanical properties of an alloy. Thus, the alloy $AuCu_3$ remains ductile during the transformation from disorder to order. But if the transformation is accompanied by a change in symmetry, as in the alloy AuCu, the ductility may be greatly affected, presumably for reasons very similar to those that produce the high

magnetic coercivity mentioned previously; indeed, the connection between mechanical and magnetic hardness is extremely close.

This is best illustrated by the work of NOWACK[106] on the Brinell hardness of the alloy CuPt as a function of time of annealing at 500°C after quenching from the disordered state. It will be seen from *Figure 36* that the hardness increases rapidly to a maximum and then decreases very slowly indeed. The initial rise is probably caused by the strains resulting from the small region of local order, the gradual reduction later being an effect of the increase in size of these regions. Unfortunately a greater range of time was not studied. The decrease shown in *Figure 36* is barely greater than the experimental error, and the decrease would have been more convincing if more results had been obtained and if the time had been plotted logarithmically.

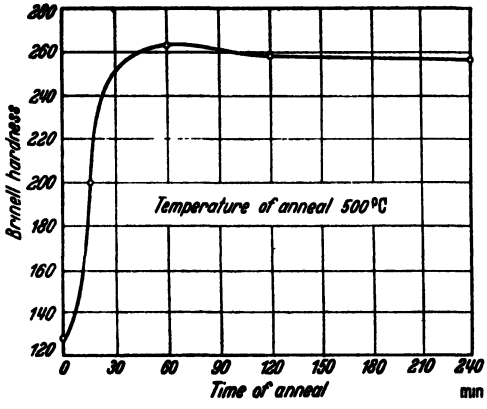

Figure 36. Age hardening curve for the alloy CuPt. *The alloy was rapidly cooled before annealing*

The opposite effect, that of mechanical deformation on ordering, has also been studied, and, as might have been expected, it is found that such deformation reduces the degree of order and may even eliminate order completely.[107] Since mechanical deformation must necessarily involve forces that are of the same order of magnitude as interatomic forces, it is not surprising that the ordering forces, which are usually much smaller, have to give way to them.

FUTURE LINES OF INVESTIGATION

Theory—It has been seen that, in general outline, the theory of the order-disorder transformation is reasonably complete, and, as compared with the theory of any other sort of transformation in the solid state, may almost be said to be perfectly satisfactory. It explains the general outlines of the process and gives reasonable agreement for the total heat of transformation. The more intimate details, such as the variation of specific heat with temperature, are not in such a satisfactory state,

and further theoretical treatment is still required. Such treatment will almost certainly be a refinement of one or other of the existing theories, and it is therefore unlikely that any revolutionary development will be forthcoming.

Kinetics of the Transformation—The theoreticians have so far chiefly aimed at accounting for the results found by experiment, and little

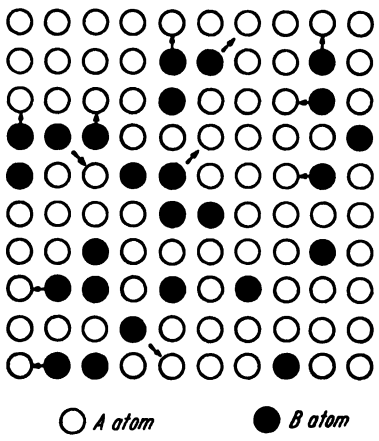

Figure 37. Random solid solution of 25% of B atoms in A. The arrows show directions in which B could interchange with A atoms in order to avoid being next to other B atoms It is assumed that each atom can interchange equally easily with each of the eight surrounding it

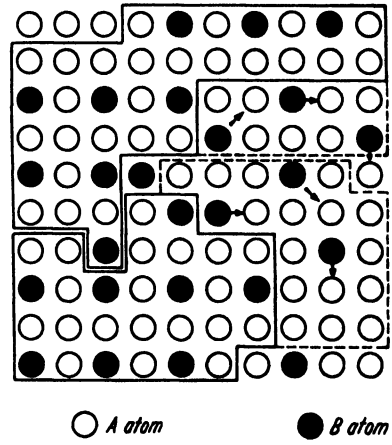

Figure 38. Structure resulting from the changes shown in Figure 37. Two anti-phase domains are shown, although the interchanges were not made in order to bring them into being. The arrows show interchanges that would further decrease the number of pairs of B atoms in contact and it will be observed that these interchanges result in increases of both anti-phase domains, as shown by the dotted lines

consideration seems to have been given to the problem of how the ordering takes place. It may be safely assumed that it is essentially a process of interchange of atoms on the various sites, but there are at least two ways in which this process can be imagined to produce a completely ordered structure.

It is more usual to assume that, when a disordered alloy is maintained rather below the critical temperature, ordering starts at specific points, and spreads outwards from these; each nucleus will thus produce a domain of similar order, and the sizes of these domains will depend upon the average distance of separation of the nuclei. In this way the structure described on p 9 is produced. Alternatively, however, we

may consider that the ordering process is completely local, starting at all points simultaneously.

It might seem that the first suggestion leads more naturally to the phenomenon of local order, but this is not necessarily true. In *Figure 37* a two dimensional disordered structure of composition A_3B is shown, and it will be noted that it contains many places where B atoms are in contact. Suppose now that the B atoms tend to avoid each other; often they cannot separate without adopting new positions where they are still in contact with the same number of B atoms, but on the whole some easement can be produced by means of the interchanges shown by the arrows. The resultant structure is shown in *Figure 38* and it will be seen that this does contain regions of similar order, although this concept of regions was not deliberately introduced.

This second suggestion has the advantage over the first that it allows a more natural explanation of the change from short-range to long-range order. On the nucleus theory, it is difficult to see how the domains increase with time of annealing, though it may be that the smaller domains are absorbed by the larger, and so an increase of the average size must always occur; but it is still difficult to see how this absorption can take place. The second suggestion however solves this problem naturally: the domains result from the avoidance of similar atoms, and as the most awkward knots of similar atoms resolve themselves by interchange, so should the domains increase in size.

It is possible that the single-crystal studies of $AuCu_3$, both above and below the critical temperature, will further elucidate these ideas. The shapes of the superlattice reflections, and the variations of these shapes with heat treatment, should give considerable information, but such experimental study will have to be accompanied by a thorough theoretical investigation of the diffraction effects to be expected in the various stages of ordering.

It is also to be hoped that alloys other than $AuCu_3$ will be found which can be studied in as much detail. This alloy is so versatile that it has attracted perhaps an unfair amount of attention, and some of the general principles deduced from its behaviour would be more firmly established if they could be supported by evidence from other alloys.

Nature of the Ordering Force—As explained previously, it is accepted that ordering can reduce the internal energy of an alloy, yet little thought has been given to the problem of the nature of the interatomic

forces that cause this ordering to take place. Nix and Shockley, in discussing this problem, state that 'we expect that accurate theories will be founded on the quantum-mechanical electronic theory of metals'.

This may well be so; indeed, if this theory is accepted as valid, and there are as yet no experimental data that cause us to doubt it, it must be so. Nevertheless, mathematical difficulties have prevented any general application of the theory to the problem of the order-disorder change, and it is natural that simpler concepts should also be considered. Simple concepts may not be precise, but science has grown by the grafting of complicated theories on to simple concepts, and it may well be that the same process will be useful here.

The lattice-strain theory of HUME-ROTHERY and POWELL[108] is based on this idea. It was pointed out on p 2 that the alloying of two elements must introduce strains in the lattice (*Figure 2*) and that these strains disappear when order is complete: Hume-Rothery and Powell suggest that the tendency to eliminate these strains provides the force that causes ordering. In other words, atoms that are too large are squeezed out of the wrong positions, and the structure will settle down only when all the atoms are in the correct positions, provided that the atoms have enough thermal energy to make the transitions possible.

This theory may seem inadequate, but as will be seen later it can account for almost all the experimental facts, including some that were not known when the theory was propounded. Before considering these facts, however, another general theory must be examined which has had considerable success in the explanation of the structures that occur in metals and alloys—the Brillouin zone theory (RAYNOR[67]).

This theory is applicable, of course, only to that part of the internal energy possessed by the free electrons in alloys, but its successes in accounting for structures and phase boundaries leads to the supposition that the energies of these electrons must form a considerable part of the total internal energy of an alloy. The theory is concerned with the interactions of the free electrons (which are envisaged as travelling waves) with the lattice of the crystal, and the results are expressed in terms of the effects of these interactions on the energies of the electrons. If the momenta of the electrons are plotted in a Cartesian coordinate system, then polyhedra, Brillouin zones, are outlined such that the energies of electrons whose momenta lie just within the surfaces are depressed below the classically expected values, and the energies of

those just outside are increased. The sequence of structures in many alloy systems is such as to keep as many electrons as possible within a zone, and to prevent their spilling over into the next zone.

The surfaces of the zones correspond with reflecting planes: these planes diffract the electron waves in the same way as they diffract

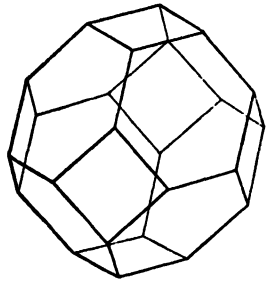

Figure 39. First Brillouin zone of the face-centred cubic structure

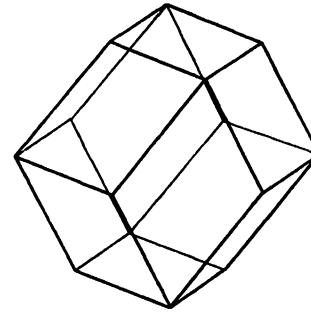

Figure 40. First Brillouin zone of the body-centred cubic structure

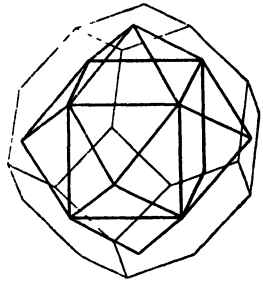

Figure 41. Formation of {100} Brillouin zone (thick lines) and {110} Brillouin zone (medium lines) within the {111} Brillouin zone (Figure 39) for $AuCu_3$

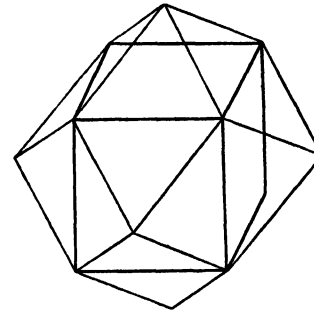

Figure 42. Formation of {100} Brillouin zone (thick lines) within the {110} Brillouin zone (Figure 40) for FeAl

x-rays. Thus for the face-centred cubic structure (*Figure 39*) the first Brillouin zone has faces {111} and {200} and for the body-centred cubic structure (*Figure 40*) it has faces {110}; these faces correspond to the lowest angle reflections from these structures (*Table 1*). But when ordering occurs, other Brillouin zones come into existence; for the $AuCu_3$ superlattice, the {100} faces and the {110} faces also come into being within what was the first Brillouin zone (*Figure 41*), and for the FeAl superlattice the {100} faces form a new Brillouin zone (*Figure 42*).

These zones must necessarily be of minor importance, since the diffraction of the electrons by the corresponding planes is much weaker than that by the planes which produce the main Brillouin zones. But then the ordering forces are expected to be much weaker than the forces which hold the crystal together. Thus the smallness of the effect cannot be held as evidence that it is of no importance.

Some brief calculations show that the superlattice Brillouin zones, as they may be called, are of about the right order of magnitude to produce some effect on the conduction electrons. The sizes must be such that the surface is close to the points representing the most energetic electrons; if these electrons are too far removed, their energies are not affected, and, if the electrons overlap into the next zone, the resultant increase of energy cancels out the earlier decrease. Now for the $AuCu_3$ structure, the superlattice Brillouin zone contains one electron per atom which is just the electron content of the alloy, since both gold and copper are monovalent. And for the Fe_3Al structure, the first superlattice Brillouin zone contains 0·5 electron per atom, which, it must be admitted, is rather less than the actual electron content of the alloy, 0·75 electron per atom; more important, perhaps, is the fact that the electron content of the alloy for which the superlattice is first noted (*Figure 24*) is almost exactly 0·5 electron per atom. When the electron content exceeds this value the electrons can overlap into the next zone, formed by the {100} faces only, and this contains 1·0 electron per atom. This zone would be the effective one for the rest of the alloys in this series up to FeAl.

It will be noted that the Brillouin-zone theory does not explain the observed facts for the $AuCu_3$ alloy and for the alloys of iron and aluminium as neatly as might have been hoped, and there are several reasons for thinking that it does not play a large part in explaining superlattice formation. For example, the complete filling of a Brillouin zone should lead to an increase of resistance, whereas we have seen that the formation of the superlattice in the alloy $AuCu_3$ is accompanied by a considerable fall in resistance (*Figures 34* and *35*). Again, one would not expect superlattice formation in alloys in which no superlattice Brillouin zone were formed, but it was seen that the alloy CuZn has a definite superlattice; the scattering factors of these two atoms are so nearly equal that the superlattice reflections are normally impossible to detect. Furthermore, from symmetry, one would expect a superlattice in the

gold-copper system at the composition Au_3Cu, since the Brillouin zone boundaries should be just as pronounced at this composition as at the composition $AuCu_3$. As *Figure 34* shows, there is no indication of a superlattice at the composition Au_3Cu.

The lattice-strain theory can account for the CuZn structure because the sizes of the atoms differ by about 10 per cent, and also for the superlattice at the composition $AuCu_3$ and for the absence of the superlattice at the composition Au_3Cu if the further assumption is made that the only strain of importance is that produced when larger atoms are accommodated among smaller ones. The presence of a smaller atom among larger ones must be assumed not to lead to a tendency to order, and thus the presence of 25 per cent of copper atoms distributed at random among the larger gold atoms is accounted for.

Finally, the recent work on $AuCu_3$, leading to the conclusion that the main process in superlattice formation in this alloy consists of the tendency of gold atoms to avoid each other, strongly supports the theory.

The lattice strain theory thus adequately accounts for many of the observed data. Its weakness is due to its purely qualitative aspect, and therefore that it cannot provide any quantitative results by which it may be tested. There is thus scope for a quantitative theory of the forces that produce order in alloys, and such a theory would have to account for the observed differences in internal energy when ordering takes place. Thus it is probable, as Nix and Shockley state, that advances in the quantum-mechanical electronic theory of metals will have to be awaited before the experimental observations can be completely accounted for.

The author wishes to thank Dr F. W. Jones, who read the first draft of this chapter and made many suggestions, most of which have been incorporated. Mr H. Steeple and Mr R. M. Hinde have also given much help in the production of most of the X-ray photographs, some of the specimens being kindly provided by Dr A. Taylor.

REFERENCES

[1] SEITZ, F. *Modern Theory of Solids* New York, 1940
[2] BARRETT, C. S. *Structure of Metals* New York, 1943
[3] HUME-ROTHERY, W. *The Structure of Metals and Alloys* London, 1944
[4] TAYLOR, A. *Introduction to X-ray Metallography* London, 1945

[5] WILLIAMS, E. J. *Sci Progr.* 125 (1937) 15
[6] NIX, F. C. *J. appl. Phys.* 8 (1937) 783
[7] —— and SHOCKLEY, W. *Rev. mod. Phys.* 10 (1938) 1
[8] GOODWIN, E. T. *Rep. Progr. Phys.* 6 (1939) 345
[9] LAVES, F., BORELIUS, G. and SCHOTTKY, W. *Z Elektrochem.* 45 (1939) 2
[10] BRADLEY, A. J., BRAGG, W. L. and SYKES, C *J. Iron Steel Inst.* 1 (1940) 63
[11] WASASTJERNA, J. A. *Soc Sci Fennica., Com Phys. Math.* 13 (1947) 5
[12] JACK, K. H. *Proc. roy. Soc. A* 195 (1948) 34
[13] —— *ibid* 195 (1948) 41
[14] BRADLEY, A. J. and TAYLOR, A. *ibid* 159 (1937) 56
[15] —— and THEWLIS, J. *ibid* 112 (1926) 678
[16] —— and RODGERS, J. W. *ibid* 144 (1934) 340
[17] FRANK, F. C. *ibid* 170 (1939) 182
[18] WANNIER, G. H. *J. chem. Phys.* 7 (1939) 810
[19] BRAGG, W. L. and WILLIAMS, E. J. *Proc. roy. Soc. A* 145 (1934) 699
[20] —— —— *ibid* 151 (1935) 540
[21] WILLIAMS, E. J *ibid* 152 (1935) 231
[22] BETHE, H. A. *ibid* 150 (1935) 552
[23] DEHLINGER, U *Z phys Chem* 26 (1934) 343
[24] BORELIUS, G. *Ann. Phys.* 20 (1934) 57
[25] —— *ibid* 24 (1935) 489
[26] PEIERLS, R *Proc roy. Soc. A* 154 (1936) 207
[27] FOWLER, R H. and GUGGENHEIMER, E. A *ibid* 174 (1940) 189
[28] EISENSCHITZ, R. *ibid* 168 (1938) 546
[29] —— *Phys. Rev.* 65 (1944) 204
[30] KIRKWOOD, J. G. *J. chem. Phys.* 6 (1938) 70
[31] CHANG, T. S. *Proc. roy Soc A* 161 (1937) 546
[32] FOKKER, A. D. *Physica* 8 (1941) 308
[33] —— *ibid* 8 (1941) 109
[34] WANG, J. S. *Sci. Rec. Acad. Sinica* 1 (1942) 116
[35] ASHKIN, J. and LAMB, W. E *Phys. Rev* 64 (1943) 159
[36] CHANG, T. S. *Proc. Camb. phil. Soc. biol. Sci.* 35 (1939) 70
[37] WANG, J. S. *Proc. roy. Soc. A* 168 (1938) 56
[38] BETHE, H. A. *J. appl. Phys.* 9 (1938) 244
[39] TEMPERLEY, H. N. V. *Proc. Camb. phil. Soc. biol. Sci.* 40 (1944) 239
[40] WASASTJERNA, J. A. *Soc. Sci. Fennica, Comm. Phys. Math* 14 (1948) 1
[41] FOKKER, A. D. *Physica* 8 (1941) 159
[42] SLATER, J. C. *Introduction to Chemical Physics* New York, 1939
[43] BRAGG, W L. *J. sci. Instrum.* 19 (1942) 148
[44] —— and NYE, J. F. *Proc. roy. Soc. A* 190 (1947) 474
[45] BORELIUS, G. *J. Inst. Met.* 74 (1947) 17
[46] SYKES, C. and EVANS, H. *ibid* 58 (1936) 225
[47] JONES, F. W and SYKES, C. *ibid* 65 (1940) 419
[48] BRAGG, W. L *Proc. phys. Soc.* 52 (1940) 105
[49] TAMMANN, G. *Z anorg. Chem.* 107 (1919) 1
[50] BAIN, E. C. *Chem metall. Engng* 28 (1923) 65
[51] JOHANNSON, C. H. and LINDE, J. O. *Ann Phys.* 78 (1925) 439
[52] JAMES, R W. *Crystalline State II* London, 1948
[53] LONSDALE, K. *Rep. Progr. Phys.* 9 (1943) 256
[54] SYKES, C. and JONES, F. W. *Proc. roy. Soc. A* 157 (1936) 213
[55] JONES, F. W. and SYKES, C. *ibid* 166 (1938) 376
[56] LONSDALE, K. *Min. Mag.* 28 (1947) 14
[57] —— *Crystals and X-rays* London, 1948

[58] SYKES, C. *J. sci. Instrum.* 18 (1941) 152
[59] WALLER, J. *Proc. roy. Soc. Sci. Uppsala II* 7 (1939) 3
[60] STOKES, A. R. and WILSON, A. J. C. *Proc. Camb. phil. Soc.* 38 (1942) 313
[61] BOUMAN, J. and DE WOLFF, P. M. *Physica* 9 (1942) 833
[62] JONES, F. W. *Proc. roy. Soc. A* 166 (1938) 16
[63] OWEN, E. A. and SIM, G. M. *Phil. Mag.* 38 (1947) 342
[64] —— and LIN, Y. H. *ibid* 38 (1947) 354
[65] WILSON, A. H. *Proc. Camb. phil. Soc.* 34 (1938) 81
[66] SYKES, C. and JONES, F. W. *J. Inst. Met.* 59 (1936) 257
[67] RAYNOR, G. V. *Progress in Metal Physics I* London, 1949
[68] MOTT, N. F. and JONES, H. *Theory of the Properties of Metals and Alloys* Oxford, 1936
[69] BRADLEY, A. J. and JAY, A. H. *Proc. roy. Soc. A* 136 (1932) 210
[70] BRAGG, W. L. *Nature, Lond.* 131 (1933) 749
[71] COMPTON, A. H. and ALLISON, S. K. *X-rays in Theory and Experiment* New York, 1935
[72] JONES, F. W. and SYKES, C. *Proc. roy. Soc. A* 161 (1937) 440
[73] HOWARTH, F. E. *Phys. Rev.* 54 (1938) 693
[74] LEECH, P. and SYKES, C. *Phil. Mag.* 27 (1939) 742
[75] ELLIS, W. E. and GREINER, E. S. *Trans. Amer. Soc. Met.* 29 (1941) 415
[76] PETCH, N. J. *J. Iron Steel Inst.* 145 (1942) 111
[77] BACON, G. E. and LOWDE, R. D. *Acta Crystallogr.* 1 (1948) 303
[78] —— and THEWLIS, J. *Proc. roy. Soc. A* 196 (1949) 50
[79] WOLLAN, E. O. and SHULL, C. G. *Phys. Rev.* 73 (1948) 830
[80] SMIRNOV, A. A. and VORONSKY, S. V. *J. Phys. U.S.S.R.* 5 (1944) 263
[81] NIX, F. C., BEYER, H. G. and DUNNING, J. R. *Phys. Rev.* 58 (1940) 1031
[82] SHULL, C. G. and SIEGEL, S. *ibid* 75 (1949) 1008
[83] WILCHINSKY, Z. W. *J. appl. Phys.* 15 (1944) 806
[84] BETTERIDGE, W. *J. Inst. Met.* 75 (1949) 559
[85] GUINIER, A. J. *Proc. phys. Soc.* 57 (1945) 310
[86] WILSON, A. J. C. *Proc. roy. Soc. A* 181 (1943) 360
[87] —— *X-ray Optics* London, 1949
[88] STRIJK, B. and MACGILLAVRY, C. H. *Physica* 12 (1946) 129
[89] GUINIER, A. J. and GRIFFOUL, R. *C. R. Acad. Sci, Paris* 221 (1945) 555
[90] —— —— *ibid* 224 (1947) 1168
[91] —— *Radiocrystallographie* Paris, 1945
[92] EDMUNDS, I. G., HINDE, R. M. and LIPSON, H. *Nature, Lond.* 160 (1947) 304
[93] WILSON, A J. C. *ibid*, 160 (1947) 304
[94] COWLEY, J. M. *J. appl. Phys.* 21 (1950) 24
[95] MACGILLAVRY, C. H and STRIJK, B. *Physica* 11 (1946) 369
[96] PATTERSON, A. L. *Z. Kristallogr* 90 (1935) 517
[97] SYKES, C. and WILKINSON, H. *J. Inst. Met.* 61 (1937) 223
[98] LIPSON, H. and WILSON, A J. C. *J. Iron Steel Inst.* 142 (1940) 107
[99] EASTHOPE, C. E. *Proc. Camb. phil. Soc.* 34 (1938) 68
[100] JOHANNSON, C. H. and LINDE, J. O. *Ann. Phys. Lzg* 25 (1936) 1
[101] PAN, S. T. *Phys. Rev.* 56 (1938) 933
[102] GRABBE, E. M. *ibid* 57 (1940) 728
[103] KUSSMANN, A. and NITKA, H. *Phys. Z.* 39 (1938) 373
[104] THOMPSON, N. *Proc. phys. Soc.* 52 (1940) 217
[105] LIPSON, H., SHOENBERG, D and STUPART, G. V. *J. Inst. Met.* 67 (1941) 333
[106] NOWACK, L. *Z. Metallk.* 22 (1930) 94
[107] DAHL, O. *ibid* 28 (1936) 133
[108] HUME-ROTHERY, W. and POWELL, H. M. *Z. Kristallogr.* 91 (1935) 23

2

RATE PROCESSES IN PHYSICAL METALLURGY

I. I. Betcherman

THE CONCEPT of the equilibrium condition of an alloy arose quite early in the development of physical metallurgy, and much effort, both experimental and theoretical, has been devoted to the study of alloys in equilibrium. As a result of important advances in physical chemistry, attention has been directed more recently to the rate of approach to equilibrium in a reacting system; the ideas that are used in this study can be applied to many problems besides the rate of chemical reactions. It is intended to indicate here how some aspects of the behaviour of metals and alloys can be considered in terms of the concept of 'activation energy'.

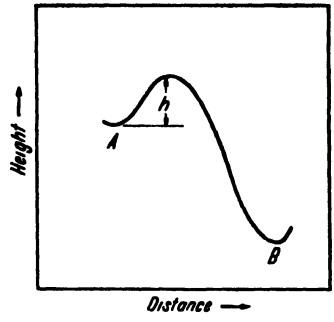

Figure 1. Concept of activation energy

APPLICATION OF THERMODYNAMICS

The atoms or molecules in any physical or chemical system constantly strive to take up positions such that the energy of the system is a minimum. However, in many cases the path leading to the position of minimum energy is obstructed. This is illustrated in the above simple example (*Figure 1*).

A ball obviously possesses a higher potential energy situated in position *A* than if lying in the valley *B*. However, in order to reach *B* the ball must be given sufficient kinetic energy to climb the barrier of height *h*. If we consider that by some agency, for example a strong wind, the ball is being constantly agitated, the rate at which it will move to position *B* will depend on the value of the height *h*. The above example is analogous to many physical and chemical processes, in which the path of atoms or molecules to equilibrium positions is obstructed by an energy barrier.

As the energies possessed by systems in equilibrium are determined by the laws of thermodynamics, the thermodynamic quantities will be briefly discussed.

Free Energy—Any system is in its true equilibrium state when its Gibbs' free energy is a minimum. The Gibbs' free energy G is defined by:

$$G = E - TS + PV \qquad \ldots . \quad (1)$$

where E is the internal energy, T is the absolute temperature, S is the entropy, P is the pressure and V is the volume of the system.

The attempts of atoms in a system to assume positions of minimum free energy constitute the driving force behind any reaction.

Entropy—Entropy is a measure of the randomness or disorder in a system. If an aggregation of $\mathcal{N}$ molecules is considered, according to the quantum theory, precisely defined energy levels are present, each of which will contain a certain number of molecules. If there are $\mathcal{N}_1$ molecules in the first energy level, $\mathcal{N}_2$ in the second *etc* the number of ways in which the $\mathcal{N}$ molecules can be assigned to the various levels is given by:

$$W = \frac{\mathcal{N}!}{\mathcal{N}_1!\,\mathcal{N}_2! \ldots} \qquad \ldots . \quad (2)$$

The fundamental principle of statistical mechanics is that the condition of affairs most closely approached is that where W is a maximum. The entropy S is defined as being equal to $k \log W$, where k is the Boltzmann constant. Entropy is defined in this manner statistically so that it is the same as the thermodynamic entropy. In pure thermodynamics entropy is defined quite abstractly as a mathematical relation between the heat absorbed by a system and its absolute temperature.

Heat Content H—If a system undergoes an operation such that thermal energy is absorbed or liberated, the number of calories involved is termed the gain or loss of the heat content of the system. For example, if x calories are liberated by a chemical reaction, the change in heat content of the system involved is $\Delta H = -x$ calories. The change in heat content:

$$\Delta H = \Delta E + \Delta(PV) \qquad \ldots . \quad (3)$$

Because of the small pressure variations to which metallic systems are normally exposed and because of the high incompressibility of metals the term $\Delta(PV)$ can usually be ignored. Therefore:

$$\Delta H \approx \Delta E \qquad \ldots . \quad (3a)$$

Chemical Kinetics—The rate at which a chemical reaction proceeds is denoted by its velocity constant k'. The velocity constant defines the number of atoms or molecules reacting per unit time. Arrhenius observed that for many reactions the velocity constant changed with temperature in a manner which can be represented by an equation of the following type:

$$\log_e k' = B - A/T \qquad \ldots . \quad (4)$$

where A and B are constants specific for each reaction. Arrhenius noted the similarity of equation 4 with the van 't Hoff isochore, which relates the equilibrium constant (K) of a reaction with temperature:

$$\log_e K = \text{constant} - \Delta H/RT \qquad \ldots . \quad (5)$$

where R is the gas constant and ΔH is the increase in heat content of the system.

By analogy, Arrhenius suggested that an equilibrium existed between 'normal' and 'active' molecules of the reacting substances and that only the active molecules can take part in the reaction. The active molecules are those possessing high energies, and because the special distribution of energies involved requires a finite time, chemical reactions are not instantaneous. The general validity of this hypothesis has since received overwhelming confirmation.

A reaction therefore occurs when molecules or atoms in a state of metastable equilibrium absorb energy, or become active, and then react to arrive in a state of lower free energy. In their transition the atoms must overcome an energy barrier. Only atoms possessing sufficient energy to overcome this barrier can react, and the rate of the reaction will be proportional to the number of activated molecules. If the energy required is denoted by ΔU, then according to the Boltzmann statistics the fraction of atoms possessing this energy is $e^{-\Delta U/RT}$ The rate of the reaction:

$$k' = A\, e^{-\Delta U/RT} \qquad \ldots . \quad (6)$$

where A is a constant.

Equation 6 may also be written as :

$$\log_e k' = \log_e A - \Delta U/RT \qquad \ldots . \quad (7)$$

and therefore if the logarithm of the reaction rate is plotted against the reciprocal of the absolute temperature, a straight line the slope of which yields the value of the activation energy should result. This does, in fact, apply to many reactions, and it is now accepted that the rate of most chemical and physical transformations varies with temperature in a

manner indicated by the above expressions. The rate of a reaction, therefore, will be higher, the lower the value of the activation energy and the higher the temperature.

Eyring's Rate Reaction Theory—EYRING's hypothesis[1] states that in any rate process in which an energy barrier must be surmounted, the atoms or molecules must first combine to form an activated complex. This activated complex is regarded as being situated on top of the energy barrier between the initial and final states, and the rate of the reaction is given by the velocity in which the activated complex travels over the top of the barrier.

It is assumed that the initial reactants are always in equilibrium with the activated complexes and that the latter decompose at a definite rate. From a consideration of statistical mechanics the following equation for the rate of a reaction may be derived:

$$k' = \frac{kT}{h} \cdot \frac{\mathcal{J}^{\ddagger}}{\mathcal{J}_n^{\ddagger}} e^{-E_0/RT} \qquad \ldots . \quad (8)$$

where k is the Boltzmann content, h is Planck's constant and E_0 is the energy of the activation process at zero degrees absolute *i.e.* the difference in internal energy between the initial reactants and the activated complexes at 0°K $\mathcal{J}^{\ddagger}$ and $\mathcal{J}_n^{\ddagger}$ are the partition functions for the activated state and the normal state respectively.

Equation 8 can be expressed in the form:

$$k' = \frac{kT}{h} \cdot e^{-\Delta G^{\ddagger}/RT} \qquad \ldots . \quad (9)$$

where $\Delta G^{\ddagger}$ is called the free energy of activation *i.e.* the difference in free energy between the atoms in the activated state and the initial reactants.

From consideration of equation 1

$$\begin{aligned} \Delta G &= \Delta(E + PV) - T\Delta S \\ &= \Delta H - T\Delta S \end{aligned}$$

therefore

$$k' = \frac{kT}{h} \cdot e^{\Delta S^{\ddagger}/R} e^{-\Delta H^{\ddagger}/RT} \qquad \ldots . \quad (10)$$

The quantities $\Delta H^{\ddagger}$ and $\Delta S^{\ddagger}$ are called the heat of activation and the entropy of activation respectively.

Equations 9 and 10 are of special significance in that they specify that the free energy of activation rather than the heat of activation is the determining factor in the rate of a reaction. From this viewpoint

the Eyring theory is more logical than other theories in which the activation energy is the controlling factor. Free energy changes are the driving force behind chemical or physical transformations, and it is to be expected that free energy changes be involved in reaction rates.

Many reactions involve only minor entropy changes and therefore the energy of activation appears to be the important factor. However, some reactions proceed with great velocity, despite high activation energies, because of large increases in entropy, resulting in a low free energy of activation.

RATE PROCESSES IN METALLURGY

Diffusion—The theory of rate processes has probably been applied to the process of diffusion more than to any other metallurgical reaction. Nevertheless many diffusion phenomena are not yet completely understood and there is a great need for further careful experimental and theoretical investigation on this process.

Many mechanisms have been proposed for the process of diffusion in solid metals. The most widely accepted are:

1 migration of atoms interstitially throughout the lattice
2 exchange of sites between two neighbouring atoms
3 migration of atoms by movement into vacant lattice sites.

Whatever the diffusion mechanism, the diffusion constant D (the amount of substance diffusing in unit time across unit area through a unit concentration gradient) can often be expressed by:

$$D = D_0 \, e^{-\Delta U/RT} \quad \ldots . \quad (11)$$

where D_0 is a constant, R is the gas constant and ΔU is the experimental activation energy of the process. A graph of log D against $1/T$ in many examples yields a straight line as shown in *Figure 2*.

Unless large differences exist between the atomic diameters of the components in a crystal lattice, interstitial movement of atoms is unlikely. Calculations made by HUNTINGTON and SEITZ,[2] for self diffusion in copper show that the calculated activation energy, on the basis of vacant lattice sites or hole diffusion, is of the same order of magnitude as the experimental value. Moreover from energy consideration it has been concluded[3] that diffusion in dilute metallic solid solutions probably occurs through the medium of vacant lattice sites rather than by the other mechanisms previously cited.

Lattice Defects—From thermodynamic reasoning, lattice defects should

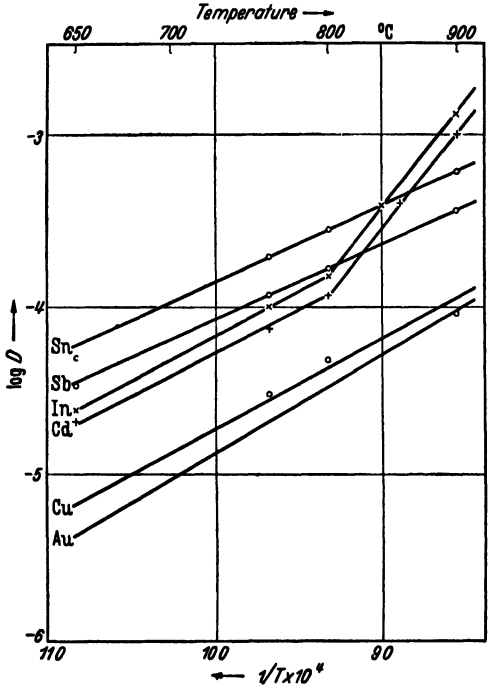

Figure 2 Diffusion constants of various metals in silver

exist in any crystal lattice. If a pure metal is considered, at °K, $G = E$ (equation 1) and therefore the stable state will be the one of minimum internal energy. This occurs when the crystal lattice is perfectly ordered *i.e.* each lattice site is occupied. At higher temperatures, however, the entropy must be considered, and the stable state is not necessarily the one of minimum internal energy. As $G = E - TS$, the minimum free energy will be attained with a compromise between a low value of E and a high value of S. If defects are introduced into an otherwise perfect crystal both the entropy and the internal energy will rise, but if the value of the TS term increases more than the rise in E, the now imperfect crystal will be in the equilibrium state. The higher the temperature, the more important will be the TS term, and therefore at very high temperatures the occurrence of many lattice defects can be expected. Despite the lack of experimental evidence, it is generally believed that lattice defects in metallic crystals are of the vacant lattice site type.

Activation Energy of Diffusion—Consider a metal which crystallizes in a lattice of coordination number z. If a hole (vacant lattice site) exists, each of the z neighbouring atoms has an equal chance of moving into the vacant position. If one atom makes this movement, all others remaining fixed, the potential energy of the atom must vary with distance as shown in *Figure 3*.

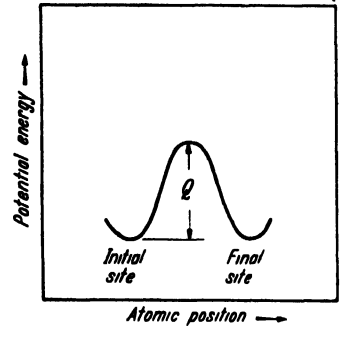

Figure 3. Variation of potential energy of atoms with distance

The atom under consideration must, by interaction with its neighbours, acquire a minimum kinetic energy of Q in order to make such a movement. The probability that the given atom will move into the hole is thus proportional to $e^{-Q/RT}$. The rate of the diffusion process will also depend on the number of holes present. This is equal to $ze^{-W/RT}$, where W is the energy of formation of a hole. The diffusion constant can then be represented by:

$$D = \text{constant } z\, e^{-W/RT} \cdot e^{-Q/RT} \quad \ldots\ (12)$$

$$= \{\text{constant } z\}\, e^{-(W+Q)/RT}$$

$$= D_0 \cdot e^{-\Delta U/RT} \quad \ldots\ (12a)$$

where $W + Q = \Delta U$, the activation energy of the diffusion process.

Effect of Solute on Activation Energy of Diffusion—STEIGMAN, SHOCKLEY and NIX[3] have shown, from accumulated data, that for a given solvent the energy of activation of the diffusion process has its greatest value for self diffusion and may be as low as half that value for dilute solutions of other elements. These authors have concluded that if hole diffusion constitutes the dominant process, the energy of formation of the vacant lattice sites W should remain the same for a given solvent, and therefore all changes of the observed activation energy with concentration should result from variations in the energy required to move into the vacant site.

It is difficult to understand why the latter term (Q in equation 12) should be appreciably lessened by the presence of solute atoms if the simple vacant site diffusion model is valid. In this model it is assumed that the solute atom migrates into a vacant lattice site when the latter approaches it, and therefore the rate of migration of the solute atom will depend on the number of vacant lattice sites, which as already shown is not seriously affected by the presence of a solute, as well as on the rate of migration of the holes. In dilute solutions the holes encounter many more solvent atoms than solute, and therefore the rate of migration of the holes should not involve much different energy consideration than in the absence of solute atoms.

JOHNSON[4] considers that vacant sites associate preferentially with solute atoms, and that molecules of hole-solute atom combinations move through the crystal. This view is reasonable from a thermodynamic aspect. The lattice must be distorted around solute atoms and around vacant sites, resulting in a high internal energy as well as a high entropy. If the solute atom and holes associate to some degree, lower

internal energies and lower entropies result, and a certain amount of this association might be necessary in order to bring about thermodynamic equilibrium. Moreover strains set up by the presence of solute atoms cause the lattice to loosen, thereby decreasing the activation energy required to move an atom from one site into another.

Table I. Diffusion of Various Elements in Copper

System	D_0 *cm² sec⁻¹*	*cal/atom*
Cu *in* Cu	11	57,200
Al *in* Cu	$1{\cdot}2 \times 10^{-2}$	37,500
Zn *in* Cu	8×10^{-1}	38,000
Sn *in* Cu	10	45,000
Si *in* Cu	$5{\cdot}2 \times 10^{2}$	39,950

Entropy of Activation—The Eyring equation 9 applies to any rate process in which the slow step involves surmounting a potential barrier. Applied specifically to the rate diffusion process, it has been shown[5] that the diffusion constant D is related to the specific rate constant k' by:

$$D = d^2k' \qquad \ldots\ (13)$$

where d is the distance travelled in a single jump *i.e.* the interatomic distance. Substituting equation 13 in 9 and 10:

$$D = d^2 \frac{kT}{h} \cdot e^{-\Delta G^{\ddagger}/RT} \qquad \ldots\ (14)$$

$$\text{or} \quad D = d^2 \frac{kT}{h} \cdot e^{\Delta S^{\ddagger}/R} \cdot e^{-\Delta H^{\ddagger}/RT} \qquad \ldots\ (15)$$

If equation 11 is considered:

$$D = D_0\, e^{-\Delta U/RT}$$

and as the experimental activation energy is approximately equal to the increase in heat content when the activated complex is formed from the reactants ($\Delta U \approx \Delta H^{\ddagger}$), then:

$$D_0 = d^2 \frac{kT}{h} e^{\Delta S^{\ddagger}/R} \qquad \ldots\ (16)$$

and therefore a large value of D_0 indicates a large entropy of activation.

Diffusion in Copper—Rhines and Mehl[6] conducted a very thorough investigation on the diffusion rates of various elements in copper. It was found that the relation

$$D = D_0\, e^{-\Delta U/RT}$$

was obeyed in all systems investigated. The results for the diffusion o some of these elements in copper are shown in *Table I* as well as data on self diffusion in copper.[3]

The decrease in the energy of activation effected by the introduction of solute atoms is readily observed. The value of D_0, and therefore the entropy of activation, is considerably lowered when solute atoms are present. Because of the entropy of solution, the introduction of solute

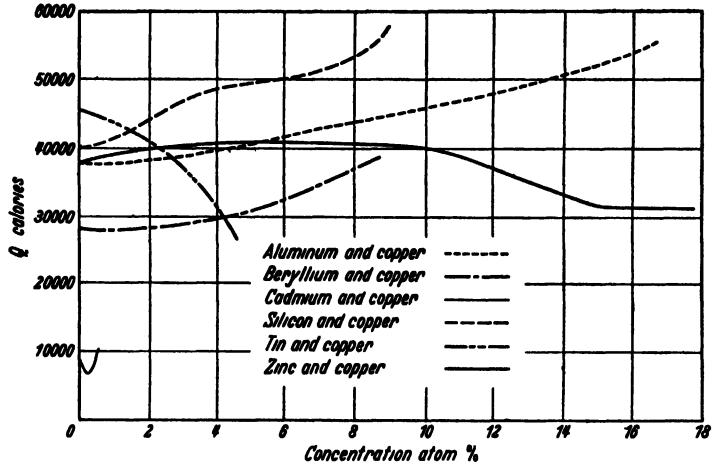

Figure 4. Experimental activation energies of copper alloys

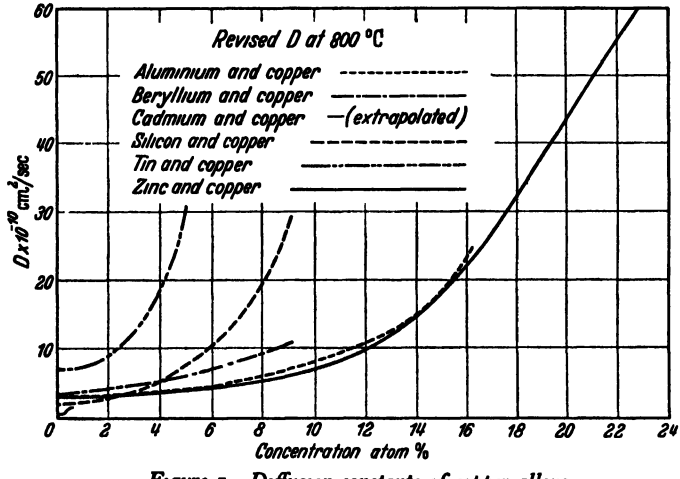

Figure 5. Diffusion constants of copper alloys

atoms increases the entropy of the system. For this reason the entropy difference between the activated state and the reactants is lowered, resulting in a small value of D_0. This interpretation by no means fully explains the decrease in the value of D_0 but does indicate in a qualitative manner why the entropy of activation is reduced when solute atoms

are added. In general, the higher the activation energy the larger is D_0, although no simple relationship between them exists.

Rhines and Mehl also examined the effect of solute concentration on diffusion. Their results are given in *Figures 4* and *5*, in which the experimental activation energy and the diffusion constant D are plotted against the solute concentration. STEARN and EYRING[7] have calculated the entropy of activation for the different solutes from the data of Rhines and Mehl, and this is given as a function of concentration in *Figure 6*. In all instances diffusion in the α-solid solution of the solute in copper is considered. The diffusion constant increases with concentration in all the examples. Therefore increasing solute concentration decreases the free energy of activation of the diffusion process. The energies and entropies of activation may increase or decrease with concentration. The reasons for the variation in ΔU and $\Delta S^{\ddagger}$ with concentration are by no means completely understood.

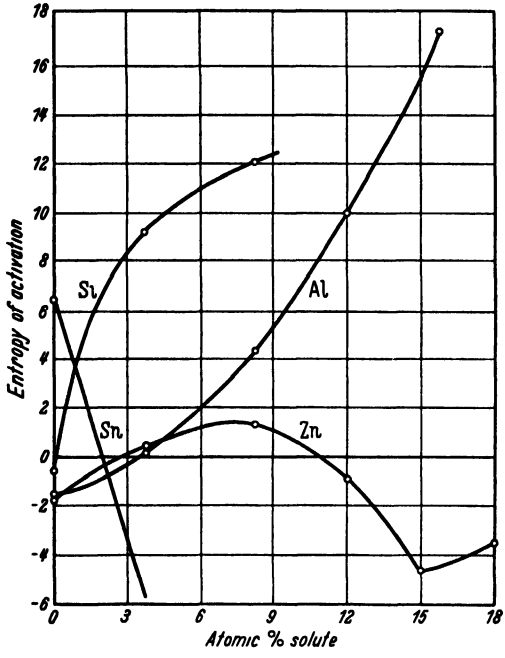

Figure 6. Entropies of diffusion of copper alloys

Discussion of Diffusion in Copper—In the following section, the data represented in *Figures 4*, *5* and *6* are discussed. An attempt is made to account qualitatively for the observed behaviour of the ΔU and $\Delta S^{\ddagger}$ terms. It must be emphasized that the conclusions which are reached are only tentative, but are made in order to stimulate further discussion.

The diffusion of tin in copper is unique in that the energy of activation decreases sharply with increasing tin concentration, while the entropy of activation increases with increasing concentration. The solubility of tin in copper is 7 atomic per cent at the temperature under consideration (800°C), whereas only traces of tin are soluble in copper at

room temperature. This fact perhaps indicates that a large amount of strain is present in the lattice of the copper-tin solid solution even at 800°C. Moreover, as indicated in *Table II*, the atomic diameter of tin deviates from that of copper more than the atomic diameter of any of the other solute elements.

Table II. Deviations of Atomic Diameters of Various Elements from that of Copper

Element	*Atomic Diameter* Å	*Deviation from* Cu %
Cu ..	2·551	0
Al ..	2·856	12
Zn	2 659	4
Sn ..	3 016	18
Si .	2 346	− 8

The large amount of strain which might be present in the copper-tin solid solution would increase the chances of migration of tin atoms and therefore lower the activation energy of the process. As the tin concentration is raised, the increasing strain would increase the lowering of the activation energy. Moreover, in an effort to relieve this strain numerous holes in the lattice might result, increasing the entropy of the system with a resultant decrease in the entropy of activation.

The solid solubility of aluminium and silicon in copper alters little with temperature, and therefore it is possible that the atoms of these elements can be accommodated in the copper lattice with much less strain than those of tin. The energy of activation for the diffusion of aluminium and silicon in copper rises with increasing solute concentration. Perhaps in these systems, as more solute is added, restrictions are imposed on the position of the solute atoms *i.e.* a certain amount of order in the lattice occurs. If any restrictions exist as to the sites which solute atoms can occupy, in order to keep the free energy of the system a minimum, the result would be to raise the energy of activation. Moreover, restrictions of this type would lower the entropy of the system and therefore increase the entropy of activation. This would account for the increase of $\Delta S^{\ddagger}$ with solute concentration.

The diffusion of zinc in copper appears to be more complex than that of the other metals considered. Both ΔU and $\Delta S^{\ddagger}$ first increase with increasing zinc content, then decrease and finally appear to remain constant, with a probable tendency for $\Delta S^{\ddagger}$ to rise again. The initial part of the curve, in which both ΔU and $\Delta S^{\ddagger}$ increase, appears to resemble the behaviour of aluminium and silicon. The second portion

of the curve, when ΔU and $\Delta S^{\ddagger}$ are decreasing, resembles the behaviour of tin. At this stage the increasing concentration of zinc may possibly cause a large amount of strain in the lattice. In the final stage ΔU is constant, but as D increases D_0 must decrease according to equation 15.

Table III. Relationship between Activation Energy and Melting Point

System	*Melting Point* °K	$\Delta U/T_m$
Cu *in* Au ..	1,336	20·5
Cu *in* Ag ..	1,233	20·1
Cu *in* Ni ..	1,728	20·6
Mo *in* W ..	3,743	21·3
Cu *in* Cu .	1,356	42
Au *in* Au .	1,336	38
Pb *in* Pb ..	600	47

Perhaps an increase in the entropy of activation at this point can be explained in terms of Johnson's suggestion *i.e.* association of holes and solute atoms, which would decrease the entropy of the system, thus raising the entropy of activation.

Effect of Melting Point of Solvent on Diffusion—As shown in *Table III*, a definite relationship may exist between the activation energy ΔU and the melting point of the solvent T_m for diffusion in a solvent as well as for self diffusion.

A correlation between the energy of activation and the melting point might be expected, since they are both measures of the binding forces in metals. Formulae proposed by BRAUNE[8] and VAN LIEMPT[9] for the velocity of diffusion make use of the relationship

$$\frac{\Delta U}{R} = 3b^2 T_m \quad \ldots . \quad (17)$$

where b is a constant which depends upon the atomic size and polarization properties of the lattice.

Table IV. Calculated and Experimental Values of Activation Energy

System	*Experimental* ΔU *cal/atom*	*Calculated* ΔU *cal/atom*
Pb *in* Pb ..	27,900	24,400
Au *in* Pb ..	13,000	13,300
Cu *in* Al ..	34,900	31,400
Zn *in* Cu ..	38,000	44,000
Zn *in* Cu + 20% Zn ..	31,000	38,500

Langmuir-Dushman Equation—LANGMUIR and DUSHMAN[10] proposed a semi-empirical equation for diffusion in cubic lattices which predicts the experimental activation energy for the diffusion process in metals

with a fair degree of accuracy. Values of the activation energy as calculated using their equation compared with the experimental values[11] are given in *Table IV.*

The Langmuir-Dushman equation was derived by considering that the lattice is composed of layers of atoms a distance d apart, where d is the interatomic distance. It was assumed that d is the free mean path of the diffusing atom. The equation is:

$$D = \frac{\Delta U}{N_0 h} d^2 e^{-\Delta U/RT} \quad \ldots . \quad (18)$$

where $N_0 = \Delta U/h\nu$, ν denoting the vibration frequency of the solid. This relationship appears to yield good results when the activation energy is small or if grain boundary processes occur.

Structure-sensitive Diffusion Processes

STEARN and EYRING[7] and BARRER[11] have discussed structure sensitive diffusion in metallic systems.

Anisotropy—Diffusion rates in some metals are strongly anisotropic. This is clearly indicated by the following data[12] on diffusion rates in bismuth.

D (parallel to (111) plane)

$$= (1{\cdot}33 - 16{\cdot}3) \times 10^{4{\cdot}5} e^{-137{,}000/RT} \text{ cm}^2 \text{ sec}^{-1}$$

D (perpendicular to (111) plane)

$$= (2{\cdot}22 - 6{\cdot}5) \times 10^{-4} e^{-30{,}000/RT} \text{ cm}^2 \text{ sec}^{-1}$$

Diffusion perpendicular to the (111) plane involves less than one quarter the amount of activation energy than diffusion in the parallel direction. Diffusion parallel to the (111) plane displays a very large entropy of activation, which seems to indicate an enormous collapse of the structure.

Effect of Grain Size—Rates of diffusion are dependent upon whether a polycrystalline or monocrystalline sample is used. Diffusion rates are more rapid in polycrystalline specimens. On passing from a single crystal to a polycrystalline brass specimen it was found[13] that both ΔU and D_0 increase, but in polycrystalline samples the ΔU values were the same but the value of D_0 increased with reduction in grain size. Some similar observations[14, 15] are shown in *Table V.*

The diffusion of molybdenum in monocrystalline and polycrystalline tungsten has also been examined[16]; the results are shown in *Table VI.*

The variation in the rate of diffusion with grain size is evidently based on changes in the entropy of activation, which appears to increase with decreasing grain size. This might be explained by assuming that diffusion takes place through the medium of grain boundaries by a different mechanism than through a crystal lattice. Interchange of sites by neighbouring atoms might be possible because of the distortion present at grain boundaries. A net movement of one interatomic distance would require two atoms being in the activated state simultaneously resulting in a greater difference in entropy between the activated and initial state than would occur by migration of atoms jumping into a hole. The latter mechanism need only involve one atom at any instant.

Table V. Effect of Grain Size on Diffusion of Thorium in Tungsten

Grain Size (μ)	ΔU *cal/atom*	D_0 *cm² sec⁻¹*
3,000	94,400	$3\cdot0 \times 10^{-3}$
7·3	95,600	$4\cdot8 \times 10^{-1}$
5·3	93,600	$7\cdot9 \times 10^{-1}$
—	94,600	$8\cdot4 \times 10^{-1}$

Table VI. Diffusion of Molybdenum in Tungsten

Specimen	ΔU *cal/mol*	$\Delta S^{\ddagger 17}$
Monocrystalline	80,500	− 9·1
Polycrystalline	80,500	− 5·5

Because D_0 is so sensitive to grain size the data found in the literature should merely be considered to give average values, and unless the grain size is known, quantitative calculations are not possible.

Table VII. Effect of Annealing on Diffusion

System	ΔU *(cal/mol)*	$\Delta S^{\ddagger 17}$
Pd *in* Cu	21,900	− 19·5
Pd *in* Cu (*annealed*)	27,400	− 14·7
Sn *in* Cu	31,200	− 4·0
Sn *in* Cu (*annealed*)	39,900	4·2

Effect of Lattice Strain— The effect of annealing to remove strain on the diffusion of palladium and tin in copper has been examined.[17] *Table VII* gives data for these systems.

The rate of self diffusion in bismuth is also increased by cold work and decreased by annealing.[12] The diffusion rates, in general, are decreased

by annealing. The energies and entropies of activation are both increased. Distortions in the lattice, which facilitate the migration of atoms, are removed by annealing. The removal of any imperfections lowers the entropy of the system, with a resultant increase in the entropy of activation.

PRECIPITATION BY NUCLEATION AND GROWTH

With a number of metals, as a solid solution is cooled a new phase appears. The simplest form of an equilibrium diagram associated with a phase separation on cooling is shown in *Figure 7*.

An alloy of composition c consists of the solid solution α at temperature T_1. On cooling to temperature T_2 the solution is saturated, and on

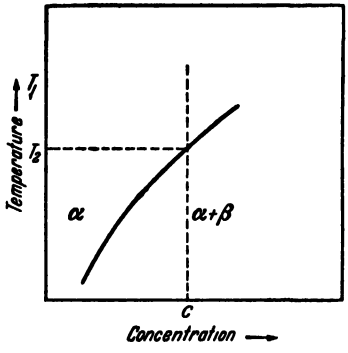

Figure 7. Equilibrium diagram of a system in which phase separation occurs on cooling

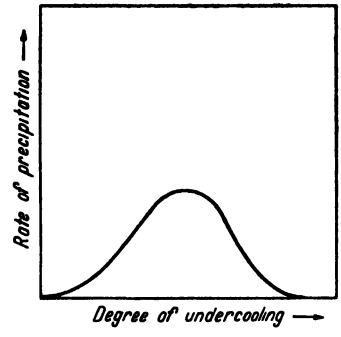

Figure 8 Rate of nucleation as a function of temperature

further decrease in temperature the solution becomes supersaturated. Therefore in order to maintain equilibrium a new phase β must precipitate. Fine particles of the new phase appear, and these subsequently grow at a rate determined by the rate of atomic migration in the alloy. As the process involves rates, activation energies must be considered. It is known that, if the alloy is cooled slightly below T_2 or if cooled much below T_2, the rate of this phase separation is very slow. The rate of nucleation is dependent on temperature in the manner shown in *Figure 8*.

At very low temperatures the slow rate of nucleation can readily be understood. Nucleation occurs through the medium of atomic migration, and the frequency with which atoms migrate has earlier been shown to be roughly proportional to $e^{-Q/kT}$, where Q is the activation energy of the process.

At temperatures just below T_2 the system possesses a minimum chemical free energy when both α and β are present. The lowering in free energy caused by the precipitation of nuclei of phase β is represented by $-\Delta G_m$. However, an increase in free energy results because of the energy produced by the formation of a surface between β-nuclei and the α-phase (ΔG_s) as well as an increase in free energy (ΔG_c) brought about by strains accompanying the formation of nuclei. The total change of free energy:

$$\Delta G = -\Delta G_m + \Delta G_s + \Delta G_c \quad \ldots . \quad (19)$$

The nuclei will not be stable unless ΔG is a negative quantity, and the

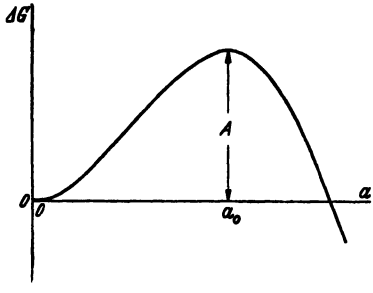

Figure 9. Free energy of formation of a cubical nucleus in a supersaturated solution as a function of the nucleus site

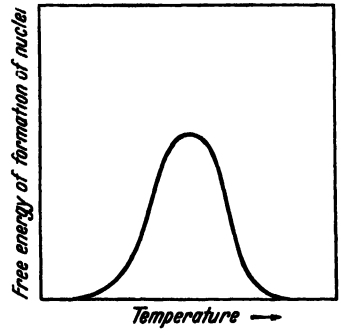

Figure 10. Number of stable nuclei formed per second as a function of temperature for the gold-platinum system

temperature must be lowered to a value where $-\Delta G_m$ is large enough to offset the increase in surface and strain energies.

Consider a nucleus in contact with the supersaturated solution at a definite temperature below T_2. In order to simplify the problem consider that the strain energy can be ignored *i.e.* $\Delta G_c = 0$. Therefore:

$$\Delta G = -\Delta G_m + \Delta G_s \quad \ldots . \quad (20)$$

The term ΔG_m will be proportional to the volume of the nucleus and ΔG_s will be proportional to its surface area. If the cube edge of the nucleus is a, then:

$$\Delta G = -k_1 a^3 + k_2 a^2 \quad \ldots . \quad (21)$$

where k_1 and k_2 are constants specific for a given temperature and composition. If a is small the ΔG_s term will predominate, and if a is large the ΔG_m term will be dominant. If ΔG is plotted against a, a curve of the type shown in *Figure 9* will result.

It is evident that a maximum in free energy occurs at $a = a_0$. Therefore a nucleus of cube edge smaller than a_0 cannot be stable, because its growth would involve a free energy increase. In other words, if the nucleus is very small, because of the high surface volume ratio the ΔG_s term will be large enough to offset the decrease in ΔG_m, resulting in a positive ΔG. A nucleus of a size smaller than a_0 will then disappear. There is then a lower limit of stable nucleus size, and with it is associated a critical value A of ΔG which can be termed the work of nucleus formation. If the diameter of the nucleus is greater than a_0 the nucleus will continue to grow, as ΔG at this point will be decreasing.

The formation of a stable nucleus then will require an increase A in the total free energy, and therefore A is the activation energy for the formation of a stable nucleus. The activation energy can be produced by fluctuations of energy in the system, and the relative probability of a fluctuation occurring which will produce a nucleus of energy A is $e^{-A/kT}$.

The creation of a nucleus is also dependent upon the process of atomic migration. The nuclei can only be formed when atoms migrate through the crystal lattice to form small clusters of suitable size and composition. BECKER[18] has proposed that the number of stable nuclei formed per second:

$$I = C\, e^{-Q/kT}\, e^{-A/kT} \quad \ldots\ (22)$$

where C is a constant.

The numerical value of Q can be obtained from the dependence of the rate of diffusion on temperature. Using the assumption that atoms possess an interactive energy with only their nearest neighbours, Becker was able to determine the change of free energy of the alloy with concentration as well as the value of the surface energy, leading to a solution for the value of A. The graph of energy of formation of nuclei I, against temperature T_1, shown in *Figure 10*, was obtained for the gold-platinum system. The maximum nucleation rate was calculated to occur at 300°C below the saturation temperature, which is in fair agreement with experimental results.

The assumptions made in the calculation of A are possibly the cause of this discrepancy. It was assumed that the atoms of both components are distributed at random in the homogeneous phase, whereas some clustering of similar atoms will occur. Moreover, the effect of surface energy on the composition of the nucleus at equilibrium was not considered.

COTTRELL[19] was able to explain the shape of the curve in a qualitative manner using equation 22. He showed that A is very large at a temperature just below T_2 (*Figure 7*) and therefore $e^{-A/kT}$ is very small, resulting in a small value for I. As the temperature falls, A diminishes rapidly, with a corresponding increase in I. At very low temperatures A is much less than Q and the term $e^{-Q/kT}$ is dominant, and I is controlled by the rate of atomic migration; at low temperatures, therefore, I decreases with increasing undercooling.

Growth of Nuclei—A very interesting and lucid discussion of the growth and coagulation of nuclei has been offered by Cottrell. A stable nucleus will grow by the continued addition of atoms; solute atoms migrating at random through the solution will join on to the nucleus. Also thermal agitation will cause atoms to acquire sufficient activation energy to leave the nucleus. If the solution is supersaturated the nuclei will grow, because the free energy is lowered when atoms attach themselves to the nucleus and is raised by the opposite process.

The degree of supersaturation affects the shape of the growing nucleus. As the nucleus grows, the strain energy associated with it will increase, but as shown by MOTT and NABARRO[20] this increase will be smallest if the new atoms attach themselves to the plate edge of the particle. If supersaturation is small, the decrease in chemical free energy accompanying growth of the nucleus may be offset by the increase in the strain free energy unless the atoms attach themselves to the plate edge of the nucleus. This fact explains the occurrence of the Widmanstatten structure, which is formed by the crystals of a precipitating phase appearing as thin plates. GUINIER[21] and PRESTON[22] independently observed that precipitation in the aluminium-copper system begins with the formation of small plate-like regions. When the solution is highly supersaturated, the strain energy factor is outweighed by the decrease in chemical free energy and atoms attach themselves fairly uniformly over the surface of the nucleus.

The high surface energy associated with small nuclei may result in a given concentration being unsaturated with respect to these and supersaturated with respect to large nuclei. The small nuclei will then dissolve and large ones will grow still larger. This process, coagulation, requires extensive atomic migration and therefore proceeds much more slowly than precipitation. Coagulation will only be extensive at high temperatures, where atomic migration is rapid.

FLOW OF SOLID METALS

KAUZMANN[23] has outlined EYRING'S[5] general statistical mechanical theory of shear rates. The shear process occurs by the flow past one another of domains in a metallic system. These domains are called units of flow. In a liquid the units of flow are believed to be molecules, and the unit process is the migration of single molecules past one another. The rate of shear is equal to the shear resulting from each jump multiplied by the number of jumps occurring in unit time. The manner in which single molecules pass one another is shown in *Figure 11*.

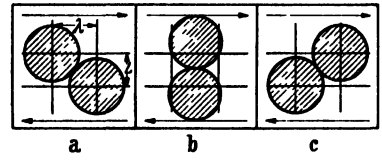

Figure 11. Schematic representation of the movement of molecules past each other

Where λ is the average distance moved by a flow unit in a single jump in the direction of shear and L is the average distance between layers of units of flow, λ/L is the shear strain in the direction indicated by the solid arrows in *Figure 11*. The shear rate:

$$S = \frac{\lambda}{L}\nu \qquad \ldots . \quad (23)$$

where ν is the net number of jumps per second made by the unit of flow in the direction of shear.

It is very likely that in order for units of flow to pass one another in the manner indicated a considerable amount of energy is required *i.e.* the process requires an energy of activation. For this reason it is to be expected that the term ν in equation will be proportional to the familiar exponential quantity $e^{-\Delta U/RT}$, where ΔU is the energy of activation of the process.

Flow of Metals—Deformation or flow in solids is, in general, caused by the tendency of the atoms or molecules in an elastically stressed body to adjust in such a way that if the deformation remains constant a release of stress would occur. If rupture does not occur, this process of relaxation causes the rate of flow to attain a final constant value, in which state the release of stress brought about by relaxation exactly counterbalances the increase of stress owing to the elastic strain on the specimen.

In metals, deformation causes a mutual displacement of atoms and the system gains potential energy, resulting in internal tensions being set up to balance the external forces. If the external forces are released,

the internal stresses act to restore the atoms to their original positions. If the original positions are regained by using the stored potential energy, the material is elastic.

Whenever a portion of the internal stress is relaxed, the equilibrium with the external force is disturbed, and further deformation occurs in order to restore equilibrium. If relaxation is continued, this process will recur continually and flow will result.

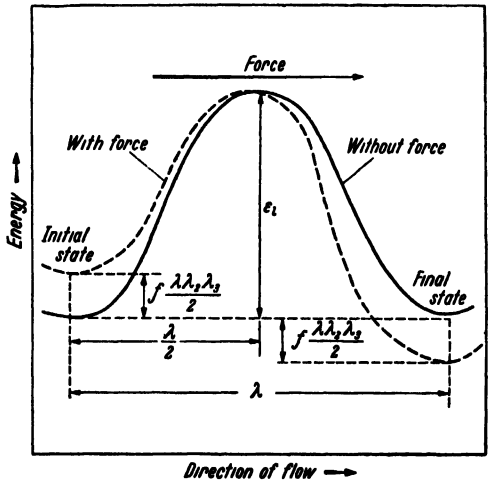

Figure 12. Rate of flow of atoms in the presence of an applied force

Even when no external force exists, the atoms in the material continually jump from one position into another, but in such a way that no net movement results. However, under the influence of an applied force the number of jumps in the direction of the force is greater than the number in the opposite direction, resulting in overall movement.

The units of force, in order to migrate from one position to another, require an activation energy. The velocity of flow:

$$V = C\,e^{-\epsilon_1/RT} \qquad \ldots\ (24)$$

where ϵ_1 is an activation energy and C is a constant. BECKER[24] postulated that the rate of flow was characterized by an equation of this type. When an external force is applied, the reaction rate is modified by the applied force, as shown in *Figure 12*.

The specific rate of the reaction in the forward direction, according to the Eyring theory, is given by:

$$n_f = \frac{kT}{h} \cdot e^{-\Delta G\ddagger/RT} \qquad \ldots\ (25)$$

and in the backward direction by:

$$n_b = \frac{kT}{h} \cdot e^{-\Delta G\ddagger/RT} \qquad \ldots\ (26)$$

When an external force is applied, the rate of reaction is modified by the applied force (*Figure 12*). If the force on a unit area of surface is f

and the projected cross sectional area of each unit of flow in the shear plane is $\lambda_2\lambda_3$, the force acting on the unit of flow is $f\lambda_2\lambda_3$. This force acts through a distance $\lambda/2$ in carrying the unit of flow from the normal to the activated state, and the work done is $f\lambda\lambda_2\lambda_3/2$. The activation energy in the direction of force is therefore lowered by the amount $f\lambda\lambda_2\lambda_3/2$ while raised by the same amount in the opposite direction. The raise in activation energy in the reverse direction is, in fact, not the same as the lowering in the direction of the force, as the distance in which the force acts is not exactly the same in forward and reverse directions. However, the error introduced is very small and will be ignored.

When the force is applied:

$$n_f = \frac{kT}{h} e^{-\Delta G\ddagger/RT} e^{f\lambda\lambda_2\lambda_3/2kT} \quad \ldots . \quad (27)$$

and

$$n_b = \frac{kT}{h} e^{-\Delta G\ddagger/RT} e^{-f\lambda\lambda_2\lambda_3/2kT} \quad \ldots . \quad (28)$$

The net number of jumps per unit time in the direction of the force:

$$\nu = n_f - n_b = \frac{kT}{h} e^{-\Delta G\ddagger/RT} (e^{f\lambda\lambda_2\lambda_3/2kT} - e^{-f\lambda\lambda_2\lambda_3/2kT}) \ldots . \quad (29)$$

Using the definition of the hyperbolic sine, $\sinh \mu = \frac{1}{2}(e^{\mu} - e^{-\mu})$:

$$\nu = \frac{2kT}{h} e^{-\Delta G\ddagger/RT} \sinh \frac{f\lambda\lambda_2\lambda_3}{2kT} \quad \ldots . \quad (30)$$

As λ is the distance moved by the flow unit in each jump, the shear rate:

$$S = \frac{\lambda}{L} \nu$$

$$= \frac{2\lambda kT}{hL} e^{-\Delta G\ddagger/RT} \sinh \frac{f\lambda\lambda_2\lambda_3}{2kT} \quad \ldots . \quad (31)$$

If the work done is small in comparison with the thermal energy of the unit of flow, $f\lambda\lambda_2\lambda_3/2kT$ will be small, and as $\sinh \mu \approx \mu$ for small values of μ:

$$S = \frac{\lambda}{hL} f\lambda\lambda_2\lambda_3 e^{-\Delta G\ddagger/RT} \quad \ldots . \quad (32)$$

This type of flow is newtonian or viscous flow such as is exhibited by water. The shear rate is proportional to the applied stress. When the thermal energy of the unit of flow is the smaller, as $\sinh \mu \approx \frac{1}{2} e^{\mu}$ for large values of μ:

$$S = \frac{2\lambda kT}{hL} e^{-\Delta G\ddagger/RT} e^{f\lambda\lambda_2\lambda_3/2kT} \quad \ldots . \quad (33)$$

Application of Theory to Creep Data—Equation 33 has been applied to the problem of creep in metals by Kauzmann. The theory outlined on the previous pages is particularly designed for the interpretation of shear processes, which require an activation energy if flow is to occur. Equation 33 can also be written:

$$S = \frac{2\lambda kT}{hL} e^{\Delta S^{\ddagger}/R} e^{-\Delta H^{\ddagger}/RT} e^{f\lambda\lambda_2\lambda_3/2kT} \quad \ldots . \quad (34)$$

The theory is useful because by substituting experimental data into the above equation an idea of the magnitude of $\Delta S^{\ddagger}$, $\Delta H^{\ddagger}$ and $\lambda\lambda_2\lambda_3$ may be obtained, and this in turn may lead to a conception of the fundamental mechanism of flow.

The rate of shear of a metal is usually measured by determining the rate at which a bar under tensile stress increases in length. The creep rate of a bar (μ) is related to the shear γ_{max} occurring along the plane of maximum shear stress[25] by:

$$\mu = \frac{2}{3}\frac{d\gamma_{max}}{dt} = \frac{2}{3}S \quad \ldots . \quad (35)$$

The true value of the force f (shearing stress per unit area) is related to the macroscopically measured shear stress σ by:

$$q\sigma = f \quad \ldots . \quad (36)$$

where q is a stress concentration factor. When $q = 1$ no stress concentration is present. The macroscopic shear stress, in the plane of maximum shear stress σ_{max}, is related to the tensile stress τ by:

$$\sigma_{max} = \frac{\tau}{2} \quad \ldots . \quad (37)$$

Substituting equations 34, 36 and 37 in 35:

$$\mu = \frac{2}{3}\frac{\lambda}{L}\frac{kT}{h} e^{\Delta S^{\ddagger}/R} e^{-\Delta H^{\ddagger}/RT} e^{q\lambda\lambda_2\lambda_3\tau/2kT} \quad \ldots . \quad (38)$$

If the logarithm of μ is plotted against τ, the slope of the curve, which is normally a straight line, yields a value for $q\lambda\lambda_2\lambda_3$. The intercept of the straight line in the y-axis at zero stress gives the value for $\frac{2}{3}\frac{\lambda}{L}\frac{kT}{h} e^{\Delta S^{\ddagger}/R} e^{-\Delta H^{\ddagger}/RT}$ at a given temperature. If the logarithm of this term is plotted against $1/T$ the slope of the resulting straight line yields $\Delta H^{\ddagger}$ and the intercept in the y-axis yields $\frac{2}{3}\frac{\lambda}{L}\frac{kT}{h} e^{\Delta S^{\ddagger}/R}$. No further resolution of the constants in the equation can be made. However,

the factor λ/L should usually be of the same order as unity and if $L \approx \lambda$, $\Delta S^{\ddagger}$ can be determined.

Kauzmann has compiled data on different materials and has discussed the significance of the data in terms of a general molecular picture. Very large values of $q\lambda\lambda_2\lambda_3$ are found for all the metals investigated. If $q = 1$ (no stress concentration), λ = one lattice distance, and $\lambda_2\lambda_3$ the cross sectional area of a single atom, a value of the order of 10 Å^3 should generally be found for metals. Instead values 100 times or more as large are usually observed.

The large value of $q\lambda\lambda_2\lambda_3$ can be accounted for in three ways *1* a large value of q *i.e.* high stress concentration *2* a large value of λ *i.e.* an atom would move a long distance before arriving in the activated state or *3* that the area of the domain is much larger than the cross section of a single atom.

The first explanation is unlikely, as stress concentration of the order required can probably only be introduced by cracks or flaws. But then the stress concentration is immobile, whereas the proper distribution of sites of unit shear processes requires that nearly every lattice site in a given shear plane be the site of a unit shear process. The second explanation is even less admissible, as it is inconceivable that an atom could move 100 atomic distances in one leap before arriving in the activated state. The third explanation, however, seems suitable. If the unit shear process occurs by the formation and movement of dislocations as suggested by TAYLOR,[26] it can be shown that the size of a dislocation is of the order required by the value of $q\lambda\lambda_2\lambda_3$.

By considering the temperature variation of the activation energy of the flow process Kauzmann was able to account qualitatively for both the very small activation energies and the negative entropies of activation that have been observed. The general features of metallic flow seem to indicate that flow occurs by means of dislocations forming at relatively few points in the lattice, the lateral dimension of which depends strongly on temperature.

The difference in the rate of flow of different metals does not seem to depend on the free energy of activation, which is very similar for all metals at a given temperature. Metals which flow very easily have a large lateral extension of dislocations, whereas metals which do not flow easily have much smaller lateral extensions.

In order to produce a material having a slow creep rate, it can be

seen on examination of equation 38 that $\Delta S^{\ddagger}$ should have as large a negative value as possible, $\Delta H^{\ddagger}$ should be as large as possible, and $q\lambda\lambda_2\lambda_3$ should be as small as possible. The factors affecting $\Delta S^{\ddagger}$ are not fully understood. $\Delta H^{\ddagger}$ can be made larger by employing a metal of high elastic modulus and the term $q\lambda\lambda_2\lambda_3$ can be made smaller by introducing barriers to limit the lateral extension of dislocations.

STRESS-STRAIN RELATIONSHIPS IN METALS

FREDRICKSON and EYRING[27] have applied the theory of rate processes to stress-strain relationships in metals. They have proposed the following model for deformation of metals under tensile stress. The stress-strain curve for metals is divided into three regions, each represented by an elastic-plastic unit. The three regions of the curve are:

i From the point of initiation of stress to the yield point. Within this region the metal is assumed to be completely elastic *i.e.* no permanent set occurs, until the proportional limit is reached, at which permanent set results if the applied stress is increased.

ii From the yield point to the maximum load point. Within this region both elastic and plastic deformation occur.

iii From the maximum load point to the point of fracture. Within this region some elastic deformation occurs but plastic deformation is dominant. At the fracture point the elastic elements in the specimen can no longer support the load.

It is considered that the total force applied to the specimen F (f is the force per unit area) is equivalent to the sum of forces f_1, f_2 and f_3, representing each of the above units respectively. Each of the units consists of an elastic element which is assumed to obey Hooke's law, and a viscous resistance which is assumed to follow the hyperbolic sine law.

As the elastic element of unit 1 is strained by application of force f_1, stress is proportional to strain until the proportional limit is reached. At this point the viscous element in unit 1 starts to flow, and when the rate of this flow is a maximum the elastic element is no longer elongating. The rate of flow is then equal to the rate of strain. The value of the strain at which the rate of flow is a maximum is defined as the yield point of the complete curve.

Simultaneously with the action of f_1 on unit 1, the application of f_2 on unit 2 causes an elongation in the latter unit in accordance with

Hooke's law. At some point in the curve the viscous element starts to flow. When the viscous flow of unit 2 is at its maximum rate the elastic element in the unit is no longer elongating, and the rate of flow is equivalent to the rate of strain. The strain at which the maximum flow rate is reached is defined as the strain at maximum load.

When force f_3 is applied to unit 3, Hooke's law is obeyed for an appreciable amount of strain, because of the low elastic modulus and high value of the viscous constants for this unit. If the testing temperature is sufficiently high and/or the rate of deformation sufficiently

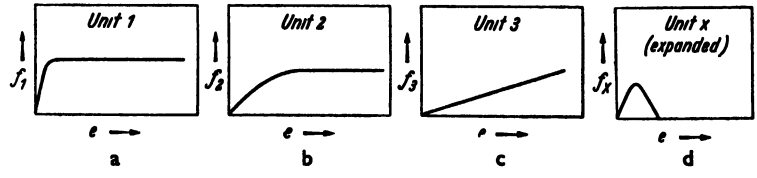

Figure 13a. Stress-strain curve for unit 1
Figure 13b. Stress-strain curve for unit 2
Figure 13c. Stress-strain curve for unit 3
Figure 13d. Stress-strain curve for unit 4
Figure 13e. Complete stress-strain curve

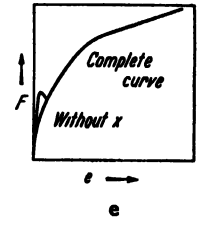

small, the viscous element in unit 3 will begin to flow at some finite value of stress and strain.

The stress-strain diagrams for the three units (*Figures 13a, b, c*) are combined to form the complete stress-strain curve for the material (*Figure 13e*). In the complete curve the modulus of elasticity is equivalent to the sum of the elastic moduli of the three units. The yield point occurs at the strain value at which the maximum flow rate of unit 1 occurs, and the strain at the maximum load point corresponds to the strain at the maximum flow of unit 2. The yield stress is determined by the sum of the stresses on the three units at the maximum flow point of unit 1, and the maximum load stress is equal to the sum of the three stresses at the maximum flow point of unit 2. Beyond the maximum load point the rates of flow of units 1 and 2 are at their limiting values, whereas the elastic element of unit 3 is being strained in accordance with Hooke's law, resulting in a straight line for this portion of the curve. The slope of the initial portion of the complete curve is determined by the sum

of the elastic moduli of the three units, whereas the slope of the final portion is equal to the elastic modulus of unit 3.

The above model has been proposed for a stress-strain relationship of a material in which the transition from apparent elastic to observable plastic deformation is gradual *i.e.* the yield point is not sharply defined. By making certain assumptions the model can be applied to metals possessing a sharply defined yield point.

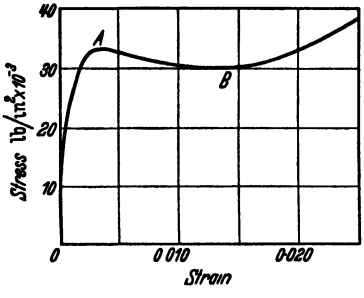

Figure 14. Stress-strain curve for an annealed mild steel

A stress-strain curve for an annealed mild steel is shown in *Figure 14*. The portion of the curve between A and B has been defined as the 'yield point elongation' and is characterized in tests at a constant strain rate by a decrease in stress with strain. Fredrickson and Eyring believe that the load at which yielding should occur is exceeded, and the yield point elongation is caused by the resistance of the metal to the high load. When plastic deformation begins the load drops, because the metal in the elastic state has more load carrying capacity than in the plastic state. Here the transition from elastic to plastic deformation is sudden.

It is assumed that the yield point elongation is structure sensitive and that this structure can be represented by a fourth unit, unit x in the model, which produces a unit stress-strain curve as shown in *Figure 13*d. Having once been broken by deformation unit x does not repair itself readily. For this reason a sharp yield point is not present when a previously deformed metal is stressed in tension. Annealing or long time aging will permit the broken bonds in unit x to re-form, and the metal will again exhibit yield point aging.

Fredrickson and Eyring, using the above model, have mathematically derived a stress-strain relationship for constant rate of strain, and point out the direct applications of the theory to various phenomena occurring in the deformation of metals.

Effect of Temperature and Rate of Deformation—The following relationship was developed for the dependence of the stress-strain curve on temperature and rate of deformation:

$$\dot{\epsilon} = B + CT^{\mu\sigma/T} \quad \ldots . \quad (39)$$

where $\dot{\epsilon}$ = strain rate, σ = stress, and C, μ and B are constants,

B being relatively independent of temperature. The strain rate varies approximately exponentially with stress and the reciprocal temperature, a fact which has been experimentally confirmed.[28, 29]

The amplitude of vibrations of atoms is irregular *i.e.* a vibration with a large amplitude may be followed by one with a small amplitude. Therefore the longer a given tensile stress is maintained, the greater the probability of an atom attaining sufficient activation energy to vibrate with a large amplitude with a subsequent migration into another site. For this reason it is evident that the rate of testing will have an influence on the nature of the stress-strain curve.

Effect of Grain Boundaries on Slip—Slip occurs by the movement of domains from one position of equilibrium to another. Although this movement requires vacant lattice sites and these predominate at the grain boundaries of a metal, as indicated by diffusion experiments, nevertheless it does not imply that slip should occur with greater ease at these boundaries. CHALMERS[30] has shown that when slip planes in two adjacent grains are not parallel it is difficult for a domain to cross the boundary from one grain into another. If a material were homogeneous it might be expected that slip would occur most easily where the density of vacant lattice sites is greatest. The general conception of a dislocation in a crystal is that of a long, straight, narrow hole some hundreds of atoms in length traversing a crystal. In this picture the successive stages by which the dislocation moves through the crystal can be visualized. However, if irregularly spaced, more numerous vacancies are present, such as probably exist at a grain boundary, although the movement of single atoms is facilitated, it is difficult to see a domain of atoms moving relative to the irregularities. Some parts of the domain would have to move farther than others, and the activation energy for this movement would be high where an irregular, non-isotropic material exists.

Strain Hardening—The increase in hardness of metals after deformation is directly attributed to the elastic element of unit 3 in the proposed model. Application of a force above the elastic limit causes the formation of internal stresses which are relieved only when the viscous elements have relaxed sufficiently. If the specimen is re-stressed prior to ultimate relaxation, these internal stresses must be overcome before plastic deformation can occur, and the specimen appears to deform elastically over a wider range of stress. The presence of internal

stresses increases the free energy of activation of the process. A change in structure of the metal, which brings about a smaller hole volume or fewer holes, will also increase the strength of the metal.

The temperature at which the tensile test is conducted has a profound influence on the magnitude of strain hardening. At high temperatures little increase in strain hardening occurs, because the viscous elements in unit 3 of the model relax so easily that the elastic element is practically inoperative.

Application of Theory to Tensile Data—Fredrickson and Eyring applied their proposed theory to tensile data determined by MacGregor and Fisher.[31] From the values of parameters required to fit the data it was shown that plastic deformation occurs by the movement of rather large domains from one position of equilibrium to another. The free energy of activation showed linear variation with temperature. The deformation appeared to be caused almost entirely by an entropy effect, with the apparent heat of activation approaching zero.

Speed of Propagation of Fracture Cracks—Saibel[32, 33] has applied the theory of reaction rates to the problem of the rate of propagation of fracture cracks in metals. He developed a thermodynamic theory of the fracture of metals, using the hole theory of the liquid state. The loss of cohesive strength was attributed to the formation of holes. It was shown that fracture took place when the critical energy density μ_c reached the value:

$$\mu_c = \left(L \frac{\Delta V}{V_s} + p\right) \qquad \ldots . \quad (40)$$

where L = latent heat of melting, ΔV = change in molecular volume on passing from the solid to the liquid state, V_s = molecular volume of the solid at the melting point, p = the hydrostatic component of the force system acting at the point of formation of the hole. When this component is compression, p is to be taken to be positive. The speed of fracture will be determined by the rate at which holes form. Each time a hole is formed the distance advanced by the crack will be equal to the diameter of the hole, and will correspond to λ in the equation:

$$\nu = \frac{2\lambda kT}{h} e^{\Delta S^{\ddagger}/R} e^{-\Delta H^{\ddagger}/RT} \sinh \frac{f\lambda\lambda_2\lambda_3}{2kT} \qquad \ldots . \quad (41)$$

which may be readily derived from equation 30.

In order that fracture may take place the heat of activation $\Delta H^{\ddagger}$

must equal the critical energy μ_c. It is furthermore assumed that the work done in forming the holes is equal to the heat of activation.

If n_h is the number of holes formed and as $f\lambda\lambda_2\lambda_3/2$ is the work done in forming each hole:

$$n_h \frac{f\lambda\lambda_2\lambda_3}{2} = \Delta H^{\ddagger} \qquad \ldots . \quad (42)$$

and

$$\frac{f\lambda\lambda_2\lambda_3}{2kT} = \frac{\Delta H^{\ddagger}}{n_h kT} = \frac{\Delta H^{\ddagger}}{n_h T.R/N} = \frac{n\Delta H^{\ddagger}}{RT}$$

where N is Avogadro's number and $n = N/n_h$.

Therefore the equation for the velocity of propagation becomes:

$$\nu = \frac{2\lambda kT}{h} e^{\Delta S^{\ddagger}/R} e^{-\Delta H^{\ddagger}/RT} \sinh \frac{n\Delta H^{\ddagger}}{RT} \qquad \ldots . \quad (43)$$

where

$$\Delta H^{\ddagger} = \mu_c = \left(L \frac{\Delta V}{V_s} + p\right)$$

Saibel was able to use the above equations to calculate the speed of propagation of a crack in iron at room temperature. The value he obtained was 69,500 in/sec (176,530 cm/sec). The average experimental value, obtained by HUDSON and GREENFIELD,[34] is 40,400 in/sec (102,616 cm/sec). The high value for ν obtained in the calculation may be explained by the assumption of a straight line motion of the crack, whereas the crack actually zigzags through the metal.

Creep—CHALMERS[35] showed that at low stresses the creep rate of single tin crystals is directly proportional to the applied stress rather than to an exponential involving the stress. At higher stresses it was found that the creep rate increases much more rapidly with the applied stress. Chalmers assumed that two different mechanisms were present, 'micro-creep' where the creep rate is proportional to the stress, and 'macro-creep' where the creep rate increases more rapidly. Kauzmann applied the hyperbolic sine equation to Chalmers' data in order to determine whether two mechanisms actually are involved.

Where the creep rate is proportional to the applied stress, and knowing the range of stresses for which this is true, an upper limit can be placed on the value of $q\lambda\lambda_2\lambda_3$. The relation used is:

$$\mu = \frac{2}{3}\frac{\lambda}{L}\frac{kT}{h} e^{\Delta S^{\ddagger}/R} e^{-\Delta H^{\ddagger}/RT} \sinh \frac{q\lambda\lambda_2\lambda_3 r}{2kT} \qquad \ldots . \quad (38)$$

The problem is merely to find the highest value for $q\lambda\lambda_2\lambda_3$ which for a given range of values of f will enable $\sinh q\lambda\lambda_2\lambda_3 r/2kT$ to be very

nearly equal to $q\lambda\lambda_2\lambda_3 r/2kT$. The upper value for $q\lambda\lambda_2\lambda_3$ is 5,000 Å^3, or about one tenth of its known value of 63,600 Å^3 for macrocreep.

However, there yet remains the possibility that the value for $q\lambda\lambda_2\lambda_3$ is of the order of 15 Å^3, which would correspond to single atoms acting as units of flow. In other words, microcreep may occur by the same process as self diffusion, and this is the reason that the creep rate is proportional to the applied stress.

Kauzmann compared the creep rate of solid lead, which was determined by McKeown,[36] with the diffusion rate of lead determined from data of Seith.[37] It was found that the creep of lead does not occur by means of a simple self diffusion mechanism. McKeown found that the creep rate was not proportional to the applied stress.

Chalmers also found that a rapid strain hardening was associated with microcreep, and the total extension in the single crystal of tin through the action of microcreep is more or less independent of the applied stress. However, the strain hardening disappears within a few hours or after a higher stress is applied for a short time. Chalmers suggested that the microcreep was the result of the flow of dislocations present in the metal and that this number of dislocations was limited.

As new dislocations form very slowly at low stresses, only the amount of creep corresponding to the dislocations already present is possible. The application of a larger stress would bring about the formation of new dislocations. Because the creep rate is proportional to the applied stress, Kauzmann believes that the rapid strain hardening associated with microcreep is caused by the exhaustion of diffusion paths favourably located for shear *i.e.* the depletion of vacant lattice sites along the given paths. The disappearance of strain hardening on standing would be caused by the slow movement of vacant sites into the paths from the surrounding medium. Kauzmann considers that the disappearance of strain hardening owing to the application of larger stresses might result from a readjustment that makes new paths of self diffusion available for causing shear.

Chalmers found that after a crystal had undergone all the microcreep of which it was capable, a small residual creep existed the rate of which was independent of the applied stress, and explained this residual creep by the formation of new dislocations in the crystal. Kauzmann's theory, however, claims that the rate of formation of dislocations is closely connected with the value of the applied stress. Kauzmann believes

that the residual creep is also caused as vacant lattice sites seep into the effective diffusion paths. He believes that since the direction of the diffusion of the holes is perpendicular to the direction of shear, the applied stress cannot have much effect on the activation energy for movement of the holes and therefore the rate of seepage remains relatively slow, thus causing the shear rate to remain sluggish.

RECRYSTALLIZATION

The latest theories on recrystallization have been discussed by Cook and Richards.[38] Krupkowski and Balicki[39] have proposed that the activation energy of recrystallization is independent of the amount of cold work, except for some materials of high deformation. Since deformation has little effect on the elastic modulus of a material, the activation energy of the recrystallization process should not be greatly affected by the degree of cold work. This theory, however, predicts that the rate of recrystallization is a maximum at the beginning of the recrystallization process, and this is in direct contradiction to experimental evidence.

Mehl and his collaborators[40–42] have expressed the rate of recrystallization in terms of two factors, the rate of nucleation N and the linear rate of grain growth G. From this theory, which involves a complex mathematical treatment, an abrupt alteration in the rate of recrystallization would be expected when growing crystals meet each other. This is not confirmed by experimental observation.

Cook and Richards believe that G is dependent on N, assuming that the growth of a recrystallized region occurs by nucleation on its surface. Only regions which are still in the cold worked state can exhibit nucleation and grain growth. The rate of recrystallization at any stage will then be dependent upon the proportion of metal in the cold worked state and the rate of nucleation of the specimen at that stage. The rate of nucleation in a cold worked sample may be different in regions remote from recrystallized domains and at points near the boundary between deformed and recrystallized regions. The rate of recrystallization must then be expressed in terms of the product of the rate of nucleation at the interface between cold worked and recrystallized regions and the fraction of metal still in the cold worked state affected by the interface and the product of the rate of nucleation inside the cold worked regions and the fraction of metal within these regions unaffected by the interface.

It is believed that for specimens subject to considerable amounts of deformation the above two rates approach the same value, and the rate of recrystallization is the product of the rate of nucleation and the fraction of metal still in the cold worked state. Cook and Richards believe that this argument is particularly applicable to recrystallization in heavily worked copper.

It is well known that a softening or recovery process occurs before recrystallization, and although it had been assumed that recovery and recrystallization are independent processes, Cook and Richards, from their investigations on copper, believe that the former is a necessary preliminary of the latter.

The lattice of severely deformed copper is highly distorted and possesses a high density of dislocations. Recovery or reduction of lattice distortion will occur by the activation of a dislocation, so that it is displaced by a slip mechanism until it is halted by a dislocation of similar sign or merges with a dislocation of opposite sign so that both vanish. Recovery then may be regarded as an atomic rearrangement of restricted range.

After considerable softening, the density of dislocations will be much lower. If one of the remaining dislocations is activated, a second type of atomic rearrangement will be initiated; recrystallized nuclei are formed. The rate of the second process will be governed by the extent to which the first has progressed.

If w is the fraction of the cold worked metal remaining in the unrecovered state at time t, and if B is the recovery rate:

$$\frac{dw}{dt} = Bw \qquad \ldots\ (44)$$

and

$$w = e^{-Bt} \qquad \ldots\ (45)$$

The fraction of recovered material (degree of recovery):

$$1 - w = 1 - e^{-Bt} \qquad \ldots\ (46)$$

and when Bt is small:

$$1 - w = Bt \qquad \ldots\ (47)$$

The process is one which must be activated, therefore B is dependent on temperature and is equal to $b\,e^{-P/RT}$, where b is a constant which varies with grain size and amount of deformation and P is the activation energy of the recovery process. Then:

$$1 - w = bt\,e^{-P/RT} \qquad \ldots\ (48)$$

It is assumed that the rate of recrystallization (dx/dt) is proportional

to the fraction $(1 - x)$ of metal remaining to be recrystallized, and to the degree of recovery $(1 - w)$ of the uncrystallized copper. Then:

$$\frac{dx}{dt} = a(1 - x)(1 - w)\, e^{-Q/RT} \quad \ldots\ (49)$$

where Q is the activation energy of the recrystallization process and a is a constant similar to b. Then:

$$\frac{dx}{dt} = abt(1 - x)\, e^{-Q/RT} e^{-P/RT} \quad \ldots\ (50)$$

and substituting $c = ab$:

$$\frac{dx}{dt} = ct(1 - x)\, e^{-(P+Q)/RT} \quad \ldots\ (51)$$

or rewriting the above equation:

$$t dt = \frac{1}{c} \frac{dx}{1-x} e^{(P+Q)/RT} \quad \ldots\ (52)$$

Integrating:

$$t^2 = \frac{2}{c} \log \frac{1}{1 - x} e^{(P+Q)/RT} \quad \ldots\ (53)$$

$$\therefore \quad \log t = \frac{1}{2} \log \left(\log \frac{1}{1 - x} \right) + \frac{1}{2} \log \frac{2}{c} + \frac{1}{2} \frac{(P + Q)}{RT} \quad \ldots\ (54)$$

The hardness of the metal, in this experiment copper, varies in an approximately linear manner with the proportion of the metal recrystallized x. Therefore from the value of the hardness at any time t and recrystallization temperature T, x can be determined. It was found from the experimental data that:

$$\log t = \frac{1}{2} \log \left(\log \frac{1}{1 - x} \right) + \text{constant} \quad \ldots\ (55)$$

thereby confirming the above theory.

If $\log t_{\frac{1}{2}}$ is plotted against T where $t_{\frac{1}{2}}$ is the time taken for each sample to reach a hardness half way between the initial and final hardness at each annealing temperature, a linear relationship is found the slope of which yields the activation energy $(P + Q)$. This has a value of about 44,000 cal/mol, which falls slightly with increasing cold rolling and decrease in initial grain size. This value applies to copper strips of 0·015 to 0·02 mm initial grain size.

When the grain size of the samples was 0·025 mm, $P + Q =$ 46,000 cal/mol, and if the grain size was 0·06 mm, $P + Q = 66{,}000$ cal/mol. The latter sample, unlike the former two, was not capable of self annealing.

The lower values of activation energy apply to samples which seem to recrystallize in regions which grow as laminae parallel to the surface of the strips. The larger value of the activation energy was obtained in samples in which the twin textures of the cold rolled strip recrystallize independently on annealing at low temperatures to form a structure with preferred orientation corresponding to that of one or the other of the initial twin textures.

Recrystallization and deformation are both processes involving atomic rearrangements, and there is probably a connection between the activation energy of recrystallization and the energy of the severest dislocation which can exist in the metal. Recrystallization can be considered to be the rearrangement of atoms to form a new lattice. If the lattice is three dimensional, three independent dislocations are necessary, each involving an energy E, and if the lattice is two dimensional, two dislocations are required. Recrystallization, in material which self anneals, involves nuclei which only grow in two dimensions, and this might account for the lower activation energies required.

SUPERLATTICES

In a substitutional solid solution the atoms of the components are arranged at random in the crystal lattice sites. For example, if we consider an alloy AB (50 atomic per cent component A : 50 atomic per cent component B), each site may be considered to be occupied half the time by an A atom and the other half by a B atom. This type of structure is called a disordered or random solid solution. With different compositions, however, certain sites will always be occupied by A atoms and the others by B atoms. This type of structure is known as a fully ordered solid solution or superlattice. An alloy consisting of 25 atomic per cent gold and 75 atomic per cent copper forms a random solid solution at high temperatures, but if annealed at low temperatures a superlattice is formed. The alloy crystallizes in a face-centred cubic lattice under both conditions, but in the superlattice the gold atoms occupy the sites at the cube corners and the copper atoms segregate in the sites at the face centres.

Several theories have been proposed for the superlattice phenomenon, but only the long-range order theory of BRAGG and WILLIAMS[43] will be discussed. Consider the solid solution alloy AB. In the fully ordered state the A atoms occupy one set of lattice sites (α-sites) and the B

atoms occupy another set (β-sites). In the random state half the α-sites are occupied by A atoms, the other half being occupied by B atoms. The degree of long-range order S is a parameter varying from 0 at complete disorder to 1 at complete order. For example, if 0·75 of the α-sites are occupied by A atoms and the other 0·25 are occupied by B atoms, $S = 0{\cdot}75 - 0{\cdot}25 = 0{\cdot}50$.

The internal energy of the alloy is a minimum when fully ordered. At low temperatures, where the entropy factor is minor, the fully ordered state ($S = 1$) will also be the one of minimum free energy. As the temperature is increased the entropy factor becomes more important, and in order to attain a minimum free energy some A atoms will interchange positions with B species.

Above some critical temperature the equilibrium state of the alloy will be that of complete disorder ($S = 0$). Therefore for each temperature below the critical value equilibrium will be characterized by a definite value of S.

The Rate of Approach to Equilibrium—Bragg and Williams have made calculations of the rate at which alloys will approach their equilibrium degree of order at a given temperature. It was assumed that the rate of approach to equilibrium is directly proportional to the discrepancy between the actual and equilibrium degree of order. The proportionality constant is taken to be the reciprocal of the time of relaxation τ where τ is the time required for an alloy to decrease its distance from equilibrium to 1/e of its initial amount. A reasonable expression for the time of relaxation as defined above is $\tau = A\, e^{W/kT}$, where W is the activation energy which a pair of neighbouring dissimilar atoms must have in order to exchange sites.

The value of τ for the system $AuCu_3$ is estimated to be 1 second at about 550°C, thereby accounting for the fact that complete disorder can be retained on quenching. In the copper-zinc system the rate of approach to equilibrium is so rapid that the disordered state cannot be retained by quenching, and this alloy is always highly ordered at room temperature.

Various possibilities which may occur in alloys are discussed by Bragg and Williams. The critical temperature T_c, above which no order is present, may have different positions with respect to three other temperatures T_a, T_q, and T_m. T_a is the temperature below which rates of migration of atoms are so slow that equilibrium can

never be attained. T_q is the temperature above which the rates of migration of atoms are so large that equilibrium is always obtained, no matter how fast the rate of cooling. T_m is the melting point. Obviously $T_m > T_q > T_a$. There are four possible positions for T_c: below T_a, between T_a and T_q, between T_q and T_m, and above T_m.

T_c below T_a. An ordered alloy will never be formed, because the totally disordered state corresponding to T_a will be produced. Such a relative position of T_c must be found in most alloy systems which do not display an ordered structure.

T_c between T_a and T_q. The structure will depend on the rate of cooling. A rapid rate of cooling will produce a disordered lattice, while a slowly cooled alloy will be partially ordered.

T_c between T_q and T_m. An ordered structure will always be produced. The fastest possible quench will not preserve a disordered structure.

T_c above T_m. The alloy will freeze directly into an ordered state. The behaviour of such an alloy will resemble an intermetallic compound rather than a solid solution.

REFERENCES

[1] GLASSTONE, S., LAIDLER, K. J. and EYRING, H. *The Theory of Rate Processes* New York, 1941
[2] HUNTINGTON, H. B. and SEITZ, F. *Phys. Rev.* 61 (1942) 315
[3] STEIGMAN, J., SHOCKLEY, W. and NIX, F. *ibid* 56 (1929) 790
[4] JOHNSON, R. P. *ibid* 56 (1929) 814
[5] EYRING, H. *J. chem. Phys.* 4 (1936) 283
[6] RHINES, F. N. and MEHL, R. F. *Trans. Amer. Inst. min. (metall.) Engrs* 128 (1938) 185
[7] STEARN, A. E. and EYRING, H. *J. phys. Chem.* 44 (1940) 955
[8] BRAUNE, H. *Z. phys. Chem.* 110 (1924) 147
[9] VAN LIEMPT, J. *Z. Phys.* 96 (1935) 534
[10] LANGMUIR, I. and DUSHMAN, S. *Phys. Rev.* 20 (1922) 113
[11] BARRER, R. M. *Diffusion in and through Solids* Cambridge, 1941
[12] SEITH, W. *Z. Elektrochem.* 39 (1933) 538
[13] BUGAHOW, W. and RYBALKO, F. *Tech. Phys. U.S.S.R.* 2 (1935) 617
[14] MEHL, R. *Trans. Amer. Inst. min. (metall.) Engrs* 122 (1936) 21
[15] FONDA, G., YOUNG, A. and WALKER, A. *Physics* 4 (1933) 1
[16] VAN LIEMPT, J. *Rec. Trav. chim.* 51 (1932) 114
[17] MATANO, C. *Jap. J. Phys.* 9 (1934) 41
[18] BECKER, R. *Proc. phys. Soc.* 52 (1940) 71
[19] COTTRELL, A. H. *Theoretical Structural Metallurgy* London, 1948
[20] MOTT, N. F. and NABARRO, F. R. N. *Proc. phys. Soc.* 52 (1940) 86
[21] GUINIER, A. *C.R. Acad. Sci., Paris* 204 (1937) 1115
[22] PRESTON, G. D. *Proc. phys. Soc.* 52 (1940) 77
[23] KAUZMANN, W. *Trans. Amer. Inst. min. (metall.) Engrs* 143 (1941) 57
[24] BECKER, R. *Phys. Z.* 26 (1925) 919

[25] NADAI, A. *J. appl. Phys.* 8 (1937) 418
[26] TAYLOR, G. I. *Proc. roy. Soc. A* 145 (1934) 362
[27] FREDRICKSON, J. W. and EYRING, H. *Amer. Inst. min. Engrs Tech. Publ.* No. 2423, 1948
[28] CLARK, D. S. and DATWYLER, G. *Proc. Amer. Soc. Test. Mater.* 38 (1938) 98
[29] MANJOINE, M. and NADAI, A. *ibid* 40 (1941) 822
[30] CHALMERS, B. *Proc. roy. Soc. A* 162 (1937) 120
[31] MACGREGOR, C. W. and FISHER, J. C. *Trans. Amer. Soc. mech. Engrs* 67 (1946) A217
[32] SAIBEL, E. *Trans. N.Y. Acad. Sci.* 11 (1939) 135
[33] —— *Amer. Inst. Min. Engrs Tech. Publ.* No. 2131, 1947
[34] HUDSON, G. and GREENFIELD, M. J. *J. appl. Phys.* 4 (1947) 405
[35] CHALMERS, B. *Proc. roy. Soc. A* 156 (1936) 427
[36] MCKEOWN, J. *J. Inst. Met.* 60 (1937) 20
[37] SEITH, W. *Diffusion in Metallen* p 42 Berlin, 1939
[38] COOK, M. and RICHARDS, T. L. *J. Inst. Met.* 73 (1946) 1
[39] KRUPKOWSKI, A. and BALICKI, M. *Ann. Acad. Sci. Tech. Warsaw* 4 (1937) 270
[40] JOHNSON, W. A. and MEHL, R. F. *Trans. Amer. Inst. min. (metall.) Engrs* 135 (1939) 416
[41] STANLEY, J. K and MEHL, R. F. *ibid* 150 (1942) 260
[42] ANDERSON, W. A. and MEHL, R. F. *Amer. Inst. min. Engrs Tech. Publ.* No. 1805, 1945
[43] BRAGG, W. L. and WILLIAMS, E. J. *Proc. roy. Soc. A* 145 (1934) 699

3

ANISOTROPY IN METALS

W. Boas and J. K. Mackenzie

SOME properties of matter, such as density, are defined by a relation between quantities (mass and volume) which are measured without reference to direction. Thus, density and similar properties are independent of direction. On the other hand, properties like electrical conductivity are defined by a relation between quantities (current density and electric field) which must be specified in magnitude and in direction. We may expect, then, properties like the electrical conductivity to depend, in general, on the direction of measurement. It is with such properties and their dependence on the direction of measurement that we shall be concerned in the following.

The physical and chemical properties of gases or crystals measured in the same direction, where direction is relevant, are the same at all points; both gases and crystals are homogeneous. Also, in a gas, the physical and chemical properties are independent of the direction of measurement *i.e.* gases show isotropy. On the other hand, in crystals, the properties in general depend on the direction in which they are measured and this is called anisotropy; all crystals show anisotropy in some of their properties. Homogeneity may be described as invariance of the measured value of a property under any translation, while isotropy is invariance under any rotation.

The fact that properties of crystals are anisotropic has been known for a very long time. The ancients used the easy cleavage of minerals along certain planes. This is due to the cohesion of crystals being weaker in some directions than in others. HUYGHENS discovered that various faces of calcite differed in hardness and so did different directions in the same plane.

Until about thirty years ago physical measurements on crystals were restricted to those on naturally occurring minerals. It is due to the development of the various techniques for producing large single-crystal specimens of metals that we now have values of the constants associated with many anisotropic properties of metals. As most of the earlier mineralogists were interested in the optical properties (refractive

index) and these are isotropic in cubic crystals, it is a widespread belief that all properties of cubic crystals are isotropic. It is therefore necessary to emphasize that this is not the case and that even cubic crystals show a very marked anisotropy in their elastic and plastic properties.

The anisotropy of the physical properties of a crystal is a consequence of its geometrical anisotropy or, in other words, of the crystal structure. Both this structure and the extent of the anisotropy of the properties depend on the forces between the atoms composing the crystal and therefore vary with the chemical composition. On the other hand, the general manner in which a property depends on the direction parallel to which it is measured is the same in crystals of the same class; it is determined by considerations of symmetry alone. All the properties of a crystal are governed by the same symmetry scheme: that of its lattice.

The derivation of the formulae giving a property as a function of the orientation requires a lengthy calculation although the results are quite simple. For this reason, the derivation will be sketched for one case only: that for which the property is defined by a linear relation between two vectors. After giving the relevant formulae for the other properties the systematic trends in the experimental values of the various constants will be discussed in relation to their physical causes. Finally, the effect of anisotropy on the behaviour of polycrystalline metals will be treated.

MATHEMATICS OF VECTOR-VECTOR RELATIONS

We shall be concerned only with properties defined by a relation between quantities which can be represented by means of scalars, vectors or tensors. For example, the relation between the change in temperature (scalar) and the resulting change in dimensions (tensor) defines the thermal expansion, the relation between the electric field (vector) and the current density (vector) defines the electrical conductivity, and that between stress (tensor) and strain (tensor) defines the elastic properties. Furthermore, it will be assumed that experiment has shown the relation to be a linear one to a sufficient degree of approximation.

The manner in which a particular property varies with direction depends not only on the symmetry of the crystal being studied but also on the nature of the physical process involved *i.e.* whether the property represents a relation between a scalar and a tensor, between two

vectors or between two tensors. The case of a linear relation between two vectors will now be considered in more detail.

For convenience, we shall assume that the property under consideration is the electrical conductivity for which the linear relation in question connects the current density **i** with the electric field **E**. However, the relations given are quite general and the vectors **i** and **E** may be taken as any pair of linearly related vectors. Then, if i_1, i_2, i_3 and E_1, E_2, E_3 are the components of these two vectors along any three mutually perpendicular axes, the most general linear relation connecting **i** with **E** is as follows:

$$\left.\begin{aligned} i_1 &= \sigma_{11}E_1 + \sigma_{12}E_2 + \sigma_{13}E_3 \\ i_2 &= \sigma_{21}E_1 + \sigma_{22}E_2 + \sigma_{23}E_3 \\ i_3 &= \sigma_{31}E_1 + \sigma_{32}E_2 + \sigma_{33}E_3 \end{aligned}\right\} \quad \ldots . \quad (1)$$

where the σ_{jk} are the conductivity coefficients. These coefficients σ_{jk} define a second order tensor, the conductivity tensor. The equations 1 may be solved to give E_1, E_2, E_3 in terms of i_1, i_2, i_3, and the resulting relations are as follows:

$$\left.\begin{aligned} E_1 &= \rho_{11}i_1 + \rho_{12}i_2 + \rho_{13}i_3 \\ E_2 &= \rho_{21}i_1 + \rho_{22}i_2 + \rho_{23}i_3 \\ E_3 &= \rho_{31}i_1 + \rho_{32}i_2 + \rho_{33}i_3 \end{aligned}\right\} \quad \ldots . \quad (2)$$

where the ρ_{jk} are the resistivity coefficients. The value of ρ_{jk} can be calculated from the σ_{jk} by means of the formula:

$$\rho_{jk} = \Sigma_{kj}/\Delta \quad \ldots . \quad (3)$$

where Δ is the value of the determinant formed from the coefficients σ_{jk} and Σ_{kj} is the co-factor of the corresponding element σ_{kj} and is $(-1)^{k+j}$ times the determinant found by striking out the k^{th} row and j^{th} column of Δ; the determinant formed from the coefficients ρ_{jk} is $1/\Delta$.

Two important deductions about the coefficients σ_{jk} can be derived from general energy considerations. First, the reciprocal relations

$$\sigma_{jk} = \sigma_{kj} \quad \ldots . \quad (4)$$

hold, and hence $\rho_{jk} = \rho_{kj}$, reducing the number of independent constants to six. Second, the determinant Δ is positive and so the expression of the E's in terms of the i's as in equation 2 is always possible. The analysis is complicated and so only the physical basis will be indicated. In these considerations it is necessary to distinguish between two classes of properties: *I* those which concern transport phenomena involving dynamical quantities such as electric current, and for which

the rate of dissipation of energy is important, and 2 those which concern static properties such as the dielectric properties and for which the stored energy is important. The typical example of such a static property will be taken to be the dielectric constant, which is defined by the relation between the electric field and the electric induction (displacement).

It can be shown that for transport phenomena the rate of dissipation of energy per unit volume is given by:

$$\partial w/\partial t = w' = i_1E_1 + i_2E_2 + i_3E_3 \qquad \ldots . \quad (5)$$

while for static properties the energy per unit volume is given by:

$$W = \tfrac{1}{2}(i_1E_1 + i_2E_2 + i_3E_3) \qquad \ldots . \quad (6)$$

and is equal to the work done in bringing unit volume of the body from an initial state with zero field to the final state. (It should be noted that $\mathbf{i}$ is the electric induction in the static case.) By substituting the values of the E's given by equation 2 into equation 5, we can express the rate of dissipation of energy as a homogeneous quadratic function of the i's. This gives:

$$w' = \rho_{11}i_1^2 + (\rho_{12} + \rho_{21})i_1i_2 + \rho_{22}i_2^2 + (\rho_{13} + \rho_{31})i_1i_3 + (\rho_{23} + \rho_{32})i_2i_3 + \rho_{33}i_3^2 \qquad \ldots . \quad (7)$$

and a similar expression with a factor $\frac{1}{2}$ for static properties.

For static properties, we now assume that the electric field is derivable by differentiation from a potential which is W *i.e.* $E_1 = \partial W/\partial i_1$ *etc.* The reciprocal relations $\rho_{jk} = \rho_{kj}$ follow immediately on comparison with the equations 2. The existence of such a potential function can be shown to be equivalent to a variational principle. This principle states that, when there is equilibrium and the values of the i's are given on the boundary of a body, the distribution of $\mathbf{i}$ inside the body is such that the total (free) energy is minimum.

With transport phenomena, it is the variational principle which is perhaps better known. Its statement is the same as for the static properties except that it is the total rate of dissipation of free energy (in general, the rate of production of entropy when the temperature is not constant) which is a minimum. This principle is known as Rayleigh's principle of least dissipation of energy and its generalization to cover the case of anisotropic media is due to ONSAGER.[1] It follows that $\frac{1}{2}w'$ is a suitable potential function and that the reciprocal relations hold. For electrical conduction Rayleigh's principle can be expressed

by the more familiar statement that the current distributes itself so that the total heating effect is a minimum.

Actually, Onsager first derives general reciprocal relations from the principle of detailed balancing and from these the generalization of Rayleigh's principle. The principle of detailed balancing asserts that when the processes occurring in a body are in dynamic equilibrium the transitions between any two (classes of) atomic configurations A and B should take place equally often in the directions A $\rightarrow$ B and B $\rightarrow$ A in a given time, independently of any other interactions involving A or B. This principle is not applicable in the presence of a magnetic field, and Onsager shows that the reciprocal relations (equation 4) must then be replaced by:

$$\sigma_{jk}(H) = \sigma_{kj}(-H) \qquad \ldots . \quad (8)$$

In the presence of a magnetic field the current lines from a point source follow spiral paths[2] and in the case of electrical conduction this leads to the well known Hall effect.

Since both the energy and the rate of dissipation of energy are essentially positive and quadratic in the components of $\mathbf{i}$ it follows from a mathematical theorem[3] that Δ is positive.

Energy considerations alone have been involved up to this point. It will now be shown what additional information can be obtained by consideration of the symmetry of the crystal.

First, the relations 1 between $\mathbf{i}$ and $\mathbf{E}$ imply that the conductivity is a centro-symmetrical property *i.e.* the same set of constants σ_{jk} apply when the direction of both the field and the current density is reversed. The geometrical configuration of the atoms has not necessarily a centre of symmetry *e.g.* in a hexagonal close packed structure, so that not all properties need have the same value on reversal of the direction of measurement. It is a matter for experiment to decide which physical properties are and which are not centro-symmetrical; the present theory applies only to centro-symmetrical properties. For these, there is no distinction between classes of crystals with and without a centre of symmetry and the number of crystal classes for which a property behaves differently is thus reduced[4] from 32 to 11.

If the crystal is triclinic and therefore has no other symmetry elements, no further reduction can be made in the number of constants. However, when the crystal has other symmetry elements, further reductions can be made. For a crystal with planes of symmetry

perpendicular to each of the crystallographic axes, the relationship between **i** and **E** must remain the same when any axis is reversed in direction. Then, consideration of the equations 1 shows that all the σ_{jk} for $j \neq k$ vanish. Further, in a cubic crystal all the axes are equivalent, so that they may be renamed cyclically (*i.e.* $x \rightarrow y, y \rightarrow z, z \rightarrow x$) without changing the relationship, thus $\sigma_{11} = \sigma_{22} = \sigma_{33}$. As will be seen below, this implies that a cubic crystal is isotropic for all properties involving linear vector-vector relationships. For other properties (*e.g.* elastic), however, this simple reduction does not occur, and even a cubic crystal is anisotropic.

For hexagonal, tetragonal and trigonal crystals their symmetry implies that $\sigma_{11} = \sigma_{22} \neq \sigma_{33}$, all the other constants being zero.[4] The z-axis is always taken along the hexagonal, tetragonal or trigonal axis; since we are using orthogonal axes the x- and y-axes cannot both be taken along the usual crystallographic axes for hexagonal and trigonal crystals. For all these crystals the relations 1 simplify to the following:

$$i_1 = \sigma_{11}E_1,\ i_2 = \sigma_{11}E_2,\ i_3 = \sigma_{33}E_3 \qquad \ldots\ (9)$$

We now return to the original equations 1 and introduce the idea of principal directions. In general, the current density **i** which results from the electric field **E** is not in the same direction as **E**. However, it may be shown[5] that when the reciprocal relations 4 hold there are always three mutually perpendicular directions such that, when the field is in any one of these three directions, the resulting current density is in the same direction; these directions are called principal directions. Clearly, when the coordinate axes are taken in these three directions the relations 1 simplify to:

$$i_1 = \sigma_{11}E_1,\ \ i_2 = \sigma_{22}E_2,\ \ i_3 = \sigma_{33}E_3 \qquad \ldots\ (10)$$

In general, these principal directions have no relation to the crystallographic axes and must therefore be defined relative to them. This requires three independent constants, and in order to specify the conductivity of a body completely these must be given in addition to the three principal conductivities σ_{11}, σ_{22}, σ_{33}. There are still six independent constants involved as in equation 1. Further, the principal directions may be different for different properties. However, when the crystal has higher symmetry this is not so, and comparison of the equations 9 and 10 shows that, for all the four crystal systems of interest in connection with metals, the principal directions must of

necessity coincide with the crystallographic axes for all properties defined by a linear vector-vector relationship. The principal directions for the resistivity are the same as those for the conductivity and $\rho_{11} = 1/\sigma_{11}$ *etc.*

Finally, we will calculate the variation in the measured properties with direction. We will take the principal directions as the axes of reference and suppose that an electric field is applied in a direction making an angle θ with the z-axis and such that the plane containing the direction of **E** and the z-axis makes an angle ϕ with the xz-plane; then the components of **E** are $(E \sin\theta \cos\phi, E \sin\theta \sin\phi, E \cos\theta)$, so that on substitution in equation 10 the resulting components of the current density are:

$$i_1 = E\sigma_{11} \sin\theta \cos\phi \qquad i_2 = E\sigma_{22} \sin\theta \sin\phi$$
$$i_3 = E\sigma_{33} \cos\theta$$

The component of the current density in the direction of **E** is found by resolving these components in the direction of **E**. This gives:

$$i_{obs}/E = \sigma_{11} \sin^2\theta \cos^2\phi + \sigma_{22} \sin^2\theta \sin^2\phi + \sigma_{33} \cos^2\theta \quad \ldots . \quad (11)$$

which is equal to the observed conductivity. When $\sigma_{11} = \sigma_{22}$ as for most metals we have:

$$\sigma_{obs} = \sigma_{11} \sin^2\theta + \sigma_{33} \cos^2\theta \quad \ldots . \quad (12)$$

which is independent of ϕ and reduces to σ_{11} for cubic metals. Thus, the electrical conductivity is isotropic in cubic metals.

In this last calculation it was assumed that the total electric field was in the direction of measurement; however, the current density is not necessarily in the same direction. In some experiments, for example with wires, it is the total current density which is in a given direction. Then, using the resistivity equations 2 by analogy with equation 12:

$$\rho_{obs} = \rho_{11} \sin^2\theta + \rho_{33} \cos^2\theta$$

i.e.

$$\rho_{obs} = 1/\sigma_{11} \sin^2\theta + 1/\sigma_{33} \cos^2\theta \quad \ldots . \quad (13)$$

It is important to notice that ρ_{obs} is not equal to $1/\sigma_{obs}$.

VARIATION OF PROPERTIES WITH DIRECTION

In the previous section, formulae giving the variation of one type of property with direction were derived. These results will now be summarized and the corresponding formulae for other types of property will also be given. In all cases the orientation of the crystal

and all other physical quantities will be referred to a set of mutually orthogonal axes related to the usual crystallographic axes as follows. The z- or c-axis will be taken parallel to the axis of highest rotational symmetry (the principal axis) *i.e.* parallel to the trigonal, tetragonal or hexagonal axes for the respective crystal systems. The x- or a-axis will be taken along a perpendicular crystallographic axis (except for monoclinic or triclinic crystals) and the y-axis perpendicular to the other two; the y-axis will not be one of the usual crystallographic axes for trigonal or hexagonal crystals. Further, an arbitrary direction in a crystal will be specified relative to these axes by its direction cosines α, β, γ.

Vector-vector relations define properties such as the electrical or thermal conductivity, the dielectric constant, the para- and diamagnetic susceptibility and the constants connected with thermoelectric effects. We have shown that all these properties can be completely specified by three principal values which determine the property in three mutually orthogonal principal directions. These directions coincide with the x-, y- and z-axes defined above, except for monoclinic and triclinic crystals. The variation with direction of any of these properties, which for generality we denote by P, is given by:

$$P = P_a\alpha^2 + P_b\beta^2 + P_c\gamma^2 \qquad \ldots\ (11a)$$

where P_a, P_b, P_c are the principal values along the three axes. In systems with a three-, four- or sixfold rotation axis the property has rotational symmetry about this axis and there are only two independent principal values. In these cases, the precise orientations of the x- and y-axes are irrelevant and the variation of the property with direction is given by:

$$P = P_a(1 - \gamma^2) + P_c\gamma^2 \qquad \ldots\ (12a)$$

where $\gamma = \cos\theta$ and θ is the angle the direction makes with the axis of rotational symmetry (z-axis). Cubic crystals are isotropic.

There are two main methods of measurement which can be most easily described by reference to a particular property, the electrical conductivity. In one method, a plate of the crystal is cut with its main faces perpendicular to the direction (α, β, γ), and the current which flows when an electric field is applied across the plate is measured. The direction of the electric field is then in the direction (α, β, γ), but the resulting current density is not in general in this direction and it is

only the component of this current density resolved in the direction (α, β, γ) which can be measured. The components of the current density are calculated from the known components of the field by using the conductivity coefficients. It was shown in the last section that the observed conductivity is given by:

$$\sigma = \sigma_a(1 - \gamma^2) + \sigma_c\gamma^2 \qquad \ldots . \quad (12b)$$

for crystals of high symmetry. In the other method, a current is made to flow along a wire, the axis of which is in the direction (α, β, γ). In this case, it is the current density which is in the direction (α, β, γ) and only the resolved component of the electric field can be measured. The components of the field are now calculated from those of the current density by means of the resistivity coefficients and the observed resistivity is given by:

$$\rho = \rho_a(1 - \gamma^2) + \rho_c\gamma^2 \qquad \ldots . \quad (12c)$$

The important point to notice is that although $\rho_a = 1/\sigma_a$ and $\rho_c = 1/\sigma_c$, in general $\rho \neq 1/\sigma$. Similar difficulties occur in measuring elastic constants.

Similar though more complicated considerations have to be made in connection with properties resulting from scalar-tensor and tensor-tensor relations. Only the results will be quoted here, and for details reference should be made to the standard text on the subject, which is the famous work on crystal physics by VOIGT.[6]

The most important examples of scalar-tensor relations are the thermal expansion and the linear compressibility, although this is really a degenerate case of an elastic property. In both, the strain is related to a scalar, either temperature or hydrostatic pressure. In these instances the strain resulting from a uniform change in temperature (or applied pressure) is homogeneous, so that straight lines will remain straight lines and planes remain planes though the interatomic distances will be altered. This means that the indices of planes and directions will remain the same, but the axial ratios and, in monoclinic and triclinic crystals, the angles between the crystallographic axes will change. As the symmetry of a crystal is maintained the angles between the crystallographic axes in the crystals with higher symmetry remain the same. However, it is obvious that, for example, in a tetragonal crystal the angle between an (hkl) plane and the c-axis will alter as the c/a ratio alters with temperature (pressure).

Because a homogeneous strain is described by a tensor of the same type as that which specifies a vector-vector relation, the thermal expansion (linear compressibility) varies with direction in the same way as a property defined by a vector-vector relation; the variation is again given by equation 11*a*. Thus, as before, there are three principal directions which coincide with at least two of the usual crystallographic axes. In orthorhombic crystals there are three distinct principal values of the thermal expansion. For trigonal, tetragonal and hexagonal crystals there is rotational symmetry about the *c*-axis and the variation of the thermal expansion with direction is given by equation 12*a*, while cubic crystals are isotropic.

The corresponding equations for the variations in the elastic properties are considerably more complicated, as these result from a tensor-tensor relation. The stress tensor is symmetrical and has for its components the three normal stresses X_x, Y_y, Z_z in the *x*-, *y*-, and *z*-directions, and the three shear stresses X_y, Y_z, Z_x. The tensor specifying a homogeneous strain is also symmetrical and has for its components the three extensions e_{xx}, e_{yy}, e_{zz} in the *x*-, *y*-, and *z*-directions and the three shears e_{xy}, e_{yz}, e_{zx}. Now, according to the generalized Hooke's law there is a linear relation between stress and strain. This relation is usually written in the form:

$$\left.\begin{aligned}
X_x &= c_{11}e_{xx} + c_{12}e_{yy} + c_{13}e_{zz} + c_{14}e_{yz} + c_{15}e_{zx} + c_{16}e_{xy} \\
Y_y &= c_{21}e_{xx} + c_{22}e_{yy} + c_{23}e_{zz} + c_{24}e_{yz} + c_{25}e_{zx} + c_{26}e_{xy} \\
Z_z &= c_{31}e_{xx} + c_{32}e_{yy} + c_{33}e_{zz} + c_{34}e_{yz} + c_{35}e_{zx} + c_{36}e_{xy} \\
Y_z &= c_{41}e_{xx} + c_{42}e_{yy} + c_{43}e_{zz} + c_{44}e_{yz} + c_{45}e_{zx} + c_{46}e_{xy} \\
Z_x &= c_{51}e_{xx} + c_{52}e_{yy} + c_{53}e_{zz} + c_{54}e_{yz} + c_{55}e_{zx} + c_{56}e_{xy} \\
X_y &= c_{61}e_{xx} + c_{62}e_{yy} + c_{63}e_{zz} + c_{64}e_{yz} + c_{65}e_{zx} + c_{66}e_{xy}
\end{aligned}\right\} \quad \ldots . \quad (14)$$

The constants c_{jk} are called the elastic moduli and they have the dimensions of stress. The corresponding set of equations for the strain components as functions of the stress components is:

$$\left.\begin{aligned}
e_{xx} &= s_{11}X_x + s_{12}Y_y + s_{13}Z_z + s_{14}Y_z + s_{15}Z_x + s_{16}Xy \\
e_{yy} &= s_{21}X_x + s_{22}Y_y + s_{23}Z_z + s_{24}Y_z + s_{25}Z_x + s_{26}X_y \\
e_{zz} &= s_{31}X_x + s_{32}Y_y + s_{33}Z_z + s_{34}Y_z + s_{35}Z_x + s_{36}X_y \\
e_{yz} &= s_{41}X_x + s_{42}Y_y + s_{43}Z_z + s_{44}Y_z + s_{45}Z_x + s_{46}X_y \\
e_{zx} &= s_{51}X_x + s_{52}Y_y + s_{53}Z_z + s_{54}Y_z + s_{55}Z_x + s_{56}X_y \\
e_{xy} &= s_{61}X_x + s_{62}Y_y + s_{63}Z_z + s_{64}Y_z + s_{65}Z_x + s_{66}X_y
\end{aligned}\right\} \quad \ldots . \quad (15)$$

where the s_{jk} are called the elastic coefficients.

As for the vector-vector relation, the existence of a strain energy function (the free energy) leads to the reciprocal relations:

$$c_{jk} = c_{kj} \quad s_{jk} = s_{kj} \qquad \ldots . \quad (16)$$

These relations reduce the number of independent moduli or coefficients from 36 to 21. The relations between the c_{jk} and the s_{jk} can conveniently be expressed by the following equations:

$$c_{1h}s_{1k} + c_{2h}s_{2k} + c_{3h}s_{3k} + c_{4h}s_{4k} + c_{5h}s_{5k} + c_{6h}s_{6k} = \begin{cases} 1 & (h=k) \\ 0 & (h \neq k) \end{cases} \ldots . \quad (17)$$

where h and k take all values from 1 to 6.

The number of independent constants can be reduced when the crystal has higher symmetry. This reduction is summarized in *Table I.* The same reductions occur for both the coefficients and the moduli, so that apart from the trivial modifications indicated in the table the two schemes are identical. In the case of the trigonal and tetragonal systems, it has been assumed that the x-axis is a twofold rotation axis or alternatively the yz-plane is one of reflection symmetry.

Table I gives the expressions for the variation with direction of Young's modulus, rigidity modulus, and linear and cubic compressibility. The linear compressibility gives the relative change in length of a line when the body is subjected to unit hydrostatic pressure. It varies with orientation, whereas the cubic compressibility is isotropic. Only in the hexagonal system, contrary to the properties discussed previously, have the elastic properties rotational symmetry about the hexagonal axis. In the cubic system, anisotropy still occurs with the exception of the linear compressibility. In these crystals the variation of both Young's modulus and rigidity modulus depends only on the quantity $(\alpha^2\beta^2 + \beta^2\gamma^2 + \gamma^2\alpha^2)$. This quantity is zero for the ⟨100⟩ direction and has its maximum value 1/3 in the ⟨111⟩ direction. Hence, if $(s_{11} - s_{12} - \frac{1}{2}s_{44})$ is positive, Young's modulus is maximum in the ⟨111⟩ direction and minimum in the ⟨100⟩ direction, while the rigidity modulus is minimum in the ⟨111⟩ direction and maximum in the ⟨100⟩ direction. If $(s_{11} - s_{12} - \frac{1}{2}s_{44})$ is negative the reverse variation occurs.

The reciprocal of the rigidity modulus is the torsion of a free cylinder under a couple of unit magnitude. It is typical of anisotropic materials that a couple produces bending in the cylinder as well as torsion. This bending vanishes only for special orientations of the cylinder.[7] For cubic crystals this occurs when the axis of the cylinder is in ⟨100⟩,

Table I. Anisotropy of Elasticity of Crystals

Property	*Trigonal System*	*Tetragonal System*	*Hexagonal System*	*Cubic System*
Scheme of elastic moduli	$\begin{matrix} c_{11} & c_{12} & c_{13} & c_{14} & 0 & 0 \\ c_{12} & c_{11} & c_{13} & -c_{14} & 0 & 0 \\ c_{13} & c_{13} & c_{33} & 0 & 0 & 0 \\ c_{14} & -c_{14} & 0 & c_{44} & 0 & 0 \\ 0 & 0 & 0 & 0 & c_{44} & c_{14} \\ 0 & 0 & 0 & 0 & c_{14} & \frac{1}{2}(c_{11}-c_{12}) \end{matrix}$	$\begin{matrix} c_{11} & c_{12} & c_{13} & 0 & 0 & 0 \\ c_{12} & c_{11} & c_{13} & 0 & 0 & 0 \\ c_{13} & c_{13} & c_{33} & 0 & 0 & 0 \\ 0 & 0 & 0 & c_{44} & 0 & 0 \\ 0 & 0 & 0 & 0 & c_{44} & 0 \\ 0 & 0 & 0 & 0 & 0 & c_{66} \end{matrix}$	$\begin{matrix} c_{11} & c_{12} & c_{13} & 0 & 0 & 0 \\ c_{12} & c_{11} & c_{13} & 0 & 0 & 0 \\ c_{13} & c_{13} & c_{33} & 0 & 0 & 0 \\ 0 & 0 & 0 & c_{44} & 0 & 0 \\ 0 & 0 & 0 & 0 & c_{44} & 0 \\ 0 & 0 & 0 & 0 & 0 & \frac{1}{2}(c_{11}-c_{12}) \end{matrix}$	$\begin{matrix} c_{11} & c_{12} & c_{12} & 0 & 0 & 0 \\ c_{12} & c_{11} & c_{12} & 0 & 0 & 0 \\ c_{12} & c_{12} & c_{11} & 0 & 0 & 0 \\ 0 & 0 & 0 & c_{44} & 0 & 0 \\ 0 & 0 & 0 & 0 & c_{44} & 0 \\ 0 & 0 & 0 & 0 & 0 & c_{44} \end{matrix}$
Scheme of elastic coefficients	$s_{66} = 2(s_{11} - s_{12})$, $s_{56} = 2s_{14}$		$s_{66} = 2(s_{11} - s_{12})$	
Number of independent constants	6	6	5	3
Linear compressibility .	$s_{11} + s_{12} + s_{13} - \gamma^2(s_{11} + s_{12} - s_{13} - s_{33})$	$s_{11} + s_{12} + s_{13} - \gamma^2(s_{11} + s_{12} - s_{13} - s_{33})$	$s_{11} + s_{12} + s_{13} - \gamma^2(s_{11} + s_{12} - s_{13} - s_{33})$	$s_{11} + 2s_{12}$
Cubic compressibility .	$2s_{11} + s_{33} + 2(s_{12} + 2s_{13})$	$2s_{11} + s_{33} + 2(s_{12} + 2s_{13})$	$2s_{11} + s_{33} + 2(s_{12} + 2s_{13})$	$3(s_{11} + 2s_{12})$
Transformation of s_{ik} into c_{ik}	$c_{11} + c_{12} = \frac{s_{33}}{s}$ $\quad c_{11} - c_{12} = \frac{s_{44}}{s'}$ $c_{13} = -\frac{s_{13}}{s}$ $\quad c_{14} = -\frac{s_{14}}{s'}$ $c_{33} = \frac{s_{11} + s_{12}}{s}$ $\quad c_{44} = \frac{s_{11} - s_{12}}{s'}$ $s = s_{33}(s_{11} + s_{12}) - 2s^2_{13}$ $s' = s_{44}(s_{11} - s_{12}) - 2s^2_{14}$	$c_{11} + c_{12} = \frac{s_{33}}{s}$ $c_{11} - c_{12} = \frac{1}{s_{11} - s_{12}}$ $c_{13} = -\frac{s_{13}}{s}$ $\quad c_{33} = \frac{s_{11} + s_{12}}{s}$ $c_{44} = \frac{1}{s_{44}}$ $\quad c_{66} = \frac{1}{s_{66}}$ $s = s_{33}(s_{11} + s_{12}) - 2s^2_{13}$	$c_{11} + c_{12} = \frac{s_{33}}{s}$ $c_{11} - c_{12} = \frac{1}{s_{11} - s_{12}}$ $c_{13} = -\frac{s_{13}}{s}$ $\quad c_{33} = \frac{s_{11} + s_{12}}{s}$ $c_{44} = \frac{1}{s_{44}}$ $s = s_{33}(s_{11} + s_{12}) - 2s^2_{13}$	$c_{11} = \frac{s_{11} + s_{12}}{(s_{11} - s_{12})(s_{11} + 2s_{12})}$ $c_{12} = \frac{-s_{12}}{(s_{11} - s_{12})(s_{11} + 2s_{12})}$ $c_{44} = \frac{1}{s_{44}}$
Linear longitudinal dilation of cylinder under axial stress (reciprocal of Young's modulus)	$s_{11}(1 - \gamma^2)^2 + s_{33}\gamma^4 + (2s_{13} + s_{44})\gamma^2(1 - \gamma^2) + 2s_{14}\beta\gamma(3\alpha^2 - \beta^2)$	$s_{11}(\alpha^4 + \beta^4) + s_{33}\gamma^4 + (2s_{12} + s_{66})\alpha^2\beta^2 + (2s_{13} + s_{44})\gamma^2(1 - \gamma^2)$	$s_{11}(1 - \gamma^2)^2 + s_{33}\gamma^4 + (2s_{13} + s_{44})\gamma^2(1 - \gamma^2)$	$s_{11} - 2(s_{11} - s_{12} - \frac{1}{2}s_{44})(\alpha^2\beta^2 + \beta^2\gamma^2 + \gamma^2\alpha^2)$
Free torsion of a cylinder (reciprocal of rigidity modulus)	$s_{44} + (s_{11} - s_{12} - \frac{1}{2}s_{44})(1 - \gamma^2) + 2(s_{11} + s_{33} - 2s_{13} - s_{44})\gamma^2(1 - \gamma^2) - 4s_{14}\beta\gamma(3\alpha^2 - \beta^2)$	$\frac{1}{2}(s_{44} + s_{66})(\alpha^4 + \beta^4) + s_{44}\gamma^4 + [4(s_{11} - s_{12}) + (s_{44} - s_{66})]\alpha^2\beta^2 + [2(s_{11} + s_{33} - 2s_{13}) + \frac{1}{2}(s_{66} - s_{44})]\gamma^2(1 - \gamma^2)$	$s_{44} + (s_{11} - s_{12} - \frac{1}{2}s_{44})(1 - \gamma^2) + 2(s_{11} + s_{33} - 2s_{13} - s_{44})\gamma^2(1 - \gamma^2)$	$s_{44} + 4(s_{11} - s_{12} - \frac{1}{2}s_{44})(\alpha^2\beta^2 + \beta^2\gamma^2 + \gamma^2\alpha^2)$

⟨110⟩ or ⟨111⟩ directions, and for hexagonal crystals when it is parallel to the hexagonal axis or at right angles to it. If the bending of the crystal is hindered by its surroundings the torsion of the crystal is smaller than if it were free.

Finally, attention may be drawn to the fact that the numerical values of the elastic constants depend on whether they are measured by static or by dynamic methods. In the latter case, any heat produced locally by the oscillations will not be conducted away if the frequency is high enough, and therefore the adiabatic constants will be obtained. Static methods will give the isothermal constants. However, the difference betweeen isothermal and adiabatic constants is small and sometimes even zero.

EXPERIMENTAL RESULTS ON BULK PROPERTIES

The results of the most reliable measurements of the elastic, electrical and thermal properties of metal crystals are summarized in *Tables II–VI.* We shall now briefly discuss how the anisotropy can be explained in physical terms and consider some qualitative relations which may be expected to hold between the extents of the anisotropy of different properties. It will be seen that the elastic properties and the magnitude of the thermal vibrations of the atoms are the basis of these relations.

In *Tables II* and *III* the elastic constants of pure metals at room temperature are given, while *Table IV* gives those of alloy crystals. In every case in which a check was made the measurements have confirmed the theoretically predicted effect of orientation. Of the cubic metals, the anisotropy of aluminium and tungsten is very small, and the same holds for the hexagonal magnesium. The quantity $(s_{11} - s_{12} - \frac{1}{2}s_{44})$ is positive for all cubic metals except molybdenum, and therefore the maximum values of Young's modulus and the minima of the rigidity modulus occur in the ⟨111⟩ directions for all these metals while for molybdenum these extreme values occur in the ⟨100⟩ directions. For copper, silver and gold, the maxima of Young's modulus and the rigidity modulus are more than 2·5 times the minimum values, whereas this factor is about 3 for lead and is still greater for zinc, cadmium and tin. In order to give a better picture of the manner in which Young's modulus and rigidity modulus depend on the orientation, these properties are represented by models for iron[14] as shown in

Table II. Elastic Coefficients in 10^{-13} *cm²/dyne*

Metal	s_{11}	s_{12}	s_{44}	s_{33}	s_{13}	s_{14}	s_{66}	*Ref.*
Aluminium ..	15 9	− 5·8	35·2					8
Nickel	7·99	− 3·12	8·44					9
Copper .. .	14·9	− 6·2	13·3					10
Silver ..	23·2	− 9·93	22·9					11
Gold ..	20·3	− 10·6	23·8					10
Lead ..	93	− 43	69					10
Sodium (80°*K*)	483	−208	169					12
Potassium (83°*K*)	823	−370	380					13
α-Iron .. .	7 57	− 2·82	8·62					14
Molybdenum .	2·8	− 0·78	9·1					15
Tungsten .	2 573	− 0·729	6·604					16
Magnesium .	22·15	− 7·7	60·3	19·75	− 4·93			17
Zinc	8·4	+ 1·1	26 4	28·7	− 7·75			18
Cadmium .	12·3	− 1 5	54·0	35·5	− 9 3			19
Mercury (83°*K*)	154	−119	151	45	−21	−100		20
Antimony ..	17·7	− 3·8	41·0	33·8	− 8·5	− 8 0		21
Bismuth ..	26 9	− 14·0	104·8	28·7	− 6 2	+ 16·0		21
Tellurium ..	48·7	− 6·9	58·1	23·4	−13·8	*unknown*		21
Tin	18·5	− 9·9	57 0	11 8	− 2 5		135	21

Table III. Elastic Moduli in 10^{12} *dyne/cm²*

Metal	c_{11}	c_{12}	c_{44}	c_{33}	c_{13}	c_{14}	c_{66}	*Ref.*
Aluminium ..	1·08	0 622	0·284					8
Nickel .. .	2·50	1·60	1 185					9
Copper	1·70	1·23	0·75					10
Silver	1·20	0·897	0 436					11
Gold ..	1·86	1·57	0·420					10
Lead	0 48	0 41	0·144					10
Sodium (80°*K*) ..	0·0601	0·0456	0 0593					12
Potassium (83°*K*)	0·0459	0 0372	0 0263					13
α-Iron	2·37	1 41	1·160					14
Molybdenum ..	4·6	1·79	1·09					15
Tungsten .	5 01	1·98	1·514					16
Magnesium ..	0 585	0·250	0·166	0·610	0·208			17
Zinc .. .	1·63	0·256	0·379	0 623	0·508			18
Cadmium ..	1·21	0·481	0·185	0·513	0 442			19
Mercury (83°*K*) ..	0·360	0·289	0·129	0·505	0·303	+ 0·05		20
Antimony ..	0 792	+0·298	0·285	0·427	0·261	+ 0·11		21
Bismuth	1·88	−0 90	1·08	0 440	0·211	− 0·42		21
Tellurium ..	?	?	?	0·700	0·231	?		21
Tin	0·839	0·487	0·175	0·967	0·28		0·074	21

Figures 1 and *2*. The large anisotropy of these properties is apparent.

For cubic crystals, the isotropy of the electrical resistivity seems to be well established,[36] although the accuracy of the measurements is not extremely high. However, in a recent x-ray investigation, it has been claimed[37] that the thermal expansion of iron is different in different crystallographic directions. Further investigations seem to be necessary

Table IV. Elastic Constants of Crystals of Solid Solutions

Alloy	s_{11}	s_{12}	s_{44}	c_{11}	c_{12}	c_{44}	*Ref*
	in 10^{-13} *cm²/dyne*			*in* 10^{12} *dyne/cm²*			
Al + 2·2 *at* % Cu	15	− 6 9	37	3 08	2 63	0 270	22
Cu + 26·5 *at* % Zn	19 4	− 8·35	13 9	1 47	1 11	0 72	23
Cu + 46 5 *at* % Zn (*ordered structure*)	38·8	−15·2	5 78	0 517	0 335	1 73	24
Cu + 24 9 *at* % Au (*ordered structure*)	13·44	− 5 65	15 08	1 91	1 38	0 663	25
Ag + 25 *at* % Au .	20·7	− 8 91	20 52	1·38	1·05	0 487	11
Ag + 50 *at* % Au	19 7	− 8 52	19 66	1 49	1 14	0·508	11
Ag + 75 *at* % Au .	20 5	− 9 09	20·63	1 66	1 32	0 485	11

to ensure that the result was not due to directional internal stresses in the material.

The isotropy of thermal expansion of cubic crystals is a consequence of the isotropy of the mean square amplitude of atomic vibrations in these crystals. However, this is only the result of the superposition of a large number of elastic waves in the crystal. The mean square amplitude of all vibrations taken together is the same in any direction in the crystal, but the distribution of the amplitudes of waves of different polarizations (having different directions of propagation) varies with the direction. Even for tungsten, which is elastically isotropic, the values of the mean square amplitudes for different types of vibration vary over a range of more than three to one. In any direction of propagation, the amplitudes of the longitudinal waves are small relative to those of transverse waves of the same frequency. Relative values of the amplitudes of waves in different directions in cubic crystals have been calculated by LONSDALE[38] from the available elastic data.

For non-cubic metals most properties are anisotropic, and *Table V* gives the best data available. The theoretical formulae for the variation

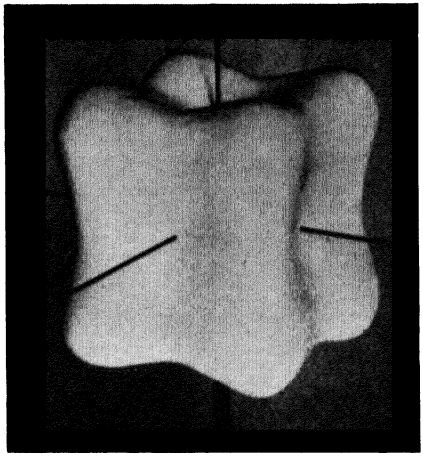

Figure 1. Elastic properties of iron crystals: the length of the vector from the centre of the model to any point on the surface is proportional to Young's modulus, the cubic axes of the crystal being indicated (Goens and Schmid[14])

Figure 2. Elastic properties of iron crystals: the length of the vector from the centre of the model to any point on the surface is proportional to the rigidity modulus, the cubic axes of the crystal being indicated (Goens and Schmid[14])

Table V. Anisotropic Properties of Non-cubic Metal Crystals

Metal	*Crystal Structure*	*c/a*	*Linear Compressibility in* 10^{-12} *cm²/dyne*		*Ref*	*R.m.s. Amplitude of Atomic Vibration in Å*		*Ref*	*Coefficient of Thermal Expansion in* 10^{-6}*/°C*		*Ref*	*Spec Electrical Resistivity in* 10^{-6} *ohm cm*		*Ref*	*Thermal Conductivity in watt/cm °C*		*Ref.*	*Atomic Susceptibility*		*Ref*
			Parallel			*Parallel*			*Parallel*			*Parallel*			*Parallel*			*Parallel*		
			c	*a*		*c*	*a*		*c*	*a*		*c*	*a*		*c*	*a*		*c*	*a*	
Magnesium 293°*K*	*c p hex*	1 624	9 9	9 5	17	0 125	0 130	26	27 0	25 4	17	3 78	4 53	17						
86°*K*						0 078	0 080		13 8	13 0										
Zinc 293°*K*	*c p. hex.*	1 856	13 2	1 75	18	0 127	0 079	27	63 9	14 1		6 05	5 83		1 24	1 24		−12 4	−9 5	35
83°*K*									64 4	5 0		1 29	1 16		1 32	1 37				
20°*K*									52 5	−2 1	29	0 044	0 037	31	7 09	5 65	31			
Cadmium 293°*K*	*c p. hex.*	1 886	16 9	1 5	19	0 182	0 118	28	52 6	21 4		8 36	6 87		0 83	1 04		−29 4	−18 0	35
83°*K*						0 100	0 067		58 9	11 7		2 02	1 63		0 90	1 13				
20°*K*									54 5	3 6		0 188	0 135		1 80	2 00				
Mercury 196°*K*	*hex*	1 94													0 341	0 264	34	−22 5	−24 3	35
86°*K*			3	14	20				47 0	37 5	20	5 87	7 78	20	0 399	0 290				
Antimony 293°*K*	*trig.*		16 8	5 4	21				15 6	8 0	21	35 6	42 6	21						
Bismuth 293°*K*	*trig.*		16 3	6 7	21				14 0	10 4	21	138	109	21				−219 0	−308 0	35
Selenium 293°*K*	*hex*	1 14							17 9	74 1	30									
Tellurium 293°*K*	*hex.*	1 33	−4 2	28 0	21				−1 6	27 2	21	283 00	613 00	32						
Tin 293°*K*	*tetrag.*	0 546	6 8	6 1	21				30 5	15 5	21	12 0	10 1	33				−20 9	−23 4	35

A recent determination on the thermal expansion on tin [CHILDS, B. G and WEINTRAUB, S *Proc phys Soc. B* 63 (1950) 267] gave values in close agreement with those given in *Table V*. Further the coefficients of thermal expansion of beryllium have been determined as $\alpha_c = 9\,4 \times 10^{-6}$ and $\alpha_a = 11\,7 \times 10^{-6}$ at 50°C [GORDON, P. *J appl. Phys.* 20 (1949) 908].

of a property with direction are confirmed by all the measurements. For zinc it should be noted that the range of values of the thermal expansion due to anisotropy is so large that it includes the values for almost all other metals. Some constants have recently been obtained on a first set of crystal rods of gallium.[39] The crystal structure of gallium is orthorhombic with the axial lengths $a = 4{\cdot}517$ *k*X, $b = 4{\cdot}511$ *k*X and $c = 7{\cdot}645$ *k*X, indicating that gallium is almost

Table VI. Anisotropic Properties of Gallium Crystals

Approximate Axial Direction	*Coefficient of Thermal Expansion between 0° and 20°C in* 10^{-6}/°C	*Spec. Electrical Resistivity in* 10^{-6} *ohm cm*		
		− 60°C	0°C	20°C
a	16 5	38 9	50·5	54·3
b	11 3	11 9	16·1	17 4
c	31	5 65	7 5	8 1

tetragonal. *Table VI* gives the experimental results for the thermal expansion and the electrical resistivity.

The values of the linear compressibility in *Table V* have been calculated from the elastic coefficients of *Table II*, using the formulae of *Table I*. This property is related to the ease of movement of a particular atom in a given direction, and its relation to the crystal structure is apparent. For zinc and cadmium, the structure is drawn out in the *c*-direction, the *c*/*a* ratio being larger than the value $\sqrt{(8/3)}$ of the ideal close-packed hexagonal structure. Therefore, deformation parallel to the *c*-axis occurs more easily than at right angles to it. Antimony and bismuth form layer lattices, the layers being at right angles to the trigonal axis. The ease of deformation along this axis is greater than that within the layers. Tellurium forms a chain lattice, the atoms approaching each other most closely along the chains, which are therefore more difficult to deform along their length.

As the properties shown in *Table V* are not independent of each other, some relations between the extents of their anisotropy may also be expected. The direction with the higher linear compressibility is obviously that along which the ease of deformation is higher. Hence the r.m.s. amplitude of the atomic vibrations is larger in this direction,

as is the amount by which the centres of vibration of the atoms are shifted *i.e.* the thermal expansion.

The anisotropy of thermal expansion of mercury[20] seems at first sight to be anomalous, as it is greater along the *c*-direction than along the *a*-direction, although the linear compressibility in the *c*-direction is smaller than that in the *a*-direction. However, the thermal expansion along any axis depends not only on the ease of elastic deformation in this direction but also on the contractions produced by thermal expansions along the other axes. In mercury, the deformation under unit applied stress along the *x*-axis is s_{11} and this is large, but so is the lateral contraction s_{12} due to the expansion parallel to the *y*-axis, whereas that due to expansion parallel to the *z*-axis, s_{13}, is small. In the *z*-direction the corresponding deformation s_{33} is about $s_{11}/3$, but the contractions due to expansions along the *x*- and *y*-axes, s_{13}, are also small and as a result α_c is slightly larger than α_a. It is clear then that both the linear compressibility and the thermal expansion in the *a*-direction are the small resultants of two comparatively large opposing effects. It is not surprising, therefore, that the relative order of the two components, in the *a*- and *c*-directions, of these properties should be reversed in this case.

The electrical or thermal resistivity is a consequence of the collisions between the electrons constituting the current and the ions of the lattice, and such collisions occur only if there are deviations from the ideal lattice *e.g.* due to thermal vibrations. The disturbance in the strict periodicity of the lattice is greater in the direction of larger amplitude of vibration *i.e.* larger thermal expansion, and this should therefore be the direction of larger electrical resistivity. *Table V* shows that this expectation is generally fulfilled and particular attention may be drawn to the case of tellurium, for which thermal expansion and linear compressibility are negative (and small) parallel to the *c*-axis, while the electrical resistivity in this direction is a half of the value parallel to the *a*-axis. It has to be noted, however, that in magnesium and antimony the electrical resistivity does not follow the general scheme, probably indicating that the distribution of the electrons in the Brillouin zones has a greater influence.

Some further insight into the relations between the extent of the anisotropy of various properties may be obtained from the variation with temperature of the elastic constants and the thermal expansion.

The effect of temperature on the elastic coefficients of sodium[12] is shown in *Figure 3*. The coefficients increase almost linearly with

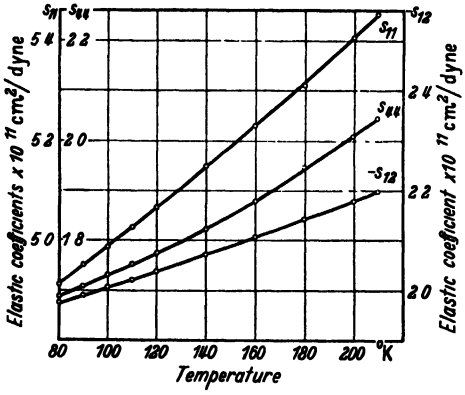

Figure 3. Effect of temperature on the elastic coefficients of sodium, the curves only give the correct relative variation with temperature (Quimby and Siegel[12])

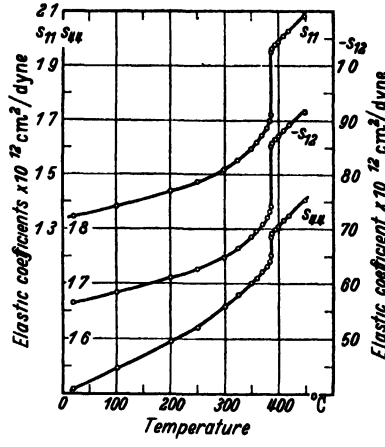

Figure 4 Effect of temperature on the elastic coefficients of $AuCu_3$: this alloy is ordered below 387 5°C and becomes a disordered solid solution above this temperature (Siegel[25])

temperature over a wide range, and this behaviour seems to be typical of a pure metal in which no phase change occurs. However, the continuous increase is interrupted when the metal undergoes a phase change or when an ordered solid solution becomes disordered. This is illustrated by *Figure 4* for the case of $AuCu_3$.[25]

The effect of temperature on the coefficients of thermal expansion of zinc[29] is shown in *Figure 5*. There is no linear increase with increasing temperature and the behaviour of the coefficients in the *c*- and *a*- directions differs widely, particularly at very low temperatures. Similar results were obtained with cadmium crystals. The curves clearly indicate that, starting from absolute zero, thermal energy is first taken up by vibrations parallel to the *c*-axis only

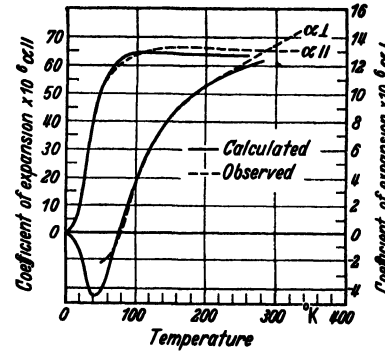

Figure 5 Effect of temperature on the coefficients of thermal expansion of zinc crystals (Grueisen and Goens[29])

and hence, owing to lateral contraction, the thermal expansion is negative in the a-direction. The reason why the vibrations occur only parallel to the hexagonal axis at the lowest temperatures is that both Young's modulus ($1/s_{33}$) and the elastic 'strength' (the reciprocal of the linear compressibility) are smaller parallel to the c-axis than parallel to the a-axis. The latter, therefore, is the direction of higher frequencies and characteristic temperature. Since a vibrating atom tends to occupy the low energy levels (low frequencies) first, the vibrations parallel to

Table VII. Anisotropy of the Rate of Self Diffusion

Metal	A_c	A_a	Q_c	Q_a	*Ref.*
	cm²/sec		*10³ cal/gm atom*		
Zinc	$4\,6 \times 10^{-3}$	$1\,6 \times 10^{2}$	19	32	41
Bismuth	$\sim 4\,4 \times 10^{-4}$	$\sim 8\,5 \times 10^{45}$	30	137	42
Tin	$1\,2 \times 10^{-5}$	$3\,7 \times 10^{-8}$	10·5	5 9	43

the c-axis will be excited first on heating from absolute zero of temperature. Only at higher temperatures will vibrations also occur parallel to the a-axis and thermal expansion take place in this direction. Then the resulting lateral contraction parallel to the c-axis slows down and even reduces the expansion along this axis.

It may be expected that the amplitude of atomic vibrations and the ease of displacing an atom from its equilibrium position are related to the rate at which an atom can migrate in a crystal of its own kind. By using radioactive tracers the rate of self diffusion has now been measured in zinc, bismuth and tin crystals and found to be anisotropic. The diffusion coefficient results from a vector-vector relation, and the two principal coefficients, D_a and D_c, can be expressed[40] as functions of temperature by equations of the Arrhenius type:

$$D_a = A_a\, e^{-Q_a/RT}$$
$$D_c = A_c\, e^{-Q_c/RT} \qquad \ldots\ (18)$$

Table VII gives the experimental constants A and Q. Neither the D values nor the constants A and Q seem to be related to such properties as linear compressibility or thermal expansion, and this is not surprising, since the rate of self diffusion depends on the depth of the potential trough as well as on the tendency of the atoms to migrate. However,

as a detailed theory of the mechanism of diffusion is lacking no final conclusions can be drawn.

Finally we shall consider two very important groups of properties, namely those associated with plasticity and strength and with ferromagnetism.

Regarding the plastic properties, a wealth of information is available on the anisotropy of elastic limit, yield point, work hardening and fracture. The anisotropy of these properties has been explained on the basis of the mechanism of plastic deformation which is slip along certain crystallographic planes and directions. The shear stress in the slip system has been shown to be the most important magnitude involved together with the amount of shear in the slip direction. In terms of the resolved shear stress and the amount of shear, the anisotropy of plastic properties becomes almost trivial and, as this subject has been treated before,[44] we will not discuss it here.

The anisotropy of the scratch hardness was discovered very early, and non-circular Brinell indentations have been observed frequently on crystal surfaces but little quantitative information is available. Recently[45] hardness indentations were made with a Wilson Tukon tester equipped with a Knoop indenter on crystals of zinc and silicon ferrite (3·5 per cent silicon). The Knoop Hardness Number showed a variation of 29 per cent (from 183 to 237) in silicon ferrite and of 184 per cent (from 15·5 to 44·0) in zinc depending on the crystal plane investigated and on the direction in the plane relative to the long diagonal of the indenter. There was a periodic variation of hardness with direction within a plane which could, to a first approximation, be explained in terms of the resolved shear stress on the slip plane of the metal and in the slip direction.

The breaking strength of brittle materials such as bismuth, antimony, tellurium and zinc (at low temperatures) should also be mentioned here. The possibility of cleaving these materials is a consequence of the anisotropy in their cohesion. The anisotropy of the mechanical strength is somewhat analogous to that of the dielectric strength of insulating crystals. Here, the breakdown in strong electric fields does not take place in the direction of the field but along certain crystallographic directions. This is illustrated in *Figure 6*, which shows a photograph of a sodium chloride plate cleaved parallel to the cubic planes.[46] The electric field has been applied between a plate and a

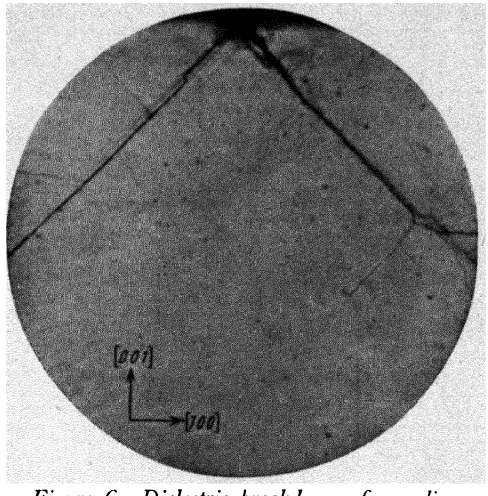

Figure 6. Dielectric breakdown of a sodium chloride crystal does not occur in the direction of the electric field nor parallel to the cleavage plane; a potential difference of 50 kv was applied between a needle (on top) and a plate (negative) for about 10^{-7} sec across a crystal of 1·8 cm thickness (Inge and Walther[46])

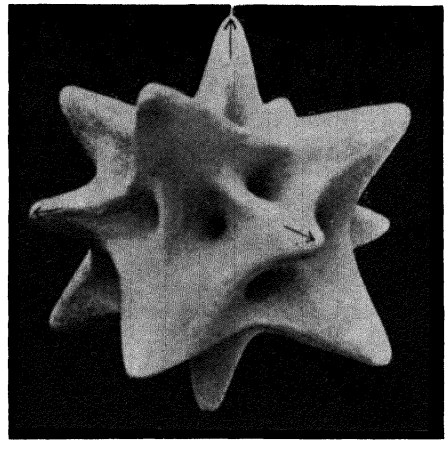

Figure 9. Rate of solution of copper in 0·3 N *acetic acid as a function of the orientation (Glauner and Glocker*[55]*)*

needle and it was found that the breakdown at room temperature usually occurs parallel to ⟨111⟩ and sometimes parallel to ⟨110⟩ directions.

The anisotropy of ferromagnetic properties is also very marked. This is illustrated in *Figures 7* and *8*. Whereas the saturation magnetization is the same for crystals of different orientations, the rate at which

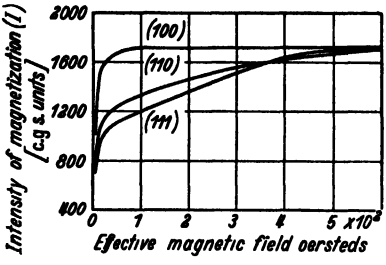

Figure 7. Magnetization curves of iron crystals (Honda and Kaya[47])

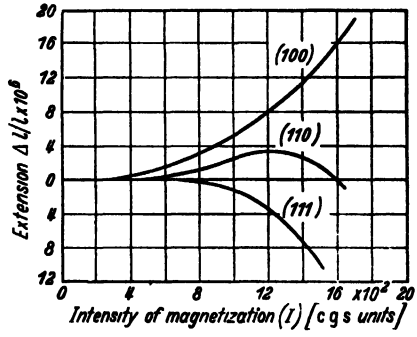

Figure 8. Magnetostriction of iron crystals (Webster[48])

saturation is reached varies with the orientation. In crystals of iron, the direction of easiest magnetization is the cubic axis and the most difficult to magnetize is the body diagonal; in nickel crystals these relations are reversed.[47] *Figure 8* shows the relative change in length of iron crystals under the influence of a longitudinal magnetic field as a function of the field.[48]

EXPERIMENTAL RESULTS ON SURFACE PROPERTIES

A satisfactory treatment of the phenomena occurring on crystal surfaces is not possible owing to the absence of a quantitative theory and of detailed measurements. However, there are many indications of the existence of anisotropy in surface properties and in the following pages we will summarize the more important of them. In ionic crystals, the anisotropy of surface tension has been calculated[49] and by analogy one would expect anisotropy also to exist in metals; however, no such calculation has yet been carried out, nor have any measurements been made on metal surfaces. Very important observations have recently been made by CHALMERS[50] on the temperature of the solid-liquid equilibrium in lead and tin. It was found that this temperature varies

with the crystallographic orientation of the interface, the difference between the melting points of two crystal faces being of the order of 0·001°C. The melting temperature is higher for interfaces which have closer packing of atoms. By thermodynamic reasoning, it follows from this observation that the free energy per surface atom is a function of the crystallographic nature of the face, and that the latent heat of fusion also depends on the crystallographic characteristics of the interface. It may then be inferred that the energy required for an atom to leave the crystal is greater for faces which are more densely occupied by atoms.

These observations provide the basis for a new explanation of the preferred orientations observed in the columnar crystals of castings. Formerly, these preferred orientations were explained in terms of an anisotropic rate of crystallization from the melt, crystals oriented with the direction of fastest rate of growth parallel to the temperature gradient suppressing the others during their advance into the liquid.[51] It is clear now that the face having the highest melting point will be in advance of the others and the direction of growth of some crystals will be inclined to the direction of the temperature gradient; thus, again some crystals will suppress the growth of their less favourably oriented neighbours.

Anisotropy in the physicochemical properties of crystal surfaces was observed when crystals were etched by vapours.[52] Single crystals were allowed to react with a gaseous reagent under conditions of temperature and pressure such that the product was volatilized away as fast as it formed. When copper crystals were subjected to halogen vapours at 444°C and about 1 mm pressure, the cuprous halide sublimed away continuously and etch pits parallel to certain crystallographic planes were produced. The relative frequency of occurrence of the facets exposed varied with the halogen vapour used.

The effect of tarnishing is similar. In the case of copper, comparison of the times required to produce oxide films giving the same interference colours on annealing in air at 260°C showed that the rate of tarnishing was greatest on the dodecahedral plane (110) and smallest on the cubic plane.[53] Also, with silver, it was found that the rate of oxidation was different for different crystallographic planes.[54] Here, the silver oxide, Ag_2O, formed is volatile at the temperature of the experiments.

The theoretical anisotropy of a property due to one particular process

is not necessarily observable, as another process may occur simultaneously and mask the expected anisotropy. For example, the rate of solution of a metal in an acid should show the anisotropy typical of a property resulting from a vector-vector relation. However, the formation of surface films on the solid or the concentration of solution products at the surface often prevents the anisotropy becoming observable. Whether the observed rate of solution is anisotropic or not depends on the particular combination of metal and acid, the concentration of the acid *etc.* An example of marked anisotropy is given in *Figure 9*, in which the rates of solution of a copper crystal in various directions are represented by vectors from the centre of the model; the three cubic axes are indicated by arrows.[55] Thus, a single crystalline sphere of copper will not remain a sphere on etching but become a body of a shape reciprocal to that of *Figure 9*. By changing the etching conditions (*e.g.* temperature, concentration of the acid) the rates of solution in the different directions will be changed and may even be reversed, and it does not seem possible at present to predict the conditions favouring the appearance of anisotropy. The same remarks have to be made regarding the rate of attack on copper crystals in various electrochemical treatments where the current density is a further important variable.[56] On cathodic treatment the rate of deposition may also be anisotropic.

The anisotropy of rate of solution has found a wide field of application in metallurgical research in which the crystallographic nature of etch pits is used to determine the orientations of crystals. A list of etchants and etching conditions producing suitable etch pits in various metals has been given by BARRETT and LEVENSON.[57]

Finally, we will mention the effect of reflection of plane polarized light by a metal surface. Generally, the light becomes elliptically polarized and the direction of maximum amplitude is rotated with respect to the original plane of polarization. Experiments on zinc crystals have shown[58] that these effects depend on the orientation of the reflecting surface, whereas in cubic crystals there is no dependence on orientation. Thus, if the surface of a non-cubic metal is observed under crossed nicols, crystals of different orientations appear with different degrees of darkness and can easily be distinguished without being etched. This effect can usefully be applied to the investigation of grain boundary migration.[59] If non-cubic surface films are present

on the metal, the effect is more complex; for instance, if a non-cubic film is formed on the surface of a cubic metal and its orientation is related to that of the underlying metal the reflection appears to be anisotropic in spite of the metal being cubic.[60]

EFFECTS OF ANISOTROPY IN POLYCRYSTALLINE METALS

The classical metallurgist and physicist considered polycrystalline metallic materials as isotropic or quasi-isotropic. It was only during the last two or three decades that he became increasingly aware of the implications of crystal anisotropy. Today, it is considered that anisotropy of polycrystalline materials is the rule rather than the exception. Although this subject is of great importance, particularly from the practical point of view, it will only be treated briefly as some parts of it have already been discussed elsewhere.[61] The three aspects of this subject will be dealt with in turn. Polycrystalline metals may exhibit anisotropy because the orientations of the crystals are not random but a preferred orientation exists. They may also show induced anisotropy as a result of a treatment which leaves permanent or temporary effects in each crystal of the metal. In addition, neighbouring crystals in the aggregate may interact under certain externally imposed conditions (stresses) in a manner depending on their relative orientations.

Preferred Orientation—This occurs after all the usual production, deformation and annealing processes and it is well known that it is extremely difficult to eliminate a preferred orientation once it exists in a metal. The origin of a preferred orientation is the anisotropy of some property of the crystals *e.g.* in the columnar crystals of castings it is the anisotropy of the melting temperature, as discussed above, and in deformed metals it is the anisotropy of the resistance of crystal planes to shear giving rise to the deformation by slip. As a consequence of preferred orientation, metals show the anisotropy of the crystals composing the aggregate. This is important not only in the fabrication of metals (earing in deep drawing) but also in testing and specification. The absence of anisotropy is not necessarily due to the absence of a preferred orientation but may be due to the simultaneous presence of orientations which counteract each other with respect to the anisotropic behaviour.[62] The alignment of crystals in an aggregate is never exact but there is some scatter of their orientations about an orientation

which occurs with highest frequency. The extent of scatter depends on the conditions of treatment *e.g.* amount of deformation or annealing temperature, and it is usually indicated in a pole-figure. However, to a first approximation, the ideal orientation can be given in terms of Miller indices, and these are set out in *Table VIII*[44] for the casting, deformation and annealing processes. Preferred orientations and their consequences have recently been described by RICHARDS,[63] and a monograph by WASSERMANN,[64] giving a complete review of the subject, was published in 1939.

Induced Anisotropy—The best known example of this is the anisotropy due to the alignment of impurities and segregations which occurs during rolling or other deformation processes. This effect is often superimposed on the anisotropy due to preferred orientation, particularly in sheet steel.[65]

After deformation processes such as drawing or rolling, directional internal stresses remain in the metal. These stresses distort the crystal structure and may constitute another source of induced anisotropy. It has been observed that the cubic structure of a cold rolled iron-nickel alloy[66] is drawn out in the rolling direction and thus becomes orthorhombic. However, this may only be a surface effect since the sign of the internal stresses in the core of the sheet is opposite to that near the surface.

As the resultant of all the internal stresses in a specimen must be zero, the overall change in any property depending linearly on the stress must also be zero. Only if a property depends non-linearly on the stress will there be any induced anisotropy. In order to test whether the electrical resistivity is such a property the resistivity of rolled cubic metals has been measured in various directions relative to the rolling direction and found to be anisotropic.[67] In a recent theory[68] it has been predicted that the change in resistivity on cold working depends on the square of the internal strains and that the ratio of the maximum to the minimum increase in resistivity depends only on Poisson's ratio and is about 2 for most metals. The latter prediction is in general agreement with the experimental results. In interstitial alloys such as those of carbon in iron there is an additional contribution to the anisotropy due to the migration of interstitial atoms to dislocations during strain aging. The effect of the rows of interstitial atoms with preferred orientations so formed has been treated theoretically.[69]

Table VIII. Preferred Orientations in Metals[44]

Metal	*Nature of Process*							
	Casting	*Drawing*	*Compression*	*Torsion*	*Rolling*		*Recrystallization after Cold Rolling*	
	Parallel to Axis of				*Parallel to Rolling*			
	Columnar Crystals	*Wire*	*Compression*	*Torsion*	*Plane*	*Direction*	*Plane*	*Direction*
Al	[100]	[111]	[110]	[111]	(110)	[1$\bar{1}$2]	(001)	[100]
Cu	[100]	[111]						
Ni		*1* [111]						
Au	[100]	*2* [100]						
Pd								
Pb	[100]	[111]						
Ag	[100]	*1* [100]			(110)	[1$\bar{1}$2]		
		2 [111]					(311)	[$\bar{1}$12]
α-Fe	[100]		[111] ([100])?	*1* [110]	*1* (001)	[110]	*1* (001)	[110]
				2 [112]	*2* (112)	[1$\bar{1}$0]	*2* (111)	[11$\bar{2}$]
					3 (111)	[11$\bar{2}$]	*3* (112)	[1$\bar{1}$0]
Mo		[110]			(001)	[110]		
Ta								
W								
Mg	[11$\bar{2}$0]	(0001)	[0001]		(0001)		(0001)	
Zn		*at* 18°*C*			*at* 20°*C*	*at* 20°*C*	*at* 20°*C*	*at* 20°*C*
	[0001]	(0001)			(0001)	[11$\bar{2}$0]	(0001)	[11$\bar{2}$0]
	is ⊥							
Cd					*at* 30°*C*			
					(0001)			
Zr		(0001)			(0001)			

Interaction of Crystals at their Boundaries—This has been investigated most extensively in connection with the plastic behaviour of metals.[70] The stress required to start plastic deformation in a crystal depends on the orientation of the slip plane relative to the direction of the stress. Hence, free crystals start deforming at different stresses. In an aggregate, crystals are hindered from deforming independently since they are in contact with each other at their boundaries, and remain in contact during the deformation. Therefore there is a large interaction between the crystals at their boundaries, and the mode of deformation is changed appreciably not only in their immediate neighbourhood but also to a considerable distance from them. The deformation thus becomes inhomogeneous, different parts of a crystal deforming differently and differences occurring from crystal to crystal. This inhomogeneity of deformation, due to the anisotropy of the plastic properties of the crystals, is inherent in all crystal aggregates. It is of theoretical importance in relation to the calculation of plastic properties of crystal aggregates from those of single crystals.[71] One of its best known effects is the roughening of the originally smooth surface of test specimens during a tensile test and the 'orange peel' effect obtained on deep drawing.[72]

A very similar surface roughening was also observed under conditions in which stresses were not applied externally. In a study of the behaviour of tin-base bearing alloys during repeated cycles of heating and cooling, signs of surface deformation by slip and the beginning of surface cracks were found, whereas these effects were absent in lead-base bearing alloys.[73] The effects were shown to be due neither to the presence of internal stresses set up by a previous treatment nor to a temperature gradient set up in the specimen during the heating and cooling (as cubic metals did not show the effects) but to stresses at the grain boundaries resulting from the different thermal expansions of crystals of different orientations. Clearly, temperature changes give rise to stresses where two crystals of different orientations adjoin and where free expansion is hindered. If these stresses are sufficiently large, plastic deformation of the crystals will occur. In a cubic metal, on the other hand, thermal expansion is isotropic and no such effect can exist. In accordance with this explanation, it was found that the rates of heating and cooling had no effect on the deformation, and that the amount of deformation increased with the number of cycles and the

temperature range employed, independently of whether the range extended to temperatures above or below room temperature. Further, material with a strongly preferred orientation showed considerably less deformation, since the change in orientation from crystal to crystal is here smaller than in a material with random distribution of orientations. This is one of the very few cases in which preferred orientations have a beneficial effect on the mechanical properties. As the stresses, and hence the deformation, depend on the anisotropy of thermal expansion, the effects are more pronounced the larger the anisotropy. The effects occur even in the half cycle of cooling of a casting from the liquid. It is therefore difficult to obtain metals with a large anisotropy of thermal expansion in a strain free condition at room temperature by casting or annealing. In non-metallic materials possessing a marked anisotropy of thermal expansion, the occurrence of stresses on change in temperature has been known and discussed for a long time.[74] For example, the weathering of rocks is at least partially due to such stresses and so is the loss of rigidity of marble.[75] It is then clear that the daily and seasonal temperature cycles produce inhomogeneous deformation of rocks or building stones and thus contribute to their disintegration.

The authors wish to acknowledge the help they have received from their colleagues in the Division of Tribophysics, Commonwealth Scientific and Industrial Research Organization, Australia.

REFERENCES

[1] ONSAGER, L. *Phys. Rev.* 37 (1931) 405; 38 (1931) 2265
[2] VOIGT, W. *Lehrbuch der Kristallphysik* p 345 Leipzig, 1910
[3] JEFFREYS, H. and JEFFREYS, B. S. *Methods of Mathematical Physics* p 123 Cambridge, 1946
[4] WOOSTER, W. A. *A Text Book on Crystal Physics* Chapter 1 Cambridge, 1938
[5] JEFFREYS, H. and JEFFREYS, B. S. *Methods of Mathematical Physics* p 85 Cambridge, 1946
[6] VOIGT, W. *Lehrbuch der Kristallphysik* Leipzig, 1910
[7] GOENS, E. *Ann. Phys.* 15 (1932) 455
[8] —— *ibid* 17 (1933) 233
[9] BOZORTH, R. M., MASON, W P., MCSKIMIN, H. J. and WALKER, J. G. *Phys. Rev.* 75 (1949) 1954
[10] GOENS, E. *Ann. Phys* 38 (1940) 456 [from *Chem. Abstracts* 35 (1941) 2048]
[11] ROHL, H. *ibid* 16 (1933) 887
[12] QUIMBY, S. L. and SIEGEL, S. *Phys. Rev.* 54 (1938) 293
[13] BENDER, O. *Ann Phys.* 34 (1939) 359
[14] GOENS, E. and SCHMID, E. *Naturwissenschaften* 19 (1931) 520
[15] DRUYVESTEYN, M. J. *Physica* 8 (1941) 439

[16] WRIGHT, S. J. *Proc. roy. Soc. A* 126 (1930) 613
[17] GOENS, E. and SCHMID, E. *Phys. Z.* 37 (1936) 385
[18] —— *Ann. Phys.* 16 (1933) 793
[19] GRÜNEISEN, E. and GOENS, E. *Z. Phys.* 26 (1924) 235
[20] —— and SCKELL, O. *Ann. Phys.* 19 (1934) 387
[21] BRIDGMAN, P. W. *Proc. Amer. Acad. Arts Sci.* 60 (1925) 305
[22] KARNOP, R. and SACHS, G. *Z. Phys.* 53 (1929) 605
[23] MASIMA, M. and SACHS, G. *ibid* 50 (1928) 161
[24] GOOD, W. A *Phys. Rev.* 60 (1941) 605
[25] SIEGEL, S. *ibid* 57 (1940) 537
[26] BRINDLEY, G. W. and RIDLEY, P. *Proc. phys. Soc., Lond* 50 (1938) 757
[27] —— *Phil. Mag.* 21 (1936) 790
[28] —— and RIDLEY, P. *Proc. phys. Soc., Lond.* 51 (1939) 73
[29] GRUNEISEN, E. and GOENS, E. *Z. Phys.* 29 (1924) 141
[30] STRAUMANIS, M. *Z Kristallogr.* 102 (1940) 432
[31] GOENS, E. and GRUNEISEN, E *Ann. Phys* 14 (1932) 164
[32] SCHMID, E. and STAFFELBACH, F. *ibid* 29 (1937) 273
[33] CHALMERS, B. and HUMPHRY, R. H. *Phil. Mag.* 25 (1938) 1108
[34] REDDEMANN, H. *Ann. Phys.* 14 (1932) 139
[35] BATES, L. F. *Rep. Prog. Phys.* 3 (1936) 185
[36] CZOCHRALSKI, J. *Int. Z. Metallogr.* 8 (1916) 1
GEISS, W. and VAN LIEMPT, J. A. M *Z anorg. Chem.* 128 (1922) 355; *Z. Metallk.* 17 (1925) 194
FRASER, M. *Phil. Mag.* 12 (1931) 112
[37] KOCHANOVSKA, A. *Physica* 15 (1949) 191
[38] LONSDALE, K. *Acta Crystallogr.* 1 (1948) 142
[39] POWELL, R. W. *Nature, Lond.* 164 (1949) 153
[40] LE CLAIRE, A. D. *Progress in Metal Physics* I p 306 London, 1949
[41] FENSHAM, P. J. *Aust. J. sci. Res. A* 3 (1950) 91 [calculated after Miller, P. H. and Banks, F. R. *Phys. Rev.* 61 (1942) 648]
[42] SEITH, W. *Z. Elektrochem.* 39 (1933) 538
[43] FENSHAM, P. *J. Aust. J. sci. Res. A* 3 (1950) 91
[44] BOAS, W. *Introduction to the Physics of Metals and Alloys* Melbourne, 1947
[45] DANIELS, F. W. and DUNN, C. G. *Trans. Amer. Soc. Met.* 41 (1949) 419
[46] INGE, L. and WALTHER, W. *Z. Phys.* 64 (1930) 830; 71 (1931) 627
[47] HONDA, K. and KAYA, S. *Sci. Rep. Tohoku Imp. Univ.* 15 (1926) 721
KAYA, S. *ibid* 17 (1928) 639, 1157
[48] WEBSTER, W. L. *Proc. roy. Soc. A* 109 (1925) 570
[49] BORN, M. and STERN, O. *S.B. preuss. Akad. Wiss.* (1919) 901
SHUTTLEWORTH, R. *Proc. phys. Soc. A* 62 (1949) 167
[50] CHALMERS, B. *Proc roy. Soc. A* 196 (1949) 64
[51] NIX, F. C. and SCHMID, E. *Z. Metallk.* 21 (1929) 286
GROSS, R. and MOLLER, H. *Z. Phys.* 19 (1923) 375
[52] ROWLAND, P. R. *Nature, Lond.* 164 (1949) 1091
[53] TAMMANN, G. and MULLER, A. *Z. Metallk.* 18 (1926) 69
[54] LEROUX, J. A. A. and RAUB, E. *Z. anorg. Chem.* 188 (1930) 205
[55] GLAUNER, R. and GLOCKER, R. *Z. Kristallogr.* 80 (1931) 377
[56] LEIDHEISER, H. and GWATHMEY, A. T. *Electrochem. Soc. Preprint* (1947) 97
[57] BARRETT, C. S. and LEVENSON, L. H. *Trans. Amer. Inst. min. (metall.) Engrs* 137 (1940) 76
[58] DAYTON, R. W. *ibid* 117 (1935) 119
[59] BRINSON, G. and MOORE, A. J. W. Private communication
[60] HONE, A. and PEARSON, E. C. *Met. Progr.* 55 (1949) 363

[61] *Progress in Metal Physics* I London, 1949
[62] YEN, MING-KAO *J. Met.* 1 (1949) 59
[63] RICHARDS, T. LL. *Progress in Metal Physics* I p 281 London, 1949
[64] WASSERMANN, G. *Texturen metallischer Werkstoffe* Berlin, 1939
[65] JACKSON, L. R., SMITH, K. F. and LANKFORD, W. T. *Amer. Inst. Min. Engrs, Met. Tech. Tech. Publ.* 2440, 1948
[66] WASSERMANN, G. *Z. Metallk.* 28 (1936) 262
[67] BROOM, T. Private communication
[68] MACKENZIE, J. K. and SONDHEIMER, E. H. *Phys. Rev.* 77 (1950) 264
[69] BHATIA, A. B. *Proc. phys. Soc. B* 62 (1949) 229
[70] KING, R. and CHALMERS, B. *Progress in Metal Physics* I p 127 London, 1949
[71] BOAS, W. *Helv. Phys. Acta* 23 (1950) 159
[72] HÉRENGUEL, J. and SCHEIDECKER, M. *Rev. Metall.* 46 (1949) 537
[73] BOAS, W. and HONEYCOMBE, R. W. K. *Proc. roy. Soc. A* 186 (1946) 57; *A* 188 (1947) 427; *J. Inst. Met* 73 (1947) 433
[74] HOWE, J. A. *The Geology of Building Stones* London, 1910
[75] RAYLEIGH, LORD, *Proc. roy. Soc. A* 144 (1934) 266

4

DEVELOPMENTS IN MAGNESIUM ALLOYS

H. G. Warrington

RELIABLE WORK on the physical metallurgy of magnesium alloys, as also on the phenomena of corrosion and protection, can be said to date from 1942 when HANAWALT, NELSON and PELOUBET[1] published their investigations on the effects of minor impurities on magnesium metal and some of the commercial alloys.

Dealing principally with corrosion resistance, these workers established tolerance limits for iron, nickel and copper for a large number of compositions and the data revealed that the corrosion rates of 'commercial purity' metal greatly exceeded those of 'high purity' metal. Whereas the lack of corrosion resistance of commercial purity magnesium was regarded as its main drawback, the high purity metal when exposed in a number of varied atmospheres reacted in general in a way comparable with many aluminium alloys and more efficiently than mild steel.[2] Subsequently the effects of other impurities such as aluminium, manganese, and silicon as well as iron, were observed in the study of alloy development, especially in those instances where the impurity will combine with a sparingly soluble addition element such as zirconium, to form a compound that is completely insoluble in molten magnesium.[3]

Prior to 1942 most magnesium produced commercially was obtained by electrolysis of fused chloride. Small amounts were produced by distillation *in vacuo* after reduction by calcium carbide or aluminium. The raw materials were not sufficiently pure to yield a high purity product, and a typical composition of pure magnesium from an electrolytic cell[4] is as follows:

	Mg	Al	Mn	Si	Cu	Ni	Fe	Ca	Pb	Zn
Cell Mg	99 85	0 01	0 08	0 01	0 003	0 001	0 03	<0 01	<0 001	<0 01
Tolerance limits of Hanawalt *et al*					0 1	0 0005	0 017	for Mg metal		
						0 001[5]	0 002	for Al containing alloys		

In 1940–41, PIDGEON at the Canadian National Research Council introduced the silicon reduction of calcined dolomite, a process which operates commercially in Canada and for a short time in the United

States of America. By the use of high purity calcined dolomite and ferro-silicon, an arc furnace product, the interfering impurities are reduced to a minimum, and since that time metal has become available for which the following composition is quoted as typical:[6]

Mg	Al	Mn	Si	Cu	Ni	Fe	Pb	Zn	Ag	Na
99·978	0 004	0·002	0 006	<0 001	<0 0005	0 001	0 001	0·001	<0·0005	<0·001

Redistilled cell metal had previously been used for investigation and research work, but as commercial quantities of very pure magnesium became available observations of far reaching importance could be made. Iron is almost completely insoluble in magnesium, and electrolytic metal can be obtained commercially in controlled purity grade, much of the iron being precipitated by maintaining the metal at a temperature just above the melting point for a sufficient length of time. The rate of precipitation is increased by addition of manganese, and zirconium is even more effective.

The alloy known commercially as M1, which contains 1·5 per cent manganese, was claimed to be the most corrosion resistant of all magnesium alloys before 1943 and some investigators attributed this to formation of a protective $Mn(OH)_2$ compound[7] in the oxide layer. Recent tests[2] demonstrate increasing corrosion resistance in most media with increasing aluminium content, and the superiority of alloys containing aluminium to the manganese alloy. It can now be seen that with metal of uncontrolled purity, the addition of manganese, usually by reduction of the chloride, causes precipitation of the iron, effectively reducing its concentration to a value below the tolerance level for this alloy.

The earliest reference to corrosion tests on alloys containing zirconium states that they 'exhibit a resistance which nearly equals that of the binary Mg–Mn alloys'.[8] Since high purity metal has been produced in quantity it was observed that alloys made up from such metal without special treatment possessed an inherently finer grain size than the older alloys, a finding which profoundly affected theories of grain refinement.[9] *Tables I* to *IV* show the properties of the various types of magnesium metal that are commercially available and the composition of some magnesium alloys.

MAGNESIUM BASE ALLOYS

In the course of thirty years' development the alloys of magnesium in commercial use have already formed a definite pattern. In addition to

Table I. Grades of Magnesium Metal Commercially Available

Grade	Mg *Minimum* %	*Typical or Specified Maxima*											
		Al	Ni	Cu	Fe	Mn	Si	Ca	Pb	Zn	Ag	Na	Sn
Electrolytic[4]	99·80		*Total* 0 001	0·02 0·02	*ASTM* B–92–45 0·03	0·06	0 01	<0 01	<0·001	<0·01			<0·001
Controlled purity[4] ..	99·80		0·005	0·05	0 005		0·01						
High purity[6] ..	99 95	0·005	*Total* 0·0005	0·005 0·0006	0·003	0·005	0·004	0·004	0 001	0·001	<0 0005	<0·001	
Redistilled[6]	99·98	0·005	*Total* 0·0005	0·0025 0·0005	0·0015	0·0005	0·003						

purely metallurgical considerations, alloy development is affected by patented composition ranges, advertising, national and local prejudice and production costs.

Far fewer alloys are used in the magnesium foundry than in the copper, iron or aluminium industries for the following reasons. Designers like to choose the highest strength material available, in the absence of other criteria. In most metals increased strength over the

Table II. Mechanical Properties of Magnesium Metal Extruded Rods

Grade	*Ult. Tensile Strength* lb/in^2	0·2% *Proof Stress* $*lb/in^2$	*Elongation* %	*Grain Size* 10^{-3} *in*
Redistilled .	22,600	7,600	8·1	11–12
High purity .	23,500	9,400	6·6	12–13
Electrolytic ..	28,000	12,200	6·6	13–14

* 100 lb/in^2 = 7·03 kg/cm^2

standard foundry alloys is only obtained at the expense of some other property, such as casting characteristics, by addition of a rare or difficult element, or by an expensive heat treatment. Cost of production, therefore, restrains the designer's choice to the alloy with the lowest mechanical or physical properties that satisfy his requirements. Hence the variety of alloys continually increases, unless an alloy showing better properties is developed at a lower cost than an existing material, when the variety of alloys decreases. The question is of interest in reviewing the reasons for differences between those alloys considered technically the best and those that are actually employed.

In magnesium sand foundry work, most applications can be satisfied by the casting alloy A8 for low and medium strength requirements and in the heat treated condition by alloy AZ91 for high strength requirements. Until the recent development of the alloys containing zirconium, magnesium alloy castings became increasingly standardized in one of these two alloys, the improvements of which resulted from the use of high purity metal and the development of methods of grain refining. For die casting, in which the liquid metal is introduced under pressure into rigid steel moulds, the ability to resist cracking at temperatures just below the solidification temperature is important and alternative alloys are sometimes used in this application. For wrought

Table III. The Composition of the Commercial Magnesium Base Alloys

Designation	Intentional Alloying Constituents % Weight								Usual Form
	Al	Zn	Mn	Ce*	Zr	Sn	Ca	Si	
*M*1 ..			1·5				0 2†		*Wrought and cast*
Eckpsaloy (trade)	1·5		1·0						*Die Cast*
*A*8 . .	8·0		0·2						*Cast*
*A*9	9·0		0·2						*Cast*
*A*10 ..	10·0		0·2						*Cast*
*A*12	12·0		0·2						*Cast*
*AS*100 .. .	10·0		0·2					0·7	*Die cast*
*AZ*21 .. .	1 6	0 6	0·25						*Wrought*
*AZ*31 . ..	3·0	1·0	0·25						*Wrought*
*AZ*51	5·0	1 0	0·25						*Wrought*
*AZ*61 .. .	6·0	1·0	0 2						*Wrought*
*AZ*80 ..	8·0	0·6	0·2						*Wrought and cast*
*AZ*91 . ..	9·0	1 0	0·2						*Cast*
*AZ*101	10 0	1·0	0 2						*Cast*
*AZ*63	6·0	3·0	0·2						*Cast*
*AZ*92	9 0	2 0	0·2						*Cast*
*TA*54	4 0		0 25			5 0			*Wrought (forgings)*
*ZK*31 . ..		3·0			0·7				*Wrought*
*ZK*51 .. .		5 0			0 7				*Cast*
*ZK*61 .. .		6·0			0 7				*Cast*
*EK*31 .. .				3 0	0 5				*Cast*
*EZK*331 .		2 5		2·5	0 5				*Cast*
Magnesium lithium alloys .. .	Li 11·5 *plus addition elements*								*Wrought (development)*

* 'Rare earth' total. † Optional. The alloy designations given above are chosen as being those in widest use on the European and American continents and most likely to be associated with the composition to which they refer by the reader not familiar with industrial terminology. On the American continent, the addition of the letter x to the designation given above denotes that in the U.S. the alloy is of controlled purity grade, and in Canada of high purity grade.

Table IV. Typical Mechanical Properties of Magnesium Base Alloys containing 8–10% Aluminium, Sand Cast

Condition	0 2% Yield Strength *lb/in²*	Ultimate Strength *lb/in²*	Elongation % on 2 in
As cast . .	14,000	26,000	4
Solution treated	14,000	38,000	10
Precipitation treated .. .	20,000	38,000	5

* 100 lb/in² = 7.03 kg/cm²

alloys, by contrast, a wider range of compositions is used. Production difficulties in rolling or extrusion operations rise with the mechanical properties of the product as the concentration of alloying element is increased, and it becomes expedient to apply the lowest strength alloy that will satisfy a given requirement.

The mechanical properties of magnesium and aluminium alloys are closely dependent on grain size (optimum properties are achieved when the grain size is a minimum) and hence the choice of alloy systems is largely influenced by the possibility of grain refinement the mechanism of which will be discussed later. The production of a fine grain size in the cast material depends on the presence of crystallization nuclei in the liquid. Grain refining was originally achieved by superheating. This was replaced more recently by the addition of carbon or one of its compounds. Zirconium, the most effective grain refiner yet discovered, forms compounds which are not soluble in molten magnesium with aluminium amongst other metals. Satisfactory mechanical properties can be obtained by additions of zinc to magnesium and a series of alloys has appeared in which zinc is the major alloying element and zirconium the grain refiner. A demand for magnesium alloys for application at elevated temperatures revived the work of HAUGHTON and PRYTHERCH[10] who demonstrated the beneficial effects of cerium additions in this respect. The grain refinement of these alloys with zirconium has introduced a further series which is of importance in engineering. Finally the theoretical interest shown by HUME-ROTHERY[11] in the system Mg-Li has promoted recent work by U.S. Navy metallurgists which shows promise of a new series of high strength alloys which can be deformed cold.

MAGNESIUM-ALUMINIUM ALLOYS

The addition of aluminium to magnesium up to a concentration of 50 per cent by weight results[12] in the formation of a compound Mg_4Al_3 (45·41 per cent aluminium). The solid solubility of aluminium in magnesium is 2 per cent at air temperature, increasing to a maximum of 12·6 per cent at the eutectic temperature of 436°C. Thermal analysis gives a eutectic point at 32·2 per cent aluminium, but in common with many metallic elements the alloys do not show the characteristic lamellar eutectic structure. Primary crystallization is that of the solid solution and interdendritic cavities are filled with the

Mg_4Al_3 compound and the solid solution. As the temperature drops the supersaturated solid solution rejects aluminium as Mg_4Al_3 in lamellar form.[13] The structure resembles that resulting from a eutectoid reaction.

Homogeneous solid solutions of metals are normally stronger than the major components and are relatively ductile. Sound castings are achieved when solidification in the form of a solid solution commences at a number of closely spaced nuclei and the interdendritic cavities are filled with a eutectic liquid to compensate for the volume contraction during solidification. These conditions are satisfied with alloys containing less than 12 per cent aluminium, which after casting and slow cooling are reheated to a temperature above that at which the Mg_4Al_3 compound will be taken into solid solution, and are then quickly cooled to retain the solid solution structure by suppressing the formation of the compound.

In practice an aluminium content of more than 10 per cent would involve considerable time at a temperature dangerously close to the eutectic melting point, and even if melting did not actually occur the negligible strength of the metal in eutectic areas would cause components to distort or even to fracture under their own weight. This is true almost quantitatively in the presence of small additions of manganese and up to 1·0 per cent of zinc, hence all the requirements of the foundry can be fulfilled with an alloy containing 8–10 per cent aluminium with small additions of zinc and manganese.

The supersaturated solid solution achieved by rapidly cooling from the heat treatment temperature can be broken down to the 'eutectoid' structure in areas of highest aluminium concentration by reheating to a temperature at which sufficient mobility allows the precipitation of the compound Mg_4Al_3 in lamellar form.[14] This introduces a physical stiffening of the metal, raising the yield point and slightly reducing the ductility. With wrought alloys, the castability of the material is a secondary consideration, the simple form of a billet rendering the problem of directional solidification and controlled temperature gradient necessary to produce a sound casting relatively easy. Cold working, even with pure magnesium, is restricted, as in other metals with the hexagonal crystal structure, slip can only occur[15] on the base planes (0001) and along the diagonal axis $[11\bar{2}0]$. This is the direction in the crystal in which the atoms are most closely spaced.

At temperatures above 250°C slip can take place on pyramidal planes as well as base planes and plastic deformation is then much easier. Also the higher the temperature, the more rapid is the recovery by relaxation from the stressed condition, allowing progressive continuation of working without fracture. The greater the aluminium content, however, the higher is the initial lattice strain, and the higher

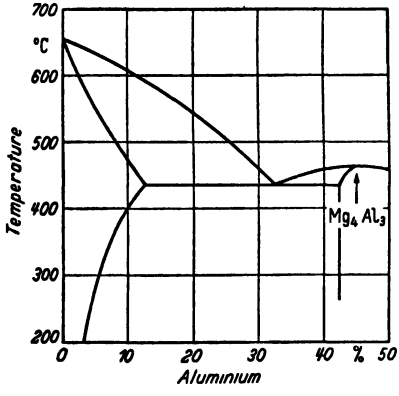

Figure 1. Magnesium-aluminium equilibrium diagram

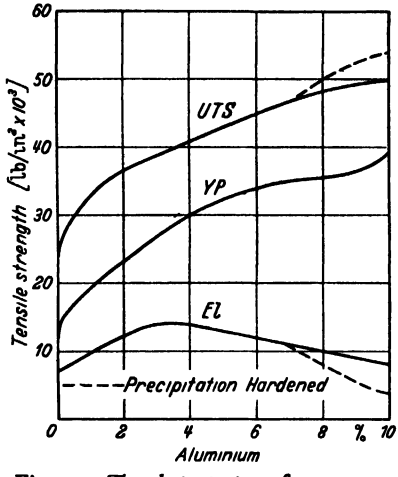

Figure 2. Tensile properties of magnesium-aluminium alloys, extruded rods

the temperature necessary to permit a given rate of deformation. Resistance to deformation by conversion of energy to heat will be compensatory to some extent, but the melting point of the eutectic forms a definite upper limit to the safe temperature. Fracture will occur at concentrations of Mg_4Al_3 compound well below this temperature, and the fractured surfaces oxidize rapidly enough when exposed to air to cause further temperature rise.

The increased difficulty in working that occurs with increased aluminium content may be exemplified by the production of tubes by extrusion at constant billet temperature of an alloy containing 2 per cent aluminium at 50 feet per minute against 1 foot (30·5 cm) per minute for an alloy containing 8·5 per cent aluminium. In general, the lowest aluminium content that will provide the necessary mechanical properties for the application is specified, and the available alloys cover the range from alloy AZ21 to AZ80, representing the single phase area on the binary Mg-Al equilibrium diagram (*Figure 1*) in which solid solutions are obtained. It might be thought that in the extrusion

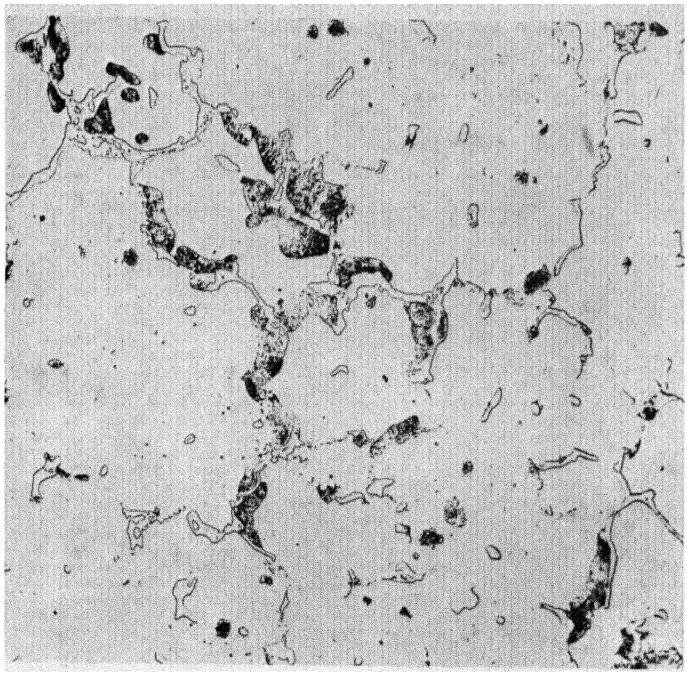

Figure 3. Photomicrograph of sand-cast magnesium alloy, as cast AZ80 *(Magnification 200 ×)*

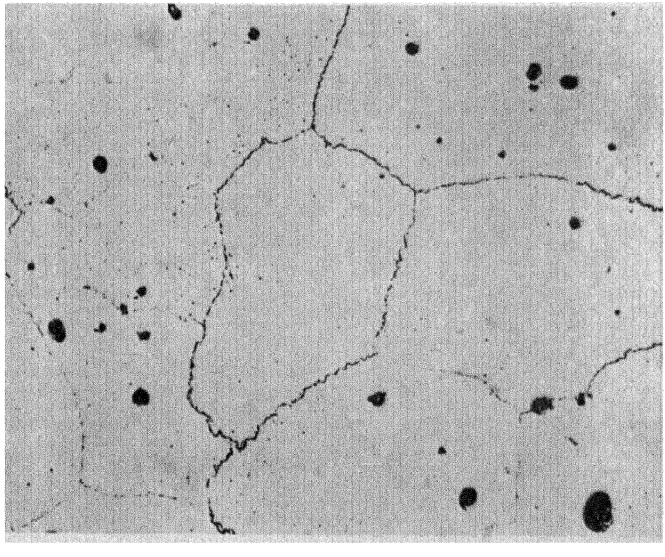

Figure 4. As Figure 3, solution treated (Magnification 200 ×)

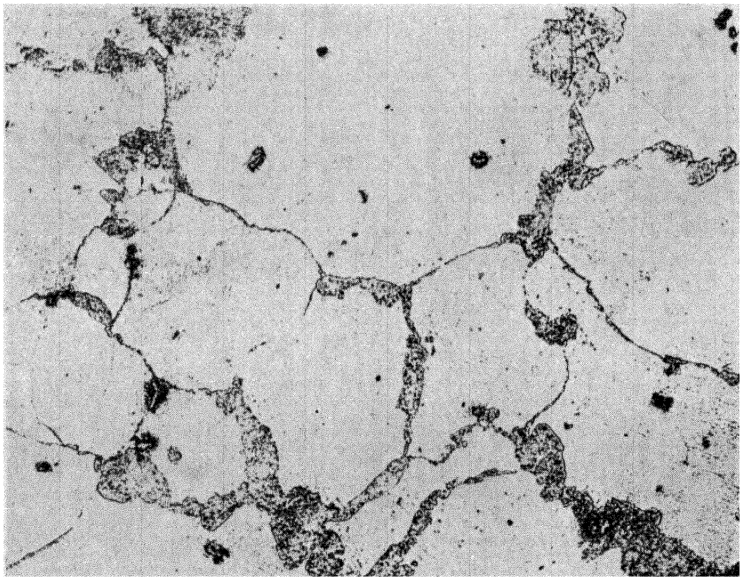

Figure 5. As Figures 3 and 4, solution treated and aged (Magnification 200 ×)

process, where the metal is totally enclosed except for the die orifice, higher working pressures could be maintained under what are apparently conditions of almost pure hydrostatic compression. However, at the die orifice friction against the die surface tends to retard the flow of the outer layers of the bar or shape being produced, with the result that it is stretched over the core, giving an external tensile layer stress system, balanced by compressive stresses in the core. The friction also raises the emergence temperature above that of the billet, so that the temperature at which the residual tensile stresses exceed the strength of the surface layers is the limiting factor. As this point is approached the metal can be seen to ripple, giving an appearance similar to Luders lines, and then to burst open at the surface with a fir tree effect. The difficulty in working the 8·5 per cent aluminium alloy under these circumstances is as much due to the increased probability of eutectic formation giving local weakness as to the increase in specific shear strength due to the higher concentration of solid solution. Tensile properties of extruded rods of magnesium-aluminium alloys are shown diagrammatically in *Figure 2*.

A finer grain size, more even distribution of Mg_4Al_3, and prolonging the preheating period to bring this compound into solution, all give improved qualities to the wrought material. To effect improvements in this direction, billet casting has progressed by three stages in the last twenty years, from the use of heavy iron moulds, through the phases of water cooled moulds of heavy cast iron to light wrought iron shells, to the method in widest use today known as direct chill casting or continuous casting. In the latter procedure, metal is poured into a water cooled collar, temporarily closed at the base by a movable plate. As soon as an outer shell and base of magnesium alloy has solidified the base plate is slowly lowered and a water spray impinges directly on the magnesium alloy. Pouring continues at a rate which maintains a constant upper level and the metal already cast becomes its own mould. If the lower part of the solid metal is cut off periodically the method is continuous as long as molten metal is available. The process may be mechanized to run with very little attention.

The depth of metal in the (α + liquid) condition is small and the time taken to pass from liquidus to solidus comparatively short, so that in spite of the high temperature gradients the concentration gradients

of the alloying elements on a microscopic scale are not as great as in other methods of casting. Due to the rapid cooling from the solidus, little or no precipitation of the compound can occur, so that within the α-phase concentration gradients on a microscopic scale are reduced and on reheating solution of the compound, if any is present, takes place rapidly and a homogeneous solid solution is quickly produced.

Table V. Effect of Grain Size on Mechanical Properties of Alloy AZ92: *Sand Cast, Solution Treated*

Grain Size Average Grain Diameter in	*Ult. Tensile Strength* *lb/in^2	*Elongation* %
0 003	40,700	10 6
0 025	31,200	4·5

* 100 lb/in^2 = 7·03 kg/cm^2

GRAIN SIZE CONTROL

The best mechanical properties of magnesium alloys are only attained when the grain size is less than a maximum value. With castings the grain size is determined by the formation of nuclei before solidification, and further heat treatment does not bring about any significant change. For wrought materials, the as-cast grain size has some influence on the final properties but the grain size finally achieved depends on the temperatures and speeds of working and on the heating and cooling cycles.

The effect of grain refinement on the mechanical properties of cast magnesium alloys is so spectacular that engineering specifications always refer to metal in the grain refined condition *i.e.* the use of these alloys as structural materials depends on the achievement of fine grain size. An example of the effect of grain size on the mechanical properties is given in *Table V.*

Considerable development work and fundamental research has taken place on this subject in recent years and the better understanding of the phenomena involved has been a big step forward in foundry development and alloy research.

The alloys of magnesium with aluminium have been grain refined for many years by an arbitrary procedure known as superheating,

without any knowledge of the fundamental mechanism involved. The procedure consisted in heating the crucible of metal to be cast to a temperature of about 850°C, and then cooling as rapidly as possible to the desired casting temperature. Holding at a lower temperature allows the effect gradually to diminish and to produce coarse-grained metal, although this is not so marked when high purity magnesium is used. The limitations which this procedure imposed on the use of permanent moulds can be realized. With sand moulds a batch of moulds can be prepared to take all the metal from one crucible as soon as it has cooled to the correct temperature. The cost of a permanent mould or metal die can only be justified, however, if it can be filled at stated intervals and not at times determined by one of a batch of moulds or a special melting cycle. Hence they are operated by ladling sufficient metal from a large crucible or bowl just to fill the mould, from which the casting is stripped as soon as it is solid, and the mould is then prepared for a repetition of the cycle. The crucible cannot be superheated and cooled for each cycle, neither is it practicable to maintain it at the higher temperature or to allow a smaller quantity to cool to the casting temperature in the smaller spoon ladle. Consequently permanent mould or gravity die castings in magnesium alloys had the reputation of being less reliable than sand mould castings, simply because of the greater difficulty in control of grain size.

The reduction in strength of a coarse-grained component compared with a fine-grained one would be greater than that which would be attributed to grain size alone if the castings were equally sound. With the higher temperature gradients induced by a metal mould, the absence of numerous nuclei allows dendrites to grow uninterruptedly from the mould wall to the hottest part of the casting, the tips of the dendrites being continuously fed with fresh metal. The last zone to solidify would therefore suffer shrinkage which is greater than average for a uniformly fine-grained casting solidifying from a large number of local centres. This shrinkage could only be compensated by a flow of liquid metal from some other part of the casting, which might be blocked off or bridged over by more rapid solidification at some change in section. This produced considerable difficulty in obtaining sound castings in permanent moulds and only recently has this method of casting been contemplated as a production method in the same way that it is by the aluminium founder.

There was ample need for fundamental research on the causes and control of grain refinement and work has been published by authors on both sides of the Atlantic, most of which has been adequately summarized by NELSON.[16] Much of the early research was contradictory. One team of investigators using ultracentrifuge methods isolated a spinel compound containing aluminium and magnesium. Others demonstrated that iron was picked up from the melting crucibles at the superheating temperature and that iron-free magnesium melted in refractory crucibles by electric resistance was not refined by superheating, but could be refined by adding iron salts. Manganese was discovered to be the cause, to be refuted by those who pointed to the impurities in the manganese salts commonly used as an addition.

As the investigations proceeded it became evident that no one element or compound could be held as exclusively responsible for the phenomenon of grain refinement by superheating. Refinement could be achieved by the addition of small amounts of a wide range of substances, including iron, manganese and zirconium amongst metals, and elemental carbon, hydrocarbons, acetylene chlorides of carbon and spinels. Iron is to be avoided for obvious reasons of contamination, although ferric chloride has been used in Germany, Sweden and other parts of Europe for many years for this purpose and this method of grain refinement gives excellent mechanical properties although it cannot be recommended unless corrosion resistance is of minor importance. In the superheating method samples taken at different temperatures show a temperature-grain size relationship, and material which was originally coarse-grained will, if heated to any given temperature, attain the same grain size as originally fine-grained material treated similarly, thus indicating equilibrium conditions at any given temperature. There was thus strong support for a theory of a liquid crystal structure. Inoculation of coarse-grained metal with grain refined metal does not affect the grain size until such quantities are added that the process becomes one of dilution rather than inoculation. A channel of molten metal connecting a coarse-grained reservoir with one containing fine-grained metal, under conditions such that no transfer by convection is likely to occur, results in grain refinement of the total quantity in about the same time interval that the presence of a metallic addition in one vessel can be detected in the other as a result of diffusion.

High purity magnesium containing iron of the order of 0·001 per cent when alloyed with similarly pure aluminium and manganese in excess of 0·15 per cent produces alloys which are inherently finer in grain than commercial grade metal. Grain refining treatment will further reduce the grain size, but only to the same specific size as that attained by coarse-grained metal. Grain coarsening treatments do not produce such coarse grain as with commercial grade metal, however. Contrarily, inoculation of molten magnesium with iron by reduction of ferric chloride produces immediate grain refinement, providing manganese is present. The use of carbon arc melting furnaces showed that contamination with carbon produced refined metal and even metal made by reduction of magnesium oxide with carbon was noted as being inherently fine-grained. Inoculation with carbon black, gaseous compounds of carbon, and eventually simultaneous degassing and grain refinement by decomposition in the melt of organic halides such as carbon tetrachloride or carbon hexachloride became established in some foundries.

The nucleation theory of grain refinement was finally given a firm foundation when work under Nelson proceeded to electron microscope studies of the phenomenon. With fine-grained metal, star shaped crystals of hexagonal habit could be observed, and in some cases identified. Compounds which have hexagonal structures above certain temperatures account for the temperature dependence. There is inadequate knowledge of the compounds that might be formed by all the various inoculents that have been observed to fit the behaviour of each into a general theory in precise detail, but sufficient is known of the compounds of manganese to trace their existence in alloys containing aluminium and manganese as follows:

$MnAl_6$ is stable below 715°C
$MnAl_4$ exists between 715°C and 850°C
$MnAl_3$ appears above 850°C

$MnAl_6$ is rhombic in structure and $MnAl_4$ is hexagonal. $MnAl_3$ is probably rhombic, as additions of iron give $(FeMn)Al_3$ compounds without change in structure and apparently in gradual transition to $FeAl_3$ which is definitely known to be rhombic. A melt of magnesium with 8 per cent aluminium and 0·25 per cent manganese when held at 715°C and cast is found by microradiographs to contain a cloud of particles that have been identified by electron diffraction to be orthorhombic in structure and similar to $MnAl_6$. The grain is coarse and

after superheating to 850°C and casting hexagonal crystals appear, believed to be $MnAl_4$, when the grain structure is refined. After superheating to 1000°C and rapidly quenching from the high temperature, coarse-grained metal is obtained.

It would appear that grain refining is caused by the presence of nuclei of hexagonal habit and of lattice constants close to those of magnesium. If such nuclei are stable within a limited temperature

Table VI. Effects of Various Methods of Grain Refinement on the Mechanical Properties of Alloy AZ80x *Sand Cast, As Cast*

Degassing Treatment	*Grain Refining Method*	*Grain Size AGC No*	*Ultimate Tensile Strength* *lb/in^2	*Elongation* %
None	*None*	12 5	23,400	4·1
Solid flux	*Superheated*	4	27,300	5·0
Chlorine	*Superheated*	4	28,400	4·8
Chlorine	*Lampblack*	3	30,000	5·5
Chlorine	CCl_4	3	30,600	6 5
Combined treatments				
Hexachlorethane		3	29,000	5 0
Hexachlorobenzene		4	29,600	5 2
Ferric chloride		4	30,200	6·0

* 100 lb/in^2 = 7 03 kg/cm^2

range, then the magnesium alloy must be heated to that range to obtain refinement of grain after casting. A number of carbides, nitrides and chlorides and also metallic zirconium apparently share the necessary physical characteristics with the compound $MnAl_4$. Nelson reports that in no case could hexagonal crystals be observed in magnesium alloys containing beryllium. It is not clear whether he examined aluminium free alloys containing beryllium and zirconium together, but it is known that with the possible exception of some zirconium containing alloys the addition of the order of parts per million of beryllium immediately and irrevocably destroys any possibility of grain refinement.

The grain refinement produced by zirconium was first mentioned by GAUTHIER[17] in a recommendation for overcoming the coarsening caused by beryllium additions. The addition of 0·005 per cent

beryllium reduces the tendency of magnesium to oxidize in the molten state, apparently by means of a surface film of low surface tension which consists of an oxide containing beryllium. As far as can be discovered by existing experimental procedure, beryllium is not soluble in liquid or solid magnesium to any appreciable extent, and its only interest is in the reduced quantities of flux and inhibitors that can be used in its presence.

The effects of zirconium, however, are more far reaching, but owing to the ease with which it forms insoluble compounds with many of the

Table VII. Effect of Zirconium on Mechanical Properties of Pure Magnesium

Material	0·2% *Proof Stress* **lb/in*²	*Ultimate Stress* *lb/in*²	*Elongation* %
Pure Mg ..	2,600	13,500	6·0
Mg 0 68% Zr ..	5,400	23,500	13 1 (*Leontis*)
Mg 0 66% Zr	8,500	25,500	18·5 (*Meier*)

* 100 lb/in² = 7·03 kg/cm²

common alloying elements, impurities present in magnesium alloys and the difficulties attendent on alloying it with magnesium, its benefits were not immediately realized. Moreover, $ZrAl_3$ has a tetragonal structure and it would not, therefore, be expected to cause grain refinement in alloys containing aluminium. Zirconium not only forms high melting point compounds of hexagonal habit with magnesium, but there is considerable evidence that a peritectic reaction occurs near the melting point. Thus its grain refining properties can be compared with the effect of titanium on aluminium. However, sufficient zirconium can be added to increase the mechanical properties by virtue of its solid solubility, so that studies initiated by its grain refining effects (such as are shown in *Table IX*) gave rise to the development of an interesting alloy series.

MAGNESIUM BASE ALLOYS CONTAINING ZIRCONIUM

Zirconium has limited liquid solubility in magnesium, owing to the formation of a high melting point compound apparently above 0·70 per cent zirconium, where the liquidus curve breaks to indicate a

peritectic reaction (*Figure 6*). At temperatures below 900°C it is difficult to alloy more than 1 per cent zirconium, but below the peritectic point the full amount added appears to be in solid solution, which diminishes rapidly with decrease in temperature, so that between 400°C and room temperature zirconium appears to have no solid solubility in magnesium. The effect of zirconium on the mechanical properties of pure magnesium in the sand cast condition is illustrated in *Table VII.*

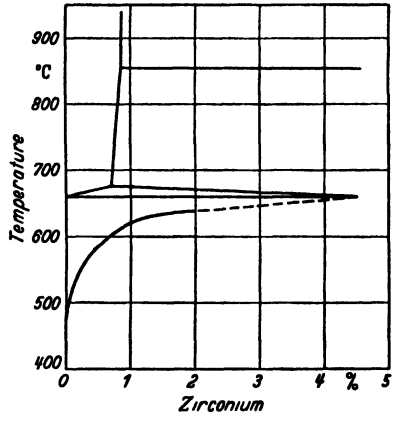

*Figure 6. Magnesium-zirconium equilibrium diagram (Sauerwald[18])**

All the above results are in the as-cast condition, but it is not stated how soon after casting the tests were made. It is possible that natural aging, which is to be expected, causes the differences in proof stress between the two authorities quoted. Also LEONTIS[19] used electrolytic cell metal and MEIER and LIVINGSTONE[20] employed Pidgeon high purity magnesium.

The grain refinement of pure magnesium by other means such as carbon inoculation or superheating is difficult to carry out, and to obtain any evidence that such is possible involves rapid cooling from the critical temperature range. There has not yet been any assessment, therefore, of the relative influence of grain refinement or the alloying effect of a sparingly soluble element of suitable characteristics on the improvement in mechanical properties of the binary magnesium-zirconium alloy. To develop ternary alloys likely to possess interesting

* More recently G. A. MELLOR of the National Physical Laboratory has published a revised and probably a more authentic diagram.[21]

mechanical properties it is now evident that those elements most obviously suited can be selected from a table of physical constants. Those metals of hexagonal crystal structure with atomic radius not too dissimilar from magnesium are shown in *Table VIII.*

Of these metals, titanium has proved difficult to alloy with magnesium in appreciable quantity, and hafnium is comparatively scarce. Both zinc and cadmium have been investigated comprehensively as alloying

Table VIII. Metals of Hexagonal Crystal Structure and Atomic Radius similar to Magnesium

Metal	*Atomic Number*	*Atomic Volume cc/gm atom*	*Atomic Radius cm* × 10^8
Magnesium .. .	12	14	1 76
Titanium ..	22	10 7	1 62
Zinc	30	9 16	1 53
Zirconium .. .	40	13·97	1 71
Cadmium .. .	48	13 01	1·73
Hafnium	72	13 98	1·76

elements with magnesium and their binary alloys develop properties second in interest only to the magnesium-aluminium alloys.

Magnesium-zinc-zirconium ternary alloys and magnesium-cadmium-zirconium alloys are known to possess mechanical and physical properties of value to fabricators and engineers; the series containing zinc, owing to a slight difference in price, is of greater use to industrialists. After the original suggestion of Gauthier, German workers initiated investigations on these alloys; in Britain the first commercial alloys were produced in 1946, followed by the United States and by the work of the Canadian Bureau of Mines. The introduction of zirconium into molten magnesium is by no means easy to accomplish and an excellent account of some of the difficulties encountered, and of the phenomena observed, has been published by EMLEY.[3] Owing to the disparity in melting points, addition of metallic zirconium gives poor efficiency and is quite impracticable. Zirconium metal is most easily produced by reduction of the oxide or salt with magnesium as a reducing agent. It is therefore advisable to select suitable compounds that will be reduced by molten magnesium to produce directly the desired alloy and an innocuous salt of magnesium. Magnesium halides are used as protective

and cleansing fluxes during melting and are stable at melt temperatures. Zirconium halides can be reduced at the usual melting temperatures, giving metallic zirconium and either magnesium chloride or magnesium fluoride, which is removed by the flux used as a protective cover. The efficiency of this operation is low, DOAN and ANSEL[21] reporting 30 per cent and MEIER 35 per cent zirconium recovery.

British investigators found that zirconium was most conveniently added in the form of an alkali metal chlorozirconate, but had

Table IX. Effects of Zinc and Zirconium on Mechanical Properties of Magnesium Alloys

Alloy	*Condition*	*Ultimate Strength* *lb/in^2	0·2% *Proof Stress* lb/in^2	*Elongation* %
Magnesium 6% *Zinc*	*As cast*	25,000	10,000	5·0
Magnesium 6% *Zinc*	*Fully heat treated*	30,000	22,500	1·5
Magnesium 6% *Zinc* 0·8% *Zirconium*	*As cast*	39,000	20,000	10·0
Magnesium 6% *Zinc* 0·8% *Zirconium*	*Fully heat treated*	46,300	29,000 *all bars sand cast*	10·0

* 100 lb/in^2 = 7·03 kg/cm^2

considerable trouble with flux inclusions. Emley demonstrated that these inclusions arise as a result of entrapment of the products of the reaction in clusters of zirconium rich particles which are insoluble in molten magnesium. These particles were due to precipitation of dissolved zirconium by the metallic impurities present in the magnesium metal, notably aluminium, silicon, iron and manganese. The composition of the magnesium used is not given, but it is certain to have been produced by the electrolytic process. Meier, using high purity magnesium and a similar technique of addition by means of chlorides, reported that no significant flux inclusions were encountered in the course of making over 150 melts of alloys containing zirconium from high purity magnesium.

The effect of zinc on the mechanical properties of magnesium is well known and has been confirmed many times. Data are given in *Table IX.* Maximum strength and ductility in the as-cast conditions are obtained with 2 per cent zinc, the elongation falling off as the zinc

content is further increased. It requires zinc in excess of 2 per cent, however, to obtain alloys susceptible to heat treatment, and a higher zinc content is desirable to promote sound castings. The properties obtained by binary alloys containing 6 per cent zinc in the fully heat treated condition do not approach those of magnesium aluminium alloys.

The zirconium addition in the range 0·65–1·0 per cent gives a ternary alloy of magnesium with 6 per cent of zinc and 1 per cent of zirconium, possessing mechanical properties in excess of any previously known magnesium base alloy.

It will be noted that the heat treated alloy containing zirconium not only possesses high strength, but retains excellent ductility in surprising contrast to the binary alloy. The heat treatments applied to the two alloys differ widely, however, because of a further unsuspected property induced by the zirconium addition.

The retention of zinc in solid solution is hindered by the presence of a eutectic melting at 341°C and therefore the binary alloy is heated at 315°–320°C to avoid damage to the structure and possible melting. After two hours the temperature was raised to 338°C, which, although the liquidus is somewhat higher, is as near the eutectic as it is practicable to go, and maintained for fourteen hours to obtain optimum solution of the constituents. After quenching, the specimens are subsequently aged at 180°C for twenty four hours. But in the presence of zirconium the solidus is raised to 510°C and it was found possible to heat the alloy without danger of melting, or even distortion, to 500°C. The heat treatment for this alloy, according to Meier, was a total of two hours at 500°C, followed by age hardening at 150°C. This effect of zirconium on the ternary alloys is of great importance in fabricating, giving much greater freedom in casting, heat treating and hot forming techniques.

Wrought Alloys—The extrusion speed of the stronger magnesium aluminium alloys is limited by the presence of a eutectic formed with the compound Mg_4Al_3 and the solidus curve dips to 430°C which is sufficient to cause local areas of fusion owing to normal inhomogeneities in structure in alloys containing over 6 per cent aluminium. Owing to the generation of heat at the die orifice, billet temperatures are about 50°–70°C cooler and the limiting temperature of 360°C generally implies high pressures and slow extrusion speeds.

The corresponding eutectic temperature with the binary magnesium-zinc alloy is 341°C and the solidus is somewhat higher with 6 per cent

zinc at 390°C. It is possible that a temperature lying between these two could be attained at the die face with high purity materials, using a billet temperature of 320°C. The addition of 1 per cent zirconium causes a rise of over 100°C in the solidus and at least an equivalent rise in eutectic temperature, and allows extrusion to proceed at much faster rates. Observed temperatures show that the section does not break up until the solidus temperature is closely approached across the die orifice. The billet temperature can thus be increased, giving a reduction in internal shear and heat generated by friction, and extrusion speeds up to 50 feet (1,525 cm) per minute can be accomplished.

The extrusion tests and micro-examination of cast and wrought specimens indicate another structural difference between the alloys containing 6 per cent zinc and 1 per cent zirconium and those containing aluminium. With the latter, the aluminium compound is difficult to get into solid solution, so that in alloys of gross composition, less than the maximum aluminium theoretically dissolvable, the local compositions vary from islands of Mg_4Al_3 to an impoverished solid solution. The temperature should not exceed that of the eutectic until the compound is all in solution. This is a lengthy process, and it is therefore difficult to conduct any operation on a magnesium alloy containing more than about 6 per cent aluminium at any temperature above that of the eutectic. The structures of the magnesium-zinc-zirconium alloys show a considerable amount of coring but little of the MgZn compound. Apparently gradients from a supersaturated solid solution to an impoverished solution are more stable in this fine-grained material than the presence of undissolved compound.

The addition of zirconium to molten magnesium effects the precipitation of a major part of any impurities present, before zirconium can be made available as an alloying ingredient. Thus these alloys are super-pure and it is possible that if the former equilibrium diagrams were repeated, using high purity materials which were not then available, the results would show better agreement with the phenomena now being explored.

The presence of zirconium appears to retard diffusion of zinc between the concentration gradients noted, and providing the higher temperatures possible are not fully exploited extrusions can be made with grain sizes of 0·0001–0·0003 in (0·0003–0·0008 cm) average grain diameter and of very high mechanical properties. High extrusion rates,

apparently by promoting diffusion, cause an increase in grain size accompanied by a reduction in strength the compressive yield point decreasing at a faster rate than the tensile yield.

Any form of heating will produce a similar result, and solution heat treatment is of little benefit. The homogenizing effect is overshadowed by a reduction in compressive yield strength due to grain growth and re-orientation. It is probable that the best combination of properties and practicable production will be attained by extruding possibly through a water cooled die or certainly into a temperature controlled quenching medium, and then to age harden by precipitation at temperatures sufficiently low to avoid grain growth.

The finest grain size is attained with all metals by extruding or working at the lowest possible temperature. The strength of the material resisting the deformation is then sufficient to produce very high residual internal stresses. The material is critically strained, either locally or generally, and on subsequent heating for solution heat treatment, relaxation and movement cause grain coarsening. With some metals it is possible to increase the temperature at the point of emergence of the extrusion so that not only is all work conducted above the recrystallization temperature, but the metal is sufficiently plastic to relax completely before cooling. The operation is thus conducted during the period where the ultimate strength of the metal exceeds the internal stresses sufficiently to resist breakdown, but the yield stress is low enough and the relaxation time of the metal short enough to permit complete annealing. Conditions would be affected by mass, light sections cooling and stiffening much more rapidly than pieces of larger bulk. A study of diffusion rates should indicate whether such conditions could be attained by the Mg-Zn-Zr alloys in a smaller time interval than is required for diffusion of zinc within the grains.

The alloy containing 6 per cent zinc has a high capacity for cold work *i.e.* a low rate of work hardening, partly demonstrated by the fact that relatively cold slow extrusion does not yield low elongation values, nor is the tensile yield strength any higher than would be expected through the finer grain size, which has the advantage of ability to resist high local strain. This combination of properties suggests good toughness, a property frequently thought to be related more closely with yield strength ultimate strength ratio and elongation values. But if we compare the toughness, as measured by energy to

rupture on a static notched bend test, of the magnesium alloy AZ80x in the fully heat treated condition, having almost identical tensile and compressive properties for yield, ultimate stress and elongation, with that of the ZK61 alloy, we find the latter superior by at least five times, 3 inch pounds and 15 inch pounds (0·035 kg metres and 0·175 kg metres) being typical examples. The zirconium bearing alloy is thus inherently less notch sensitive than the older magnesium alloys and forms an excellent basis for fundamental study.

The mechanical properties can be varied to suit widely differing conditions, but *Table X* gives the results of a number of tensile tests in

Table X. Mechanical Properties of Alloy ZK61*: Magnesium, 6 per cent Zinc, 0·85 per cent Zirconium Extruded Rod*

Condition	*Yield Point* **lb/in²*	*Ultimate Stress* *lb/in²*	*Elongation* %
As extruded 15 *ft/min* . .	35,000	45,000	10 0
Age hardened 160°*C* .. .	40,000	50,000	8 0
Solution treated 500°*C* .. .	28,000	41,500	18 0
Solution treated and aged 160°*C*	42,000	50,000	8·0

* 100 lb/in² = 7 03 kg/cm²

the form of easily reproducible, or minimum median, figures under general conditions, such as could be used for establishing engineering specifications.

The compression yield in the directly age hardened condition is within 95 per cent of the yield in tension, whereas in the solution heat treated and age hardened condition the compression yield is reduced to 80 per cent of the tensile figure. The greater increase in strength obtained by aging the solution treated material suggests the problem overcoming the diffusion and grain growth that delays the development of an even higher strength material as an intriguing field of study.

Magnesium-Cerium-Zirconium Alloys—Haughton and Prytherch have published investigations undertaken at the National Physical Laboratory on a number of magnesium base alloy systems, with the object of developing materials suitable for use at elevated temperature.[10] For this purpose the most promising results were obtained by the addition of cerium calculated as total rare earths—amounts up to 6 per cent being added as *mischmetall* which is mainly composed of

cerium and lanthanum. The mechanical properties of alloys containing 3–6 per cent rare earths are comparable at temperatures of 250° to 300°C with the more commonly used aluminium alloys. At air temperature, and particularly in the sand cast condition, their total efficiency was still lower than that of many aluminium base alloys.

The rare earth metals crystallize in the close packed hexagonal system, and should not interfere with the grain refining effects of zirconium. These alloys were studied by MURPHY and PAYNE[22] in England and by LEONTIS in the United States, and they developed two main types of alloy, one containing 3 per cent cerium with 0·5 per cent zirconium nominated EK31 and the other containing 2·5 per cent zinc, 2·5 per cent cerium, 0·5 per cent zirconium. The addition of zinc does not appreciably affect the room or elevated temperature properties, but is claimed to assist in casting. Cerium forms a compound Mg_9Ce as a result of peritectic reaction of Mg_3Ce. The former compound gives a eutectic at 21 per cent rare earths, and at 590°C, Haughton reported a solid solubility of 1·6 per cent, reduced to zero below 400°C, so that some increase in strength is obtained by precipitation hardening after a solution treatment.

Whereas the alloying of zinc with magnesium raises the mechanical properties, the addition of rare earths either to pure magnesium or to the magnesium-zinc alloy results in alloys of almost exactly similar mechanical properties, the further addition of zirconium raising the properties of both alloys by an equal amount. Furthermore, the zirconium addition is less sensitive in the presence of cerium than with a binary magnesium-zinc alloy. With the latter, the highest properties are not achieved until almost 1 per cent zirconium is present, the increase in strength being due both to grain refinement and the zirconium rich alloying constituent. The presence of rare earth metals determines the dominant characteristics of the alloy and the zirconium would appear to behave purely as a grain refiner.

During solidification the alloys containing rare earth behave very differently from those containing aluminium and zinc. These traditional alloys develop a close dendritic network in cooling from the liquidus to the solidus and the final alloy-rich solution although of eutectic composition breaks down to islands of compound. Gaps are produced in the network and it is difficult to avoid shrinkage porosity.

With the alloys containing cerium and zirconium, a typical eutectic

structure is apparently present and can be confirmed radiographically, filling the micro-cavities remaining in the last parts to solidify. The major portion of a casting is homogeneous in structure with little coring and no sign of micro-shrinkage cavities. The last portion of the melt to solidify behaves as a true eutectic, and the solidus is indicated by a sudden surface shrinkage as the eutectic composition is reached and solidification is complete.

Table XI shows that at air temperature the addition of zinc is of no apparent benefit to the alloys containing cerium. Leontis finds that the

Table XI. Mechanical Properties of Magnesium Alloys containing Cerium, Zinc and Zirconium Sand Cast, As Cast

Alloy			0·2% Yield Stress	Ultimate Stress	Elongation
Ce	Zn	Zr	*lb/in²	lb/in²	%
—	3·0	—	6,000	25,000	10·0
3·0	—	—	8,800	15,500	2·5
3·0	3·0	—	9,900	15,400	1·5
3·0	—	0·5	15,200	24,800	7·0
3·0	3·0	0·5	14,700	23,200	4·0

* 100 lb/in² = 7·03 kg/cm²

creep properties suffer in rather a different way. In this table the alloys containing both metals behave similarly to that which contains cerium alone. In creep at temperatures of 150° and 200°C the alloys containing both metals behave similarly to those containing zinc alone. *Table XII* gives creep limits, expressed as the limiting stress required to give a creep extension of 0·1 per cent in 100 hours of test, taken from curves published by Leontis.

The above tests are carried out in the heat treated and aged condition, which, though slightly improving the mechanical properties at air temperature, considerably increases the creep resistance at slightly elevated temperatures.

MAGNESIUM-LITHIUM ALLOYS

Hume-Rothery has drawn attention[11] to the well known diagonal relation of the elements of the first short period and to the readiness with which magnesium and lithium can replace one another in their compounds. The phase diagram[23] shows two series of solid solutions,

that of lithium in magnesium up to 21 atomic per cent and from 30 atomic per cent of lithium, either a solid solution of magnesium or an intermediate phase based on Mg_2Li in lithium. This corresponds to an alloy of 11 per cent by weight lithium, so that whilst industrially it would be regarded as a magnesium-base alloy, it is more properly a lithium-base alloy containing a high proportion of magnesium by metallurgical considerations.

The physical characteristics of alloys containing more than 11 per cent of lithium are undoubtedly those of a lithium alloy the melting point of

Table XII. Creep Limits required to give Creep Extensions of 0·1 per cent in 100 hours of Test

Alloy	*Temp. of Test* °C	*Creep Lmit* * *lb/in²*
Mg–3Zn–3Ce ..	149°C	8,300
Mg–6Zn–3Ce .	149°C	6,900
Mg–3Ce ..	204°C	10,000

* 100 lb/in² = 7 03 kg/cm²

which has been raised by the addition of a solute element. The structure represents a body-centred cubic, with coordination number 8, so that plastic deformation at normal temperatures should occur relatively easily in contrast to the hexagonal structure of magnesium *i.e.* deformation by cold work is possible. As the magnesium and lithium atoms apparently replace one another in complete disorder, for the purpose of further alloy development the alloy of magnesium with 11 per cent lithium can be treated as though it were lithium metal. It is reasonable then to expect that silver, a more electro-negative element would alloy with this metal to produce electron compounds with a tendency to order typified by the CsCl structure in which the like atoms (of silver) would be situated at the centres of unit cubes.[24] To procede to quarternary alloys, the system silver-cadmium shows a disordered body-centred cubic β-phase, and it is probable that the system cadmium-lithium depends rather on electron concentration than on valency bonds. The investigation thus forms a study of the superlattice arrangements of the body-centred cubic system and a distinct contrast to that of magnesium base alloys where the hexagonal structures are of great importance.

Some U.S. Navy investigators also appear to have adopted this reasoning and have released information on the following alloys, developed in collaboration with the Battelle Memorial Institute:[25]

1 binary alloy 89 per cent magnesium, remainder lithium,

2 quarternary alloy 68·5 per cent magnesium, 15 per cent cadmium, 5 per cent silver, 11·5 per cent lithium.

The quarternary alloy gives 0·2 per cent yield strength of 43,000 lb/in^2 with 8 per cent elongation when tested in tension from wrought specimens, but has relatively poor corrosion resistance. The binary alloy shows corrosion resistance under intermittent sea water immersion tests corresponding to loss of weight from 2–10 mg/cm^2/day. This is not inferior to that of controlled purity magnesium alloys, and so might be used as a cladding material for the stronger alloy produced in sheet form.

The more complex alloys suffer a loss of strength if subjected to prolonged aging at temperatures as low as 66°C, although they are stable at normal atmospheric temperatures. More extensive knowledge of the effect of trace elements may improve the properties which can be obtained as it is already reported that extreme brittleness can be caused by the presence of as little as 0·01 per cent sodium.

The comparative rarity of lithium metal may retard rapid commercial development of these alloys, but their physical and mechanical properties may prove of use to the aircraft engineer. The specific gravity is as low as 1·5 and the body-centred cubic lattice implies not only better cold forming properties than are possible with hexagonally structured materials, but that the properties in compression[26] will more nearly equal those in tension.

REFERENCES

[1] HANAWALT, J. D., NELSON, C. E. and PELOUBET, J. A. *Trans. Amer. Inst. min. (metall.) Engrs* 14 (1942) 299

[2] DIX, E. H. *Corrosion of Metals* p 164 New York, 1946

[3] EMLEY, E. F. *J. Inst Met.* 75 (1949) 481

[4] DOW CHEMICAL CO. Magnesium Division, Midland, Mich. U.S.A.

[5] DAVIES, J. K. *Magnesium Rev. and Abs.* 8 (1948) 46

[6] DOMINION MAGNESIUM LTD, Haley, Ontario, Canada

[7] KROENIG, W. O. and PAWLOW, S. E. *Korrosion u. Metallsch.* 9 (1933) 268

[8] MARTINSON, M. Private communication

[9] NELSON, C. E. *Trans Amer. Foundrym Ass.* 56 (1948) 1

[10] HAUGHTON, J. L. and PRYTHERCH, W. E. *Magnesium and its Alloys* London, 1937

[11] HUME-ROTHERY, W. *The Structure of Metals and Alloys* London, 1936

[12] KURNAKOW, M. S. and MIHEERA, V. I. *Abs. J. Inst. Met.* July (1938) 252

[13] BECK, E. A. *Technology of Magnesium*, p 50 London, 1940
[14] WARRINGTON, H. G. *Metal Ind. Lond.* 62 (1936) 256
[15] BECK, E. A. *Technology of Magnesium*, p 21 London, 1940
[16] NELSON, C. E. *Amer. Inst. Min. Engrs, Tech Publ. No.* 1708; *Metals Technol.* 2 (1944)
—— *Amer. Inst. Min. Engrs I.M.D. Symposium* (1946)
—— *Trans. Amer. Inst. min. (metall.) Engrs* 52 (1944) 159, 392
[17] GAUTHIER, G. *Canadian Patent No. 396, 383 (1940)*; *French Patent No. 829, 316 (1937)*
[18] SAUERWALD, F. *Z. Metallk.* 40 (1949) 41
[19] LEONTIS, T. E. *Metals Technol., Tech. Publ. No.* 2371, 1948
[20] LIVINGSTONE, H. and MEIER, J. W. Private communication
[21] DOAN, J. P. and ANSEL, G. *Metals Technol., Tech. Publ. No.* 2107, 1946
[22] MURPHY, A. J. and PAYNE, R. J. M. *J. Inst. Met.* 73 (1946) 105
[23] BECK, E. A. *The Technology of Magnesium and its Alloys* p 2 London, 1940
[24] HUME-ROTHERY, W. *Atomic Theory* London, 1946
[25] NELSON, C. E *A.S.M.* Ottawa, 1949
[26] JACKSON, J. H., FROST, P. D., EASTWOOD, L W. and LORIG, C. H. *J. Met.* 1 (1949) 149
[27] MELLOR, G. A *J. Inst. Met.* 77 (1950) 163

BIBLIOGRAPHY

ACHENBACH, K., NIPPER, H. A. and PIWOWARSKY, E. Contribution to the Question of Melting Practice for Cast Magnesium Alloys *Giesserei* 26 (1939) 597, 621
—— The Effect of Superheating on the Technological Properties of Magnesium Casting Alloys *Aluminium* 21 (1939) 209
MURPHY, A. J., WELLS, S. A. E. and PAYNE, R J The Melting of Light Alloys *Metal Industry* 55 (1939) 7, 33
CHUBB, W. F. The Casting of Magnesium Alloys *Light Metals* 3 (1940) 191
FOX, F. A. The Time and Temperature of Superheating *Metal Industry* 58 (1941) 550
SIEBEL, G. Influence of Certain Volatile Organic and Inorganic Substances upon the Mechanical Properties of Cast Electron *Research Rept.* 19 (1942)
Report from Research Dept. I.G. Farbenindustrie B. Herfeld RTB—TIB 3C
TINER, N. Superheating of Magnesium Alloys *Metals Technol.* 12 (1945), *Amer. Inst. Min. Engrs, Tech. Publ. No.* 1935
FOX, F. A. and LARDNER, E. An Exploration of the Problem of Superheating in Magnesium Base Alloys *J. Inst. Met* 71 (1945) 1
—— —— *Magnesium Rev. and Abs.* 5 (1945) 68
MAHONEY, C. H., TARR, A L. and LE GRAND, P. E. A Study of Factors Influencing Grain Size in Magnesium Alloys and a Carbon Inoculation Method for Grain Refinement *Metals Technol.* 12 (1945), *Amer. Inst. Min. Engrs, Tech. Publ. No.* 1892
HULTGREN, R., MITCHELL, D. W. and YORK, B. Grain Refinement of a carbothermic Magnesium Alloy by Superheating *Trans. Amer. Inst. Min. (metall.) Engrs* 161 (1945) 315
—— —— Grain Refinement of Magnesium Alloys without Superheating *Trans. Amer. Inst. Min. (metall.) Engrs* 161 (1945) 323
HALL, H. T. A Note on Attempts to Produce Superheating Effect by Addition of Alumina to Electron A–8 *Magnesium Rev. and Abs.* 3 (1945) 68, 86
DAVIS, J. A., EASTWOOD, L. W. and DE HAVEN, J. C. Grain Refinement of Magnesium Casting Alloys *Trans. Amer. Foundrym. Ass.* 53 (1945) 352; *Amer. Foundryman* (1945) 35
—— —— —— Recent Developments in Magnesium Foundry Melts *Light Metal Age* 4 (1946) 8, 17, 22, 25

TSENTER, A. Technology of Magnesium Alloy Production in Germany *Tsvetnye Metal* 19 (1946) 55

PARTRIDGE, G. B. Production of Magnesium Melting Technique and Grain Refinement *Metallurgia, Mnchr* 35 (1947) 241

MEIER, J. W., KOZLOWSKI, H. and MARTINSON, M. W. Refining of Magnesium Casting Alloys CIM Sept (1949) Reprint

STRAUSS, K. Improvement in or relating to the degassing and grain refinement of Magnesium *U.K. Patent No. 606,072*

I.G. Farbenindustrie *Belgian Patents No. 444, 757; 444, 770*

Developments in Magnesium Production and Fabrication *B.I.O.S. Report No.* 1338

The German Magnesium Industry *B.I.O.S. Report No.* 5

Metallurgical and Industrial Developments in Magnesium *F.I.A.T. Report No.* 89

Production and Fabrication of Magnesium Alloys *C.I.O.S. Report No.* 21

Battelle Reports 1–8

Investigation of Cast Magnesium Alloys and of Existing Foundry Techniques and Practices *War Metallurgy Board, U.S.*

SYMPOSIUM ON POLYGONIZATION

5

INTERNAL STRAINS AND RECRYSTALLIZATION

R. W. Cahn

THE PROCESSES that occur during the annealing of deformed crystalline solids are usually classified in four groups: recovery, primary recrystallization, grain growth, and secondary recrystallization. It is the main purpose of this paper to discuss a fifth type which has only recently been studied systematically, and to explore its connection with the others, particularly with primary recrystallization. The discussion centres largely on the internal strains present in deformed solids, because these are a common factor in all the processes in question. The theory of dislocations introduced by TAYLOR[1] and OROWAN,[2] and now well established, is adopted throughout the paper; it has not been thought necessary to discuss the evidence for this theory, particularly since full accounts are readily available.[3, 4]

Recovery is defined as a change in the physical properties of a cold worked solid when annealed, in which no structural change is discernible either microscopically or by X-rays. An inevitable uncertainty is encountered in assigning a change in properties to this process, owing to the limited resolving power of microscopes and the averaging over extended volumes inherent in ordinary X-ray techniques. BURGERS[5] showed that X-rays are the more sensitive tool in this respect, and more recent work by GUINIER and TENNEVIN[6] has proved that when a material increase in resolving power is attained, structural changes can be detected which had previously been missed. On the basis of these results and of investigations reported below, it appears probable that much of what has been called recovery in fact involves detectable structural changes.

Primary recrystallization is the mechanism by which the disturbance remaining in the crystal lattice after recovery is almost completely removed; it occurs at temperatures higher than those required to bring about recovery. Primary recrystallization takes place by growth from nuclei to form an entirely new structure. The circumstances under

which the nuclei are formed are not yet entirely clear. Some views on the subject will be advanced in this chapter.

Grain growth generally follows primary recrystallization and consists of a uniform coarsening of the structure, involving a reduction in the number of grains. The nature of this phenomenon has been clarified principally by SMITH,[7] BURKE,[8] HARKER and PARKER[9] and BECK *et alii*.[10] It is primarily connected with the surface energies of the grain boundaries and reflects the tendency of the material towards a structure in which this energy is a minimum. Since internal strains are not fundamentally involved in this process, they will not be further discussed here.

Secondary recrystallization occurs when the structure resulting from primary recrystallization after very heavy cold work is subjected to further annealing, and consists in the selective growth of a few grains only, as distinct from uniform coarsening. The reasons for this occurrence are still far from clear. In some of the most recent work[11, 12] it is ascribed to the imperfect elimination of internal strains by primary recrystallization, while other workers consider the dominant factor to be a marked dependence of the rate of grain boundary migration on the relative orientations of the growing grains and their neighbours.[13, 14]

POLYGONIZATION

A structural change has recently been definitely recorded by x-rays after a deformed specimen has been annealed, in which the relation of the new structure to the old is much closer than is usual in primary recrystallization. This relation is manifested by the fact that the asterisms found in a Laue photograph made from a deformed specimen remain in the same positions in a photograph made from the same specimen after annealing, though the asterism is split into many separate spots with little or no blackening of the film between them. CRUSSARD,[15] for example, found this occurred when he annealed single crystals of aluminium elongated by a few per cent in tension. *Figures 1* and *2* are enlarged reproductions of one asterism due to a crystal extended by 12 per cent before and after annealing at 555°C, respectively. The enlargement is such that 1·5 cm represents 1° rotation of the normal to the reflecting plane. (Before the first photograph was made the specimen had been given a recovery anneal at 200°C.) *Figure 2* differs markedly from the Laue photographs obtained after primary recrystallization of single crystals, where a number of new spots are found on the

photograph, often distributed almost at random. When the preceding deformation has been heavy, there is a preferred orientation or texture, which causes the Laue spots due to the new grains to bunch together, but it is never found that the bunches coincide with the original asterisms.[16] Crussard called the phenomenon he had found 'recrystallization *in situ*', because it appeared that each portion of the lattice had kept its orientation intact, while losing its elastic strain. *Figure 2* reveals that the structure formed gradually as annealing was continued. Laue photographs, taken after successive anneals, showed the spots becoming gradually sharper and then decreasing in number, but always occupying the area of the previous asterism. This behaviour is quite unlike that of grains formed by primary nucleation. The Laue spots corresponding to such grains appear suddenly and grow in size until the new grains fill the x-ray beam or impinge on other grains, thereafter remaining constant in size. Recrystallization of this type was in fact observed in most cases to follow a recrystallization *in situ*. The latter was accompanied by a gradual decrease of the elastic limit of the specimen, while nucleation was accompanied by a sharp fall in this property. Prior to Crussard's work, COLLINS and MATHEWSON[17] made a study of the recrystallization of aluminium. In a few of their specimens they observed recrystallization *in situ* before nucleation; from the published photograph it appears that the subdivision of the asterisms was coarser than that described by Crussard.

Probably the first observation of this phenomenon was recorded by KONOBEEVSKI and MIRER;[18] a Laue photograph taken after annealing a strongly bent rocksalt crystal revealed recrystallization *in situ*. Here the subdivision of asterisms was also coarser than that found by Crussard. They did not pursue the matter, considering perhaps that it represented simply a marked example of preferred orientation after primary recrystallization, an opinion also expressed by Burgers in his book on recrystallization.[5]

Some years later, ANDRADE and his collaborators [19, 20] discovered that crystals of sodium and potassium, when extended at room temperature, invariably gave Laue photographs with spotted asterisms. Assuming that this was due to recrystallization at this temperature, they tried extending and photographing a sodium crystal under liquid nitrogen. The asterisms were now continuous, confirming their opinion. As a complementary experiment, iron crystals were extended at high

temperatures and then further annealed in stages. As expected, the asterisms exhibited increasing discontinuity, while at the same time spots due to new grains became more numerous. Examination of the sodium crystals revealed that in addition to the slip bands, the surface showed a number of bands transverse to the latter, which became more marked with increased slip. Collins and Mathewson found the same on aluminium crystals. It is probable that this observation is intimately connected with the type of recrystallization under discussion and the point will be raised again later.

Recrystallization *in situ* has been observed under various circumstances on several occasions during the last few years. BUNGARDT and OSSWALD[21] took Debye-Scherrer photographs of weakly rolled, coarse-grained aluminium. After annealing at temperatures insufficiently high to cause primary recrystallization, the coarse patches constituting the Debye-Scherrer rings decomposed into a finer structure. The fact that they used monochromatic X-rays probably prevented them from observing the full range of orientations present. Again, Debye-Scherrer photographs of extended and annealed mild steel taken by CHITRUK[22] showed the same effect, though it was much less marked.

MADDIN[23] has detected recrystallization *in situ* in a strongly stretched crystal of α-brass remaining from some earlier experiments.[24] The crystal, in spite of the considerable deformation, was only slightly disturbed internally, as was shown by the sharpness of the Laue spots. These small spots became minutely subdivided on annealing, rather as in Crussard's experiments, and only very localized signs of nucleation could be detected. This finding tallies with CRUSSARD and AUBERTIN's observation[25] that single crystals of zinc, even after extremely heavy extensions, exhibit only very slight asterism, and that they recrystallize *in situ* before nucleation; the latter is true also of polycrystalline zinc. HIRST[26] had evidence of recrystallization *in situ* in lead crystals subjected to tensile creep at elevated temperatures, while DUNN[27] observed it in Laue patterns taken near deformation bands in deformed silicon ferrite.

Recrystallization *in situ* has even been found to occur in specimens subjected to creep at moderately high temperatures, without the necessity of any subsequent annealing. Thus, CRUSSARD and AUBERTIN[28] took Laue photographs of coarse-grained aluminium after prolonged creep at 200°C and obtained clearly split asterisms in them. This source of softening has not been taken into account previously in

Figure 1. Aluminium crystal, extended 12 per cent, annealed 16 hr at 200°C (Crussard)

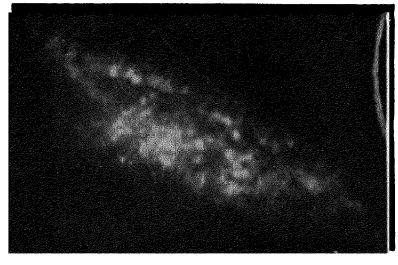

Figure 2. Aluminium crystal, extended 12 per cent, annealed ½ hr at 555°C (Crussard)

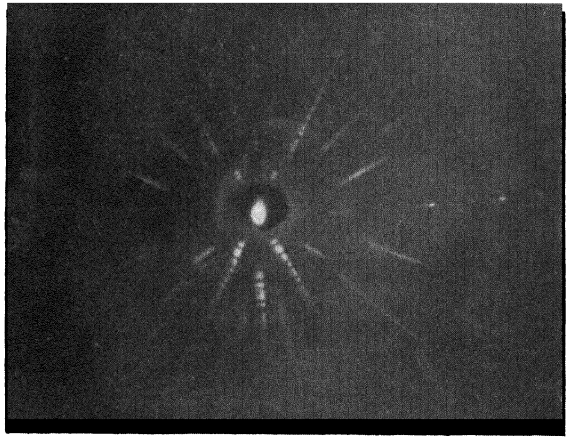

Figure 4. Zinc crystal, bent to 0·35 cm radius, annealed 2 hr at 400°C: Laue photograph with x*-ray beam perpendicular to glide plane*

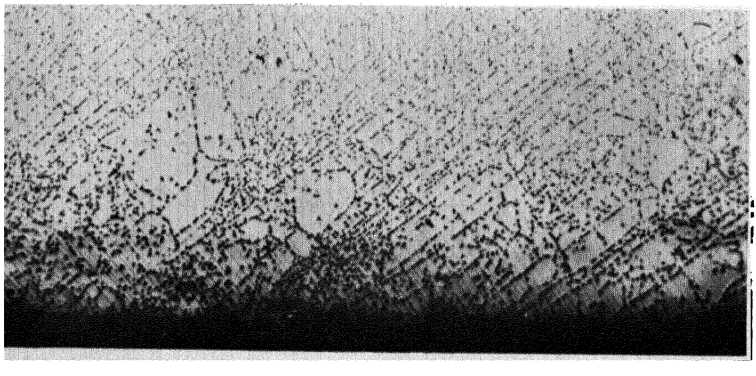

Figure 5. Aluminium crystal, bent to 3 cm radius and annealed 18 hr at 625°C. Etched and bent further (Magnification 55 ×)

quantitative considerations of creep; it would seem to be a relevant factor, particularly in those recent theories based upon the motion of dislocations.

In most of these experiments the evidence gained by x-rays was not supplemented by other measurements which might give a better insight into the nature of the type of recrystallization in question, except in Crussard's work with aluminium crystals, in which he sought to

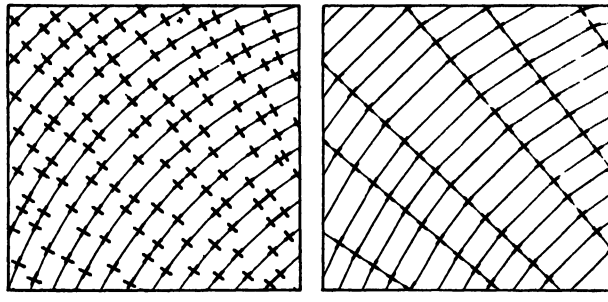

a b

Figure 3. Nature of polygonization (schematic): a *as bent* b *annealed, the crosses represent excess positive dislocations*

correlate the changes in Laue photographs with the course of the elastic limit with annealing temperature. There was no doubt that recrystallization *in situ* was accompanied by a marked softening of the specimens; the softening at those stages at which the modification of the Laue photographs became visible was stated to be distinct from the softening due to recovery. Crussard was therefore led to the remark that 'il s'agite donc d'un phénomène bien tranché, avec l'apparition d'édifices cristallins nouveaux quoique très petits et orientés presque comme le cristal initial'. If this were so, it seemed worth while to seek microscopic confirmation of the existence of new crystallites and to try to correlate any microstructure with the nature of the applied deformation and the crystallography of the specimens. The present author has carried out some experiments with this purpose.[29, 30]

In the course of this work it soon became clear that most information could be obtained by using bent single crystals after the manner of Konobeevski and Mirer's original experiment. The subdivision of the asterisms was demonstrated very clearly by this means in zinc, magnesium and aluminium as well as rock salt. Thus, cylindrical zinc crystals 1 mm in diameter were bent in such a way that almost pure

plastic bending would occur with the operation of a single glide system. The nature of the recrystallization observed is shown schematically in *Figure 3*; the glide planes are perpendicular to the plane of the paper and the glide direction is in it. This type of recrystallization has been named polygonization, for a reason obvious from the sketch. *Figure 4* is a Laue photograph taken with the x-ray beam directed perpendicular to the glide planes, the glide direction is vertical and it will be seen that the equatorial asterisms which are due to practically undeformed lattice planes are not elongated or subdivided. *Figure 5* is a specimen photomicrograph of the Y-surface (see *Figure 6*) of a polygonized aluminium crystal. This crystal had the shape and orientation shown in *Figure 6*, was bent to a radius of 3 cm and annealed at 625°C for 18 hours. Before the photograph was made, the crystal was bent a little further to develop fresh slip lines and these can be seen at the edge of *Figure 5*; they serve to show up the crystallographic direction of the polygonization boundaries. (The polygonization boundaries in zinc are shown in COTTRELL,[4] *Figure 1*.) It will also be seen that the boundaries etched up as rows of etch pits, giving an appearance quite unlike that of a normal grain boundary. This peculiarity was found in all the specimens examined, both zinc and aluminium, and, as will be seen later, it casts some light on the mechanism of polygonization.

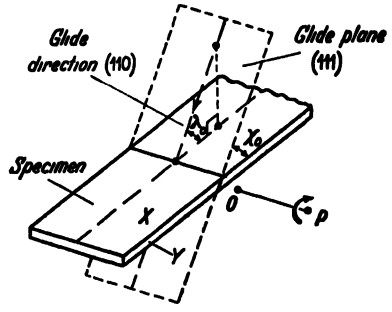

Figure 6. Orientation of aluminium crystals used in author's experiments

In these experiments polygonization was detected in the x-ray photographs with radii of curvature from about 22 mm downwards, and even with radii as small as 3·5 mm the specimens usually recrystallized in this way instead of undergoing primary recrystallization. Guinier and Tennevin's work has now made it clear that the observed limit of 22 mm was due to insufficient sensitivity of the ordinary x-ray technique and that, for aluminium at any rate, a very weak bending suffices. Very sharply bent crystals also polygonized, showing that even quite considerable distortions can be relieved by this means.

It has been suggested by LACOMBE[31] that confusion might be avoided

if the terms polygonization and recrystallization *in situ* are given slightly different meanings. Polygonization is to refer to the very fine blocks described by Guinier and Tennevin in the present volume, which can be detected only by their special focusing technique. The other term is to describe the later stage when the blocks have become larger and the angles between them increased sufficiently for them to become visible in ordinary Laue photographs. This division is of course arbitrary and approximate and depends not only on the x-ray technique used, but also on the dimensions and x-ray absorption of the specimen. Furthermore, the present author was able to show up polygonization boundaries quite clearly by etching, while the Laue photographs gave no sign of the phenomenon. Nevertheless the distinction is worth making if only because the criterion of change in the x-ray pattern is frequently used to differentiate between recovery and recrystallization, and the relevance of polygonization to recovery is thus emphasized.

Similar experiments were carried out with crystals of magnesium, aluminium and rock salt, to discover whether the results were peculiar to zinc; all exhibited polygonization. HONEYCOMBE[32] has extended this finding to include cadmium. His results are very striking, since before bending his crystals he stretched them by as much as 200 per cent. There was hardly any asterism in the Laue photograph and annealing did not lead to any change in the pattern. When, however, the stretched crystal band was bent and re-annealed, clear evidence of polygonization was obtained by x-rays. *Figures 7* and *8* represent two of the photographs taken by Honeycombe; they show in particular how the number of grains decreases with prolonged annealing.

THEORETICAL CONSIDERATIONS

Before considering how these results assist the interpretation of the various observations mentioned, it is necessary to discuss theoretically the nature of polygonization in bent crystals. In the first volume of this series[4] Cottrell has advanced an explanation in terms of dislocations and it is indeed impossible to give a satisfactory account of the phenomenon on any other basis.

Plastic bending is characterized by the presence of excess dislocations of one sign along the surfaces of the glide lamellae. These dislocations provide for continuity of the lattice between adjacent lamellae, because the lattices in the surfaces of two lamellae in contact are expanded

in one and contracted in the other, and the same thing is true of the lattices on the two sides of a dislocation line. From another consideration it can also be seen that a large number of dislocations must be present. The amount of slip or shear on each slip plane varies from zero to a positive or negative maximum in passing from the neutral axis of the specimen to the outer or inner edge respectively. Since one unit slip is held to occur by the passage of a dislocation right along a slip plane, it is obvious that a shear gradient such as just described is associated with the presence of dislocations which have become stuck on the slip plane. To be more precise, an excess of dislocations of one sign over those of the other sign is required; this distinguishes a bent crystal from a crystal deformed in an externally homogeneous way, for in the latter the numbers of the two types of dislocations (which are responsible for work hardening) must balance.

If these excess dislocations now diffuse along the glide plane and gather at intervals, two consequences arise. The lattice between the two dislocation bunches straightens out *i.e.* loses its macroscopic flexure, and the bunches of dislocations separate unbent regions of slightly different orientations. BRAGG[33] and BURGERS[34] have shown that any boundary between two regions of slightly differing orientation is in effect a row of dislocation lines, which may be of edge type or screw type only or of both types. Bragg discussed the present ideal case (*Figure 3*), where only edge dislocations are involved because adjacent unbent regions are related by rotation about an axis which is parallel to edge dislocation lines. A simple calculation shows that the number of dislocations required to form, at equal intervals, boundaries with the correct inclinations between the adjacent regions is the same as that necessary to establish continuity between the lamellae, and that number is independent of the glide lamella thickness and of the spacing of the boundaries. The mechanism described for polygonization is therefore crystallographically self-consistent.

It remains to consider the energetics of the process. The final state must have a lower free energy than the initial state or polygonization would not take place and primary recrystallization would occur instead. There is, of course, a decrease in elastic energy when the bent lattice planes straighten out into segments, but at first sight it would appear that there must be a large increase of free energy due to the grouping of large numbers of edge dislocations of the same sign, which are known

to repel each other. However, the repulsion between such dislocations is a minimum when they collect in a boundary plane which is perpendicular to the glide direction. The repulsion must be still further decreased if the dislocations are spaced at uniform intervals in the boundary plane and the lattices on the two sides of the boundary plane are inclined at the corresponding angle. Then the elastic fields associated with the dislocations are restricted to the immediate region

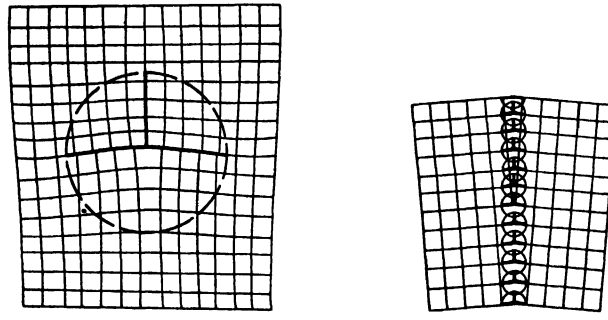

Figure 9

a *Schematic section of an isolated edge dislocation*
b *schematic section of an array of edge dislocations forming a polygonization boundary*
The circles delimit the approximate areas over which the elastic strain is appreciable

of the boundary, while the elastic field in the case of an isolated dislocation extends over a wide volume around it. (This is only true when the boundary is perpendicular to the glide plane,[4, 34] an orientation which was observed in all cases examined.) *Figure 9* illustrates the point diagrammatically, the circles about the dislocations indicating the regions in which elastic strain is appreciable. In actual fact the dislocations cannot be spaced quite regularly, but must occur in small groups on each active glide plane, which in turn consists of many active planes very close together.[35] This should not affect the above considerations, which show qualitatively that a boundary created during polygonization must have a low free energy. Thus according to this model polygonization results in a decrease of free energy and the structure formed must be thermodynamically stable.

GROWTH OF SUB-GRAINS

Once a macroscopically bent crystal has undergone polygonization, it appears to be in a relatively stable state, for no nucleation has been

found to occur on prolonged annealing except in very sharply bent crystals. However there appears to be a form of grain growth. As Guinier and Tennevin mention in the following chapter, the x-ray patterns after successive anneals show different arrangements of spots even if the identical part of the specimen is examined on each occasion. Furthermore, LACOMBE and BEAUJARD[36] describe a system of sub-grains in aluminium crystals which, as will be shown, must be due to polygonization. The configuration of this system of sub-grains is completely changed by an anneal, confirming that polygonization boundaries are very mobile. Examining bent aluminium crystals which had been annealed for a long time, the present author found that a few of the sub-grains revealed by etching had grown very large compared with their neighbours. Some such large blocks may be seen in *Figure 5*. In his previously mentioned experiments on extended and bent cadmium crystals, Honeycombe took Laue photographs at different stages of annealing. He found that the spots along the asterisms became more widely spaced with prolonged annealing near the melting point, as may be seen by comparing *Figures 7* and *8*. This means that coalescence of some of the grains has occurred. Such coalescence is presumably due to the decrease of the total area of boundary present and consequent decrease of the free energy of the system. Since they often extend right across the specimen, the grain-boundaries can wander freely; when two of them meet at one point, the tendency will be for the grain included between them to be swallowed up for reasons which have been explained[7] in detail by Smith. As the boundaries separate regions of only slightly differing orientation the energy of the boundary must be very low, the change in energy due to coalescence must be small and this accounts for the high temperature and long annealing required to bring it about.

BEHAVIOUR OF STRETCHED CRYSTALS

When polygonization occurs in crystals deformed in tension, as in Crussard's experiments with aluminium and zinc, coalescence is again observed on prolonging the heat treatment. This is manifested by a decrease in the number of spots within the area of the original asterism, but as this process progresses, primary recrystallization *i.e.* nucleation, often supervenes, so that the structure giving rise to the fine spots is entirely consumed. To understand this, the nature of polygonization

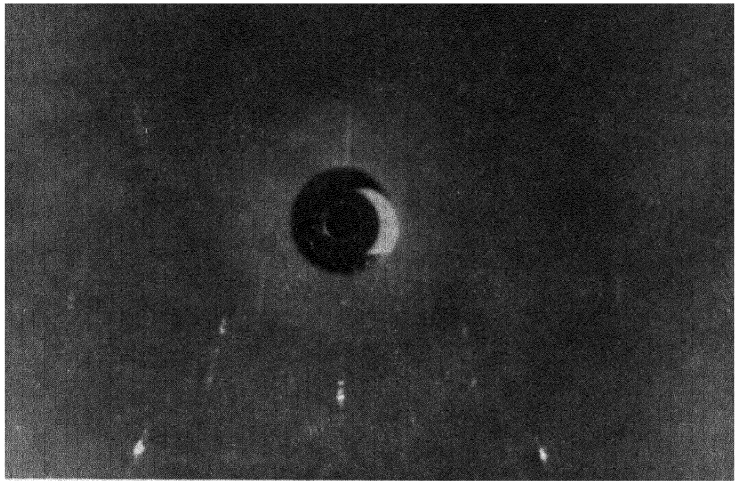

Figure 7. Cadmium crystal, extended 200 per cent, then bent 0·35 cm radius and annealed 2 hr at 285°C. Laue back reflection photograph (Honeycombe)

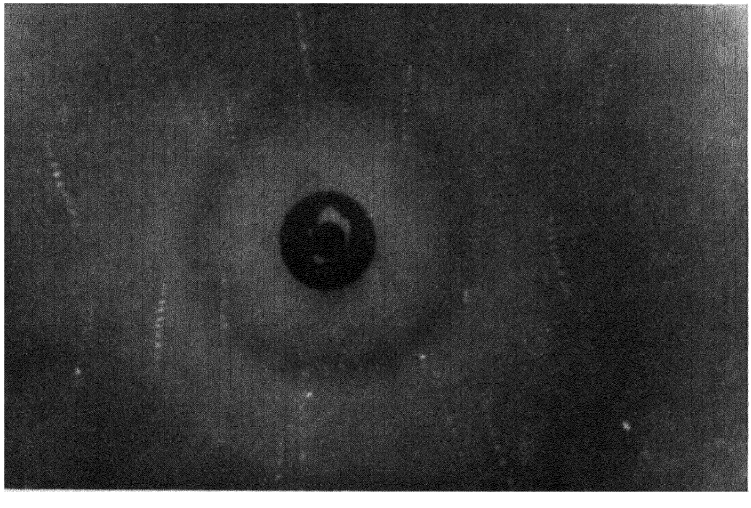

Figure 8. As Figure 7, annealed a further 90 hr at 300°C (Honeycombe)

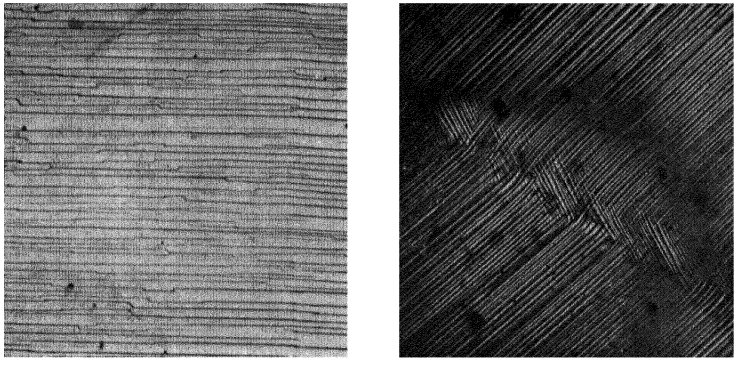

a b

Figure 10

a *Aluminium crystal, extended 7 per cent (X surface) (Magnification 120 ×)*

b *Aluminium crystal, extended 25 per cent (Y surface) (Magnification 126 ×)*

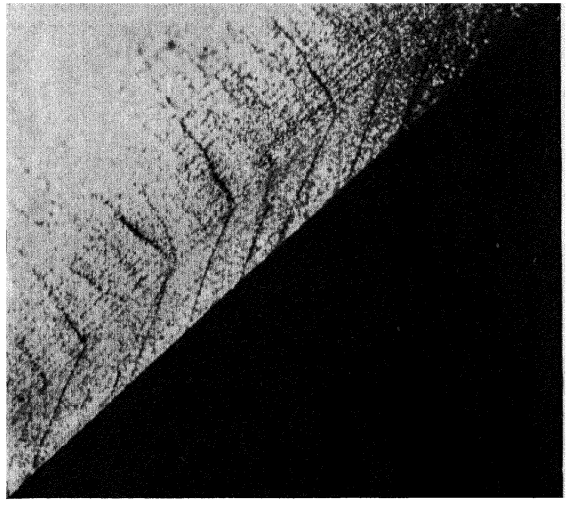

Figure 11. *Aluminium crystal, extended 20 per cent, annealed at 435°C, macroetched. Oblique illumination, showing both X and Y faces (Magnification 11 ×)*

in stretched crystals, which bears close resemblance to polygonization in bent crystals, must first be discussed.

It is practically certain that polygonization must be associated with some departure from homogeneous deformation during the elongation; in other words, some regions of the lattice must be bent, because polygonization by its nature can only occur in such regions. An ideal crystal after plastic elongation is in a physical state indistinguishable by x-rays from its original condition, except for restricted regions near the grips in which there has been flexural glide. This ideal seems to be approached with some metals. As previously mentioned, Honeycombe reports[32] a complete absence of asterism in cadmium stretched by more than 100 per cent, while Crussard and Aubertin record[25] that after 260 per cent elongation Laue back reflection patterns from zinc represent a rotation of only 4°. MADDIN, MATHEWSON and HIBBARD[24] state that there is an almost complete absence of asterism in α-brass crystals extended by 10–20 per cent, as well as an absence of any work hardening. Even in these instances, however, the lattice must be slightly bent, for recrystallization *in situ* has been observed both in zinc and α-brass. The change of lattice by stretching is shown by the fact that the slip bands can often be revealed when etching a polished section of a deformed specimen (BURKE and BARRETT,[37] MCLEAN,[38] JACQUET[38a,b]). Moreover, when a crystal is deformed in pure shear asterism does not always occur but hardening takes place, showing that the lattice has been changed.[53] The residual distortion along the active glide planes was clearly revealed by BERG[39] and BARRETT[40] by means of their microdiffraction technique. This type of distortion has been held by some authors to be the sole cause of asterism, at any rate in weakly deformed single crystals, but as distortion can be present (shown by means other than Laue photographs) without leading to asterism this theory is doubtful. It is probable that distortion on a sub-microscopic scale in the slip bands is always accompanied by distortion on a coarser scale where considerable asterism is found.

Some experiments carried out by the present author confirm this in the specific instance of aluminium. Thin plate shaped crystals of high purity aluminium (99·99 per cent) were made from the melt with a predetermined orientation by using a crystal of the required orientation as a seed. A sketch of such a specimen is shown in *Figure 6*. The top surface *X* and the side surface *Y* were ground flat and given a high

polish by electrolytic means. The crystals were pulled in tension by amounts varying from 7 to 27 per cent. The orientation was so chosen that a large deformation could be given within the domain of single glide and also so that the flexural glide necessary to accommodate the change in orientation of the crystal involved a rotation about the axis *OP*. The specimen had only to bend about its thickness and distortion due to this cause was relatively slight. After extension, photomicrographs were taken of the slip lines on both surfaces (slip lines were visible on the side surfaces because these were not exactly parallel to the slip direction). *Figure 10a* demonstrates the appearance of slip lines on the *X*-surface of a crystal extended by 7 per cent, *Figure 10b* shows the *Y*-surface of another specimen extended by 25 per cent. Different specimens were used for the two photographs to emphasize that *i* the slip lines on the top surface are broken up by elements of cross slip similar to those found with α-brass[24] by Maddin, Mathewson and Hibbard, practically no cross slip appearing on the side surface *ii* on the latter, the whole family of slip planes goes through a slight bend. The line of this bend appeared more clearly if the specimen was etched and so illuminated that the unbent matrix only appeared bright. These bends were more easily seen in strongly pulled crystals, but they existed even in those extended by small amounts. It was found that the specimens contained many such lines of flexure or deformation bands, approximately perpendicular to the glide planes. They become more marked and numerous with increased elongation. *Figure 11* shows the considerable contrast between the bands and matrix in a crystal stretched by 20 per cent and etched. The etchant used was that recommended by BARRETT and LEVENSON,[41] which gives accurately crystallographic etch pits. When the specimens were measured on a two circle goniometer it was found that the lattice in the bands was rotated about axis *OP i.e.* that axis which is also operative for flexural glide and the rotation was in the same sense as that associated with flexural glide.

It is clear that these bands are due to uneven extension of the crystal. They are formed if isolated parts of the crystal slip first and are followed by other parts and this is repeated at later stages of slip. The uneven extension of the crystal was confirmed directly by measuring after extension the distances between a number of scratches on its surface. *Figure 12* indicates diagrammatically how the bands are formed.

Annealing the crystals at 450–550°C, depending on the degree of elongation, led to recrystallization *in situ*. A detailed examination of the Laue patterns showed that asterism was largely due to the deformation bands and consequently the recrystallization *in situ*, which was deduced from the decomposition of the asterisms into spots, was also largely confined to these bands. This localization was clear only in weakly extended crystals, but microscopic examination showed it to exist also in more heavily deformed crystals. *Figure 13* illustrates the Y-surface of a crystal pulled by 31 per cent and annealed for 1 hour at

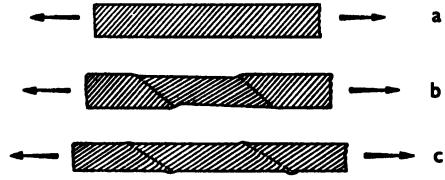

Figure 12. Creation of deformation bands as a consequence of inhomogeneous extension of crystal, a *before extension,* b *after local yielding,* c *after further extension*

450°C; the specimen was then repolished and extended by 2–3 per cent. The fresh slip lines go through sharp bends when they pass through a polygonized deformation band, instead of curving continuously as in *Figure 10*b. Any polygonization that may have occurred in the weakly bent regions between the bands is not revealed by this technique. It is suggested that polygonization occurs first in the strongly flexed bands and the sub-grains grow quickly there. In the regions between the bands the lattice is bent much more weakly, if at all, and polygonization is slower there; in weakly pulled crystals it may not occur at all. This picture is unfortunately complicated by the fact that crystals prepared from the melt are originally imperfect. The sub-grain structure due to this cause was also examined and was found to be different from that just described and much coarser. The type of deformation here described is an artificially simple one, used so that the results should be capable of a clear interpretation. Generally in deformation of a polycrystal, the operative slip systems and consequently the sets of deformation bands will be more numerous and diverse. It seems justifiable to say that polygonization and recrystallization *in situ* in extended or otherwise deformed crystals is primarily associated with the sharp lattice curvature present in deformation bands; these do not arise, of course, with uniform macroscopic bending.

These observations serve to explain Dunn's discovery[27] that recrystallization *in situ* occurred near deformation bands in silicon ferrite.

Surface markings have also previously been observed on extended crystals which are almost certainly equivalent to those just described, though their nature was not closely investigated. They were found on unetched aluminium and sodium crystals and were always associated, under suitable temperature conditions, with split asterisms. ANDRADE and TSIEN[19] attributed the bands they observed in crystals pulled by 10 per cent or more to the onset of double slip. It is now suggested that these are deformation bands, which lead to a visible crinkling of the unetched surface if the deformation is relatively heavy; this was detected by the present author with aluminium crystals. The remarkable clarity of the discrete spots in the sodium extensions is presumably due to the fact that the deformation bands in this metal are widely spaced, so that the X-ray beam would only intersect one or two of them. This is also suggested by the regular spacing between the spots and the regularity of the dependence of the angle between the spots on the degree of extension.

ANDRADE and CHOW[20] found that the range of rotation calculated from the asterism from sodium crystals was higher the lower the temperature of deformation. On the present interpretation this implies that slip in the single crystals is more inhomogeneous at low temperatures of deformation, leading to greater persistence of the bands; to put it more precisely, a band is formed earlier on during the deformation and one part of the crystal extends a considerable amount before the adjacent parts begin. This will cause greater lattice rotation inside the band. (The process sketched in *Figure 12* is really an example of yield, as once a portion of the crystal has begun to deform, it goes on deforming in preference to adjacent portions. Yield is known to be more marked at low temperatures.) According to the same authors it is also associated with greater hardening. It follows from the very mode of formation of the bands that they act as traps for dislocations and their efficiency in doing so must increase with the distortion of the lattice in them. It may also readily be understood why polygonization in an extended crystal brings about a fall in the elastic limit.[15] Before polygonization, a dislocation travelling along a glide plane meets a region where this plane is sharply bent and therefore full of immobilized dislocations through which the moving dislocation will consequently have difficulty in passing. After polygonization, this region is replaced by a number of relatively perfect crystalline blocks, inclined to each

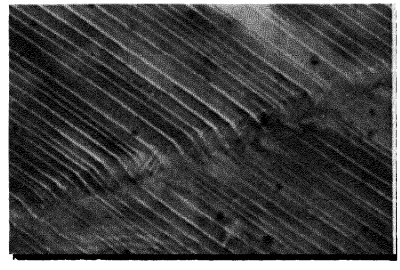

Figure 13. Aluminium crystal, extended 31 per cent and annealed 1 hour at 450°C (Y surface). Repolished and extended 3 per cent. Showing polygonized deformation bands (Magnification 260 ×)

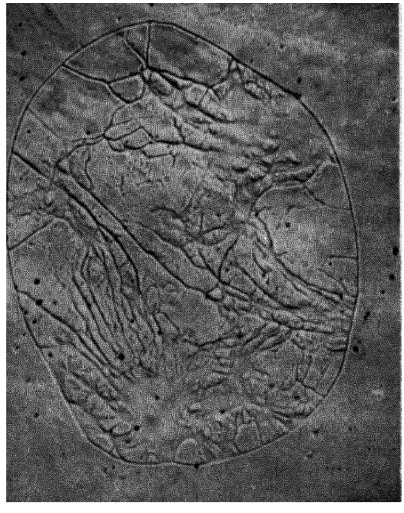

Figure 14. Included grain showing polygonization in a large crystal of Al-Zn *alloy made by recrystallization, electrolytically polished* (*Lacombe*) (*Magnification 70* ×)

other at small angles. These blocks will offer a smaller resistance to the passage of the dislocations than the continuously bent lattice.

The temperature of deformation affects not only the development of deformation bands but also the ease of polygonization. In general, the higher the temperature at which deformation has been carried out, the more readily polygonization occurs. Thus CAHN[30] found that zinc crystals bent under a stream of liquid air would not polygonize sufficiently, on subsequent annealing at 400°C, for the Laue asterism to become appreciably split. Again, in the experiments with aluminium crystals described previously, and in those mentioned by Guinier and Tennevin, the minimum temperature required to bring about polygonization was about 450°C. Their specimens were deformed at room temperature. CRUSSARD[42] found that crystals which had undergone creep for some time at 200°C had recrystallized *in situ*. Here the temperatures of deformation and of annealing coincided and the latter was much lower than the 450°C quoted. WOOD and his collaborators[43] have confirmed Crussard's observations with polycrystalline aluminium slowly deformed at temperatures ranging from 110–500°C. These observations are readily accounted for in terms of dislocations. The higher the temperature at which a metal is deformed, the less it is hardened for a given deformation. This implies that fewer dislocations have been trapped, and therefore less resistance is offered to the passage of mobile dislocations. Plastic deformation and polygonization both operate through the motion of dislocations, and anything which reduces the resistance to one must necessarily reduce the resistance to the other.

LACOMBE'S WORK

A digression may be made at this point to discuss the conclusions of LACOMBE and his co-workers,[33, 44] which affect the question of the energy of the boundaries between polygonization blocks. They showed that aluminium specimens consisting of a few large crystals, made by Carpenter and Elam's method, were often composed of a number of sub-grains or blocks inclined to each other at small angles. (GUINIER[45] has remarked that he has frequently obtained by this method crystals which were highly perfect. The reasons for the variability in this respect are not yet clear.) The boundaries between these blocks, in spite of their close similarity in orientation, showed up after etching with a special solution of mixed anhydrous acids as loci along which

crystallographic etch pits were concentrated. The ordinary boundaries between the main crystals, however, etched as continuous grooves as long as the crystals differed in orientation by more than a few degrees. Where they did not, as in aluminium which had been cold rolled and annealed, the boundaries were not revealed at all by etching. This makes it quite clear that the sub-boundaries differed in nature from the main crystal boundaries. But it does not mean that the energy of the sub-boundaries is greater. Where these meet the main boundaries no change in direction is discernible in the latter even at high magnification. Following the arguments[7] advanced by Smith, this means that the sub-boundaries have energies negligible compared with those of the main boundaries. Exactly the same discontinuous type of etching was noted by the present author with polygonized zinc and aluminium crystals; indeed the different modes of etching of ordinary and sub-grain boundaries give a possible clue to their respective natures. Cahn found that with both zinc and aluminium crystals, the mean spacing of slip lines in the bent crystal was often about equal to the mean spacing of etch pits on the Y-surface of the specimen. (However, this was not invariably so and there was sometimes a factor of two or three difference.) This can be understood when it is remembered that polygonization boundaries are surfaces on which groups of dislocations collect after diffusing along the active glide planes. A small group of dislocations furnishes an imperfection likely to start off an etch pit; and some such imperfection is probably necessary, just as it seems to be for the reverse process of crystal growth.[46] In between the groups of dislocations the lattice is continuous between the sub-grains, and these places remain unetched unless etching is continued long enough for the pits to grow sizable. An ordinary grain boundary is somewhat different. In BURGERS' view,[34] any boundary consists essentially of a uniformly spaced set of dislocations of edge and screw types, in suitable proportions. There is then no reason why any one point on a boundary should nucleate an etch pit rather than another and as a result one obtains a uniform groove instead. When two crystals have almost the same orientation, the dislocations composing the boundary are widely spaced, and if, as is probable, single dislocations are insufficient to nucleate an etch pit, the boundary will not etch up at all; which is, as already remarked, in sharp opposition to the behaviour of sub-grain boundaries.

Since the sub-grains discovered by Lacombe and Beaujard etch up in the same way as boundaries in bent and annealed aluminium crystals (*Figure 5*), it is probable that they are also the product of polygonization and this view is now held by GUINIER and LACOMBE.[47] Evidence has been advanced [48, 49] that, during primary recrystallization, the grains which are formed first upset the balance of internal stresses in the unrecrystallized matrix and are slightly distorted by the latter. Plate shaped crystals such as those used by Lacombe and Beaujard could most readily become distorted by a very gentle flexure about some axis lying approximately in the plane of the specimen. The resultant polygonization structure would consist of long prismatic sub-grains going right through the specimen, as found[36] by Lacombe and Beaujard. X-ray evidence of polygonization can also be obtained in undeformed crystals made from the melt, on prolonged annealing. This is presumably due to stresses induced in some way during growth.

LACOMBE and BERGHEZAN[50] have discovered that the sub-grain boundaries may attract solute atoms away from the neighbouring lattice. They found that it was possible, with crystals of aluminium-zinc alloy (8–12 per cent zinc) to reveal the sub-grain boundaries by electrolytic polishing alone without recourse to etching; but they could only do this after the crystals had been allowed to age for some hours at room temperature. They argued that during the aging period a concentration of zinc atoms built up along the sub-grain boundaries; this would lead to a local difference of electrode potential during electrolytic polishing and therefore to differential attack at the boundaries. *Figure 14* shows a polygonized grain with the sub-boundaries revealed in this way, embedded in a larger unpolygonized crystal.

CASTAING and GUINIER[51] have studied a similar concentration of copper in the sub-grain boundaries in aged 4 per cent aluminium-copper alloy, by means of the electron microscope. Minute discrete plates of $CuAl_2$ were found spaced out along the sub-grain boundaries but not, curiously enough, on the main grain boundaries, where only a few coarse precipitates occurred. The spacing of the plates was so small that, it was estimated, there was one plate per dislocation line. This finding contrasts with the previous suggestion, that the dislocations are present in bunches. It is probable that the $CuAl_2$ plates grew from minute regions on the contracted side of the dislocations, where the small copper atoms had been locally concentrated. This would agree

with Cottrell's calculations on the tendency of small atoms to form atmospheres around dislocations.[4] Similar observations with the same alloy have been made by Lacombe and Berghezan (quoted by CHAUDRON[52]) using ordinary microscopy.

PRIMARY RECRYSTALLIZATION

Returning to the main discussion, the later stages of the recrystallization of an extended crystal, during which new grains of quite different orientation form by primary nucleation and growth, must be considered. First, recovery occurs, presumably throughout the crystal, and this is followed, or rather accompanied, by polygonization, which takes place in regions where the lattice is curved. There is as yet insufficient experimental evidence to decide how much of the softening ascribed to recovery is in fact due to polygonization. But it is fairly certain that the two processes are distinct. Thus KOCHENDORFER[53] showed that naphthalene crystals deformed in pure shear *i.e.* perfectly homogeneously, were capable of some recovery, while polygonization would seem to be out of the question under such conditions. Recovery of the elastic limit is only partial; this is true *a fortiori* of softening by polygonization, because this affects only the lattice in the deformation bands.

Even when both recovery and polygonization are complete, the effects of cold work have not been entirely removed. Arguments have been advanced (p 161) implying that some of the retained energy goes to distort the lattice in the immediate vicinity of the active glide planes, even though there is no microscopically visible bending and the volume distorted may be too small to affect the Laue pattern. This energy can only be removed by primary recrystallization.

Nucleation of primary crystals—Much work has been done with the aim of elucidating this phenomenon.[5] Although so simple at first sight, there are many particulars the explanation of which is still the subject of speculation. The growth of the new grains, once they have nucleated, seems to be relatively straightforward; it is their nucleation which is still something of a mystery. It is remarkable that nucleation should occur at all, for the difference in free energy between a cold worked and an annealed metal[54] is very much smaller than that between crystallographically distinct phases. The transformation between two such phases is often sluggish; particular instances of such changes are now

well understood, for example the breakdown of the quenched α-phase in the aluminium-copper system.[55] Here the new phase is formed by a gradual process involving the diffusion of copper atoms into restricted zones which experience a progressively greater elastic force tending to break their continuity with the parent lattice; when this happens, nuclei are formed which are then able to grow. Another instance in which the free energy change is almost certainly very small, is the decomposition of one face-centred solid solution into two, with slightly differing parameters.[56] Here no nucleation in the ordinary sense occurs at all, but a periodic fluctuation in composition gradually develops in the lattice. We may suppose that nucleation in primary recrystallization is of an analogous nature, in the sense that some gradual change takes place which eventually culminates in the appearance of a visible grain. This supposition is strengthened by the existence in all cases of a finite induction period during which no sign of new grains can be detected. Evidence for this view is supported further since a relation exists between the orientations of the parent crystal and those of the new grains formed from it, as there is also between the phases in the analogous cases mentioned. After heavy homogeneous deformation this relation is very sharply marked[16] and even a weak tensile extension suffices to bring out a clear statistical connection.[57] If nuclei formed by chance conglomerations of atoms, as envisaged in BECKER and DÖRING's classical theory,[58] it would be difficult to account for this fact, but if we assume that most of the nuclei formed approximate to some preferred orientation, we have an explanation. The only alternative explanation would be in terms of a preferential growth of nuclei of particular orientations, and this possibility is discussed below.

It has already been pointed out that the elastic strain present in a deformed single crystal is very unevenly distributed; if this were not so, the difference in mean free energy as measured by TAYLOR and QUINNEY[54] would certainly be too minute to allow of any nucleation at all. This is true to an even greater extent in polycrystalline metals, where the restraining action of grain boundaries leads to very marked distortion in their vicinity, both on a relatively coarse and on a submicroscopic scale. Thus most of the nuclei are formed at the boundaries. In single crystals, nuclei form preferentially at deformation and twin bands and particularly in slip bands. This has been shown particularly clearly in a recent paper by JACQUET,[59] by means of a refined

microscopic technique. Minute grains first form on and grow along slip bands in rolled copper crystals.

The existence of particular orientation relationships has led Burgers to suggest that nuclei were formed at points of high energy lying in active glide planes. From his x-ray studies, he concluded that very small portions of the lattice were rotated about an axis lying in the glide plane, perpendicular to the glide direction. The justification of

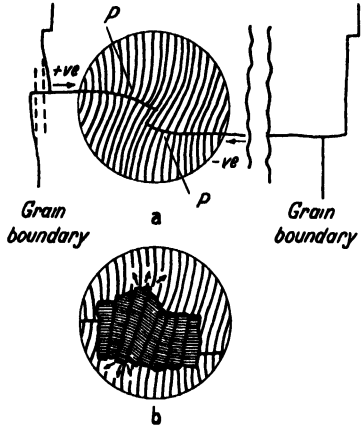

Figure 15

Creation of local curvatures where groups of positive and negative dislocations are immobilized

a *Local curvature near a grain boundary*
b *Generation of recrystallization nuclei in the curvature*

drawing these conclusions from Laue photographs of deformed crystals is questionable, as we have seen earlier. Their existence is, however, a direct consequence of the dislocation theory of work hardening. Hardening is held to be due to the interactions of dislocations of opposite sign which have become lodged in the lattice because of their mutual attraction. When many such dislocations stick in one vicinity, as the multiple nature of the glide planes[35] readily enables them to do, the lattice necessarily becomes rotated about just the axis postulated by Burgers. One would expect the actual axes of rotation of local curvatures to show a fair degree of spread. *Figure 15*a represents an attempt to illustrate this diagrammatically for two groups of dislocations (drawn, for simplicity, on two glide planes only). From his experiments Burgers concludes that nuclei must form from local curvatures in some way allowing them to retain the orientation of the lattice in the curvature. *Figure 15*b demonstrates how this could occur; the curved portion of the lattice polygonizes and when the process has gone far enough the crystallites break their continuity with the matrix, just as do the zones in age hardening and one of them grows. These experiments on extended crystals showed that polygonization can occur in

narrow bent bands surrounded by a matrix which is only very weakly bent. There is in principle no reason why this should not occur in much smaller regions still, if they are bent strongly enough.

Making use of certain assumptions, the author has made an attempt at a quantitative theory of nucleation based on this model.[61] (BECK[62] has suggested independently that nuclei are polygonized regions of high stress.) In a deformed crystal there will be curvatures with different rotations, distributed statistically. It is assumed that the distribution of curvatures is gaussian, with a large standard deviation and a mean value increasing with the deformation. The greater the curvature *i.e.* the smaller the radius, the more quickly polygonization and coarsening of the consequent structure will proceed; all the experiments described earlier point to this. The somewhat arbitrary supposition is made that the time required for a nucleus to become ready to start growing is proportional to the radius of curvature. The strain energy in a local curvature must be approximately proportional to the density of dislocations and hence to the curvature, and since the energy of polygonization boundaries is small, the decrease of free energy on polygonization is also approximately proportional to the curvature. Thus it is assumed that the time required by the nucleus to finish polygonizing is proportional to the free energy gained in the process.

When the rate of nucleation N is plotted as a function of time calculated on these assumptions, a graph is obtained exhibiting an induction period, a steep rise and well defined maximum, followed by a long tail. Various points, all normalized to the same scale, of experimental data of N as a function of t, under different conditions of deformation and temperature,[63] can be plotted on the same graph. Agreement is good, and is not much affected by the exact value chosen for the standard deviation of the distribution of curvatures.

This model for nucleation has not yet proved amenable to theoretical treatment by the quantitative theory of dislocations. When it becomes possible, this and other models for recrystallization processes can be subjected to more stringent tests than hitherto. So much is certain: the internal strains present in worked metals are largely associated with dislocations and the various thermally activated processes by which these strains can be removed must clearly be related to the motion of dislocations.

At the time of writing, a very interesting article by PETERSEN[60] came

to the author's attention. Here nucleation is pictured as being due to the diffusion of atoms under the action of elastic stress gradients, which under certain circumstances is held to relieve the originally highly stressed nucleus of most of its strain energy, enabling it to grow. Orientation relationships are partly accounted for by supposing that atomic diffusion actually permits the nuclei to rotate. The model is worked out in some detail and merits careful consideration. It appears to be superior, in its explanation of experimental facts, to a theory based on chance conglomeration of self diffusing atoms such as that advanced by TURNBULL.[64]

Growth of primary crystals—The state of internal strain of the deformed lattice has a profound effect on this growth. Jacquet showed[59] that in the initial stages of their growth new grains in copper crystals formed as narrow plates along the slip bands in which they were nucleated. Slip bands are regions of high internal stress and by growing in this way the nuclei release a maximum of elastic strain energy. This release of strain energy is essential to growth, and when it is no longer possible growth stops. Crussard and Aubertin observed[25] that the nuclei forming at the highly stressed curved twin boundaries in zinc often stopped growing when they reached the less stressed regions in the interior of a grain, where there was little distortion in spite of considerable slip. The behaviour of primary grains when they approach the deformation bands in elongated aluminium crystals gives another example. The present author and also COLLINS and MATHEWSON,[17] found that the growing grains very often had boundaries parallel to the deformation bands. If the boundary of a large grain advancing into an extended single crystal was examined, it was seen to contain a number of pointed tongues which terminated in deformation bands. Evidently the growing grain had a greater tendency to consume the strongly bent portions of the lattice than the intervening regions, even though some polygonization had occurred in these regions. Nevertheless, thorough polygonization can render a deformed grain stable towards a growing grain in its vicinity. Lacombe and Berghezan in seeking to account for a residue of unabsorbed grains by Carpenter and Elam's method, showed that one category of such grains had arbitrary orientations with respect to the growing crystal; but while the latter appeared to be perfect, the included grains were all strongly polygonized.[50] This is illustrated in *Figure 14* showing an included grain

in a large crystal of aluminium-zinc alloy (with this material, electrolytic polishing alone suffices to show up the sub-grain boundaries, for a reason previously explained).

Another striking instance of the importance of the local states of internal strain has recently been reported by CLAREBOROUGH.[65] Two silver-magnesium alloys containing similar amounts of α- and β-phases were made, one by quenching from a high temperature and the other by slowly cooling from a lower temperature. Each of these samples was then heavily cold drawn and annealed. The β-phase of the slowly cooled alloy recrystallized, but that of the quenched alloy, in which some fine precipitation took place, did not recrystallize. This may be explained by assuming that the highly localized misfits associated with precipitation act as dislocation traps, relieving the β-phase of strain and at the same time removing sites of potential nucleation, and the possibility of growth of new grains. An observation by SANDEE[66] and BURGERS[67] also emphasizes the influence of the state of strain in the lattice immediately surrounding a nucleus or its growth; it was that sometimes in strained polycrystalline aluminium a nucleus, previously invisible, would suddenly begin to grow when another grain approached close to it. The latter grain evidently alters the state of strain in the matrix in its immediate vicinity and this in turn allows the nucleus to start growing.

SECONDARY RECRYSTALLIZATION

Opinions still differ regarding the causes of secondary recrystallization; some metallurgists even doubt whether it is justifiable to give the phenomenon a separate name. BOWLES and BOAS[11] regard it as being closely connected with the orientation relationship between the giant secondary grains and the remaining primary grains. They state that a few grains become very large because of the ease with which they can grow, rather than because of a positive tendency to grow. RATHENAU[12] regards their tendency to grow as also important, and has carried out experiments giving support to the theory that a selection of those primary grains which grow just before all the matrix has been consumed, give rise to the giant crystals which are formed on continued annealing. He considers this due to the perfection of these grains, for the primary grains that are formed earlier are liable to become slightly distorted through the action of the elastic strains present in the remaining

unrecrystallized matrix.[48, 49] There is a difference of opinion also on the important question whether the secondary grains are already present after primary recrystallization or are produced by a second nucleation.

Very recent work[14, 15] has emphasized the importance of the variation of rate of growth with the orientation relationship between a secondary grain and the primary, highly textured material into which it advances. BECK and HU[14] showed that the orientation of the secondary grains were similar whether growing from the body of the specimen or from a sawcut where the primary texture obtained elsewhere in the specimen did not exist. This appears to eliminate any possibility of the nucleation of secondary grains in specific relative orientations. It has been suggested[68] and the view has been supported by KRONBERG and WILSON'S results[13] that preferred growth is also of importance in primary recrystallization. They prepared twin free copper sheet with a highly preferred cubic texture. Strips of this material were deformed in tension by a few per cent and subsequently annealed to recrystallize them. The newly formed grains had a well marked texture, although the deformation had been weak, in contrast with the very feeble, merely statistical correlation between the orientations of a weakly deformed single crystal and of the grains formed by recrystallizing it. Beck argues that this poor correlation is due to the formation of so few nuclei in the single crystal that hardly any will possess orientations specially favoured for growth. Kronberg and Wilson's highly textured materials contained grain boundaries, and many nuclei would be expected to form there even after a fairly weak extension. Of these, only nuclei in a favoured orientation would grow quickly. It is highly probable that primary (as distinct from secondary) recrystallization textures are due to combined preferred nucleation and preferred growth of grains of specific orientations. Preferred growth must be less important for primary recrystallization than for secondary, because in the former case the difference in free energy between the deformed structure and the new nuclei is bound to be a predominating factor and will tend to cause growth of the nuclei, whatever their orientation relative to the deformation texture.

The author is greatly indebted to Professor C. Crussard and Mr R. W. K. Honeycombe, who provided X-ray photographs, to Professor P. Lacombe for a photomicrograph, and to Dr R. Maddin for information. Thanks are due to Professor Crussard, Professor Lacombe and Dr A. Guinier for their valuable comments on the manuscript.

REFERENCES

[1] TAYLOR, G. I. *Proc. roy. Soc. A* 145 (1934) 362
[2] OROWAN, E. *Z. Phys.* 89 (1934) 634
[3] BARRETT, C. S. *Structure of Metals* p 334 New York, 1943
[4] COTTRELL, A. H. *Progress in Metal Physics* Chapt. 2 London, 1949
[5] BURGERS, W. G. *Handbuch der Metallphysik* Vol 3 ii Leipzig, 1941
[6] GUINIER, A. and TENNEVIN, T. *C.R. Acad. Sci., Paris* 226 (1948) 1530
[7] SMITH, C. S. *Trans. Amer. Inst. min. (metall.) Engrs* 175 (1948) 15
[8] BURKE, J. E. *ibid Tech. Publ. No.* 2472, 1948
[9] HARKER, D. and PARKER, E. R. *Trans. Amer. Soc. Met.* 39 (1945) 156
[10] BECK, P. A., TOWERS, J. and MANLEY, W. D. *Amer. Inst. min. (metall.) Engrs, Tech. Publ. No.* 2326, 1948
—— HOLZWORTH, M. L. and SPERRY, P. R. *ibid, Tech. Publ. No.* 2475, 1948
[11] BOWLES, S. and BOAS, W. *J. Inst. Met.* 74 (1948) 501
[12] RATHENAU, G W. *ibid* 74 (1948) 753
—— and CUSTERS, J. F. *Philips Res. Rep.* 41 (1949) 241
[13] KRONBERG, M. C. and WILSON, F. H. *Trans. Amer. Inst. min. (metall.) Engrs* 185 (1949) 501
[14] BECK, P. A. and HU, HSUN *ibid* 185 (1949) 627
[15] CRUSSARD, C. *Rev. Métall.* 41 (1944) 111, 133
[16] BURGERS, W. G. and LOUWERSE, P. C. *Z. Phys.* 67 (1931) 605
[17] COLLINS, J. H. and MATHEWSON, C. H. *Trans. Amer. Inst. min. (metall.) Engrs* 137 (1940) 150
[18] KONOBEEVSKI, S. and MIRER, I. *Z. Kristallogr.* 81 (1932) 69
[19] ANDRADE, E. N. DA C. and TSIEN, L. C. *Proc. roy. Soc. A* 163 (1937) 1
[20] —— and CHOW, Y. S. *ibid* 175 (1940) 290
[21] BUNGARDT, W. and OSSWALD, E. *Z. Metallk.* 31 (1939) 45
[22] CHITRUK, V. Private communication
[23] MADDIN, R. Private communication
[24] —— MATHEWSON, C. H. and HIBBARD, W. R. *Amer. Inst. min. (metall.) Engrs, Tech. Publ. No.* 2331, 1948
[25] CRUSSARD, C. and AUBERTIN, F. *Métaux et Corrosion* 21 (1946) 45, 66
[26] HIRST, H. *Proc. Aust. Inst. Min Met.* 121 (1941) 11, 29
[27] DUNN, C. G. *Trans. Amer. Inst. min. (metall.) Engrs* 167 (1946) 373
[28] CRUSSARD, C. and AUBERTIN, F. *Rev. Métall.* 42 (1946) 310
[29] CAHN, R. W. *Report of Conference on Strength of Solids* Phys. Soc. (1948) 136
[30] —— *J. Inst. Met.* 76 (1949) 121
[31] LACOMBE, P. Private communication
[32] HONEYCOMBE, R. W. K. *J. Inst. Met.* Discussion to reference 30. In press
[33] BRAGG, W. L. *Proc. phys. Soc.* 52 (1940) 54
[34] BURGERS, J. M. *Proc. kon. Acad. Wet. Amst.* 42 (1939) 239, 315, 378
—— *Proc. phys. Soc.* 52 (1940) 23
[35] HEIDENREICH, R. D. and SHOCKLEY, W. *Report of Conference on Strength of Solids* Phys. Soc. (1948) 57
[36] LACOMBE, P. and BEAUJARD, L. *J. Inst. Met.* 74 (1947) 1; *Report of Conference on Strength of Solids* Phys. Soc. (1948) 91
[37] BURKE, J. E. and BARRETT, C. S. *Trans. Amer. Inst. min. (metall.) Engrs* 175 (1948) 106
[38] MCLEAN, D. *J. Inst. Met.* 74 (1947) 95
[38a] JACQUET, P. A. *C.R. Acad. Sci., Paris* 218 (1944) 790
[38b] —— *Rev. Métall.* 47 (1950) 355
[39] BERG, W. F. *Z. Kristallogr.* 89 (1934) 286
—— *Wiss. Veroff. Siemens-Konz.* 9 (1930) 119

[40] BARRETT, C. S. *Trans. Amer. Inst. min. (metall.) Engrs* 161 (1945) 15
[41] BARRETT, C. S. and LEVENSON, L. H. *Trans. Amer. Inst. min. (metall.) Engrs* 137 (1940) 76
[42] CRUSSARD, C. *Rev. Métall.* 43 (1946) 307
[43] WILMS, G. R. and WOOD, W. A. *J. Inst. Met.* 75 (1949) 693
RACHINGER, W. A. and WOOD, W. A. *ibid* 26 (1949) 269
[44] LACOMBE, P. and BERGHEZAN, A. *C.R. Acad. Sci., Paris* 226 (1948) 2152
[45] GUINIER, A. Private communication
[46] FRANK, F. C. *Report of Discussion on Crystal Growth* Faraday Soc. (1949) 49
[47] GUINIER, A. and LACOMBE, P. *Métaux et Corrosion* 24 (1948) 212
[48] POLANYI, M. and SACHS, G. *Z. Metallk.* 17 (1925) 227
[49] BONZEL, M. *Rev. Métall.* 34 (1937) 372, 429
[50] LACOMBE, P. and BERGHEZAN, A. *C.R. Acad. Sci., Paris* 228 (1949) 95
—— —— *Métaux et Corrosion* 281 (1949) 1
[51] CASTAING, A. and GUINIER, A. *C R. Acad. Sci., Paris* 228 (1949) 2033
[52] CHAUDRON, G. *J. Inst. Met.* 76 (1949) 1
[53] KOCHENDORFER, A. *Z. Kristallogr.* 97 (1937) 263
[54] TAYLOR, G. I. and QUINNEY, H. *Proc. roy. Soc. A* 143 (1934) 307; 163 (1937) 157
[55] GUINIER, A. *Nature, Lond.* 142 (1938) 669
PRESTON, G. D. *ibid* 142 (1938) 157
[56] DANIEL, V. and LIPSON, H. *Proc. roy. Soc. A* 181 (1943) 368; 182 (1944) 378
[57] BURGERS, W. G. and BASART, J. C. M. *Z. Phys.* 51 (1928) 545
[58] BECKER, R. and DOERING, W. *Ann. Phys.* 24 (1935) 719
[59] JACQUET, P. A. *Rev. Métall.* 42 (1945) 133
[60] PETERSEN, C. *Metallforschung* 2 (1947) 289
[61] CAHN, R. W. *Proc. phys. Soc. A* 63 (1950) 323
[62] BECK, P. A. *J. appl. Phys.* 20 (1949) 633
[63] ANDERSON, W. and MEHL, R. F. *Trans. Amer. Inst. min. (metall.) Engrs* 161 (1945) 140
[64] TURNBULL, D. *ibid* 175 (1948) 774
[65] CLAREBOROUGH, L. M. *Nature. Lond.* 165 (1950) 39
[66] SANDEE, J. *Physica* 9 (1942) 741
[67] BURGERS, W. G. *ibid* 9 (1942) 987
[68] BECK, P. A. and HU, H. *Trans. Amer. Inst. min. (metall.) Engrs* 185 (1949) 627
—— SPERRY, P. R. and HU, H. *J. appl. Phys.* 21 (1950) 420

6

RESEARCHES ON THE POLYGONIZATION OF METALS

A. Guinier and J. Tennevin

THE OBSERVATIONS on polygonization which are to be described were made as a result of a new experimental technique. It was only owing to the improvement of technique that new facts have emerged and it is therefore necessary first to discuss in detail the scope and limitations of our method. This will, in particular, allow us to compare our results with those of earlier investigations and to interpret the latter.

EXPERIMENTAL METHOD

Only the principle of the method will be recalled, since the experimental details have already been published.[1] The purpose of the investigation is to detect differences in orientation of the lattice planes within a crystalline block. Let us consider a small, perfect block, the direction of planes of a particular family being strictly constant at all points in the block. With the ordinary Laue method, the collection of rays impinging on the block, which is assumed to have a volume of the order of 0·5 mm^3, is delimited by a collimator that also determines its divergence. We will assume that the collimator consists of two holes 0·5 mm in diameter and 50 mm apart, the second hole being in contact with the specimen. The maximum divergence of the rays is then 70′ and on a film placed 50 mm from the specimen a spot about 1·5 mm in diameter will be produced. Let us suppose the specimen to be composed of two blocks at an angle ϵ; then the two corresponding spots will not be resolved unless ϵ is greater than 1° 30′. If ϵ is 10′, only a single spot enlarged by 10 per cent would be observed *i.e.* the change in the Laue pattern would be virtually imperceptible.

To increase the sensitivity of the Laue method it is necessary to use collimators which are longer and have finer pinholes, but at the same time this reduces the volume irradiated to a point at which it is no longer representative of the mean structure of the specimen. Our new method permits us to explore, with great sensitivity, a specimen

several mm³ in volume. The principle is very simple, and so is the experimental arrangement. A divergent polychromatic beam from a point source S (*Figure 1*) impinges on a crystalline lamella. It can be shown geometrically that all rays reflected by a family of lattice planes constitute a beam converging to a line perpendicular to the plane of incidence; the trace M of this line lies on the circle C, which passes through the symmetry point S' (defined by $SO = OS'$), and is also

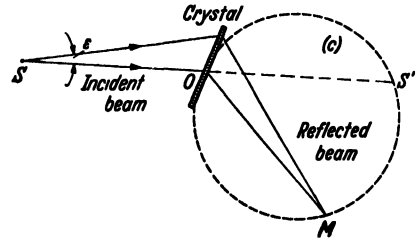

Figure 1
Experimental arrangement for taking focused Laue diffraction photographs

tangent to the lamella at O. When the lamella is approximately normal to the beam and the deflection of the diffracted beam is small, it will be seen that the distance from the specimen to the focus is nearly equal to that from the specimen to the source. The width of the image P is independent of the divergence of the beam and of the distance OS and is of the order of the source width, provided that the thickness of the lamella is very small compared to the distance OS.

A perfect crystal, then, yields a narrow image which defines its orientation with a precision increasing with the distance OS. It is calculated that a source of 0·05 mm projected width and a perfect crystalline lamella 0·3 mm thick gives an image 0·1 mm wide. If the distances OS and MS are about 1 metre, this width corresponds to an angular resolution of the reflecting plane normals of 10 seconds of arc. Photographs can in fact be made at such distances without excessive exposure times, provided the crystal is very good.

With deformed metallic crystals we generally arranged specimen-source distances of about 25 cm, giving a resolution which is more than a hundred times better than that obtained with the normal Laue method. A surface area of 30–50 mm² can be examined without difficulty, and for a specimen thickness of 0·5 mm this corresponds to a volume of some 25 mm³.

In these experiments it was essential to use a tube with a fine focal spot. We employed a demountable tube having a hot cathode provided with electrostatic focusing. The tungsten filament is surrounded by a

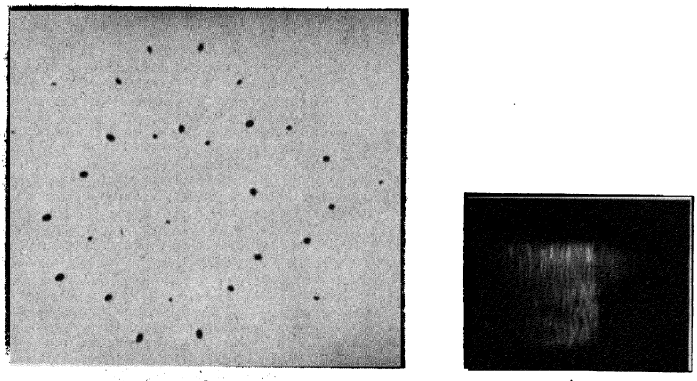

a b

Figure 2. Diffraction photographs of a polygonized aluminium crystal a *ordinary Laue photograph* b *focused Laue spot*

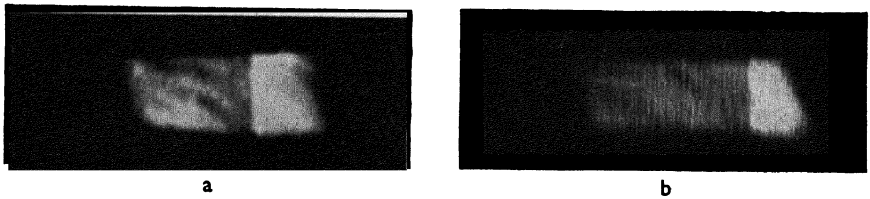

a b

Figure 3. Comparison of focused Laue spots obtained with a *X-ray tube with coarse focal spot* b *X-ray tube with fine focal spot*

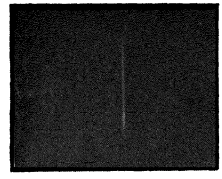

Figure 4. Focused Laue spot of a perfect single crystal of aluminium

a

Figure 5. Focused Laue spots of an aluminium crystal **a** *extended by 2 per cent* **b** *after annealing 14 hours at 520°C* **c** *after annealing 14 hours at 565°C* **d** *after annealing 14 hours at 610°C*

b

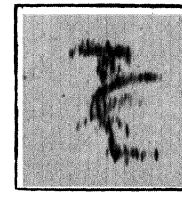

c

d

shield at a negative potential. The focal point has the shape of a small ellipse with axes 1 × 0·5 mm; seen at a glancing angle of 6° this appears as a short line, 0·05 mm wide and 1 mm in height. With a tube of this kind the arrangement is very simple. The photographic plate can be placed in the position calculated for the focus of a diffracted beam and it is unnecessary to locate this position with precision. The specimen is so orientated that an intense Laue spot is formed in this favourable position. *Figure 2*a represents a crystal pattern prepared by the ordinary Laue method; the spots do not differ in appearance from those given by a perfect crystal. *Figure 2*b shows the detail in one of the spots revealed by the use of the focusing arrangement with fine source. *Figure 3*a shows the result of applying the same method when the source is the anti-target of an ordinary sealed tube; the dimensions of the source are too great and the detail in *Figure 3*b has disappeared.

THE POLYGONIZATION OF A METAL CRYSTAL

We shall first describe a set of experiments which display the conditions under which we observed the phenomenon of polygonization.

1 Initial State of the Metal—We worked with aluminium specimens 1 mm in thickness, in which very large crystals had been produced by the method of Carpenter and Elam (a high temperature anneal following an extension of 2 per cent). The aluminium was refined and of 99·99 per cent purity. *Figure 4* shows a diffraction spot given by such a crystal. A surface portion of the specimen 6 mm square was examined. The width of the line corresponds to an orientation range of 25″. Since the crystal is so perfect it had to be handled with the greatest care to avoid any bending. This degree of perfection is a rather surprising result when it is remembered that aluminium has always been considered, from its observed line intensities, to be 'ideally imperfect'. We see, then, that the mosaic structure of the crystal, if it exists, involves only very slight orientation differences in the body of the crystal. (In measurements of line intensities, the surface layer has an importance which it did not have in our experiments.)

2 Deformation of the Metal—The crystals were deformed in tension to an extension of 5 per cent. After such deformation the diffraction spots become wider (*Figure 5*a); the extent of widening depends on the orientation of the reflecting plane in relation to the axis of tension. It was also found that the widening of the spots (which corresponds to

the so-called asterism in ordinary Laue patterns) was not the same for different parts of the specimen. This is due to the heterogeneous distribution of lattice curvatures brought about by extension. These various factors, however, did not enter appreciably into the present set of experiments. The phenomena to be described depend neither on the identity of the plane giving rise to the observed spot nor on the relative orientation of this plane and the specimen.

3 Annealing the Metal—Specimens deformed in this way were annealed progressively. Here two factors are of importance, the time and the temperature of annealing. In the first set of experiments the time of each anneal was kept constant at 4 hours while the temperature was continually increased. After each anneal, the specimen was allowed to cool slowly and examined by x-rays. The specimen was always carefully replaced in the same position so that the same diffraction spot was obtained each time and the progressive changes in it could be studied. Finally the metal was subjected to a very complex treatment of interrupted anneals; it will be seen later whether this form of heating produced any special effect.

The following phenomena were observed:

i Up to a temperature of 450°C, annealing leads to no perceptible alteration in the spot.

ii Above 450°C the spot became striated in appearance; fine, compact striations were superimposed on the continuous background (*Figure 5b*). At first these were faint and each of them had the same height as the reflection from an infinitely small crystal in the specimen (this height being proportional to the height of the focal spot). As the annealing temperature was raised from 450° to 520°C these striations became more intense after each anneal. Some became very prominent, others remained weak, but none grew wider; they all retained the width of the reflection from a perfect crystal.

iii From 520° to 580°C (*Figure 5c*) the intensity and sharpness of the striations increased progressively, and at the same time the intensity of the continuous background was diminished. From 580° to 600°C the background disappeared entirely, and the spot took the form of an assembly of small, separate striations which between them cover the same area as the original spot obtained from the cold worked metal. Further annealing at these high temperatures led to a reduction in the number of striations *Figure 5d*.

When the anneals were carried on beyond 630°C, one of two phenomena was observed in specimens which had undergone identical prior treatments:

i The specimen recrystallized, that is, new crystals were formed of orientations quite different from those of the original crystal. The focused reflections from these new crystals were very narrow, and their perfection was thus comparable to that of the crystal with which we started (*Figure 6*).

ii After short anneals there was no sudden change in the appearance of the spots, but the striations were less numerous and some became more intense. After very long anneals, however (over 10 hours), it was observed that all the striations disappeared, with the exception of 3 or 4 which became very strong (*Figure 7*); these did not remain narrow. At this stage, the separation of these spots was so marked that the asterisms on ordinary Laue photographs were divided into several separate spots.

INTERPRETATION OF THE RESULTS

The widening of the diffraction spot from the deformed crystal reveals distortion of the corresponding lattice planes; the direction of the normal to the planes varies continuously, but not uniformly. When, on the other hand, striations appear in the spot, there must exist in the specimen small packets in which the direction of the normal is constant, and of sufficiently large volume for the diffracted image to stand out sharply against the continuous background. At a later stage, when the background has disappeared and a number of sharp, distinct striations remain, the specimen has been transformed into a collection of crystalline blocks having slightly differing orientations, the overall range of orientations being the same as before the anneal. The word polygonization provides a good picture of this transformation.

The variable number of striations obtained from a given volume of irradiated metal indicates that the size of the elementary blocks varies according to the treatment. After annealing at 500°C the striations are not all clearly separated. The continuous band may derive from the unpolygonized parts of the specimen, or alternatively from the accumulated reflections due to very small, and therefore very numerous, blocks. In view of this, it is important to be clear about the minimum block dimensions we can resolve by our method. Thus, the specimen

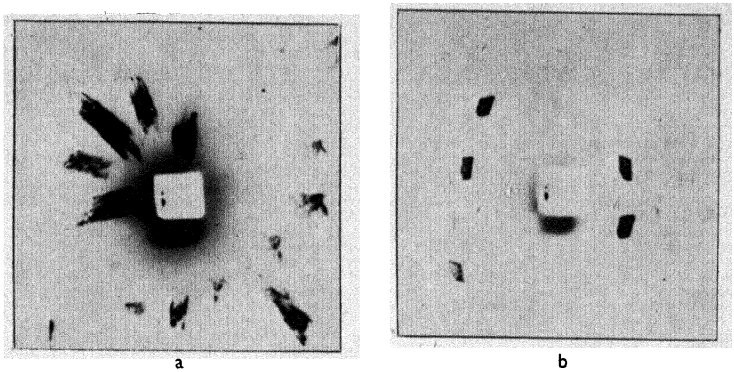

Figure 6. Ordinary Laue photographs of an aluminium crystal extended by 10 per cent **a** *polygonized by a 2 hour anneal at 620°C* **b** *recrystallized by a 2 hour anneal at 630°C*

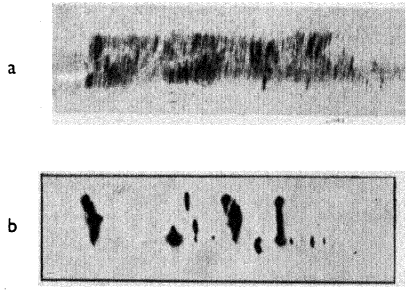

Figure 7. Focused Laue spots showing the sub-grains after polygonization **a** *aluminium crystals extended 2 per cent, and annealed 2 hours at 640°C* **b** *same specimen after 14 hours' anneal at 640°C*

a

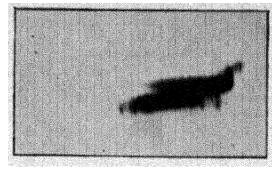

b

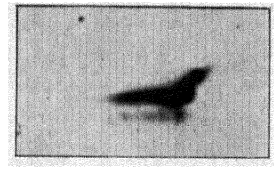

c

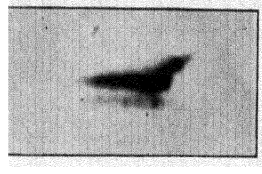

d

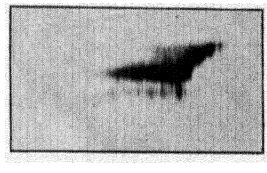

Figure 8. Focused Laue spots of an aluminium crystal extended by 2 per cent, taken **a** *at room temperature after annealing at 550°C* **b** *at 580°C, from 5th to 6th hour of annealing* **c** *at 580°C, from 7th to 8th hour of annealing* **d** *at room temperature after 8 hours' annealing at 580°C*

This result is readily interpreted in the following way. The sub-grains of a polygonized crystal do not remain immobile; the boundaries separating neighbouring sub-grains are displaced, the grains rotate through very small angles and are joined to their neighbours. Thus the diffracted beams from the several sub-grains undergo slight displacements. This experiment shows that the boundaries between sub-grains are very mobile, much more so than the boundaries between ordinary grains, which under these conditions do not undergo any change. This is one aspect of the fundamental difference between the boundaries of the sub-grains and ordinary grain boundaries. The former can be revealed micrographically. LACOMBE and BEAUJARD[2] have shown that the arrangement of the sub-grains is altered by an anneal; this displacement of their boundaries accompanying their change of orientation is another aspect of the mobility of the sub-grains. It is to be noted, however, that both Lacombe's and our own observations reveal that a long anneal at high temperature leads to a stabilization of the sub-grains, suggesting that a state of equilibrium is approached.

COMPARISON WITH PREVIOUSLY DESCRIBED PHENOMENA

Polygonization, as we have presented it, is essentially the same as certain phenomena described by earlier investigators. (See the review of earlier work in Chapter 5.) Any differences are due merely to the variations in sensitivity between our method and the methods previously employed. We were able to detect polygonization where previous experiments missed it, and it is now shown to be a much more common phenomenon than had formerly appeared; the new results obtained by means of the greater sensitivity permit us to extrapolate with some confidence and to put forward reasonable hypotheses as to what occurs in domains as yet inaccessible to direct investigation.

The Laue method only permits study of the final stage, reached by continued annealing, that is, the production of large blocks called recrystallization *in situ* by CRUSSARD. This is quite rare, since ordinary recrystallization often intervenes. CAHN[3] has listed a number of conditions required for polygonization to appear. For coarse-grained polygonization to occur these conditions are, in fact, necessary, but none of them is requisite for polygonization on a fine scale.

We have studied the influence of several factors on polygonization for aluminium.

a Deformation was at first imparted by extension. Later, bending of the specimens was attempted. It was confirmed that the phenomenon was visible more readily if the diffracting planes used were in the radial position; the diffraction spot is then well spread out. The specimens were bent very weakly (the radius of curvature was 15 cm). Also, with extension, curvature of lattice planes occurs, but this is here indirectly due to deformation.

b The orientation of the crystal relative to the axis of deformation has no marked effect. The single crystals of aluminium used were orientated at random and the diffracting plane was not chosen systematically, but we never found any differences due to this on our plates.

c As regards the annealing temperature, data for aluminium were given in a preceding paragraph. According to our observations an anneal of several hours at a temperature 40°C below the melting point of aluminium will lead to the coarse polygonization observed by Cahn.

d After the initial experiments, which were carried out with aluminium of high purity, we went on to study the behaviour of commercial aluminium. We started with a single crystal made, as before, by critical extension, and in spite of the low purity of the metal (99·4 per cent) the crystal was of good quality, the orientation range being less than 1·5′. This crystal was extended by 5 per cent and given successive anneals. It was found that polygonization occurred in this case also, but the temperature at which it reached detectable proportions was higher (580° to 600°C). The striations were very numerous and fine, and remained so even after prolonged annealing, showing that the sub-grains increased in size much less readily than in the pure metal. We did not encounter any instance of recrystallization *in situ*, that is, growth of a few of the blocks already present, a phenomenon we observed, though rarely, with pure aluminium.

e All deformations were carried out at room temperature, and the effects of deformation at low temperature mentioned bv Cahn were not studied.

f Polygonization was observed with other metals besides aluminium. Large grains of iron and copper after annealing gave sharply striated diffraction spots.

Thus, it would appear from these first experiments that the transformation of the cold worked state into the polygonized state is normal when a single crystal is annealed after a weak deformation leading to lattice curvature.

INFLUENCE OF THE DEGREE OF DEFORMATION OF A SINGLE CRYSTAL

Next we examined the influence of the degree of deformation on polygonization, and also studied the behaviour of a deformed polycrystalline aggregate. These two sets of experiments were carried out with high purity aluminium.

A number of aluminium crystals were extended by various amounts *viz* 5 per cent, 10 per cent, 15 per cent, and by extension to fracture. Each of the deformed crystals was cut with the utmost care into several small specimens, which were then deeply etched to remove the effects of sawing. It was found imperative to carry out the experiments on numerous specimens, since the results, more especially those relating to recrystallization, were highly variable. From this point of view a series of separate specimens behave quite differently from the undivided crystal, since the whole of the latter can be consumed by the growth of a single nucleus formed by recrystallization. The various temperatures which will be quoted have no absolute or precise significance. The specimens were given short anneals (2 hours); had the anneals been longer, the phenomena to be described would have been observed at different temperatures.

From these experiments it may be concluded that annealing a deformed specimen can have two consequences: polygonization and recrystallization. While the degree of deformation has a powerful influence on the temperature of recrystallization, its influence on the temperature at which polygonization first appears is smaller.

For weak extensions (less than 5 per cent) the diffraction patterns sometimes include small spots due to new grains, but these remain small. Appreciable recrystallization was observed in three instances at 500°C and in six instances above 600°C. Polygonization became

perceptible in most of the specimens pulled by 5 per cent, at a temperature of about 450°C, whereas all the specimens made from the crystal pulled by 15 per cent recrystallized completely at 380°C. It was not possible to detect polygonization before recrystallization had begun with any of the other specimens. It may be concluded that the threshold temperature for polygonization was still around 400°C, but that the fall in the recrystallization temperature had masked this fact. For the specimens pulled by 10 per cent, the threshold temperature for polygonization was about 400°C.

POLYCRYSTALLINE METALS

The starting material consisted of a piece of high purity aluminium which had been heavily rolled and recrystallized by a 2 hour anneal at 350°C. The piece had a small grain size (0·2 mm) and the normal recrystallization texture of rolled aluminium. The focused diffraction pattern exhibited fine spots, showing that the grains were perfect. After an extension of 2 per cent, the spots were smeared out much more than with a single crystal extended by the same amount; this is in accord with the well known fact that a polycrystal shows more Laue asterism than a single crystal, the presence of grain boundaries accentuating the lattice curvature in the individual grains. When the extension exceeded 5 per cent, the spots were so far dispersed that they could no longer be registered on films placed at a distance from the specimen, even with long exposures. On account of this limitation imposed by the experimental method, we restricted ourselves to the study of very weak extensions.

As before, the specimens were annealed at progressively higher temperatures. We found that polygonization began at 320°C in the specimen pulled by 2 per cent, and at 280°C in that pulled by 5 per cent; at these temperatures the smeared spots due to the various grains became striated, but when the temperature exceeded 350°C or 310°C, respectively, recrystallization began before polygonization could go to completion (*Figure 9*).

We reach the same conclusion as before: increasing amounts of deformation hardly affect the polygonization temperature, whether of single crystals or polycrystals, while the temperature of recrystallization is considerably lowered. In a polycrystal which is even more deformed,

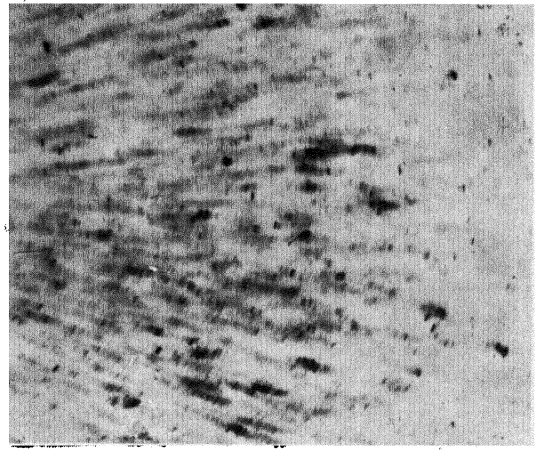

Figure 9. Focused Laue pattern of a polycrystalline aluminium specimen extended by 2 per cent and annealed 2 hours at 350°C

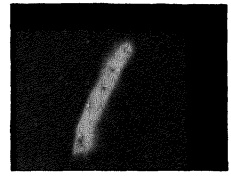

Figure 10. Focused Laue spot of an aluminium crystal made from the melt

it is probable (though the supposition cannot be checked) that recrystallization takes place before any detectable polygonization has developed. Then, to observe polygonization clearly, it is essential that the onset of recrystallization be retarded, and this is best achieved with weakly deformed single crystals.

INFLUENCE OF POLYGONIZATION ON RECRYSTALLIZATION

We attempted to resolve the following problem: assuming that after a given deformation the metal recrystallizes above a certain temperature T, is this temperature changed when a preliminary anneal at a temperature below T transforms the cold worked metal into the polygonized state?

The answer to this question is not as yet clear. A series of experiments with crystals extended to fracture failed because all the specimens recrystallized at a temperature too low for polygonization to develop. Another series with crystals pulled by 5 per cent did not prove to be conclusive, because the recrystallization temperatures of apparently identical specimens are extremely variable; it was consequently impossible to ascertain whether a rise in recrystallization temperature after polygonization was significant and due to the polygonization. The experiments throughout underlined the 'inconsistent' character of recrystallization in contrast to the greater regularity of polygonization.

OTHER INSTANCES OF POLYGONIZATION

The phenomenon of polygonization has also been observed in slightly different circumstances from those described in the preceding paragraphs.

When a crystal is formed from the liquid, it has always been found to be in a very distorted condition; thus, aluminium crystals made from the melt contain variations of orientation of the order of one degree (*Figure 10*). This also occurs with artificial crystals of rock salt in spite of the utmost care taken for their slow and regular solidification. Moreover, such crystals are birefringent, demonstrating the existence of internal strains. It is known that these strains can be dissipated by a long anneal at a temperature close to the melting point. After such treatment it was found that the rock salt produced the diffraction pattern of a polygonized crystal. Similarly, it was observed that an

aluminium crystal made from the melt and then annealed for a long time gave a striated diffraction spot; but the striations were too badly resolved for reproduction.

However long the period of annealing may be for a cast crystal the total range of orientations of the lattice is not reduced, but the transformation of the bent crystals into a number of polygonized blocks brings about a release of internal strains. This behaviour is very similar to that previously observed, the difference being that the deformation of the lattice is not the result of an externally applied deformation, but of the mode of formation of the crystal.

Another observation made on polygonization is less easy to account for. It was found on occasion, both with aluminium of commercial purity and with iron, that the grains formed in the course of recrystallization were in a polygonized condition, although they had not, to our knowledge, been subjected to any deformation. The reason for the occurrence of polygonization in these rare instances is obscure.

CONNECTIONS BETWEEN RECOVERY, POLYGONIZATION AND RECRYSTALLIZATION

The effects of a heat treatment on the cold worked state have been divided into two processes, recovery and recrystallization. Recovery, according to BURGERS,[4] is to be regarded as a rearrangement of the deformed lattice through the elimination of the dislocations present, whereas recrystallization proceeds through the formation and growth of new crystal nuclei. Not only do the usual x-ray methods fail to reveal any change in crystals annealed at a temperature high enough to bring about recovery, but no trace of polygonization can be detected even by means of our method. But it does not follow that recovery and polygonization are different in nature; as has been shown, the existence of separate sub-grains cannot be recorded experimentally as long as their dimensions are below 10–100μ, which is large in comparison with the size of the unit cell.

It is possible to form a simple image of a deformed lattice by invoking dislocations. It is easy to see (*Figure 11*) that the introduction into the lattice of an extra plane of atoms in the upper half (constituting a positive dislocation) occasions a curvature of one sense, while its introduction in the lower half causes the opposite curvature. A disturbed crystal block with zero mean curvature must contain

practically equal numbers of dislocations of opposite signs; if, however, the block is macroscopically curved, one of the two kinds must predominate.

In the course of recovery at a temperature at which only limited atomic displacements can take place, pairs of dislocations of opposite signs will, according to Burgers' ideas, annihilate each other and thereby eliminate the corresponding lattice defects. It remains then

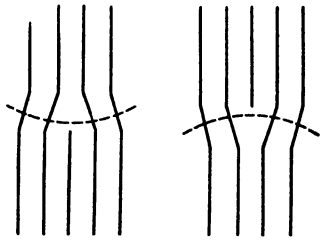

Figure 11. Curvatures produced by positive and negative dislocations (schematic)

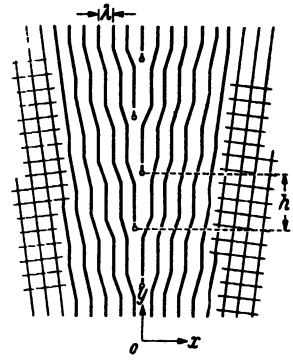

Figure 12. Row of positive dislocations separating two sub-grains (schematic, after Burgers)

to account for the excess dislocations of one sign. It would seem that polygonization provides an answer to this problem. Two crystal blocks with nearly identical orientations can be schematically represented as being separated by a row of dislocations of the same sign (*Figure 12*); the angle between the two blocks is the reciprocal of the number of lattice parameters between successive dislocations. If the angle is 1′, the dislocations are spaced at intervals of 3,000 parameters. Simultaneously with the mutual annihilation of positive and negative dislocations, we may suppose the excess dislocations of one sign to be arranging themselves in lines, at any rate within restricted regions. In this way a deformed crystal block, which is distorted locally and also bent as a whole, is progressively changed into an assembly of smaller blocks of increasingly perfect structure and slightly differing orientations. The sub-grains thus formed are imperfect in the early stages, since they still contain a number of dislocations and have badly defined boundaries. At this stage, diffraction photographs do not reveal the sub-grains, since their diffraction images are so wide and so numerous that they are not resolved. Only when the blocks have become well

defined does polygonization become apparent. Nevertheless it seems to us that there is complete continuity between recovery and polygonization.

The curvature present in the metal constitutes an important consideration. If this is very weak, that is, the numbers of the two kinds of dislocations are almost equal, the lattice will regain its perfection without polygonizing sharply, while polygonization will be most marked when there are strong curvatures present. It is known that dislocations are concentrated in the active glide planes, consequently the number of glide systems taking part in the deformation will influence the final distribution of dislocations. It will be seen that the example studied by Cahn (single crystals of zinc bent with the base plane parallel to the axis of curvature) is particularly favourable for the formation of large sub-grains making quite large angles with each other.

Two adjacent blocks are separated by a widely spaced line of dislocations, indicating that almost everywhere the lattices are continuous with each other. This fact permits us to explain the following observations relating to polygonization.

The line of dislocations may readily be displaced, that is, one block can easily grow at the expense of the other; presumably it will be the more nearly recovered, and therefore more perfect, of the two blocks which has the tendency to grow. Apart from this, as is pointed out by CAHN,[5] the disappearance of the boundaries of separation in itself reduces the energy of the metal, and therefore tends to occur. With continued annealing then, the blocks grow, are reduced in number and become more perfect, and thus will be resolved on the photographs. The appearance of the diffraction patterns recorded at the annealing temperatures and their variation with the time of annealing also show that the block boundaries are mobile, at least for an extended period before an equilibrium configuration is set up at a given temperature. The division of a crystal into blocks of progressively increasing size continues as long as the process is not interrupted by polygonization.

The boundaries between sub-grains are quite different from the ordinary grain boundaries present in recrystallized metal.[2] It must be remembered that the angles between the lattices of the sub-grains are extremely small. There are not, as between grains of markedly different orientations, one or two atomic layers displaced from their

normal lattice positions.[6] This explains why the sub-grain boundaries are so much more mobile than ordinary grain boundaries, and why they are not attacked in the same way by chemical reagents. The considerations advanced by Burgers regarding the growth of nuclei in recrystallization are also applicable at the recovery stage, because recovery is accompanied by polygonization during which sub-grains grow at the expense of their neighbours; these considerations may even be more justifiable here, since the orientation deviations between the blocks are so much smaller and because of the absence of intercrystalline layers of displaced atoms.

Polygonization can only proceed at a particular temperature if there is no recrystallization at this temperature. The rearrangement of the lattice by recovery and polygonization proceeds in a regular manner which depends little on the state of the metal. In contrast to this, recrystallization is dependent on the production of nuclei which appear with a particular probability at a given temperature. This probability is closely connected with the temperature and the degree of deformation of the metal, and there are few nuclei in weakly deformed single crystals. The statistical character of recrystallization accounts for the irregular results obtained with a number of specimens which had undergone the same treatment.

In the case of a weakly deformed single crystal, recovery and polygonization between them have brought the metal into a fairly stable condition, and the formation and growth of a nucleus are then a rare event, which may not take place even at a temperature near the melting point. In ordinary recrystallization the new grains have quite a different orientation from the parent crystal. As has been remarked, however, there are instances of polygonization progressing to a stage where only a few blocks remain. It is conceivable that in this case recrystallization would occur by the growth of nuclei having the orientations of some of these large blocks. This is unlikely, however, since a grain formed by true recrystallization at high temperature is characterized by great perfection, showing fine striations in the diffraction pattern, while the striations of *Figure 7* are not fine, each consisting of several components close together. The growth of the grains under these two conditions cannot therefore have taken place by the same mechanism.

The growing grain, in the second case, had to absorb other grains of

almost the same orientation, which Burgers has shown to be the least favourable condition for such growth; moreover, long anneals are required for the phenomenon to occur. As we propose to show elsewhere, a grain which grows by swallowing other recrystallization grains does not retain its perfection. Recrystallization *in situ* should be considered as an exaggerated growth of one of the grains formed by polygonization rather than as an instance of recrystallization giving rise to a new and perfect grain.

The authors wish to thank Dr R. W. Cahn for his comments on the manuscript and its translation.

REFERENCES

Collected references on the subject are given on p 175

[1] GUINIER, A. and TENNEVIN, J. *Acta Crystallographica* 1 (1948) 188

[2] LACOMBE, P. and BEAUJARD, L. *J Inst. Met.* 74 (1947) 7

[3] CAHN, R. W. *Conference on Strength of Metals* London 1948 p 136; *J. Inst. Met.* 76 (1949) 121

[4] BURGERS, W. G. *Proc. K. Akad. Wet. Amst.* 50 (1947) 452

[5] CAHN, R. W. This volume: Chapter 5

[6] ZENER, C. *Amer. Inst. Min. Engrs Met. Tech. Publ. No.* 1992, 1946

7

POLYGONIZATION IN STRONGLY DEFORMED METALS

C. Crussard, F. Aubertin, B. Jaoul and G. Wyon

THE EXISTENCE of polygonization has been established on single crystals or coarse-grained metals annealed after slight or moderate cold work, these observations having been carried out by means of micrography or x-rays. It will be our aim here to present the experimental evidence for polygonization in fine-grained metals heavily cold worked before annealing, this evidence being based on micrography and x-ray studies, and also indirectly on observation of other physical properties (plasticity, thermoelectric power) which are influenced by polygonization, as will be shown later.

POLYGONIZATION IN COLD ROLLED COPPER

If, after the electropolishing of copper in the Jacquet bath[1] the electrodes are short circuited, a selective deposit of copper is produced on the metal, which reveals very fine details. This fact was utilized in the study of strips of copper annealed at 850°C and cold rolled from 7·7 to 1 mm. The observed markings are related to the structure of the metal itself, and not to irregular conditions of the deposit, as is proved by the fact that, after re-polishing and re-etching, the same markings appear in their original places. The pattern of markings formed on cold rolled copper is shown in *Figure 1*: bright patches on the surface correspond to parts of the metal where a (100) plane is nearly parallel to the surface. Lines appear at these places that are fairly continuous and somewhat bent or forked, suggesting some kind of bending in the lattice, which is certainly due to flexural glide.

After 100 hr annealing at 125°C different patterns are sometimes displayed (centre of *Figure 2*): the etchings consist of short segments, broken at rather large angles; the breaking points of all the lines draw contours dividing the initial grain into sub-grains, and are very similar to LACOMBE's intracrystalline contours.[2] This only occurs

where the initial curvature was marked and suggests an incipient polygonization.

After annealing for 2 hr at 190°C, some new grains appear (centre of *Figure 3*); thus actual recrystallization has begun. But where recrystallization has not taken place and where the surface is bright the appearance has changed: instead of being continuous the lines are fragmented into small segments or curves, having well defined ends, which form contours having roughly the same orientation within each grain (*Figure 4*). Thus the bending of the lattice is no longer distributed over all the grains, but concentrated along some sub-boundaries. This again suggests generalized polygonization.

INFLUENCE OF POLYGONIZATION ON MECHANICAL PROPERTIES

If any polygonization occurs in heavily cold worked metals by annealing at temperatures just below the recrystallization point, it may be possible to detect it by a change in the mechanical properties. Recrystallization *in situ* was first observed on aluminium by such a change.[3] For this purpose the exact shape of the stress-strain curve was studied as a function of temperature.

The metal used in this investigation was aluminium (99·99 per cent purity) containing 0·004 per cent iron (after hot extrusion). Samples were machined out of these rods, annealed at various temperatures for 5 hours, and tested in Chevenard's tensile micromachine. The photographic registering of the tensile curve facilitates very accurate analysis of the shape of the curve. *Figure 5* represents the elastic limits (measured limit of proportionality) and the stress for an elongation of 1 per cent as a function of the annealing temperature. The sharp decrease of the curve at 300°C indicates that recrystallization is taking place, as is proved by x-ray analysis: at 300°C the samples are wholly recrystallized; at 265°C there is no recrystallization; at 290°C there is a mixture of new grains and distorted matrix (asterism).

One of the Debye rings consists of very small spots. This ring is a $K\alpha$ doublet; the pattern of the spots is about the same on each component of the doublet and one can be approximately deduced from the other by translation. This corresponds to a polygonized state. It is possible that some of the spots indicate the formation of a few new grains; but on the transmitted part the halo due to the continuous

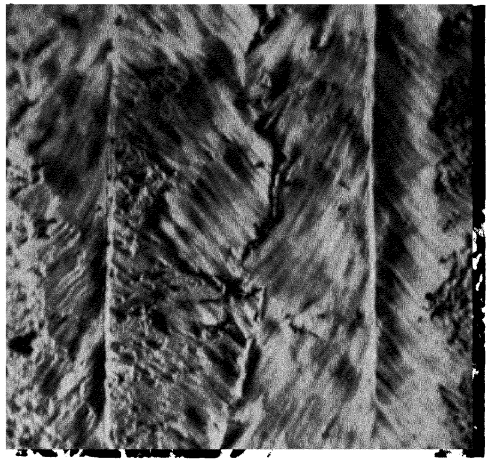

Figure 1. Cold rolled copper (Magnification 1,000 ×)

Figure 2. Cold rolled copper after 100 hr at 125° C (Magnification 1,000 ×)

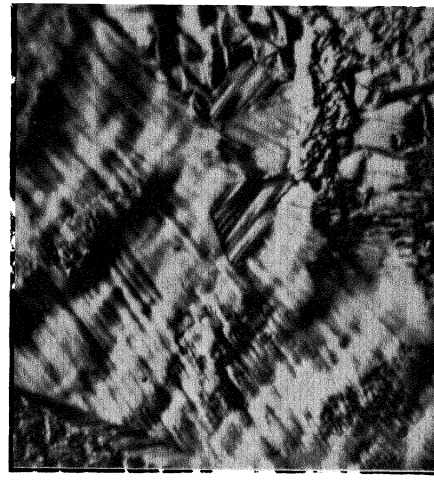

Figure 3. Cold rolled copper after 2 hr at 190°C; nucleus (Magnification 1,000 ×)

Figure 4. Cold rolled copper after 2 hr at 190°C (Magnification 1,000 ×)

spectrum of x-rays still shows a pronounced asterism, proving that the sample is not really recrystallized at 265°C. Great care must be taken in the interpretation of these x-ray diagrams because the outer layers of the samples, heavily cold worked by the cutting tool, recrystallize at lower temperature than the remainder of the material. Mistakes are best avoided by the removal of these layers, through electropolishing or etching, prior to annealing.

It can be seen quite clearly from *Figure 5* that between temperatures of 250° and 280°C the elastic limit shows an initial drop, while the

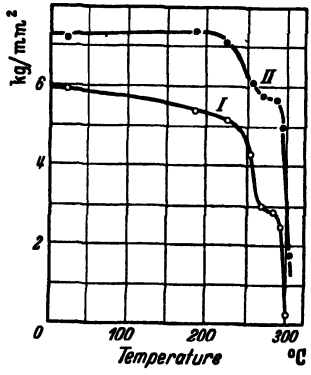

Figure 5. Variation of elastic limit (I) and 1 per cent proof stress (II) as a function of annealing temperature, aluminum 99·99 per cent cold drawn

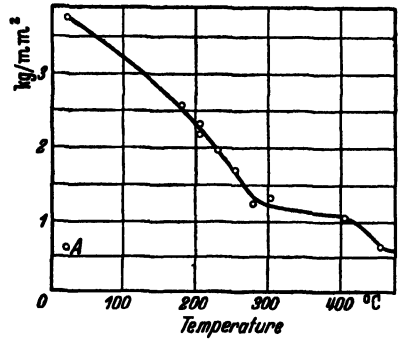

Figure 6. Variation of elastic limit as a function of annealing temperature, aluminum 99 99 per cent stretched 3·5. A = elastic limit of unstretched specimen

stress for 1 per cent elongation does not decrease much. This premature drop is one of the anomalies of this zone of annealing temperature.

The shape of the initial part of the stress-strain curve in this region is also quite peculiar: it is known that a stress-strain curve has a roughly parabolic shape, that is, the stress σ is related to the elongation ϵ by a formula[4] of the type

$$\sigma = \sigma_0 + a\epsilon^m$$

The elastic strain is deduced from the measured strain to give ϵ.

Careful investigation shows that the value of m is not universal for the whole range of the curve. For a small region of the curve m can best be computed by a differential method which was proposed by DE LACOMBE for the analysis of creep curves,[5] by which any change of shape along the curve is clearly revealed.

Let us now study the shape of the first 2 per cent of the curve, after which m changes. For recrystallized samples a and m are positive, the latter being of the order of 0·5 to 0·8 (we have detected values as high as 1·0); then σ_0, as computed by the above method, approaches the observed elastic limit, which is generally higher, direct observation being less accurate than calculation. For cold worked samples m has a negative value of the order of — 0·9 to — 1·1; here σ_0 is not related to the elastic limit. When the material is annealed at 265° and 280°C m equals zero, that is, the curve is logarithmic. The change is abrupt, m still being equal to — 0·95 for samples annealed at 250°C.

Thus, immediately below the temperature of genuine recrystallization there is a narrow zone of temperature where annealing produces a stress-strain curve of a special shape.

It is interesting to compare these observations with materials where polygonization occurs, that is on coarse-grained slightly cold worked crystals. Samples of the same metal were recrystallized to a grain size of 0·1 mm diameter, stretched 3·5 per cent and annealed at various temperatures for 0·5 hr. Recrystallization as seen by x-ray occurs between 400° and 450°C.

Figure 6 shows the variation of the elastic limit with temperature of annealing up to 450°C. As in *Figure 5*, the drop from the cold worked state to the recrystallized one occurs in two stages. It was thought that the metal is polygonized at the intermediate stage at about 350°C. X-ray analysis confirmed this supposition: each grain produces a cluster of sharp spots, thus the metal is recrystallized *in situ*, that is heavily polygonized. Also, as was remarked in the cold worked or the recrystallized state, the value of m changes at this intermediate stage. Thus, in heavily as in slightly cold worked metals, recrystallization is preceded by an intermediate stage; as this corresponds to polygonization in the latter, it is reasonable to assume the same thing for the former.

Other experiments were performed on wires of impure aluminium containing 0·41 per cent iron and 0·28 per cent silicon (no other impurities). Special grips had to be made to enable pieces of wire to be tested in Chevenard's micromachine. *Figure 7* shows the variation of elastic limit as a function of the temperature of annealing. The shape of the curve is the same as for pure aluminium: the drop occurs in two stages, separated by a zone of temperature where x-rays show the metal to be polygonized.

THERMAL ANALYSIS

The energy stored in a cold worked metal is evolved as heat during annealing. A differential thermal analysis between a cold worked sample and an annealed one of the same metal enables us to determine at which temperature this heat evolution occurs. The method was used in a sensitive device with the pure aluminium mentioned. Although the experiments have only recently been initiated, it appears that the heat evolution is very small during recovery and begins

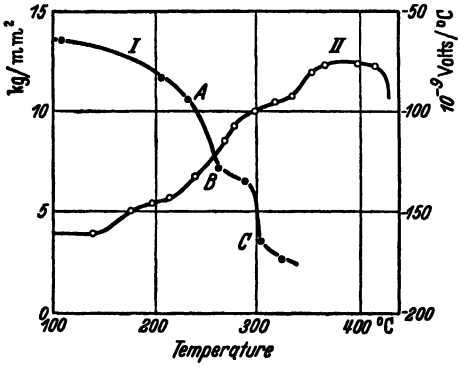

Figure 7. Variation of elastic limit (I) and thermoelectric power (II) as a function of annealing temperature, aluminium 99 3 per cent cold drawn. X-rays show sample A to be polygonized

sharply between 280° to 285°C. Thus the stored energy is dissipated mainly at recrystallization, which occurs at the temperature indicated by other experiments.

X-RAY STUDY

Some observations made on x-ray diagrams lead to a better understanding of the facts. In polygonized polycrystals each block or crystallite of the structure gives a sharp spot. If the metal is coarse-grained these spots are clustered along arcs of the Debye rings, extending over a few degrees; each arc corresponds to a whole grain. These spots are quite distant for high Bragg angles. If the grain is finer, the different arcs merge together; thus it is difficult to distinguish between a polygonized metal and a recrystallized one with very fine grains. But the distinction can be effected by observing $K\alpha$ doublet on back reflection, as mentioned earlier: in the polygonized state the pattern of spots from one component of the doublet to the other correspond due to asterism. It is also characteristic that, by transmission, the continuous spectrum of x-rays produces a pattern which, for polygonized metals, still shows a great asterism. By these means we were able to

prove that the cold drawn aluminium crystals were polygonized after annealing at about 270°C.

It is important to note that, even in the cold worked state, the Debye rings are often not continuous but consist of spots (back reflection). These spots are perhaps not as sharp as in the polygonized state, but have about the same density. It is well known that in the cold worked state the deformation is heterogeneous. In other words, cold working generally leads to fragmentation,[6] except for single crystals deformed in a homogeneous way.

A study of this fragmentation has been made[7] (see particularly *Figures 8* and *9* of this reference) and it was concluded that high purity aluminium is always fragmented. The average size of the fragments or crystallites could sometimes be deduced from the number of spots produced by a grain of known value and it was found to be of the order of 5 microns. A picture (*Figure 8*) obtained by means of BARRETT's x-ray microscopic method[8] shows the shape of the fragments of a grain in a sheet of slightly bent aluminium; the size is somewhat larger than mentioned above, but cold work is slight, so that it is probable that the type of fragmentation is the same in both samples.

With impure aluminium fragmentation cannot be detected in single crystals, where it is probably too fine, but it appears quite distinctly in polycrystals. The phenomena cannot generally be observed in metals other than aluminium, excepting those having a low melting point. If deformation is carried out at high temperatures or at low rates the fragmentation is much more pronounced and distinct, indicating a relationship with density of slip lines and size of the mosaic block after deformation. But it is not yet clear whether the observed fragments or crystallites form the mosaic blocks themselves or if they are larger. They may rather be related to deformation bands.

This fragmentation greatly hinders the detection of the start of polygonization by means of x-rays. It is, in fact, questionable whether a fragmented cold worked metal is not already polygonized. This involves a question of terminology which will be discussed later.

THERMOELECTRIC MEASURES

As polygonization implies a movement of dislocations, in an impure metal it must also lead to a displacement of the foreign atoms by the Cottrell mechanism. As thermoelectric measurements have been shown

Figure 8. Coarse-grained sheet of aluminium, bent, Barrett's method (Magnification 100 ×)

to provide a very sensitive method of observing the changes in repartition of foreign atoms,[9] the study of the variation of thermoelectric power during annealing at increasing temperatures is implied.

Dislocations alone have been shown to have a very small effect on thermoelectric power of aluminium[10] (variation smaller than 10^{-8} volt/degree). Thus any appreciable variation of the thermoelectric power must be due to some kind of precipitation or dissolution of impurities, or possibly the formation of large Cottrell atmospheres. The method for measuring the thermoelectric power directly at a given temperature has been described elsewhere.[11]

The metal tested was the same wire of impure aluminium as above. It was annealed at 500°C in order to dissolve about 0·006 per cent iron and all the silicon present, air-quenched and cold drawn from 4 to 1 mm diameter. (Silicon and iron both decrease the thermoelectric power of aluminium. Thus an increase of this quantity corresponds to a precipitation.) *Figure 7* represents the thermoelectric power of the wire as a function of temperature; the graph displays a sharp increase from 160°C and tends towards the value of pure aluminium: some kind of precipitation is occurring. The variation occurs in three stages at temperatures of about 170°, 260° and 320°C respectively. These stages seem to correspond rather well to the processes of recovery, polygonization and recrystallization, although the temperature of 320°C is too high for the latter and it is still not known how recrystallization can lead to a precipitation of impurities.

A similar study has been carried out on an aluminium wire of similar composition, which consists of a few cylindrical grains and can therefore be considered to behave like a single crystal. The wire was annealed at 600°C and stretched 18 per cent: its thermoelectric power shows no variation before 430°C, at which temperature genuine recrystallization occurs as shown by x-ray analysis, which reveals no fragmentation below 430°C. Here the precipitation is very pronounced but accompanies recrystallization. In an intermediate sample of a coarse-grained wire stretched 20 per cent precipitation begins at 270°C, while true recrystallization is observed only at 310°C.

Thus thermoelectric studies on an impure aluminium crystal show that, as it is increasingly fragmented by cold work, more precipitation precedes recrystallization. The relation of this precipitation with polygonization has been suggested by GALT.[12] It will be discussed later.

DISCUSSION OF RESULTS

A metal is said to be polygonized when, within each grain, lattice rows are not continuously bent but broken into small segments, each of them making small angles with its neighbours. Two problems arise from this definition:

1 A question of scale: by the atomic scale, all bent crystals are polygonized. It is not intended to account for this 'polygonization'. Therefore a lower limit must be assigned to the length of the segments involved in the definition. Since x-rays show that, even in heavily cold worked metals, coherent domains of reflection have a length of about 10^{-5} cm, it is appropriate to select this limit. Thus the lower limit of polygonization is the mosaic structure.[13]

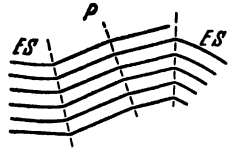

Figure 9. Arrangement of an atomic row in a metal displaying polygonization P and elastic stresses ES

2 The question also presents itself whether these segments must be straight, or whether they can be slightly bent when two kinds of imperfections occur along the atomic rows: local breakings, and bending over longer parts (*Figure 9*). The assumption that the word polygonization expresses only a trend to localize the curvature with angular discontinuities, but does not exclude elastic curvature, seems to be the most suitable solution here.

Thus, where x-rays show fragmentation, a cold worked metal exhibits polygonization and internal stresses together. The x-ray study mentioned in this chapter indicates that in aluminium this polygonization is on a rather large scale (order of 10^{-3} cm). It is more pronounced on polycrystals, due to heterogeneity in the stress distribution. Impurities decrease the scale of polygonization, so that it hardly can be detected by x-rays: single crystals of impure aluminium reveal no fragmentation or polygonization when deformed. Nevertheless one must remember that Guinier has observed polygonization on single crystals of impure aluminium after annealing at a very high temperature (600°C). For other cubic metals the scale of polygonization seems smaller and must descend to the mosaic structure; also internal stresses are higher. Thus, there is a more or less continuous passage from the

small and continuous curvature of bent single crystals to the mosaic structure of heavily deformed metals, going through an intermediate state of polygonization at the scale of the deformation bands.

When such structures are annealed, the pattern of dislocations and the related stresses will tend to reach a more stable state (more localized rearrangements, which may have an effect on magnetic or electric properties, are not considered here). This can *a priori* happen in two ways:

i Annihilation of + and −, as suggested by BURGERS. This process can be called 'local recovery' and does not change the curvature at the mosaic scale.

ii Movements of dislocations, with a trend to group along sub-boundaries *i.e.* polygonization.

This process is hindered by inadequate size of curvatures or by a predominance of impurities. Thus, polygonization occurs much more easily in a metal already fragmented by cold work and progresses during annealing by an increase of the distance between the sub-boundaries.

Our thermal analysis experiments have shown that most of the dislocations present in the cold worked state disappear only during recrystallization; thus, if 'local recovery' occurs in aluminium, it annihilates only a few dislocations. Only the thermoelectric curve of *Figure 7* can suggest a first stage recovery, as distinct from polygonization; but the bend in this curve at 215°C may be due to experimental error.

Other experiments on aluminium (variation of elastic limit, or shape of the stress-strain curve of x-ray diagrams and of thermoelectric power) all show that, where a metal is already fragmented or partly polygonized by cold work, polygonization progresses further during annealing, and just before recrystallization reaches a relatively stable state of coarse polygonization (or recrystallization *in situ*). This state is not essential for recrystallization, as it is absent in the case of single crystals of impure aluminium which are not fragmented, or at least where it may occur on a much smaller scale.

The precipitation of foreign elements accompanying polygonization can either be actual precipitation or formation of large Cottrell atmospheres. The fact that the variation in thermoelectric power continues during recrystallization can be best explained by the second

hypothesis: a genuine precipitation occurring at the places where the atmospheres had united many atoms.

Micrography also shows a trend to polygonization in a fine scale for copper, so that the phenomenon appears to be quite general, at least for cubic metals.

SUMMARY

A special micrographic technique shows that in cold rolled copper annealing develops sub-boundaries within the grains before actual recrystallization occurs.

In heavily cold worked aluminium the crystals are fragmented as shown by x-rays, so that a partial polygonization is already present. This is not true for slightly cold worked, impure aluminium.

During annealing of fragmented aluminium the drop of the elastic limit occurs in two stages. The first one corresponds to a progress of the polygonization, the second one to recrystallization.

The state of coarse polygonization thus reached corresponds to a special shape of the stress-strain curve.

Thermoelectric study proves that this progression of the polygonization is accompanied by a partial precipitation of impurities.

Recrystallization can occur in single crystals without previous polygonization (at least on an observable scale).

REFERENCES

[1] JACQUET, P. *Rev. Métall.* 37 (1940) 214
JAROSZEWICZ-BORTNOWSKI, M. and SCHOOFS, J. *Rev. univ. Min.* 5 (1949) 9
[3] LACOMBE, P. and BEAUJARD, L. *J. Inst. Met.* 74 (1947) 1
[5] CRUSSARD, C. *Rev. Métall.* 41 (1944) 11
[4] —— *ibid* 41 (1944) 45
[5] DE LACOMBE, J. *ibid* 36 (1939) 178
[6] HOMES, G. *Bull. Acad. Belg. Ce. Sci* 23 (1936) 653
[7] CRUSSARD, C. *Communication au Congrès de Liége 1947* Rev. univ. Min. p 41, 1949
[8] BARRETT, C. S. *Amer. Inst. Min. Engrs, Met. Technol. Tech. Publ. No.* 1865, 1945
[9] CRUSSARD, C. and AUBERTIN, F. *Rev. Métall.* 45 (1948) 410
[10] —— *Bristol Conference Rep. 1947* p 119; *Publ. Phys. Soc.* 1948
[11] —— and AUBERTIN, F. *Rev. Métall.* 46 (1949) 661
[12] GALT, J. K. *Phil. Mag.* 7, 40 (1949) 309
[13] CRUSSARD, C. and GUINIER, A. *Rev. Métall.* 46 (1949) 61

AUTHOR INDEX

SUBJECT INDEX